NUCLEOPHILIC BORYL MOTIFS AND ALPHA-BORYLCARBANIONS: REACTIVITY AND TRENDS

Ricardo José Maza Quiroga

UNIVERSITAT ROVIRA i VIRGILI

Nucleophilic boryl motifs and alpha-boryl carbanions: reactivity and trends

Ricardo José Maza Quiroga

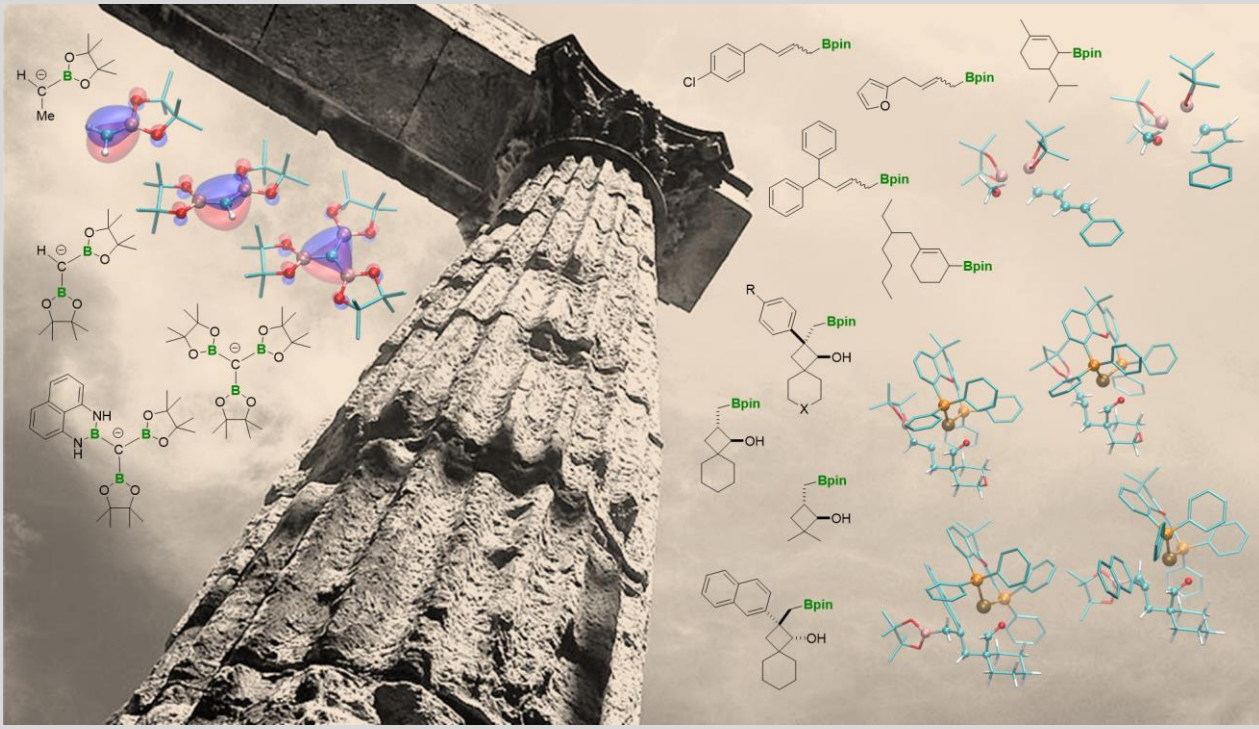

DOCTORAL THESIS
2021

Ricardo José Maza Quiroga

Nucleophilic boryl motifs and alpha-borylcarbanions: reactivity and trends

Doctoral Thesis

Supervised by:

Prof. María Elena Fernández Gutiérrez

Prof. Jorge Juan Carbó Martín

Departamento de Química Física e Inorgánica (URV)

UNIVERSITAT ROVIRA i VIRGILI

Aniversari Universitat Rovira i Virgili

Tarragona, December 2021.

Dr. María Elena Fernández Gutiérrez y Dr. Jorge Juan Carbó Martín, profesores titulares del Departamento de Química Física e Inorgánica de la Universidad Rovira i Virgili,

HACEMOS CONSTAR que el presente trabajo, titulado:

"Nucleophilic boryl motifs and alpha-borylcarbanions: reactivity and trends"

que presenta Ricardo José Maza Quiroga para la obtención del título de Doctor, ha sido realizado bajo nuestra dirección en el Departamento de Química Física e Inorgánica de la Universidad Rovira i Virgili.

Tarragona, 4 de noviembre de 2021

Los directores de la Tesis doctoral

María Elena Fernández Gutiérrez

Jorge Juan Carbó Martín

El presente trabajo se ha desarrollado mediante una beca FPI (BES-2017-079801). El contenido descrito en la presente Tesis ha sido financiado por:

- El Ministerio de Economía, Industria y Competitividad de España (MINECO) mediante proyectos CTQ2016-80328-P, PGC2018-100780-B-I00 y PID2019-109674GB-I00.
- La Generalidad de Cataluña mediante el proyecto 2017SGR629 de ayudas a los grupos reconocidos y consolidados.
- La Universidad Rovira i Virgili mediante los proyectos 2015PFR-URV-B2-21 y 2016PFR-URV-B2-22 del *Programa de Foment a l' Activitat de la Recerca* (PFR).

Agradecimientos

A veces echo la vista atrás y me da vértigo del tiempo que ha pasado y de todo lo que he avanzado como persona y como químico. Y esto no he podido conseguirlo sin la ayuda directa e indirecta de ciertas personas que han estado a mi lado en este camino.

Quiero empezar esta sección de agradecimientos a las personas que hicieron posible dicho camino, mis supervisores Elena Fernández y Jordi Carbó. Elena, creo que no hay palabras para describir el agradecimiento tan profundo que tengo por haberme no solamente darme la oportunidad de realizar un trabajo de investigación como este, sino por confiar en mí, siendo yo un auténtico desconocido de Málaga del que nada sabías. A día de hoy sigo recordando aquel correo, hace ya unos cuantos años, con tu respuesta e interés en mí, marcando en mi vida uno de esos puntos de inflexión que marcan en el interior de una persona. Más adelante recuerdo que, en una reunión, me comentaste si quería empezar un proyecto en Química computacional, lo cual me abrumó y alegró a partes iguales, puesto que tenía la sensación de que esa confianza iba en aumento y ahí es cuando empieza mi historia con Jordi Carbó. A él le quiero agradecer haberme introducido en esta parte apasionante de la Química, además de su infinita paciencia y esfuerzo para que pudiera ser mínimamente independiente en esta área. De nuevo, gracias por haber compartido vuestros conocimientos conmigo y por ser los supervisores que sois.

También me gustaría agradecer a Manuel Soriano, quien hizo posible la entrada en el grupo mediante su contrato industrial de la empresa Maystar en el grupo de Elena para desarrollar ceras depilatorias en frío. Recuerdo las reuniones que teníamos con Elena comentando las fórmulas y cuáles podrían ser mejores. Al final conseguí una que arrancase pelo, y prueba de ello eran los “parches” que me dejaba en el brazo intentando probar la propia fórmula en mí mismo, lo cual me dio una gran satisfacción por haber cumplido con el objetivo.

En otro lugar nos encontramos a los chicos del laboratorio. Comenzaré por Oriol, así no te haré difícil buscarte en la parte de agradecimientos. Si nos ponemos a ser estrictos, entraste prácticamente a la par que yo, solo que tú estabas realizando el graduado y yo estaba comenzando en el grupo, así que eres casi igual de perro viejo que yo. Eres una persona inteligente, perspicaz y humilde, demostrando tener una gran capacidad para manejarte en el laboratorio y supervisar a otras personas bajo tu tutela y manteniendo la moral alta con tus *performances* en mitad del laboratorio. Sigue así, te esperará un gran futuro en la vida tanto en lo profesional como en lo personal.

Todavía recuerdo aquella vez que apareció aquella vez aquel italiano con acento acento andaluz en nuestro grupo, Riccardo Gava. Tuvimos que sufrir las confusiones a veces con el nombre, lo cual se agravaba aún más al darme cuenta que nuestras respectivas novias se

llamaban de igual manera…pero se sobrellevaba de manera graciosa. A él le quiero agradecer toda la ayuda prestada durante su estancia en la Universidad, y a las regañinas que me echaba cuando alguna cosa no la hacía de manera correcta, que de alguna forma me han hecho mejorar poco a poco a base de palos. Eres una de las personas más inteligentes que conozco, muy metódico y cuestionándotelo todo, como un buen químico que eres. En la época que te marchaste para labrar tu futuro en la empresa, no dude que te iría genial, y a la vista está que es cierto. Todo lo que te propones lo haces, y es algo que también admiro de ti. Nunca cambies.

Otra gran Post-doct que paso por nuestro grupo fue Macarena, quien anteriormente estuvo en el departamento de Orgánica realizando el doctorado. Estuvimos unos pocos meses juntos, pero los suficiente para darme cuenta de la gran persona y profesional que eres. Cuando me fui de la estancia y supe que encontraste una posición en la empresa me apenó por una parte al saber que ya no podríamos seguir en el mismo proyecto juntos, pero de igual manera me alegré enormemente puesto que al fin podrías crecer profesionalmente y cumplir tus objetivos. Estoy seguro que todo te irá genial en la vida. El proyecto que dejamos no cayó en el olvido, sino que las llevo a cabo la recién llegada Mireia, que ha ido progresando a pasos agigantados. No me cabe la menor duda que ha caído en muy buenas manos. Por otro lado, tenemos a Paula, quien también ha demostrado ser una crack en el mundo de los borillos. Tenéis potencial y auguro que vais a dar vuestro 150 % en vuestra carrera investigadora. Luego está Sara, la ponferradina del grupo y mi sustituta en las compras del grupo. Ya comenzaste tus pasos por el laboratorio en el grupo vecino y efectivamente veo que hizo muy bien Elena al introducirte en el “boron group”. También quiero agradecer a la persona que en primer lugar me tutorizó en el laboratorio, Nuria Miralles. Fuiste una gran profesional, ayudándome y supervisándome en mis comienzos en el grupo. También a Jordi Royes, con quien tuve el placer de trabajar juntos antes de su defensa de su defensa de Tesis. Finalmente tenemos a Jana, una gran química y escaladora. No te desearé suerte en la recta final del doctorado puesto que lo más probable es que no lo necesites. No solamente están los chicos del grupo, también otros como Joan, peculiarmente conocido por ser el *hater* del grupo. Eres una persona muy inteligente con un “gran” corazón, aunque no se aprecie a simple vista. A los demás chicos del laboratorio 216 y 217, Pol, la almeriense Lola, Jordi, Daniel (el recién llegado de Bath) y Jessica, gracias por haber compartido esta etapa.

En otro lugar tenemos a los chicos del departamento de computacional, empezaré por Toni Salom. Creo que no te lo dije, pero la primera vez que te escuché creía que eras un doctorando proveniente de Italia, luego me contaron que eras de Mallorca y que el acento era bastante más marcado. Gracias por toda la ayuda que me has prestado en mis inicios y durante mi doctorado. No querría dejarme atrás a Gerard, otro reciente fichaje en el grupo.

Ya en el trabajo de fin de grado mostraste potencial y profesionalidad. Estoy convencido que tendrás una próspera carrera investigadora ahora con el Máster, ¡sigue así campeón! Al resto de chicos del departamento, Yannik, Albert y Gonzalo, también tienen su hueco aquí por hacer los momentos del café más amenos con las innumerables charlas que mantuvimos de diversos aspectos de la vida.

Por otro lado, querría agradecer a mi amigo de la infancia Alexander Behzenar (igualmente conocido como *Oleksankobich*), por su ayuda y sus consejos a la hora de mejorar la estética de la portada. Eres un grande, y espero que consigas lo que te propongas. Otro amigo a quien tengo que agradecer es a Gaspar Carrasco, quien, sin su consejo de venir a Tarragona a realizar el doctorado, probablemente no estuviera aquí. Fue una pena que te marchases de Tarragona a Madrid a comenzar de nuevo tu etapa doctoral, pero sé que hiciste bien. Con tu gran capacidad e inteligencia estoy segurísimo que todo te irá genial.

También querría dejar un pequeño espacio a las personas que hacen posible que el trabajo del laboratorio funcione correctamente. Comenzaré por nuestra técnica de laboratorio por excelencia, Raquel. Sinceramente, tenerte en el departamento es una bendición, siempre intentando ayudarnos para resolver cualquier problema del laboratorio de manera rápida y eficiente. También a Josep, por estar ahí ante cualquier problema y recordarnos constantemente la falta de bidones de pentano. Por otro lado, tenemos a las chicas de masas, siempre ayudando para cualquier problema/duda con el GC-MS y ESI-TOF. Y finalmente Ramón, nuestro técnico experto en el RMN ¡muchísimas gracias por toda la ayuda prestada!

During my research stay in Vienna I also shared moments with people which would be unfair to not be included in this section. They were Davide Castiglione, Laura Ielo, Monica Malik, Carola Ricciardelli, Francesco Baso y Veronica Pillari, to all of them, grazie mille per avermi ricevuto a braccia aperte. In a special way, I would mention to Raffaele Senatore, for his great help and support provided during this three month in Vienna. Non c'é dubbio che la carriera che hai Alle spalle parla per te e sono sicuro che raggiungerai tutti GLI obbiettivi che ti sei prefissato. I would also like to specially thanks to Margherita Miele to share really good times and also help me in the laboratory during my beginnings. Buena fortuna per l'ultima parte del dottorato campionessa!

En últimos lugares quiero agradecer a la persona que ha estado todo este tiempo a mi lado, desde mi inicio hasta ahora, Natalia (o también llamada *Zihquita*). No tengo palabras para describir el agradecimiento profundo y lo mucho que te debo por estar a mi lado al pie del cañón dándome tus mejores consejos y animándome cada día a ser mejor persona. Te quiero inmensamente, esta tesis en parte también es un éxito tuyo.

Finalmente querría agradecer a las personas que me dieron la vida y el amor incondicional que haya llegado hasta donde estoy, mis Padres. Recuerdo a mi madre el día que le confirmé la fecha exacta de mi partida de mi querida Málaga. La pobre, en una mezcla de sentimientos, se emocionó. A mi padre creo que no le pesó tanto puesto que tiene la compañía de sus pájaros. Fuera de bromas, a él es a quien le debo haber empezado mi carrera como Químico. Eres la principal fuente de inspiración para mí, te quiero y te admiro por igual, y espero que al menos haya llegado a ser una décima parte de lo que eres. A mi hermana Rosita, por sus muchos consejos y ayudas a lo largo del doctorado. Eres otra fuente de inspiración y estoy muy orgulloso por ver hasta donde has llegado.

Así pues, me gustaría terminar con una acertada frase que nos dejó en sus novelas el famoso J.R.R. Tolkien mediante el gran personaje Gandalf: *No es importante saber cuánto tiempo te queda, sino qué hacer con el tiempo que se te ha concedido*. Termino una etapa, para empezar otra nueva, teniendo siempre en mente la finalidad de aprovechar ese tiempo otorgado para estudiar, mejorar y ser mejor persona.

De nuevo,

Gracias a todos.

Thanks to all.

Gràcies a tots.

"Un país no es rico porque tenga diamantes o petróleo. Un país es rico porque tiene educación, en definitiva, la riqueza es conocimiento"

Antonio Escohotado

Contents

Chapter 1 Introduction and General Objectives 1

1.1 Borylation of π-systems via copper(I) catalysis 3

1.1.1 Intramolecular borylative alkylation 4

1.1.2 Intramolecular copper-catalyzed borylative cyclization involving ketones or aldehydes 7

1.2 Transition-metal-free borylation of π-systems 12

1.3 Computational insight into the nucleophilic character of trivalent boron compounds 19

1.4 α-Borylcarbanions as a promising set of homologating reagents 23

1.4.1 α-Boryl carbanions 23

1.4.2 Reactivity of borata-alkene compounds 32

1.5 Objectives 38

1.6 References 39

Chapter 2 Nucleophilic Cu-B addition to alkenes with concomitant intramolecular coupling with aldehydes 53

2.1 Abstract and specific objectives 55

2.2 State of the Art 56

2.3 Results and Discussion 57

2.4 Conclusions 70

2.5 Computational Details 71

2.6 References 72

Chapter 3 Allylic Borylation of conjugated dienes catalyzed by alkoxides 75

3.1 Abstract and specific objectives 77

3.2 State of the Art 78

3.3 Results and Discussion 79

3.4 Conclusions 89

3.5 Computational Details 89

3.6 References 90

Chapter 4 α-Boryl Carbanions: Mapping the structure and the reactivity trends 95

4.1 Abstract and specific objectives 97

4.2 State of the art 98

4.3 Results and Discussion 100

4.3.1 Influence of the nature of the boryl moiety 100

4.3.2 Influence of the substituents on the carbanionic carbon 103

4.3.3 Influence of the number of boryl substituents 104

4.3.4 Mapping the nucleophilicity of α-boryl carbanions 107

4.3.5 Influence of the nature of the metal 110

4.3.6 Trend map for the metal salts and complexes 113

4.4 Conclusions 115

4.5 Computational details 116

4.6 References 118

Chapter 5 Conclusions 123

Chapter 6 Experimental Section 127

6.1 General Considerations 129

6.2 Experimental section for Chapter 2 130

6.2.1 General procedure for the protection of amines with sulfonyl chloride derivative 130

6.2.2 Characterization of sulfonyl chloride derivative 130

6.2.3 General procedure for the preparation of alkyl bromides 130

6.2.4 Characterization of 1,1-disubstituted products prepared via Wittig Reaction (Method A) 131

6.2.5 Characterization of products from bromination Reaction (Method B1) 132

6.2.6 Characterization of products from Bromination Reaction (Method B2) 133

6.2.7 General procedure for the alkylation of ester substrates with alkyl bromides followed by reduction to alcohols and oxidation to aldehydes 133

6.2.8 Characterization of alkylated esters and aldehydes 134

6.2.9 General procedure for the alkylation of aldehyde substrates with alkyl bromides 136

6.2.10 Characterization of alkylaldehydes from alkylbromides 136

6.2.11 General procedure for the alkylation of aldehyde substrates with allyl alcohols 137

6.2.12 Characterization of alkylated aldehydes from allyl alcohols 138

6.2.13 General procedure for the copper catalyzed borylative cyclization 139

6.2.14 Characterization of spirocyclic borylcyclobutanol products 139

6.2.15 General procedure for the oxidation of spiroboronate compounds 144

6.2.16 Characterization of spirocyclic 2.23 146

6.3 Experimental section for Chapter 3 147

6.3.1 General procedure for the preparation of 1,3-dienes via Wittig olefination 147

6.3.2 Characterization of 1,3-dienes via Wittig Olefination 147

6.3.3 General Procedure for the preparation of cyclic 1,3-dienes via Kumada Coupling 150

6.3.4 Characterization of cyclic 1,3-dienes via Kumada Coupling 150

6.3.5 General Procedure for the transition metal-free 1,4-hydroboration reaction for non-cyclic 1,3-dienes 151

6.3.6 Characterization of 1,4-hydroborated non-cyclic 1,3-dienes 151

6.3.7 General Procedure for the transition metal-free 1,4-hydroboration reaction for cyclic 1,3-dienes 154

6.3.8 Characterization of 1,4-hydroborated cyclic 1,3-dienes 154

6.3.9 General procedure for the transition metal free 1,2-diboration reaction 155

6.3.10 Characterization of 1,2-diborated and 1,2,3-triborated products 156

6.3.11 General procedure for oxidative reaction of borylated 1,4-hydroborated compounds 156

6.3.12 Characterization of allylic alcohols 157

6.4 Experimental section for Chapter 4 161

6.4.1 Descriptors 161

6.4.2 Cambridge Structure Database (CSD) search 165

6.5 References 167

Chapter 7 Summary 169

Chapter 8 List of publications, conferences and research stay 175

8.1 List of publications 177

Chapter 1 Introduction and General Objectives

1.1 Borylation of π-systems via copper(I) catalysis

The development of catalytic C-B bond formation is a powerful tool in organic chemistry. Organoboron compounds are generally considered nontoxic and are therefore environmentally benign.[1,2] The borylation of π-system represents a remarkably versatile method to install new functionalities, giving access to essential natural products or useful precursors for pharmaceutical purposes.[3–9]

In that context, copper complexes have emerged as an efficient catalyst to install boron across π-unsaturation since they can promote nucleophilicity through unreactive diboron compounds under homogeneous catalysis conditions.[10] The copper-catalyzed borylation was first reported by Miyaura and co-workers in 2000, suggesting that the *in situ* formed species Cu-Bpin catalyzed the β-borylation of α,β-enones.[11,12] Fernández and co-workers described the copper-catalyzed borylation of alkenes in the presence of Cu(I) complexes modified with N-heterocyclic carbene ligands.[13] The general mechanism for copper-catalyzed borylation of unsaturated substrates has been suggested to proceed through initial Cu-B bond formation via σ-bond metathesis, between diboranes reagents (bis(pinacolato)diboron B_2pin_2 (**1.1**)) and Cu-OR, followed by coordination of the π-systems with the concomitant 1,2-insertion to form the C-B bond and the C-Cu bond, which eventually react with an electrophile to generate the corresponding product (Figure 1.1). This mechanism describes most reactions involving unsaturated substrates,[14,15] and it was explored in depth by Sadighi,[16,17] Tsujhi,[18] Marder[19] and Kleeberg[20], who could isolate the key catalytic intermediates **I2** and **I3** described in Figure 1.1.

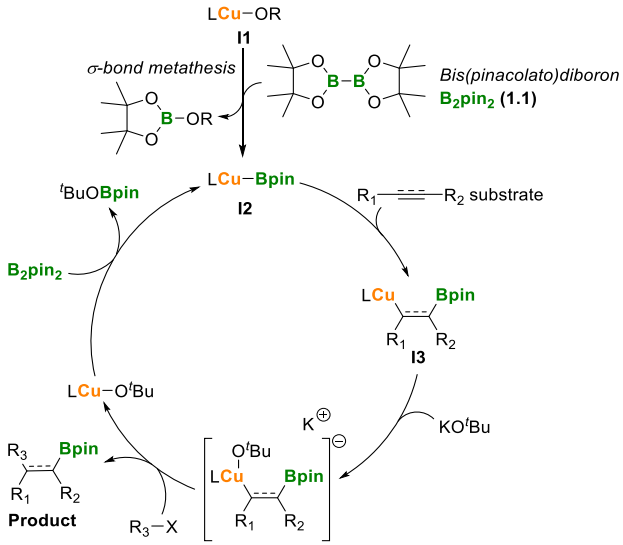

Figure 1.1. A general mechanism for copper-catalyzed borylative difunctionalizations.

A broad range of π-systems has been studied to be difunctionalized through copper-catalyzed borylative reactions. Alkenes, allenes, dienes and alkynes are the most widely studied, but also ketones, aldehydes, imines alkyl halides, and epoxides have been examined.[14]

Intermolecular copper-catalyzed borylative difunctionalizations reactions were studied by Yoshida and co-workers as the three-component carboboration to generate multisubstituted boryl-alkanes from alkenes (Scheme 1.1).[21] The same authors extended this study to the borylalkylation of alkynes to boryl-alkenes towards the generation of alkenylboranes (Scheme 1.1).[21] This new protocol could be applied later to the total synthesis of Equol which has potential bioactivity against osteoporosis and breast cancer diseases.[22]

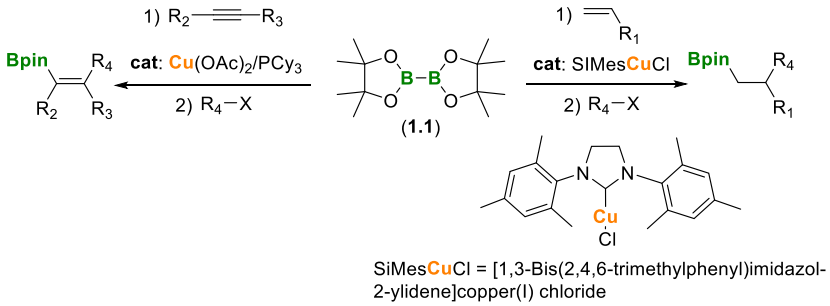

Scheme 1.1. Copper-catalyzed borylative difunctionalization of alkenes and alkynes.

1.1.1 Intramolecular borylative alkylation

Unlike intermolecular borylative alkylation of π-systems, intramolecular borylative functionalization is based on a two-component borylative process within subsequent cyclization. Ito and co-workers initially demonstrated the borylative cyclization of γ-silylated allylic carbonates providing access to bifunctional cyclopropanes (**1.4**) (Scheme 1.2). This borylative cyclization involved a regioselective addition of borylcopper(I) to the alkene through an *endo*-cyclization, in which boryl moiety is bonded to the internal part of the olefin due to electronic directing groups, such as trialkylsilyl groups. Surprisingly, both stereoisomers of the substrate generated the same diastereomer of the product. However, improved reactivity was observed with the *Z*-alkene **1.2** (Scheme 1.2).[23] The same authors postulated that once the LCuBpin complex is formed, it attacks regioselectively to the olefin. *E*-alkene **1.3** can suffers a posterior rotation of the C-C bond to be accessible to the attack of the nucleophile carbon (Scheme 1.3). This protocol was extended to the borylative cyclization of allylic phosphates.[24]

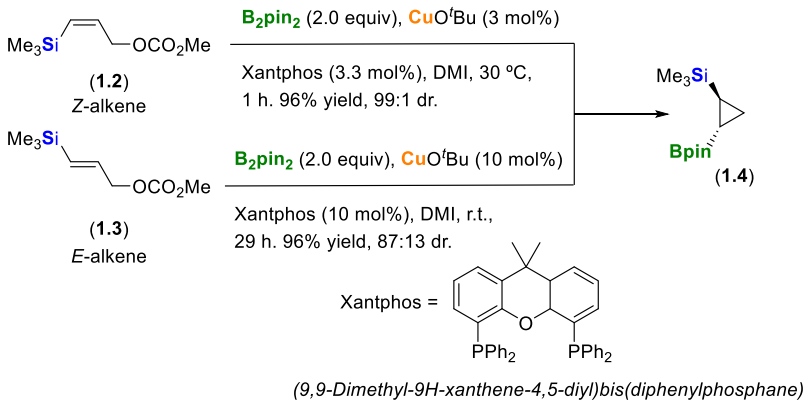

Scheme 1.2. First copper-catalyzed borylative cyclization reported by Ito and co-workers.

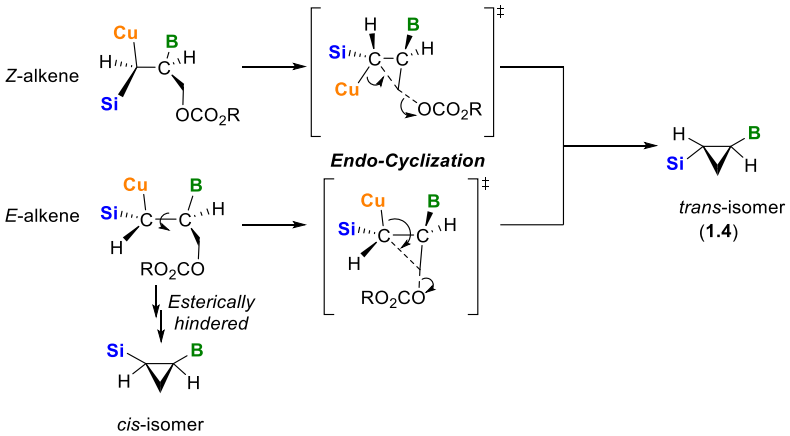

Scheme 1.3. Postulated pathways for cyclopropanation via borylative *endo*-cyclization of γ-silylated allylic carbonates.

Ito and Sawamura launched an interesting copper-catalyzed borylative cyclization of *Z*- and *E*-homoallylic methanesulfonates towards the corresponding *trans*- and *cis*-cyclobutane derivates.[25] Subsequently, Marder and co-workers described the borylcupration of alkenyl halides, via *exo*-cyclization, when they studied the borylation of alkyl halides using diboron reagents.[26] Ito and co-workers improved this discovery, and they carried out the optimization of this methodology.[27] Using unactivated terminal alkenes, they optimized the synthesis of spirocyclic boronates in high yields, generating up to five-member ring size. A good example is the borylative cyclization of substrate **1.5** towards the synthesis of spirocyclic boronate **1.6**, which could be subsequently oxidized and coupled with the amide to obtain a histamine H3 receptor compound **1.9** (Scheme 1.4). Following this study, the

authors also postulated a plausible mechanism in which a Cu(III) plays a fundamental role (Figure 1.2).[27]

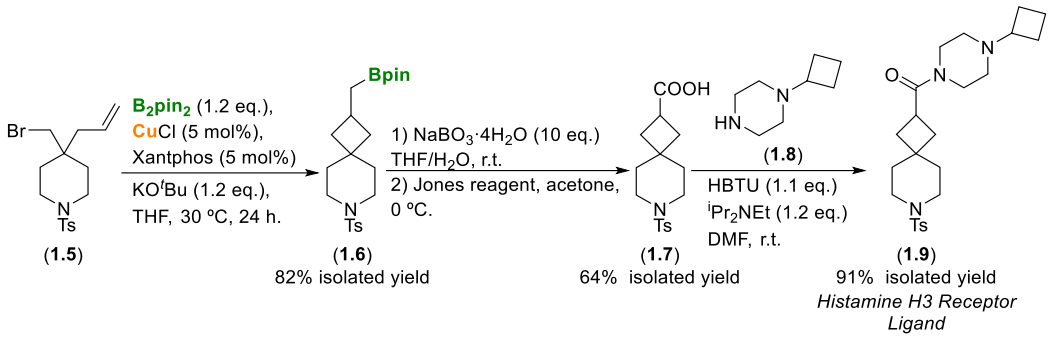

Scheme 1.4. Reaction pathway reported by Ito and co-workers for the synthesis of Histamine H3 Receptor Ligand via borylative *exo*-cyclization.

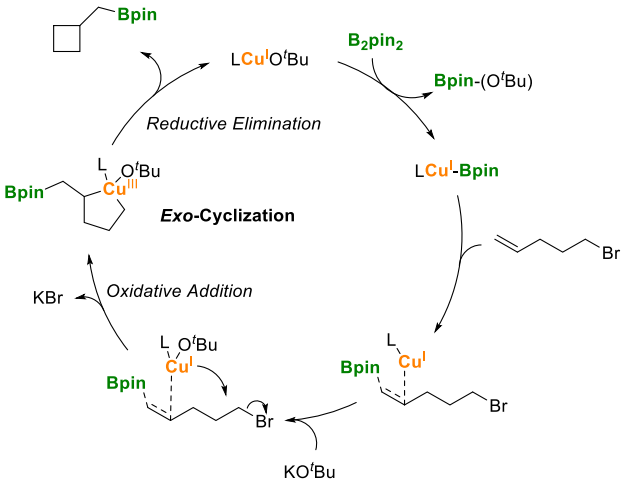

Figure 1.2. Proposed mechanism for Cu(I) catalyzed intramolecular borylative cyclization of alkenyl halides.

In 2018, Fernández, Carbó and Maseras reported a similar strategy for generating borylated spirocyclic products with various ring sizes, improving Ito's methodology to compounds with six-member ring.[28] The authors also postulated a plausible mechanism via Density Functional Theory (DFT) calculations, in which they demonstrated that Cu(III) intermediate is not kinetically relevant. A total of 28 different free energy profiles were computed, varying the influence of the leaving group, the cation of the base, the size of the member ring, and the number of explicit THF that might coordinate with the counterion. Figure 1.3 shows a representative energy profile for the mechanism of the formation of five-membered ring spiro molecules where the rate-determining process correspond to the energy difference between the transition state **spiro-A-TS2** and the intermediate **spiro-A-**

I4 with a free energy increment of 25.7 kcal·mol^{-1}.[28] The intramolecular copper-catalyzed borylative cyclization was extended to alternative π-systems with remarkable control of diastereo and enantioselectivity by selecting the appropriate ligand.[29–45]

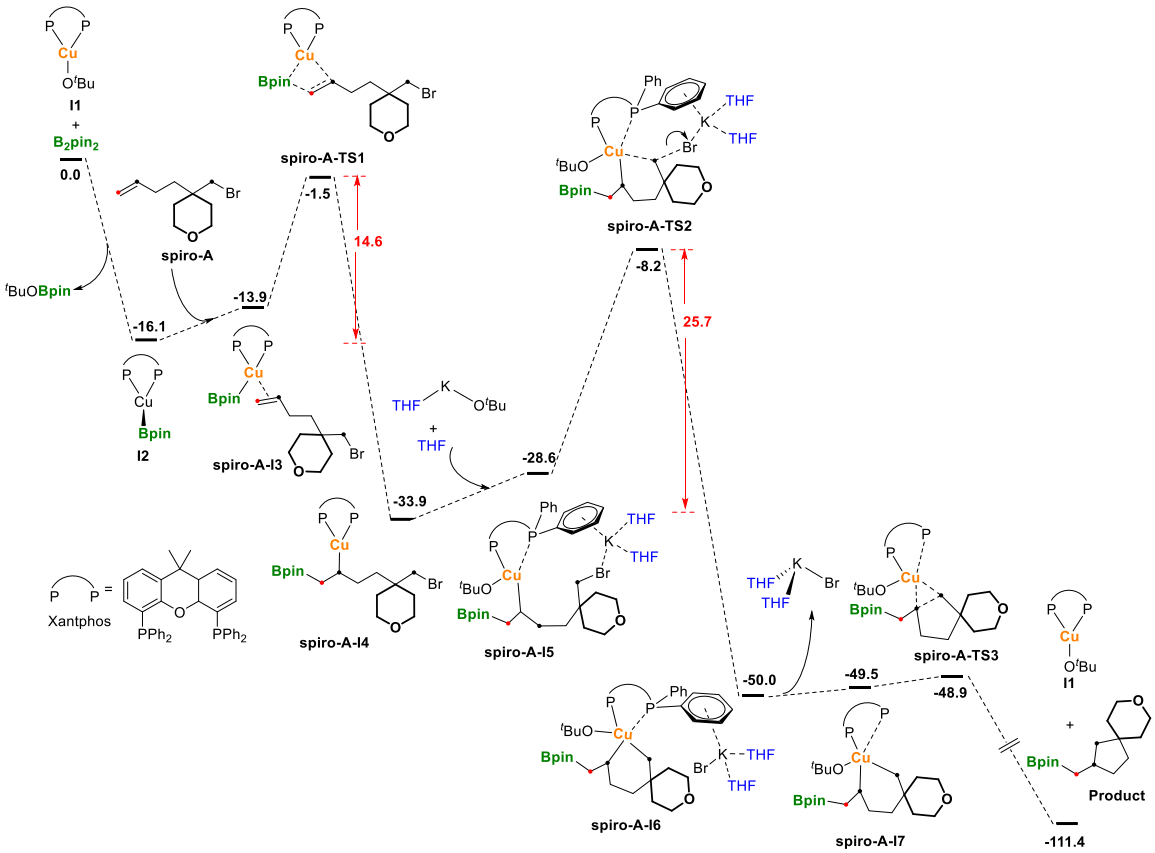

Figure 1.3. Computed free energy profile (in kcal·mol^{-1}) for the formation of 5-member ring spiro.

1.1.2 Intramolecular copper-catalyzed borylative cyclization involving ketones or aldehydes

The first example of boryl cupration of π-systems and subsequent cyclization with ketones was first reported by Lam and co-workers.[46] They developed an enantioselective copper-catalyzed domino conjugate borylation/aldol cyclization of enone-diones, using Cu/Josiphos catalyst and ^{t}BuOH as additive, to give a range of highly functionalized bicyclic decalins (Scheme 1.5a), hydrindanes (Scheme 1.5b) and diquinanes (Scheme 1.5c), the last ones with lower diastereoselectivity.[46]

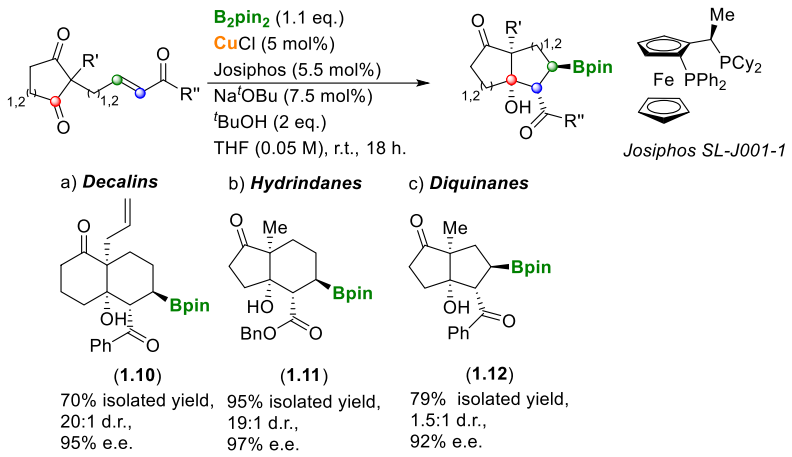

Scheme 1.5. Borylative aldol cyclization of enone diones developed by Lam and co-workers.

To explain the diastereoselectivity, the authors postulated a key transition state using the Zimmerman-Traxler model through chair-like *Z*-enolate, where the Bpin fragment is in pseudoequatorial position in the linker position connecting the dione and enolate (Scheme 1.6).[46]

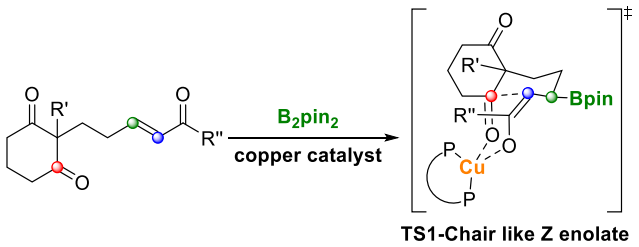

Scheme 1.6. Zimmerman-Traxler-type transition state postulated by Lam and co-workers to justify the diastereoselectivity.

In 2017, Meek and co-workers studied an efficient enantio- and diastereoselective hydroxy(bisboronates) through Cu(I) catalyzed intermolecular 1,2-addition on vinylarenes and further intermolecular interaction with aldehydes, using chiral diphosphine (R)-(+)-Cl-MeO-BIPHEP (Scheme 1.7).[47]

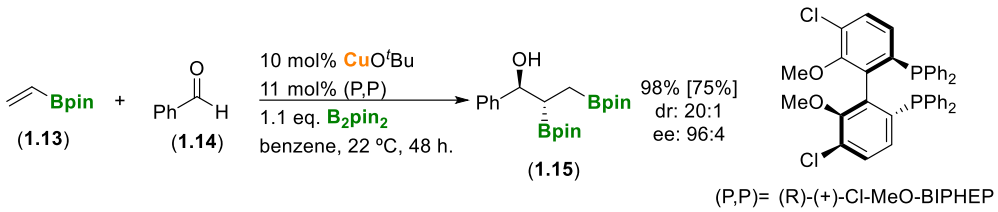

Scheme 1.7. Borylation/1,2-addition of benzaldehyde through Cu(I) catalysis. Yields reported without brackets were given by ^{1}H NMR spectra with hexamethyldisiloxane as internal standard and isolated yield in brackets.

Figure 1.4 shows the mechanism postulated by Meek and co-workers, where Cu-Bpin (**I1**), coming from the Cu-O^{t}Bu/B$_2$pin$_2$ σ-bond-metathesis, is responsible for the borylation of the vinylborane system to form α-borylalkyl–Cu intermediate **I2**, that further interacts with the carbonyl, via 1,2-addition, to provide the 1-hydroxi bis(boronate) ester.[47]

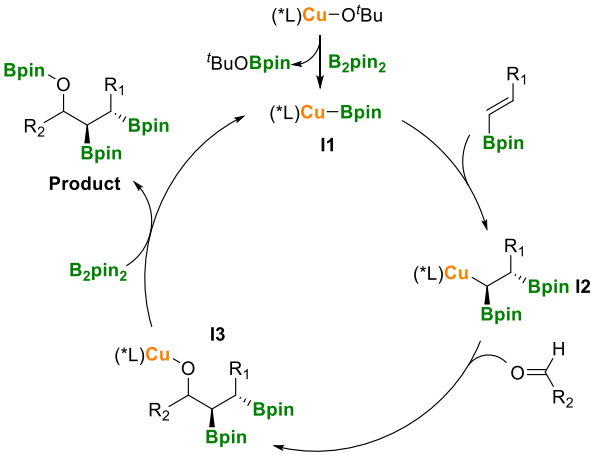

Figure 1.4. Mechanism for borylcupration of vinyl boronates followed by carbonyl 1,2-addition, postulated by Meek and co-workers.

The same authors expanded the scope for intramolecular borylcupration of vinylboranes and eventual trapping with aldehydes or ketones. The borylcupration of an aldehyde (**1.16**) resulted in the expected product **1.18** in 49% yield with good enantio- and diastereoselectivity (98.5:1.5 and 20:1, respectively). Although the process proceeds with very high selectivity, the yield was not as high as the one through the intermolecular version, because undesirable product was formed by competition of 1,2-addition of Cu-B to the aldehyde to get the secondary α-hydroxyboronate ester (**1.19**).[48,49] To solve this problem, similar experiments were carried out with sterically encumbered ketone (**1.17**), resulting in a significantly improved yield in product **1.20**, maintaining the high stereoselectivity (Scheme 1.8).

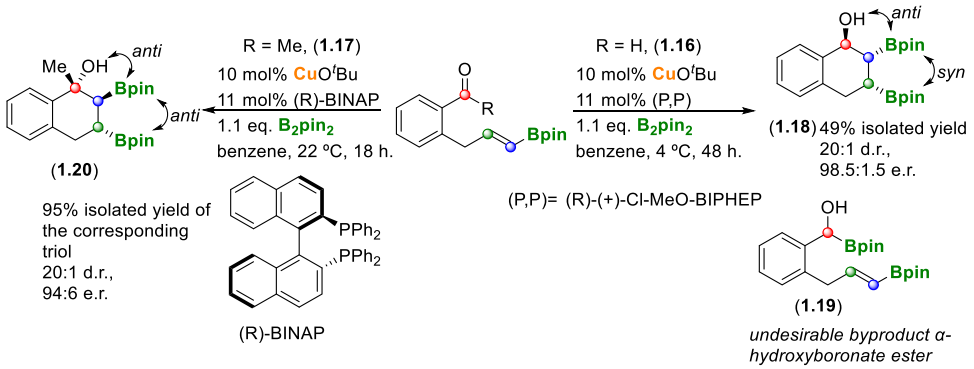

Scheme 1.8. Diastereo- and enantioselective intramolecular borylcyclization between vinylboranes and aldehydes.

Following this discovery, the same authors reported a similar reactivity using an alkyne instead of an alkene group. The authors demonstrated the Cu-catalyzed enantio- and diastereoselective tandem hydroboration/borylative cyclization of alkynes with ketones to synthesize carbocycles via desymmetrization. The method provides rapid access to [6,5]- and [5,5]-bicycles and cyclopentane products using CuCl/(S)-2-Furyl-MeOBIPHEP catalyst and methanol as an additive (Scheme 1.9).[50] The authors proposed a copper-catalyzed tandem mechanism in which dual catalytic cycles process contemporaneously. Firstly, the alkyne is hydroborated to give **1.22**, which following suffers a diastereoselective borylative cyclization yielding the product **1.23** by an excess of B_2pin_2.

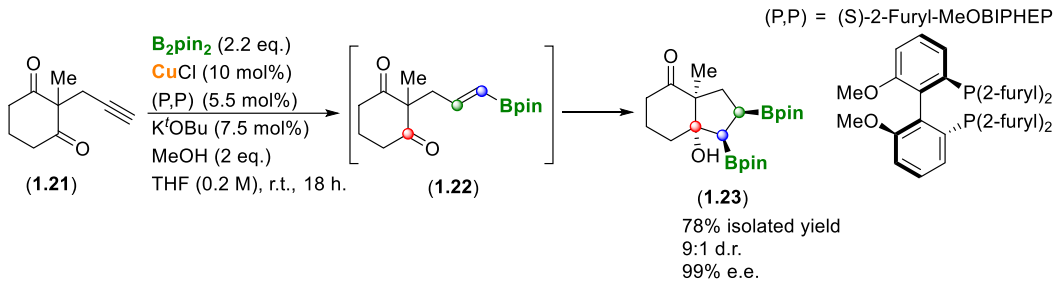

Scheme 1.9. Borylative aldol cyclization of alkyne diones developed by Meen and co-workers.

When small phosphine is used as ligand, the authors observed that the intramolecular borylative cyclization occurs with stereoretention, giving the *syn-anti-syn* diastereoisomer (Scheme 1.10a). Alternatively, with larger phosphine ligands, the cyclization was more likely to occur with stereoinversion to give the *syn-anti-anti* diastereoisomer (Scheme 1.10b).[50]

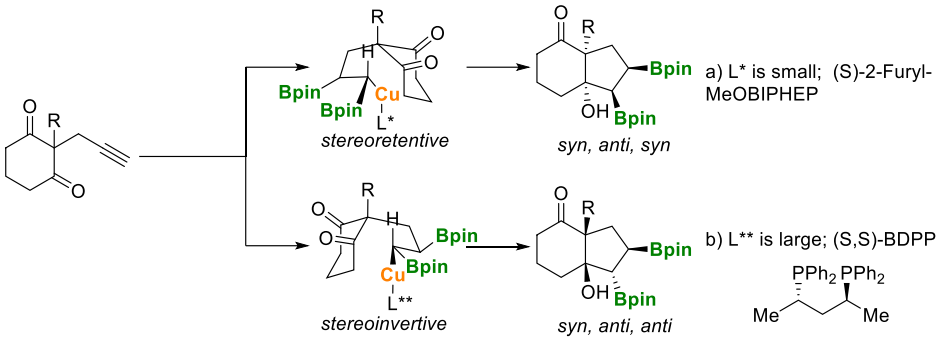

Scheme 1.10. The model used by Meek and co-workers to explain the observed diastereoselectivity.

Ito and co-workers, besides the preliminary study about *exo*-intramolecular borylative cyclization, developed an interesting method for diastereoselective *exo*-borylative cyclization of γ- or δ-alkenyl aryl ketones via copper(I)/Xantphos catalyst system, affording 4 and 5 member-ring products with *syn* diastereoselection (**1.26** and **1.27**) (Scheme 1.11).[51]

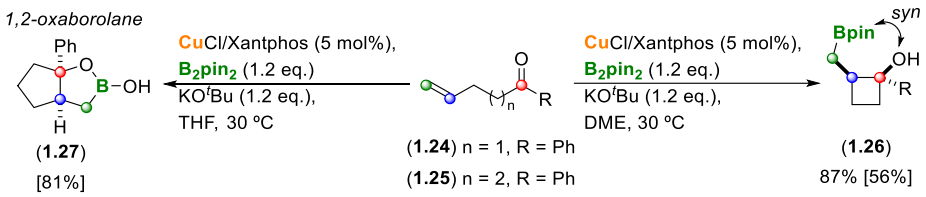

Scheme 1.11. Complementary borylative cyclization of γ- or δ-alkenyl aryl ketones. Yields reported without brackets were given by ^{1}H NMR spectra and isolated yield in brackets.

More recently, in 2019, Lautens and co-workers reported a similar intramolecular borylcyclization of γ-alkenyl aryl/alkyl ketones towards boryl-functionalized cyclobutanols (see product **1.29** in Scheme 1.12), using $Cu(MeCN)_4PF_6$ as the copper source and (S,S)-BDPP as chiral ligand and isopropanol as additive.[52] The reaction scope was broad and could tolerate a variety of electron-donating and electron-withdrawing groups and aromatic heterocycles, providing products with high enantio- and diastereoselectivity (Scheme 1.12).

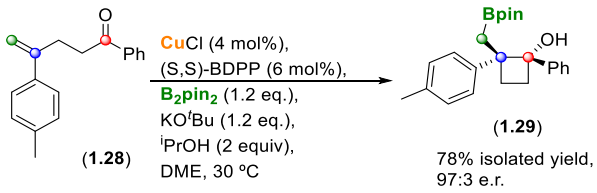

Scheme 1.12. Intramolecular borylcyclization of γ-alkenyl aryl/alkyl ketones.

In order to further understand the mechanism, the authors generated a quadrant diagram representation of the catalyst to predict the migratory insertion step from borylalkyl-copper intermediate **1.30**, pointing out the diastereomeric preference between **1.31** or **1.32**, due to the interaction between the two phenyl groups during the cyclization step (Scheme 1.13).[52]

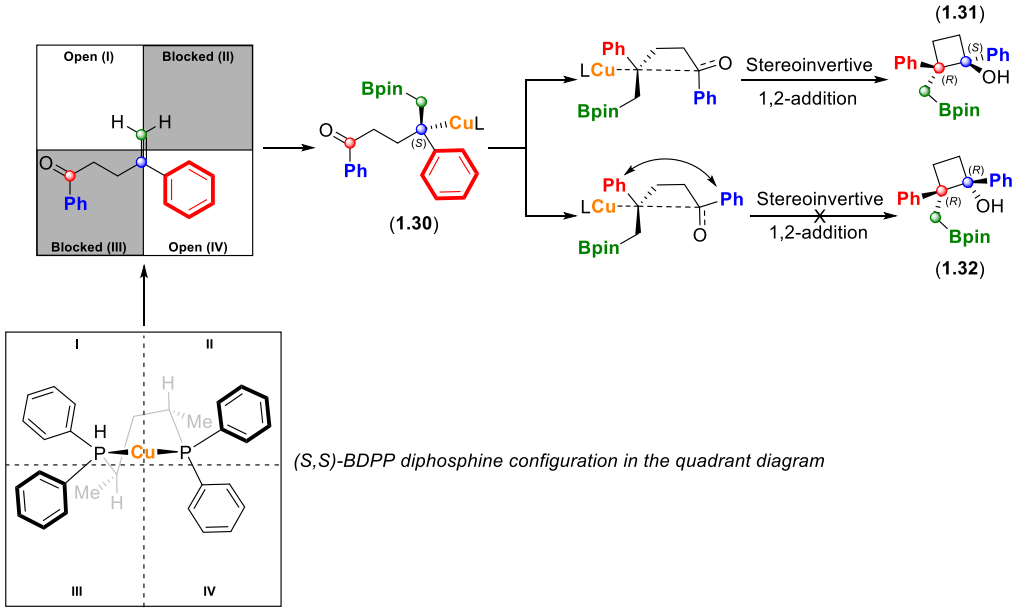

Scheme 1.13. Proposed quadrant diagram of (S,S)-BDPP diphosphine ligand and γ-alkenyl ketone to predict the migratory insertion of boryl-copper intermediate.

With all these precedents in mind, we realized the interest of intramolecular copper-catalyzed borylative cyclization, giving added value in cases that are highly stereoselective, towards polysubstituted cyclobutane formation. For this reason, we focused our effort to explore a novel copper-catalyzed borylative cyclization of γ-alkenyl-aldehydes in order to generate target product formation in a diastereoselective manner but also to understand the intrinsic mechanism that governs the activity as well as the selectivity fully disclosed in Chapter 2.

1.2 Transition-metal-free borylation of π-systems

The development of transition metal-catalyzed C-B formation represents a powerful tool in organic chemistry nowadays. It is thus noteworthy that C-B bond formation has been efficiently performed in the presence of transition metal-based catalysis.[48,53–55] Principally, complexes based on Pt,[56–58] Rh,[59] Ni,[60,61] and Cu[12,62–68] are examples of efficient transition metal complexes for catalytic C-B bond formation. Since organoboranes are very important

in organic synthesis and biomedicine,[69–75] the transition-metal-free approach might be a very appealing alternative, and its development is critical to the advance of modern chemical synthesis. Such protocols are valuable since reduces the toxicity and cost-associated to metal catalysts. Transition-metal-free borylation has emerged in the last decade as a convenient synthetic methodology toward selective C–B bond formation.[76] Schlesinger and co-workers were pioneers in 1954 to report olefin diboration with diborontetrachloride (**1.33**) in a transition-metal-free context, (Scheme 1.14a).[77] Four years later, in 1958, the same group reported the same reactivity using acetylene instead of ethylene (Scheme 1.14b).[78] In this work, the researchers also extended the reactivity of B_2X_4 (X=Br, F) to different unsaturated compounds.

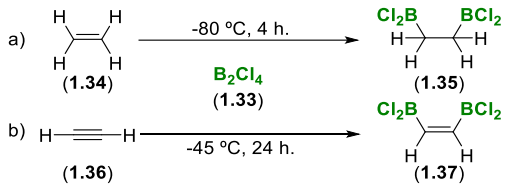

Scheme 1.14. Transition-metal-free diboration of alkene and alkyne by Schlesinger and co-workers.[76,77]

Diboron tetrahalides used in these reactions are thermally unstable and cannot be easily handled, so it has been necessary to develop a new methodology for transition-metal-free borylation. Some years earlier, in 1949, the same group reported for the first time the isolation of a mono-adduct of diborane **1.39** as a "liquid monoetherate" or a "solid dietherate" upon addition of varying amounts of diethyl ether.[79] Similar results were reported using tetrafluorodiborane,[80] resulting in a "crystalline, non-volatile solid at 0 °C" claimed to be the corresponding monoetherate (**1.40**) (Scheme 1.15a). With this evidence, sp^2-sp^3 diborane was suggested, in which the empty boron orbital of the diborane can be partially electron-filled by a rich-electron molecule, thus hybridizing the boron B(sp^2) empty orbital into B(sp^3) one (Scheme 1.15a). In 1970, Musgrave and co-workers reported an interesting sp^2-sp^3 anionic adduct, isolating a pentabutoxydiborate (**1.41**) (Scheme 1.15b).[81] Marder and co-workers isolated, characterized and studied similar adducts formed between B_2pin_2 and different anions, such $^tBuO^-$, MeO^-, $(4\text{-}^tBuC_6H_4)O^-$ and F^-.[82,83]

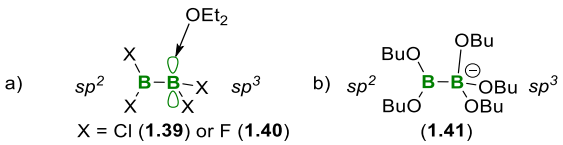

Scheme 1.15. An early example of a) sp^2-sp^3 mono-adduct of diboron tetrahalides with diethyl ether reported by Schlesinger group and b) pentabutoxydiborate reported by Musgrave group.

In 2009 Hoveyda and co-workers reported a novel conversion of non-polarized B-B bond,[84] from commercially available B_2pin_2 into pinacolboryl nucleophile through the addition of readily available N-heterocyclic carbenes (NHC) (Figure 1.5). The authors explored the conjugated addition to enones such as cyclohexanone (**1.42**) in the presence of 10 mol% of NHC catalyst, 1.1 equiv of B_2pin_2 at 22 °C in THF for 12 hours. Giving access to the corresponding β-borylated product **1.43** in high yields (Scheme 1.16). Kleeberg and co-workers isolated and studied the solid-state and solution behavior of the B-B-NHC adduct together with computationally thermodynamic data.[85]

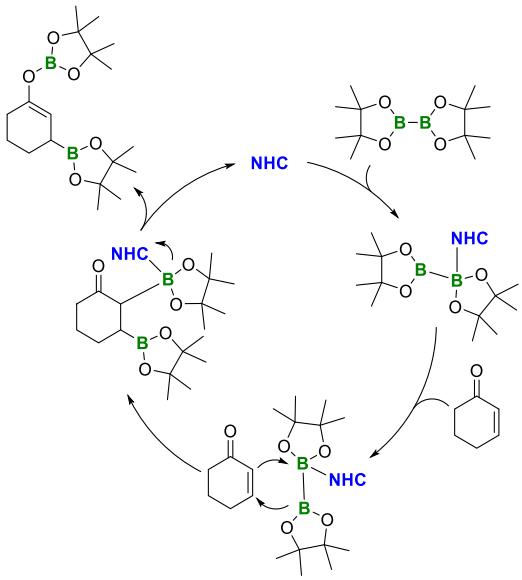

Figure 1.5. Proposed model for borylative conjugate addition to an enone catalyzed by NHC.

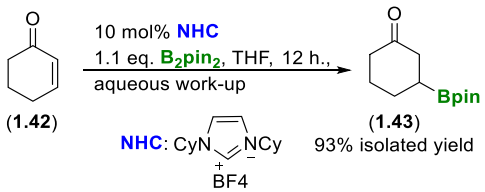

Scheme 1.16. Optimal reaction conditions for borylative conjugate addition through B-B-NHC adduct.

The new concept of metal-free catalysis opened a broad range of synthetic approaches such as the enantioselective version of the NHC-catalyzed boron conjugate addition process via transition-metal-free catalysis[86,87] or hydroboration of multiple bonds like alkynes, ketimines, aldimines and α,β-unsaturated molecules,[88] becoming a powerful tool in the field of organoboron synthesis.

An interesting observation by Hosomi and co-workers[62] was that PBu_3 could induce slight conversion of benzylideneacetophenone (**1.44**) into the β-borated ketone **1.45** in the absence of the catalyst precursor CuOTf (Scheme 1.17). This study served as a precedent to Fernández and co-workers in 2010 to develop a transition-metal-free asymmetric boron-addition reaction with achiral boron reagents.[89] They described a method for the synthesis of β-borated carbonyl compounds by reacting B_2pin_2 with either α,β-unsaturated esters or ketones in the presence of phosphine catalyst. The metal-free reaction only requires tertiary phosphorus compounds, MeOH, and a base as additives (Scheme 1.18a). The authors identified the appropriate conditions using chiral mono or di-phosphorous compound instead of achiral ones. Interestingly, (R)-(S)-Josiphos-type ligands provided much higher activities, but the asymmetric induction was susceptible to the structure of the substituents of the phosphorus donor atoms (Scheme 1.18b).[89]

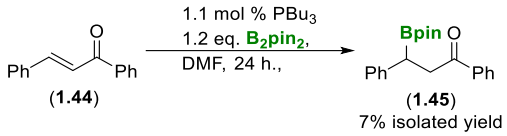

Scheme 1.17. Boration of benzylideneacetophenone promoted by PBu_3.

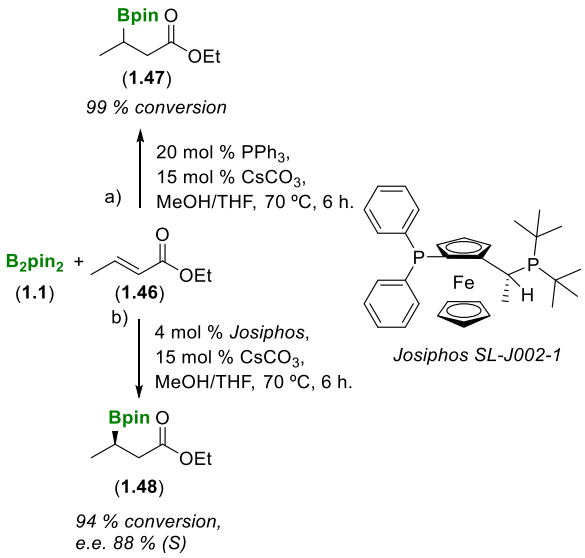

Scheme 1.18. Phosphine-mediated catalytic β-boration of ethyl crotonate with B_2pin_2.

Although the authors initially suggested that the phosphines might interact with the diboron reagent to activate the B-B bond and promote the asymmetric induction, a deeper study prompted them to postulate that the phosphine might play the role of pre-activation

of the substrates via phosphonium enolate intermediate.[90] To prove that they conducted stoichiometric experiments mixing PMe_3, *E*-hex-4-en-3-one (**1.49**) and B_2pin_2 in MeOH, observing the quantitative formation of the ion-pair ([α-H,β-PMe_3-3-hexanone]$^+$[MeO-pinB-Bpin]$^-$ which was full characterized experimentally and computationally as a global minimum in the potential energy surface.[90] It was postulated that the phosphine directly interacts with the most electrophilic carbon of the α,β-unsaturated carbonyl compound resulting in the formation of a strongly basic zwitterionic phosphonium enolate species (Scheme 1.19). This intermediate can be protonated by the excess of MeOH, a process that is particularly favoured by the presence of bis(pinacolato)diboron that stabilizes the MeO^- anion, thus forming the Lewis acid-base adduct [MeO-pinB-Bpin]$^-$ that acts as counteranion (Scheme 1.19). The ion-pair ([α-H,β-PR_3-3-hexanone]$^+$[MeO-pinB-Bpin]$^-$ might be responsible for the Bpin delivery, and in the presence of chiral phosphines, the nucleophilic Bpin transfer could be influenced by the chiral environment of the ion-pair.

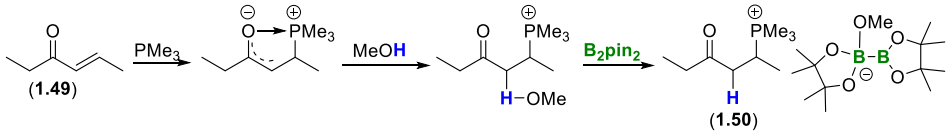

Scheme 1.19. Sequential illustration for the suggested role of phosphines in β-boration of activated alkenes.

In 2011, Fernández and co-workers developed the transition-metal-free borylation of non-activated unsaturated compounds using the anionic adduct [MeO-pinB-Bpin]$^-$.[91] Unlike conjugation addition of α,β-unsaturated esters, the phosphine additive was unnecessary for diboration catalysis. The catalytic system for the nucleophilic diboration of non-activated olefins or allenes combined base and methanol (Scheme 1.20).

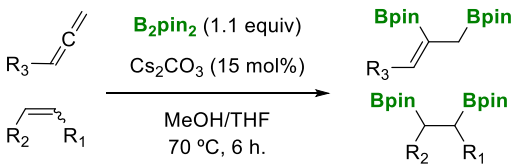

Scheme 1.20. Transition-metal-free diboration reaction of alkenes and allenes.

This reactivity has several significant aspects, such as product formation by a reaction between a nucleophilic substrate and a reagent that also has a pronounced nucleophilic character, that represented an almost unknown reactivity. And, unlike in the case of conjugate additions, both boryl units of the reagent are introduced to the substrate, resulting in an atom-economic addition reaction of great practical importance. It was an unprecedented discovery since up to date, the only known method to add

tetralkoxydiboron compounds to non-activated alkenes was the application of transition-metal complexes as catalysts.[53,92–105]

Different bases and diboron reagents have been explored in the β-boration of the α,β-unsaturated esters.[106] A combination of DFT studies, NMR spectroscopy and ESI-MS experiments were performed to understand the role of the base on the mechanism Quantitative conversion was observed for B_2pin_2 (**1.1**), bis(catecholate)diboron (**1.51**) and bis(hexyleneglycolato)diboron (**1.52**), but only moderate conversion was achieved with bis(neopentylglycolato)diboron (**1.53**) as shown in Scheme 1.21, even with Verkade organic base.

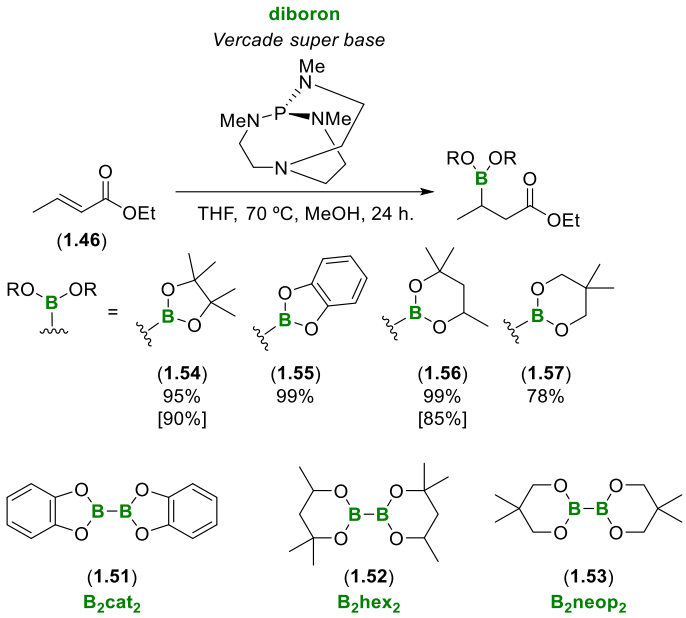

Scheme 1.21. Verkade base mediates β-boration of ethyl crotonate with different diboron reagents. Conversion is given by GC-MS analysis and isolated yield in brackets.

With this background, many studies were developed through transition-metal-free borylation of unsaturated systems, such as borylation of aryl halides,[107] diboration of propargylic alcohols,[108] borylative of sulphonamides,[109] ring-opening of vinyl epoxides and aziridines,[110] mixed diboration of alkenes with unsymmetrical diboron reagents[111], borylation of tertiary allylic alcohols,[112] etc.

In 2018, Fernández and Davenport reported an unprecedented 1,2,3-triboration of conjugated dienes via 1,4-hydroboration followed by an *in situ* diboration reaction of the internal double bond.[113] This reactivity was unpredicted since borylation of conjugated

dienes had been only reported via transition-metal catalysis.[18,114–116] Initial substrate evaluation was conducted with *E*-1-phenyl-1,3-butadiene (**1.58**), and they found that under optimal conditions (30 mol% of Na_2CO_3 and 3 equiv of B_2pin_2 in methanol at 90 °C overnight), the triborated product **1.60**, could be obtained, avoiding the 1,4-hydroborated byproduct **1.59** (Scheme 1.22). The study was extended to analyze the scope of *E*-1-phenyl 1,3-dienes, showing an efficient 1,2,3-triboration in almost all cases, even with sterically hindered 1,3-dienes.

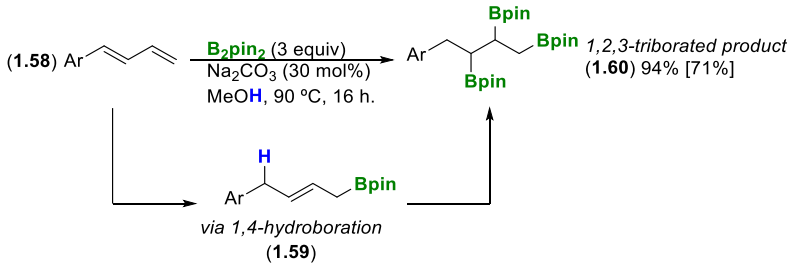

Scheme 1.22. Synthetic approach towards 1,2,3-triborated products via transition-metal-free borylation of 1,3-dienes. Yields were given by ^{1}H NMR spectra with naphthalene as internal standard and isolated yield in brackets.

When *E*-1-methyl-1,3-butadiene (**1.61**) reacted with lower equivalents of B_2pin_2, (1.1 instead of 3.0 equiv), the 1,2-diboration of the terminal alkene took place mainly, and instead diborated product **1.62** was obtained (Scheme 1.23a). However, an excess of B_2pin_2 (3 equiv) and base favoured the quantitative formation of 1,2,3,4-tetraborylated product **1.63** (Scheme 1.23b), suggesting that in higher quantities of B_2pin_2, the reaction proceeds through a double 1,2-diboration.

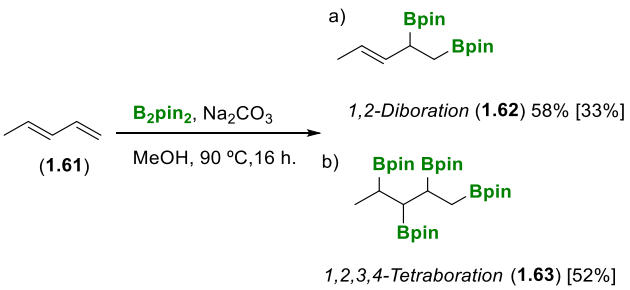

Scheme 1.23. Synthetic approach towards 1,2-diborated and 1,2,3,4-tetraborated products via metal-free catalysis for unactivated 1,3-dienes. Yields were given by ^{1}H NMR spectra with naphthalene as internal standard and isolated yield in brackets.

With this evidence, there was no doubt that transition-metal-free borylation of 1,3-dienes is a valuable tool. Thus, the next goal of this Thesis is the development of chemo- and

regioselectively 1,4-hydroboration of 1,3-dienes in a transition-metal-free context, and Chapter 3 discloses the corresponding study.

1.3 Computational insight into the nucleophilic character of trivalent boron compounds

Since the development of quantum mechanics methods, their applications to the understanding molecular structures and reaction mechanisms have evolved drastically. Therefore, this tool has become an essential part of the daily work of synthetic and catalytic studies. In boron chemistry, quantum mechanism-based DFT methods have been largely applied to understand the mechanism involved in the generation of C-B bonds.

As discussed above, diboron reagents in the presence of alkoxides can form a Lewis acid-base anionic adduct, [MeO-pinB-Bpin]$^-$. Computational studies on the electronic structure of this adduct showed that the methoxide induces polarization of the B-B bond towards the non-quaternized sp^2 boron, which can behave as nucleophilic synthon.[91] This concept was used by Fernández and Bo to explain the transition-metal-free diboration of unactivated alkenes, where the strongly polarized Highest Occupied Molecular Orbital (HOMO) formally corresponding to the B-B σ-bond overlaps with the Lowest Unoccupied Molecular Orbital (LUMO) of the C=C π-bond of the alkene (Figure 1.6).[91]

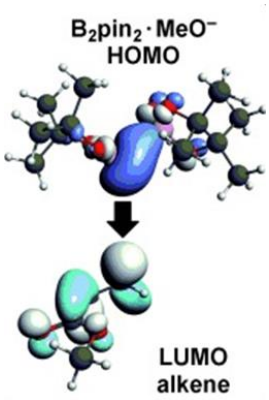

Figure 1.6. [MeO-pinB-Bpin]$^-$ HOMO is overlapping with the olefin LUMO to explain the olefin diboration reproduced from ref. 91.

According to DFT calculations carried out on B_2pin_2 and its Lewis acid-base adduct [MeO-pinB-Bpin]$^-$,[91] the B(sp^3) boron atom loses negative charge density upon the charge transfer from the alkoxide, while the B(sp^2) unambiguously gains electron density.[91] The loss of electron density on the B(sp^3) boron atom, despite the direct charge transfer from the Lewis

base, can be rationalized by considering that upon rehybridization, the boron atom loses the *p*-symmetric electron donation from the oxygen atoms of the pinacolate moiety. The net result of these structural changes is that adduct [MeO-pinB-Bpin]$^-$ becomes considerably polarized, and the B(sp^2) atom gains a strong nucleophilic character.[91] From this analysis, it was possible to propose a mechanism, as illustrated in Figure 1.7, for the diboration of alkenes with diboron reagents activated by a base that is consistent with the stereospecific *syn*-addition of diboron to internal and cyclic alkenes observed experimentally.[91] The mechanism can be divided into three main steps. Firstly, the B(sp^2) of the diboron Lewis acid-base adduct attacks the terminal carbon of the alkene double bond, increasing the negative charge supported by the other carbon atom of the double bond. Secondly, the first transition state connects with a second transition state through a bifurcation point, in which the developed negative charge at the internal alkene carbon attacks the B(sp^2) moiety, forming two C-B bonds. Finally, the methoxide is released, and the diborated product is formed.

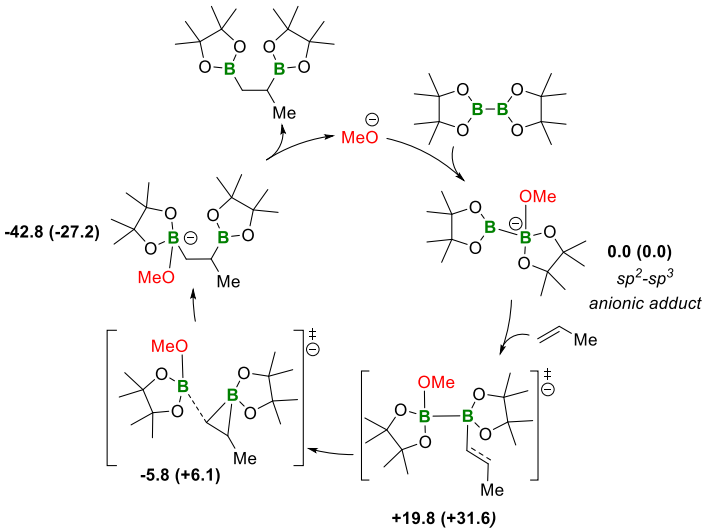

Figure 1.7. Suggested catalytic cycle for the diboration of unactivated alkenes by diboron reagents activated by Lewis bases. Electronic energy (kcal·mol^{-1}) and Gibbs free energy (kcal·mol^{-1}; in parentheses) relative to [MeO-pinB-Bpin]$^-$ adduct and propylene.

An alternative mechanism for the diboration of alkenes by [MeO-pinB-Bpin]$^-$ adduct have been proposed by Haeffner in 2018.[117] The author postulated that the adduct would interact with uncomplexed acidic B_2pin_2 diboron resulting in trimeric boron $(Bpin)_3^-$ species and a BpinOMe compound. Then, the $(Bpin)_3^-$ undergoes a *syn* addition to the alkene to yield an anionic diborated intermediate to finally interact with BpinOMe, which would regenerate the [MeO-pinB-Bpin]$^-$ adduct and release the *syn* diborated product (Figure 1.8).

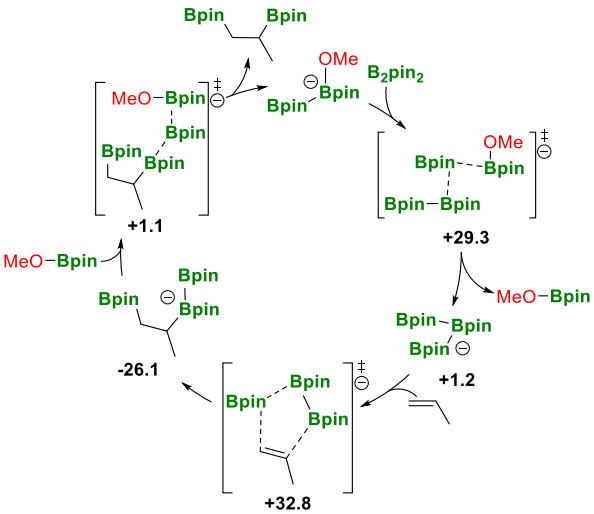

Figure 1.8. The mechanism proposed by Haeffner for the diboration of propene through trimeric boron $(Bpin)_3$.[117] Relative Gibbs free energies are in kcal·mol^{-1}.

Further studies on nucleophilic boryl species using computational descriptors have allowed to build a tendency map[118] and quantitative structure-activity relationships (QSAR)[119] classifying and evaluating the nucleophilic and electrophilic reactivity of a broad range of trivalent boron compounds. These works proved the nucleophilicity of the B(sp^2) fragment in the activated diboron, analyzing its transfer to a model substrate (formaldehyde)[119] as illustrated in Figure 1.9. The nucleophilic attack of B(sp^2) to the electrophilic carbon of the formaldehyde is preferred to the electrophilic attack to the oxygen of the formaldehyde by 2.7 kcal·mol^{-1}. Using this model substrate, it was also possible to establish a reactivity order for representative trivalent boron compounds (Figure 1.10). The [MeO-pinB-Bpin]$^-$ adduct shows a moderate nucleophilic character in comparison to strong nucleophiles such as boryl-lithium and boryl-copper complexes. On the other hand, species with other late transition metals such boryl-palladium or boryl-rhodium tend to act as electrophiles.[118]

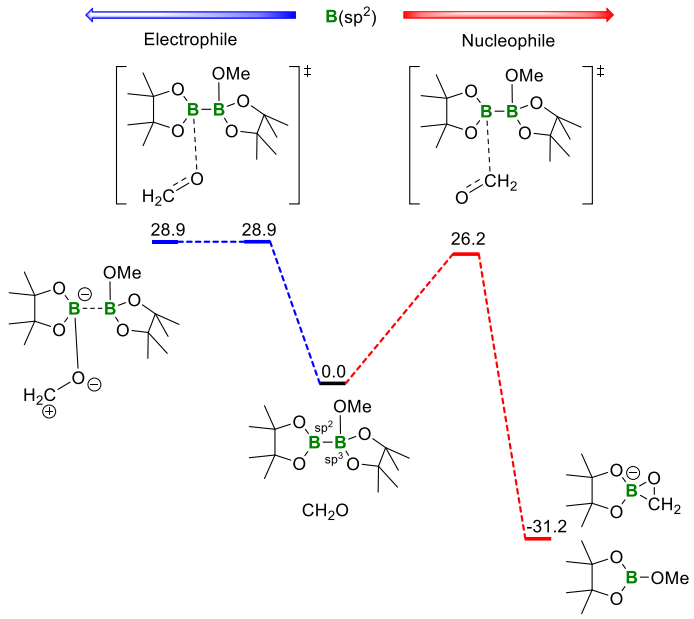

Figure 1.9. Computed free energy profiles (kcal·mol^{-1}) for the electrophilic and nucleophilic transfer from B(sp^2) [MeO-pinB-Bpin]$^-$ adduct to formaldehyde model substrate.

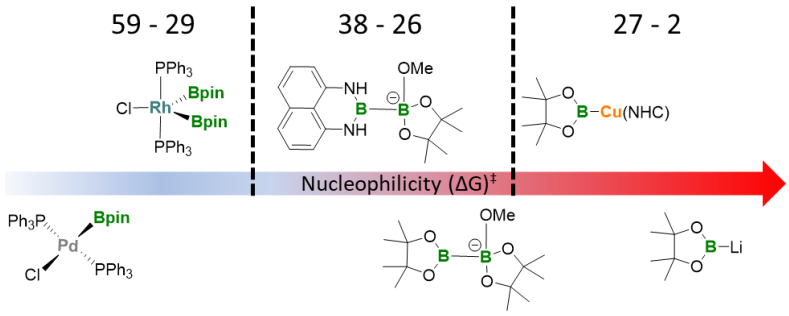

Figure 1.10. Reactivity order for representative trivalent boron compounds. Computed free energy barriers for the nucleophilic boryl transfer to formaldehyde in kcal·mol^{-1}.

Figure 1.11 shows the tendency map constructed from two electronic descriptors: the charge of the boryl fragment [BX_2] and the boron p/s ratio in the M-B σ-bond.[118] The map includes three types of boryl moiegies: 1) bonded to the main-group metals, 2) coordinated to transition metals and alkaly metals, and 3) bonded to an sp^3 boryl unit. For constructing the QSAR model,[119] both electronic descriptors were used along with a steric parameter, the *distance-weighted volume* (V_w).[120,121] The V_w was used to measure the effectiveness of the fragment bulkiness on the reactivity resulting in an inverse correlation trend with the nucleophilicity. Overall, the study resulted in a three-term easy-to-interpret QSAR model with statistical significance and predictive ability.

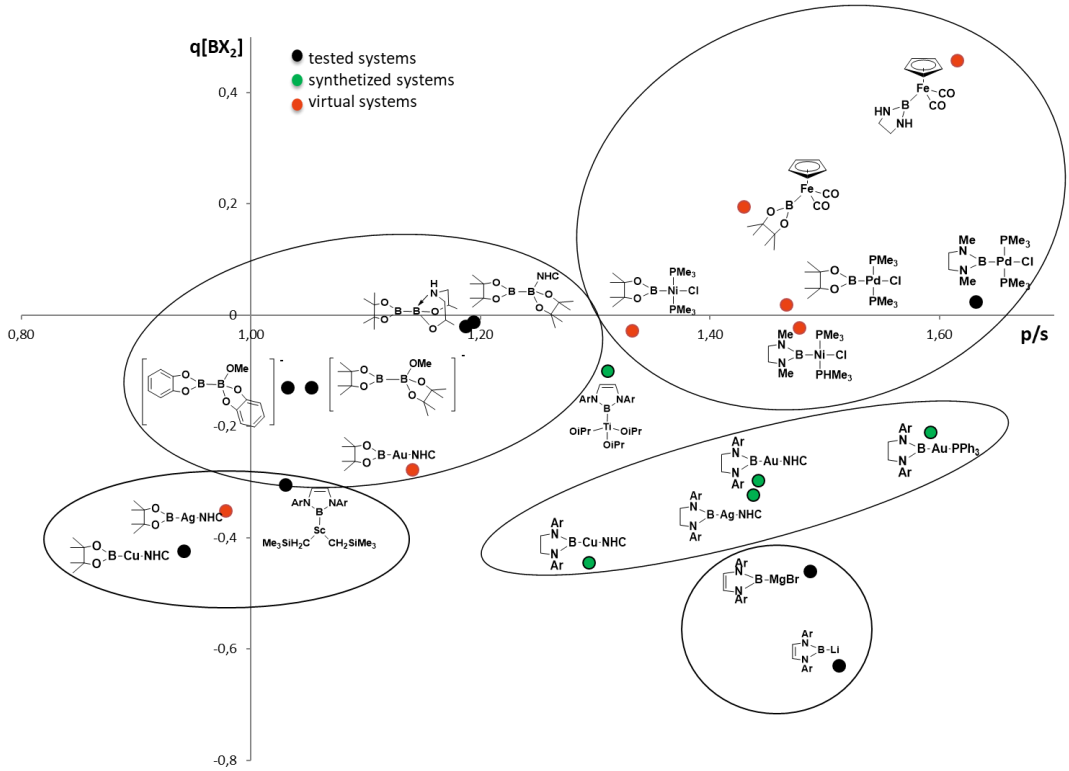

Figure 1.11. Correlation between the charge on the $[BX_2]$ fragment and the boron p/s-population ratio for synthesized and reactivity tested systems (black circles); synthesized systems (green circles); and for virtual systems (red circles).

1.4 α-Borylcarbanions as a promising set of homologating reagents

1.4.1 α-Boryl carbanions

The borata-alkene synthon $[R_2B{=}CH_2]^-$, represents the formal expression of stabilized α-boryl carbanions due to the valence deficiency of the adjacent three-coordinate boron centre (Scheme 1.24).[122]

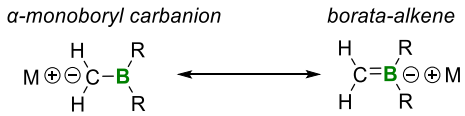

Scheme 1.24. Resonance structures for α-monoboryl carbanion and borata-alkene.

The C=B bond in borata-alkene species was initially depicted by H. C. Brown and G. Zweifel in 1961, considering the instability of 1,1-diborylalkanes towards hydrolytic cleavage, the authors assumed assuming that the corresponding α-boryl carbanion could be rewritten as borata-alkene intermediate (Scheme 1.25).[123,124]

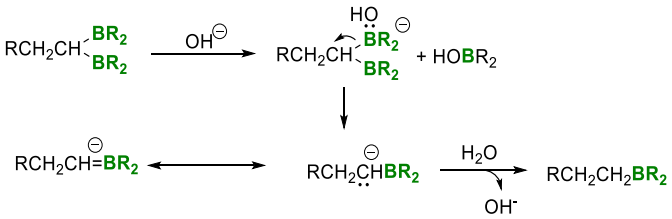

Scheme 1.25. H. C. Brown and G. Zweifel's proposal for stabilizing borata-alkene intermediate through the hydrolytic cleavage of *gem*-diboryl alkanes.

The generation of α-boryl carbanions species can be performed through complementary strategies that are described as follow.

Deborylation of *gem*-diboryl alkanes

Alkyl lithiated bases, such MeLi or BuLi, are used for deborylation of *gem*-diboryl alkanes. Zubiani and co-workers conducted this methodology in 1966 (Scheme 1.26),[125] and subsequent works by the same authors and other research groups confirmed the viability of this strategy to form the α-monoboryl carbanion within a wastage of one boron residue per carbanion formed.[126–131]

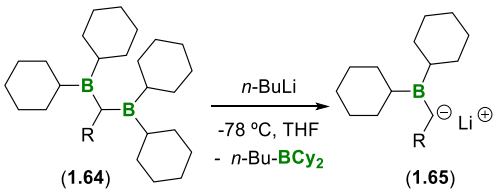

Scheme 1.26. Generation of α-monoboryl carbanions via deborylation of *gem*-diboryl alkanes.

On another hand, the deborylation of trialkoxyboronates gives the α-diboryl carbanions, developed by Matteson and co-workers in 1970.[132] The commercially available diborylmethane can also be activated via deborylation with specific bases to generate the α-monoboryl carbanion in the presence and absence of transition metal complexes. Shibata and co-workers were pioneers in developing the carbanion formation through the Pd(II) complex (Scheme 1.27a).[133] Alternatively, Morken and co-workers observed that diborylmethane can be deborylated by adding significant amounts of alkoxide (Scheme 1.27b).[134]

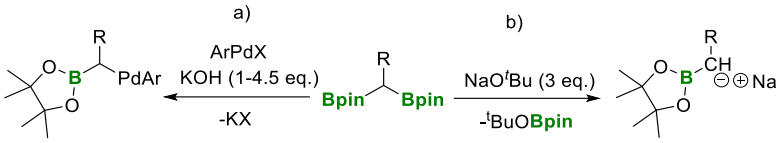

Scheme 1.27. α-Monoboryl carbanion formation via a) Pd(II) deborylation and b) alkoxide mediated deborylation.

Deprotonation of α-boryl alkanes

Alternatively, Rathke and Know reported the deprotonation of B-methyl-9-borabicyclo [3.3.1]nonane (*B*-methyl-9BBN-H, **1.66**) with lithium 2,2,6,6-tetramethylpiperidine (LiTMP, **1.67**) to form the corresponding α-monoboryl methide lithium salt **1.68** (Scheme 1.28).[135,136]

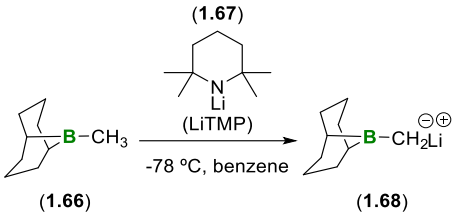

Scheme 1.28. Generation of α-monoboryl carbanions via deprotonation of borylalkanes.

Subsequent studies demonstrated that the proton abstraction from 1-phenyl-1,4-dihydro-bora benzene with ^{t}BuLi, in pentane-THF, produced a stabilized B-phenylborabencene anion (Scheme 1.29a).[137] Stabilized borata-alkene salts also can be formed from the generation of indenyl boranes through proton abstraction of the α-CH-B fragment, as developed by Erker and co-workers (Scheme 1.29b).[138] Another type of conjugative borata-alkene system is reported by Ramsey and Isabelle, which carried out experiments to abstract the aromatic proton from the mesytil group using BuLi at room temperature (Scheme 1.29c).[139] Deprotonation of *gem*-diboryl and triboryl alkanes have broadly been studied, following the pioneering work by Matteson and co-workers.[140,141]

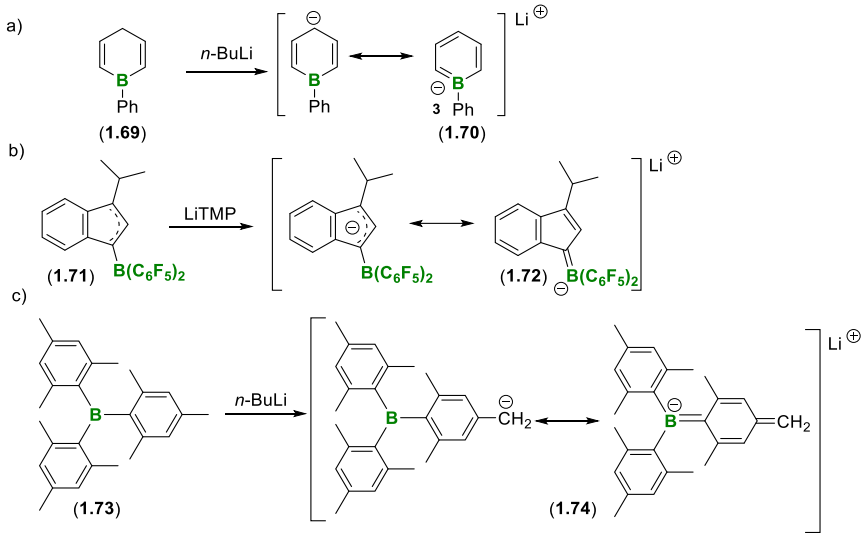

Scheme 1.29. Deprotonation strategies towards a) generation of B-phenylborabencene anion, b) synthesis of conjugated stabilized borata-alkene compound, c) formation of the anion $[CH_2C_6H_2(3,5\text{-}Me_2)(4\text{-}B\{2,4,6\text{-}Me_3C_6H_2\}_2)]^-$

The use of large aromatic groups on boron such as Mes_2B (Mes = mesityl, 2,4,6-$Me_3C_6H_2$) to inhibit the corresponding boron-"ate" complex formation when reacting with Cy_2NLi or MeLi bases was reported by Pelter and co-workers (Scheme 1.30).[142–145] The formation of the borata-alkene species was suggested by the lack of rotation effects around the B-C, giving an ΔG = 92 KJ·mol^{-1}.

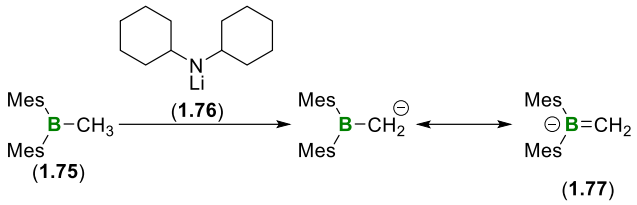

Scheme 1.30. Dimesitylboranes enable the formation of useful α-boryl carbanions through deprotonation reactions.

Cu/Zn transmetalation from α-halo boronic esters

Boron-stabilized carbanions were prepared by reaction of α-halo boronic esters with Zn and Cu to generate the α-(dialkoxyboryl)alkyl zinc/copper compounds, making this methodology a good option for the preparation of highly substituted alkyl groups (Scheme 1.31).[146]

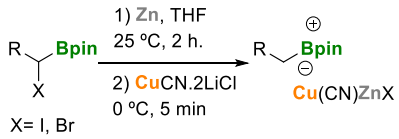

Scheme 1.31. α-Halo boronic esters as precursors of α-monoboryl carbanions stabilized by Zn and Cu.

Nucleophilic addition of electron-deficient α-boryl alkenes

Electron deficient α-monoboryl alkenes are susceptible to nucleophilic addition, with the concomitant α-monoboryl carbanion formation.[147] Scheme 1.32 shows the intramolecular version via a metal-halogen exchange that initiates the nucleophilic addition reaction conducted at -100 °C, towards the formation of compound **1.79**.

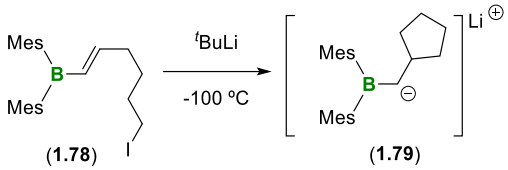

Scheme 1.32. Intramolecular nucleophilic addition to vinyldimesitylborane.

Transmetallation of α-boryl methide species

Through transmetallation with lithium bases, boron-stabilized carbanions may also be produced by selective cleavage of α-monoboryl methide metal salts.[148,149] Scheme 1.33a illustrates the transmetallation of borylstannylalkanes with lithium thiophenoxide (PhSLi) or MeLi, leading to the cleavage of the stannyl moiety. Interestingly, the reaction of LiF with dimesitylboryl(trimethylsilyl)alkanes also gives access to α-boryl carbanions via $FSiMe_3$ elimination (Scheme 1.33b).

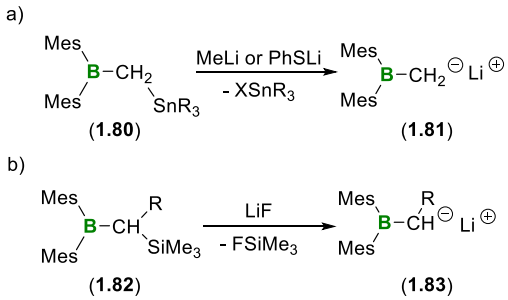

Scheme 1.33. Transmetallation of a) borylstannylalkanes with lithium PhSLi or MesLi, b) borylsilylalkanes with LiF.

Partial reduction of diverse functional C-C, C-B or B-B bond

Berndt and co-workers developed direct access to 1,3-diborataallene **1.86**[150,151] from compounds containing a partial boron-carbon triple bond, such as borataalkyne ion **1.85**,[152] which was prepared from 1,1-bis(boryl)ethene (**1.84**) with an excess of lithium in diethyl ether (Scheme 1.34).

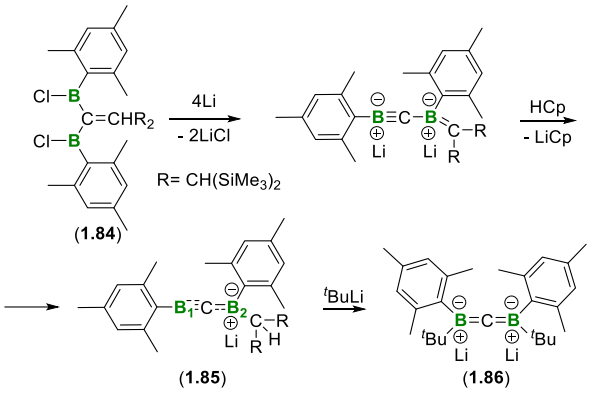

Scheme 1.34. Synthesis of 1,3-borataallene type compound.

Braunschweig and co-workers demonstrated that CO could be efficiently added to a boron–boron triple bond, diboryne **1.87** at room temperature and atmospheric pressure, resulting in a compound where four equivalents of CO are incorporated, identified as a flat-bicyclic, bis(boralactone) **1.88** where the boron atoms are in an environment of borata-alkenes motifs (Scheme 1.35).[153]

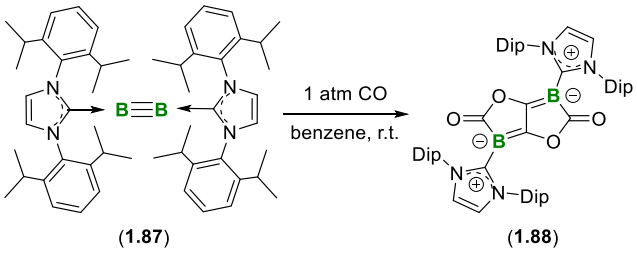

Scheme 1.35. Synthesis of bis(boralactone) from carbonyl addition to diboryne.

More recently, Nogi and Yorimitsu have developed the diborative reduction of alkynes towards 1,4-diboratabutadiene dianions **1.90**, employing B_2pin_2 and alkali metals (Scheme 1.36).[154] A possible reaction mechanism has been suggested by the authors considering that the electron reduction of the alkyne would generate a radical anion that further reacts with B_2pin_2 to form borate intermediates.

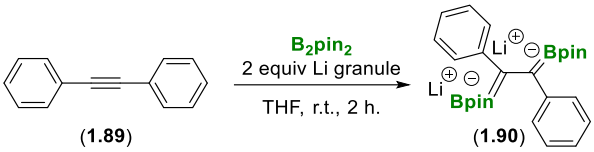

Scheme 1.36. Diborative reduction of alkynes towards 1,4-diboratabutadiene dianions.

Gabbaï and co-workers explored reducing α-boryl carbocation **1.91** with K to produce the corresponding α-boryl carbanion **1.92** (Scheme 1.37).[155] This protocol results in a sequential population of the boron-carbon bond that is confirmed by an apparent shortening of the B-C bond, as well as an increase in the order of the B-C bond upon reductions, as it is shown in computational studies.

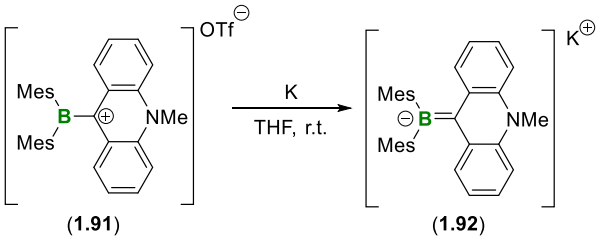

Scheme 1.37. Synthesis of borata-alkene via reduction of α-boryl carbocations with K.

Borylation of Frustrated Lewis pair

Erker and co-workers have developed an intramolecular reaction pathway of suitable frustrated Lewis pairs (FLPs), efficiently yielding the respective B=C systems.[156,157] This protocol is based on the intramolecular addition of the phosphane nucleophile to the adjacent dienyl borane moiety allowing the borata–diene system, which is neutral to the outside because they bear their (phosphonium) countercation inside the new structure **1.95** (Scheme 1.38a). Erker group also demonstrated that specific frustrated P/B Lewis pairs (FLPs) could deliver internal proton transfer from the α-CH-boryl substituent to the phosphane Lewis base (Scheme 1.38b).[158] The attachment of strongly electron-withdrawing C_6F_5 substituents at boron greatly enhances the CH acidity in the α-position.

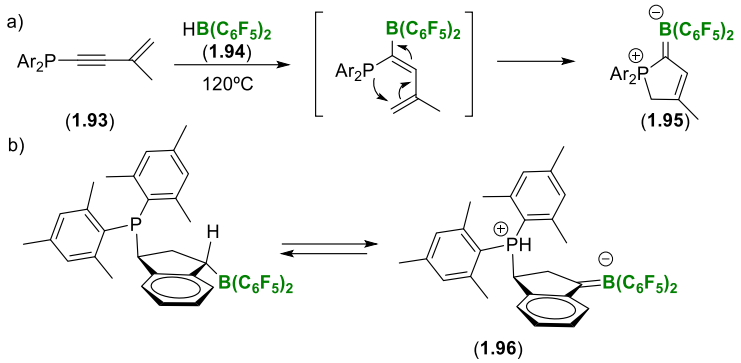

Scheme 1.38. Formation of stable zwitterionic borata–alkenes by frustrated Lewis pair pathway.

Erker and co-workers also conducted a synthetic approach towards frustrated N/B Lewis pairs in which a pronounced π-conjugative interaction could be structurally established across the π-system of the organic linker (Scheme 1.39)[159,160] Following a synthetic protocol through a $B(C_6F_5)_2$ induced rearrangement of a bulky propargyl amine, the iminium/borata-alkene **1.99** can be formed, showing a *trans*-arrangement between the two antagonistic π-components.

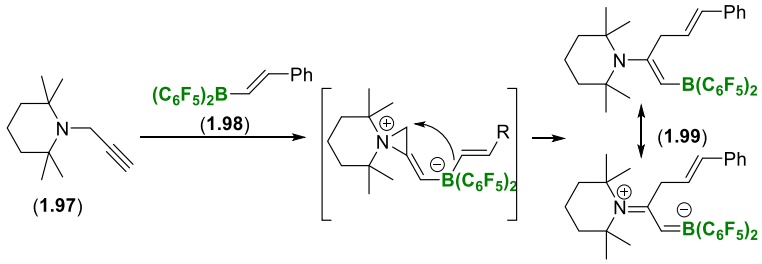

Scheme 1.39. Formation of π-conjugated frustrated N/B pairs by borane induced propargyl amine rearrangement.

Isomerization of anionic boron peri-bridged naphthalene derivative

Dimesityl-1,8-naphthalenediylborate **1.100** undergoes the heterolytic cleavage of one of the boron peri-carbon bonds followed by nucleophilic attack at the ortho-carbon of one of the mesityl groups to afford the conjugated hexa-1-boratatriene system **1.101** (Scheme 1.40).[161] The reaction was performed at room temperature in toluene for an extended period of time.

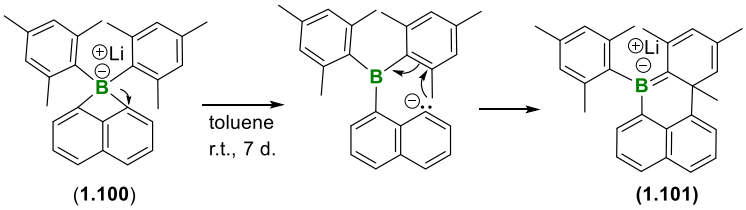

Scheme 1.40. Isomerization of dimesityl-1,8-naphthalenediylborate towards cyclic borata-alkene.

Borylation of phosphorous substituted nucleophilic carbon

Boese, Bertrand and co-workers reported that bis(diisopropylamino)phosphanyl trimethylsilyl carbene **1.102** react through formal 1,2-additions with dimesitylfluoroborane to obtain a valuable C-borylated phosphorus ylide **1.103** that can also be considered as C-phosphonio-substituted borata-alkene **1.104** (Scheme 1.41).[162] The reaction resembles the well-known haloboration of alkynes, although mechanistic studies suggest a carbene-type attack to dimesitylfluoroborane.

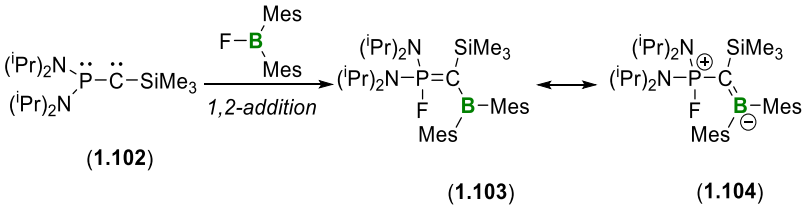

Scheme 1.41. Synthesis of C-phosphonio-substituted borata-alkenes.

The reactivity of geminal dianions toward $BH_3{\cdot}SMe_2$ has also been established as an alternative methodology to prepare borata-alkene species. Scheme 1.42 illustrates the direct nucleophilic attack of the phosphorus-stabilized dianion **1.105** to BH_3, with the subsequent formation of the zwitterionic species **1.106**, described recently by Mézailles and co-workers.[163]

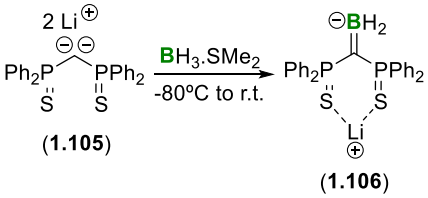

Scheme 1.42. Formation of zwitterionic species by nucleophilic attack of phosphorus-stabilized dianions to BH_3.

1.4.2 Reactivity of borata-alkene compounds

Boron-Wittig reaction

α-Boryl carbanions are convenient synthons towards homologation reactions through electrophilic trapping strategies.[164,165] The homologation protocols via single carbon chain extension involve a facile introduction of the C–B bonds, which can be transformed into functionalized target products containing C-O, C-N or C-C bonds, principally. One of the most extended applications of α-monoboryl carbanions/borata-alkene synthons is the boron-Wittig reaction,[166] and the first example of this condensation of *gem*-bis(boryl)alkanes with aldehydes and ketones to yield olefins was observed by Zubiani and co-workers in 1966.[125] These authors observed that benzaldehyde and a series of aliphatic, aromatic and alicyclic ketones could efficiently be converted to the corresponding olefin by reaction with the α-(boryl)carbanion lithium salt, through nucleophilic attack followed by B-O elimination (Scheme 1.43). In this approach, both boryl moieties were eliminated from the starting compound, via deborylation with n-BuLi and subsequent B-O elimination.

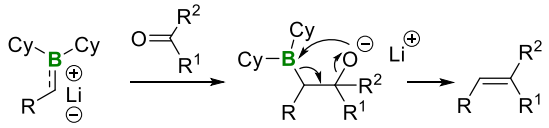

Scheme 1.43. First observed condensation of α-monoboryl carbanions / borata-alkene synthons with aldehydes and ketones.

Matteson and co-workers expanded the general access to α-mono- and α-polyboryl carbanions and proved their reactivity through similar condensation sequences.[167,168] Pelter and co-workers[169–172] were pioneers to use the α-boryl carbanion systems stabilized by an adjacent dimesityl boron group, in the nucleophilic addition to aldehydes and ketones to prepare the corresponding 1,2-disubstituted alkenes (Scheme 1.44a). The reaction of benzaldehyde (**1.14**) with octyldimesitylborane (**1.107**) gives the product *E*-1-phenylnon-1-ene (**1.109**) as the major isomer indicating that the boron-Wittig protocol was essentially stereospecific.[169–172] The same authors found that the condensations of dimesitylboryl stabilized carbanion **1.107** with aliphatic aldehydes (**1.108**), in the presence of N-chlorosuccinimide (NCS), accomplished a condensation-redox reaction towards ketone **1.110** production (Scheme 1.44b).[173] Similarly, Pelter and co-workers developed the boron-Wittig reaction between boron-stabilized alkenyl carbanions with aldehydes to give allenes in the presence of trifluoroacetic anhydride (TFAA), illustrated in Scheme 1.45.[174]

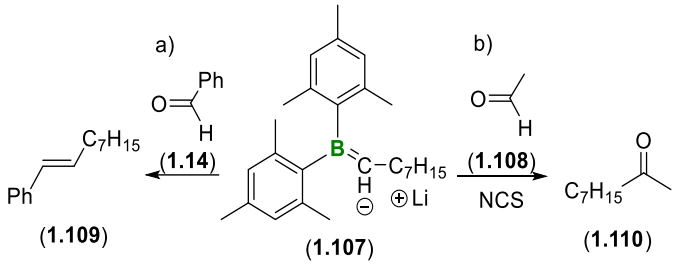

Scheme 1.44. Boron-Wittig with α-dimesitylboryl carbanion systems.

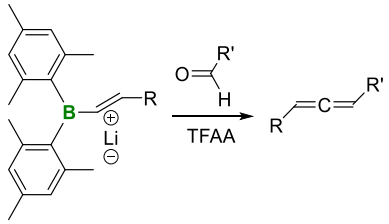

Scheme 1.45. Boron-Wittig with boron-stabilized alkenyl carbanions with aldehydes to give allenes.

Okazaki and co-workers isolated and characterized, by X-ray diffraction, the structure of the first example of a tetracoordinated 1,2-oxaboretanide **1.111**, which is considered an intermediate of the boron-Wittig reaction under basic conditions. Further thermolysis of **1.111** eventually gave the olefin **1.112** (Scheme 1.46).[175]

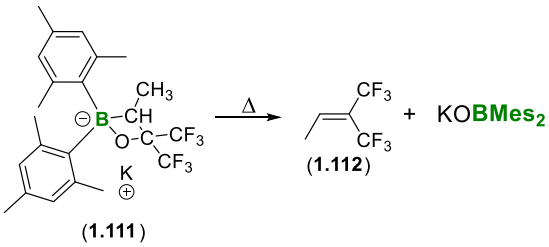

Scheme 1.46. Isolation of tetracoordinate 1,2-oxaboretanide as an Intermediate of the boron—Wittig reaction under basic conditions.

Erker and co-workers also found a different reaction mode of the stabilized indenyl based borata-alkene **1.72**, which can undergo different cycloaddition reactions with carbonyl compounds.[138] The reaction of **1.72** with a chalcone in toluene gives the formal [4+2] cycloaddition product **1.115** that was isolated and characterized by X-ray diffraction (Scheme 1.47a).[138] The X-ray crystal structure analysis of **1.115** shows that the nucleophilic borata-alkene ring carbon atom was added to the chalcone Michael position, and the boron atom of the borata-alkene trapped the chalcone oxygen atom. Alternative stepwise

cycloaddition pathway of the borata-alkene **1.72** with phenylmethylketene seems to be supported by forming the formal [6+2] cycloaddition product **1.116** (Scheme 1.47b).[138] The X-ray crystal structure analysis of compound **1.116** shows that the ketene sp-carbon atom is attached to the central carbon atom of the indene five-membered ring, and the ketene oxygen is bonded to boron.

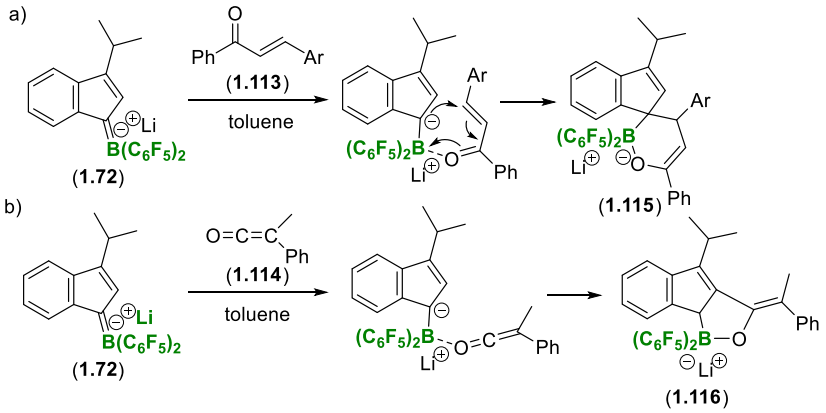

Scheme 1.47. Cycloaddition reactions of borata-alkene **67** with a) α,β-unsaturated ketones, b) ketenes.

Nucleophilic substitution through deprotonate borylalkanes and metal deborylate *gem*-borylalkanes

Nucleophilic substitution reactions have been generally established in the reactivity of α-boryl carbanions. Pioneer work by Pelter and co-workers showed that the alkylation of $MesB{=}CH_2^-$ in an efficient and general process led to a broader range of alkyldimesitylboranes (Scheme 1.48a).[143] Similarly, the same authors also reported the nucleophilic substitution of boron stabilized allylic anion with alkyl halides to react regioselectivity through the γ-position (Scheme 1.48b).[144]

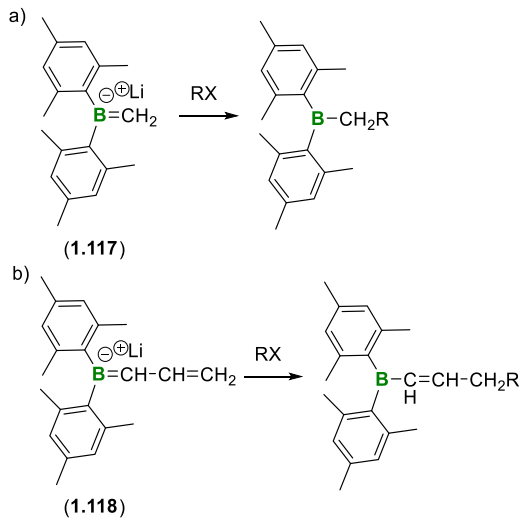

Scheme 1.48. Alkylation of borata-alkenes with alkyl halides.

Within the last decade, there has been significant development on the alkylation of α-pinacolboryl carbanions, varying the nature of the counterion. Endo and Shibata's group reported in 2010 the use of 1,1-diborylalkanes in palladium-catalyzed cross-coupling at room temperature.[133,176–178] The authors suggested that transmetalation between RPdX and the stabilized α-boryl carbanion generates a σ-borylmethylPdR intermediate, which undergoes reductive elimination to produce the coupled product (Figure 1.12). The use of chiral ligands in the Pd complex allowed to induce asymmetry in the reactions sequence.[179,180]

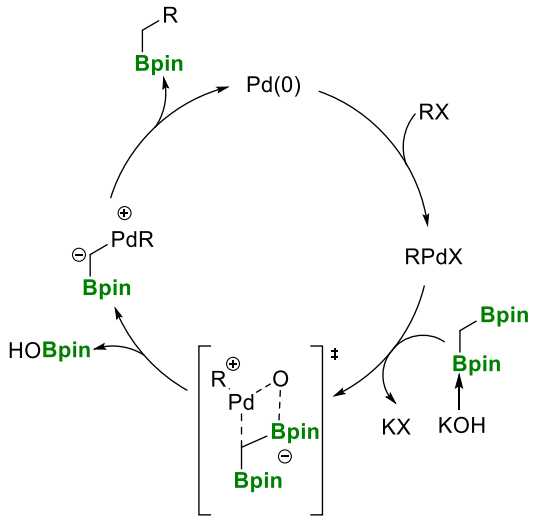

Figure 1.12. Pd catalyzed cross-coupling of *gem*-diboryl alkanes with RX.

Fu, Marder and co-workers have explored the copper-catalyzed alkylation reaction throughout the reaction of a variety of alkyl bromides with diborylmethane in the presence of 10–20 mol% CuI as the catalyst.[181–184] A S_N2 mechanism has been suggested as the most plausible for the alkylation of copper stabilized α-pinacolboryl carbanions. The copper complex can be modified with diverse ligands, even chiral ones, to perform the corresponding asymmetric alkylation.[181,183–187] The addition of LiO^{t}Bu favours the reaction outcome, probably by activating the diborylmethane reagent and stabilizing the borata-alkene intermediate. From a mechanistic point of view, it has been suggested that copper alkoxide complex [Cu(IMes)O^{t}Bu] can be generated from [Cu(IMes)Cl] in the presence of LiO^{t}Bu. The copper(I) complex undergoes transmetalation with the activated diborylmethane to afford the complex **I2** with the α-borylmethyl ligand that in the case of allylic substrates, promotes the subsequent S_N2' substitution reaction (Figure 1.13).

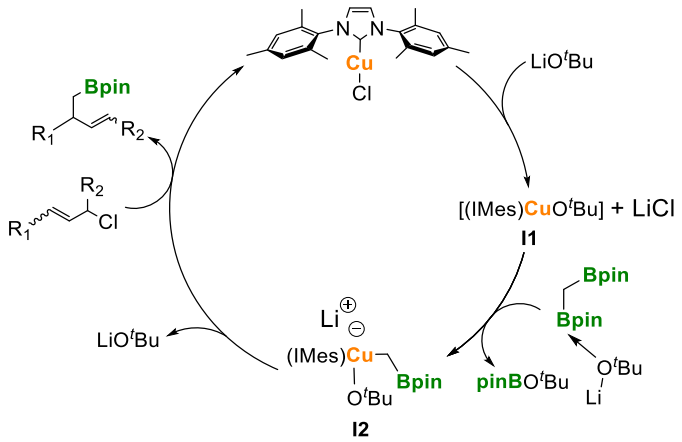

Figure 1.13. Proposed catalytic cycle for copper alkylation or arylation of α-boryl carbanions.

The nucleophilic borylmethylation reaction through copper(I)-catalyzed S_N2' allylic alkylation of vinyl cyclic compounds has been successfully developed, and representative examples are shown in Scheme 1.49. Vinyl epoxides **1.120** act as allylic electrophiles in the copper-catalyzed addition of CH_2Bpin moiety on the terminal position of the vinyl epoxide to generate S_N2'-selective products with the concomitant ring-opening (Scheme 1.49a).[182] Vinyl cyclic carbonates **1.121** also followed a nucleophilic attack of the α-pinacolboryl methyl group to the terminal double bond with concomitant carbonate ring-opening reaction under favoured stereocontrol on the *E*-isomer formation (Scheme 1.49b).[188]

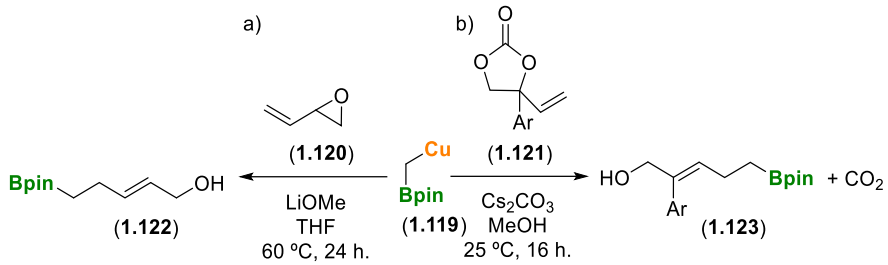

Scheme 1.49. Nucleophilic borylmethylation of a) vinyl epoxides and b) vinyl carbonates.

Nucleophilic substitution through boryl-Cu/Zn complex

Early experiments by Knochel demonstrated that α–boryl carbanion from (Bpin)CH_2Cu(CN)ZnI shows excellent reactivity toward electrophiles such as allyl halides and acyl halides.[146] Scheme 1.50 illustrates the reactivity of tert-butyl α-(bromomethyl)-acrylate (**1.125**) with (Bpin)CH_2Cu(CN)ZnI (**1.124**), at low temperatures, remarking the chemoselectivity of the process since the α,β-unsaturated ester group remains inert, whereas the alkyl bromide substitution takes place efficiently.

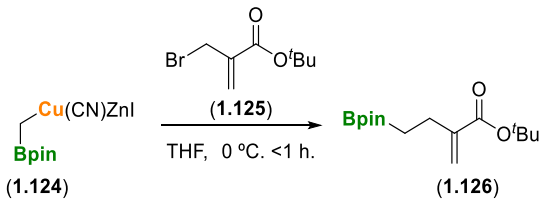

Scheme 1.50. Alkylation of borylmethide through (Bpin)CH_2Cu(CN)ZnI species.

With the aim to contribute to generate relevant knowledge towards the reactivity of α-boryl carbanions, we have developed and compiled in Chapter 4 a map of trends based on computational studies, using chemically meaningful descriptors to understand the key points about the nucleophilic character of α-boryl carbanions.

1.5 Objectives

This doctoral Thesis aims to develop the synthesis of organoboron compounds via transition-metal and transition-metal-free borylation of a specific type of π-systems, as well as their mechanistic rationalization by computational methods. In addition, this doctoral Thesis also focuses explicitly on studying the reactivity of α-borylcarbanions from a theoretical point of view. The specific objectives of the different chapters are described below:

Chapter 2 aims to study the copper-catalyzed borylation of alkenyl-aldehydes with bis(pinacolato)diboron. The borylated organocupprated intermediate suffers an intramolecular cyclization that evolves towards cyclobutanols with remarkable stereoselectivity. In addition, a theoretical study intends to rationalize the experimental results, determining the key intermediates and transition states to understand the chemo- and diastereoselectivity observed.

Chapter 3 is focused on the experimental study about transition-metal-free borylation of conjugated dienes through $[MeO\text{-}pinB\text{-}Bpin]^-$ adduct and the mechanistic rationalization of the stereo- and regioselectivity observed by means of DFT calculations.

Chapter 4 compiles the study of the reactivity of α-borylcarbanions from a theoretical point of view. It pursues the determination of the appropriate descriptors to develop a map of trends to classify and predict the nucleophilicity of a large set of α-borylcarbanions, tunning diverse structural and electronic features.

1.6 References

(1) Yang, W.; Gao, X.; Wang, B. Boronic Acid Compounds as Potential Pharmaceutical Agents. *Med. Res. Rev.* **2003**, *23* (3), 346–368.

(2) Neeve, E. C.; Geier, S. J.; Mkhalid, I. A. I.; Westcott, S. A.; Marder, T. B. Diboron(4) Compounds: From Structural Curiosity to Synthetic Workhorse. *Chem. Rev.* **2016**, *116* (16), 9091–9161.

(3) Shinokubo, H. Transition Metal Catalyzed Borylation of Functional π-Systems. *Proc. Japan Acad. Ser. B* **2014**, *90* (1), 1–11.

(4) Mun, B.; Kim, S.; Yoon, H.; Kim, K. H.; Lee, Y. Total Synthesis of Isohericerin, Isohericenone, and Erinacerin A: Development of a Copper-Catalyzed Methylboronation of Terminal Alkynes. *J. Org. Chem.* **2017**, *82* (12), 6349–6357.

(5) Meng, F.; McGrath, K. P.; Hoveyda, A. H. Multifunctional Organoboron Compounds for Scalable Natural Product Synthesis. *Nature* **2014**, *513* (7518), 367–374.

(6) Jia, T.; Cao, P.; Wang, B.; Lou, Y.; Yin, X.; Wang, M.; Liao, J. A Cu/Pd Cooperative Catalysis for Enantioselective Allylboration of Alkenes. *J. Am. Chem. Soc.* **2015**, *137* (43), 13760–13763.

(7) Chen, B.; Cao, P.; Liao, Y.; Wang, M.; Liao, J. Enantioselective Copper-Catalyzed Methylboration of Alkenes. *Org. Lett.* **2018**, *20* (5), 1346–1349.

(8) Hancock, E. N.; Kuker, E. L.; Tantillo, D. J.; Brown, M. K. Lessons in Strain and Stability: Enantioselective Synthesis of (+)-[5]-Ladderanoic Acid. *Angew. Chem. Int. Ed.* **2020**, *59* (1), 436–441.

(9) Dherbassy, Q.; Manna, S.; Shi, C.; Prasitwatcharakorn, W.; Crisenza, G. E. M.; Perry, G. J. P.; Procter, D. J. Enantioselective Copper-Catalyzed Borylative Cyclization for the Synthesis of Quinazolinones. *Angew. Chem. Int. Ed.* **2021**, *60* (26), 14355–14359.

(10) Dang, L.; Zhao, H.; Lin, Z.; Marder, T. B. DFT Studies of Alkene Insertions into Cu−B Bonds in Copper(I) Boryl Complexes. *Organometallics* **2007**, *26* (11), 2824–2832.

(11) Takahashi, K.; Ishiyama, T.; Miyaura, N. Addition and Coupling Reactions of Bis(Pinacolato)Diboron Mediated by CuCl in the Presence of Potassium Acetate. *Chem. Lett.* **2000**, *29* (9), 982–983.

(12) Takahashi, K.; Ishiyama, T.; Miyaura, N. A Borylcopper Species Generated from Bis(Pinacolato)Diboron and Its Additions to α,β-Unsaturated Carbonyl Compounds and Terminal Alkynes. *J. Organomet. Chem.* **2001**, *625* (1), 47–53.

(13) Lillo, V.; Fructos, M. R.; Ramírez, J.; Braga, A. A. C.; Maseras, F.; Díaz-Requejo, M. M.; Pérez, P. J.; Fernández, E. A Valuable, Inexpensive CuI/N-Heterocyclic Carbene Catalyst for the Selective Diboration of Styrene. *Chem. – Eur. J.* **2007**, *13* (9), 2614–2621.

(14) Whyte, A.; Torelli, A.; Mirabi, B.; Zhang, A.; Lautens, M. Copper-Catalyzed Borylative Difunctionalization of π-Systems. *ACS Catal.* **2020**, *10* (19), 11578–11622.

(15) Liu, Z.; Gao, Y.; Zeng, T.; Engle, K. M. Transition-Metal-Catalyzed 1,2-Carboboration of Alkenes: Strategies, Mechanisms, and Stereocontrol. *Isr. J. Chem.* **2020**, *60* (3–4), 219–229.

(16) Laitar, D. S.; Müller, P.; Sadighi, J. P. Efficient Homogeneous Catalysis in the Reduction of CO_2 to CO. *J. Am. Chem. Soc.* **2005**, *127* (49), 17196–17197.

(17) Laitar, D. S.; Tsui, E. Y.; Sadighi, J. P. Copper(I) β-Boroalkyls from Alkene Insertion: Isolation and Rearrangement. *Organometallics* **2006**, *25* (10), 2405–2408.

(18) Semba, K.; Shinomiya, M.; Fujihara, T.; Terao, J.; Tsuji, Y. Highly Selective Copper-Catalyzed Hydroboration of Allenes and 1,3-Dienes. *Chem. – Eur. J.* **2013**, *19* (22), 7125–7132.

(19) Dang, L.; Lin, Z.; Marder, T. B. DFT Studies on the Borylation of α,β-Unsaturated Carbonyl Compounds Catalyzed by Phosphine Copper(I) Boryl Complexes and Observations on the Interconversions between O- and C-Bound Enolates of Cu, B, and Si. *Organometallics* **2008**, *27* (17), 4443–4454.

(20) Borner, C.; Anders, L.; Brandhorst, K.; Kleeberg, C. Elusive Phosphine Copper(I) Boryl Complexes: Synthesis, Structures, and Reactivity. *Organometallics* **2017**, *36* (24), 4687–4690.

(21) Yoshida, H.; Kageyuki, I.; Takaki, K. Copper-Catalyzed Three-Component Carboboration of Alkynes and Alkenes. *Org. Lett.* **2013**, *15* (4), 952–955.

(22) Kageyuki, I.; Yoshida, H.; Takaki, K. Three-Component Carboboration of Alkenes under Copper Catalysis. *Synthesis* **2014**, *46* (14), 1924–1932.

(23) Ito, H.; Kosaka, Y.; Nonoyama, K.; Sasaki, Y.; Sawamura, M. Synthesis of Optically Active Boron–Silicon Bifunctional Cyclopropane Derivatives through Enantioselective Copper(I)-Catalyzed Reaction of Allylic Carbonates with a Diboron Derivative. *Angew. Chem. Int. Ed.* **2008**, *47* (39), 7424–7427.

(24) Zhong, C.; Kunii, S.; Kosaka, Y.; Sawamura, M.; Ito, H. Enantioselective Synthesis of *Trans*-Aryl- and -Heteroaryl-Substituted Cyclopropylboronates by Copper(I)-Catalyzed Reactions of Allylic Phosphates with a Diboron Derivative. *J. Am. Chem. Soc.* **2010**, *132* (33), 11440–11442.

(25) Ito, H.; Toyoda, T.; Sawamura, M. Stereospecific Synthesis of Cyclobutylboronates through Copper(I)-Catalyzed Reaction of Homoallylic Sulfonates and a Diboron Derivative. *J. Am. Chem. Soc.* **2010**, *132* (17), 5990–5992.

(26) Yang, C.-T.; Zhang, Z.-Q.; Tajuddin, H.; Wu, C.-C.; Liang, J.; Liu, J.-H.; Fu, Y.; Czyzewska, M.; Steel, P. G.; Marder, T. B.; Liu, L. Alkylboronic Esters from Copper-Catalyzed Borylation of Primary and Secondary Alkyl Halides and Pseudohalides. *Angew. Chem. Int. Ed.* **2012**, *51* (2), 528–532.

(27) Kubota, K.; Yamamoto, E.; Ito, H. Copper(I)-Catalyzed Borylative *Exo*-Cyclization of Alkenyl Halides Containing Unactivated Double Bond. *J. Am. Chem. Soc.* **2013**, *135* (7), 2635–2640.

(28) Royes, J.; Ni, S.; Farré, A.; La Cascia, E.; Carbó, J. J.; Cuenca, A. B.; Maseras, F.; Fernández, E. Copper-Catalyzed Borylative Ring Closing C–C Coupling toward Spiro- and Dispiroheterocycles. *ACS Catal.* **2018**, *8* (4), 2833–2838.

(29) Zuo, Y.-J.; Chang, X.-T.; Hao, Z.-M.; Zhong, C.-M. Copper-Catalyzed, Stereoconvergent, *Cis*-Diastereoselective Borylative Cyclization of ω-Mesylate-α,β-Unsaturated Esters and Ketones. *Org. Biomol. Chem.* **2017**, *15* (30), 6323–6327.

(30) Kubota, K.; Iwamoto, H.; Yamamoto, E.; Ito, H. Silicon-Tethered Strategy for Copper(I)-Catalyzed Stereo- and Regioselective Alkylboration of Alkynes. *Org. Lett.* **2015**, *17* (3), 620–623.

(31) Kim-Lee, S.-H. H.; Alonso, I.; Mauleón, P.; Arrayás, R. G.; Carretero, J. C. Rationalizing the Role of NaO^{t}Bu in Copper-Catalyzed Carboboration of Alkynes: Assembly of Allylic All-Carbon Quaternary Stereocenters. *ACS Catal.* **2018**, *8* (10), 8993–9005.

(32) Zhang, F.; Wang, S.; Liu, Z.; Bai, Y.; Zhu, G. Copper-Catalyzed Borylative Cyclization of 1,n-Enynyl Phosphates Leading to Five- to Eight-Membered Cyclic 1,4-Dienyl Boronates. *Tetrahedron Lett.* **2017**, *58* (15), 1448–1452.

(33) He, T.; Li, B.; Liu, L.-C.; Wang, J.; Ma, W.-P.; Li, G.-Y.; Zhang, Q.-W.; He, W. Copper-Catalyzed Trifunctionalization of Alkynes: Rapid Formation of Oxindoles Bearing Geminal Diboronates. *Chem. – A Eur. J.* **2019**, *25* (4), 966–970.

(34) Liang, R.-X.; Chen, R.-Y.; Zhong, C.; Zhu, J.-W.; Cao, Z.-Y.; Jia, Y.-X. 3,3'-Disubstituted Oxindoles Formation via Copper-Catalyzed Arylboration and Arylsilylation of Alkenes. *Org. Lett.* **2020**, *22* (8), 3215–3218.

(35) Liu, P.; Fukui, Y.; Tian, P.; He, Z.-T.; Sun, C.-Y.; Wu, N.-Y.; Lin, G.-Q. Cu-Catalyzed Asymmetric Borylative Cyclization of Cyclohexadienone-Containing 1,6-Enynes. *J. Am. Chem. Soc.* **2013**, *135* (32), 11700–11703.

(36) He, C.-Y.; Li, Q.-H.; Wang, X.; Wang, F.; Tian, P.; Lin, G.-Q. Copper-Catalyzed Asymmetric Borylative Cyclization of Cyclohexadienone-Containing 1,6-Dienes. *Adv. Synth. Catal.* **2020**, *362* (4), 765–770.

(37) Sakae, R.; Hirano, K.; Miura, M. Ligand-Controlled Regiodivergent Cu-Catalyzed Aminoboration of Unactivated Terminal Alkenes. *J. Am. Chem. Soc.* **2015**, *137* (20), 6460–6463.

(38) Whyte, A.; Burton, K. I.; Zhang, J.; Lautens, M. Enantioselective Intramolecular Copper-Catalyzed Borylacylation. *Angew. Chem. Int. Ed.* **2018**, *57* (42), 13927–13930.

(39) Li, D.; Kim, J.; Yang, J. W.; Yun, J. Copper-Catalyzed Asymmetric Synthesis of Borylated *Cis*-Disubstituted Indolines. *Chem. – An Asian J.* **2018**, *13* (17), 2365–2368.

(40) Zhang, G.; Cang, A.; Wang, Y.; Li, Y.; Xu, G.; Zhang, Q.; Xiong, T.; Zhang, Q. Copper-Catalyzed Diastereo- and Enantioselective Borylative Cyclization: Synthesis of Enantioenriched 2,3-Disubstituted Indolines. *Org. Lett.* **2018**, *20* (7), 1798–1801.

(41) Li, D.; Park, Y.; Yun, J. Copper-Catalyzed Regioselective and Diastereoselective Synthesis of Borylated 1-Benzo[b]Azepines. *Org. Lett.* **2018**, *20* (23), 7526–7529.

(42) Wang, H.-M.; Zhou, H.; Xu, Q.-S.; Liu, T.-S.; Zhuang, C.-L.; Shen, M.-H.; Xu, H.-D. Copper-Catalyzed Borylative Cyclization of Substituted N-(2-Vinylaryl)Benzaldimines. *Org. Lett.* **2018**, *20* (7), 1777–1780.

(43) Bi, Y.-P.; Wang, H.-M.; Qu, H.-Y.; Liang, X.-C.; Zhou, Y.; Li, X.-Y.; Xu, D.; Shen, M.-H.; Xu, H.-D. Stereoselective Synthesis of All-*Cis* Boryl Tetrahydroquinolines via Copper-Catalyzed Regioselective Addition/Cyclization of o-Aldiminyl Cinnamate with B_2pin_2. *Org. Biomol. Chem.* **2019**, *17* (6), 1542–1546.

(44) Larin, E. M.; Loup, J.; Polishchuk, I.; Ross, R. J.; Whyte, A.; Lautens, M. Enantio- and Diastereoselective Conjugate Borylation/Mannich Cyclization. *Chem. Sci.* **2020**, *11* (22), 5716–5723.

(45) Kubota, K.; Uesugi, M.; Osaki, S.; Ito, H. Synthesis of 2-Alkyl-2-Boryl-Substituted-Tetrahydrofurans via Copper(I)-Catalysed Borylative Cyclization of Aliphatic Ketones. *Org. Biomol. Chem.* **2019**, *17* (23), 5680–5683.

(46) Burns, A. R.; Solana González, J.; Lam, H. W. Enantioselective Copper(I)-Catalyzed Borylative Aldol Cyclizations of Enone Diones. *Angew. Chem. Int. Ed.* **2012**, *51* (43), 10827–10831.

(47) Green, J. C.; Joannou, M. V; Murray, S. A.; Zanghi, J. M.; Meek, S. J. Enantio- and Diastereoselective Synthesis of Hydroxy Bis(Boronates) via Cu-Catalyzed Tandem Borylation/1,2-Addition. *ACS Catal.* **2017**, *7* (7), 4441–4445.

(48) Laitar, D. S.; Tsui, E. Y.; Sadighi, J. P. Catalytic Diboration of Aldehydes via Insertion into the Copper-Boron Bond. *J. Am. Chem. Soc.* **2006**, *128* (34), 11036–11037.

(49) McIntosh, M. L.; Moore, C. M.; Clark, T. B. Copper-Catalyzed Diboration of Ketones: Facile Synthesis of Tertiary α-Hydroxyboronate Esters. *Org. Lett.* **2010**, *12* (9), 1996–1999.

(50) Zanghi, J. M.; Liu, S.; Meek, S. J. Enantio- and Diastereoselective Synthesis of Functionalized Carbocycles by Cu-Catalyzed Borylative Cyclization of Alkynes with Ketones. *Org. Lett.* **2019**, *21* (13), 5172–5177.

(51) Yamamoto, E.; Kojima, R.; Kubota, K.; Ito, H. Copper(I)-Catalyzed Diastereoselective Borylative *Exo*-Cyclization of Alkenyl Aryl Ketones. *Synlett* **2016**, *27* (2), 272–276.

(52) Whyte, A.; Mirabi, B.; Torelli, A.; Prieto, L.; Bajohr, J.; Lautens, M. Asymmetric Synthesis of Boryl-Functionalized Cyclobutanols. *ACS Catal.* **2019**, *9* (10), 9253–9258.

(53) Burks, H. E.; Morken, J. P. Catalytic Enantioselective Diboration, Disilation and Silaboration: New Opportunities for Asymmetric Synthesis. *Chem. Commun.* **2007**, 45, 4717–4725.

(54) Beletskaya, I.; Pelter, A. Hydroborations Catalysed by Transition Metal Complexes. *Tetrahedron* **1997**, *53* (14), 4957–5026.

(55) Ishiyama, T.; Ishida, K.; Miyaura, N. Synthesis of Pinacol Arylboronates via Cross-Coupling Reaction of Bis(Pinacolato)Diboron with Chloroarenes Catalyzed by Palladium(0)-Tricyclohexylphosphine Complexes. *Tetrahedron* **2001**, *57* (49), 9813–9816.

(56) Lawson, Y. G.; Lesley, M. J. G.; Marder, T. B.; Norman, N. C.; Rice, C. R. Platinum Catalysed 1,4-Diboration of α,β-Unsaturated Ketones. *Chem. Commun.* **1997**, 21, 2051–2052.

(57) Ch, B.; Ali, H. A.; Goldberg, I.; Srebnik, M. Addition Reactions of Bis(Pinacolato)Diborane(4) to Carbonyl Enones and Synthesis of (Pinacolato)2BCH2B and (Pinacolato)2BCH2CH2B by Insertion and Coupling. *Organometallics* **2001**, *20* (18), 3962–3965.

(58) Bell, N. J.; Cox, A. J.; Cameron, N. R.; Evans, J. S. O.; Marder, T. B.; Duin, M. A.; Elsevier, C. J.; Baucherel, X.; Tulloch, A. A. D.; Tooze, R. P. Platinum Catalysed 3,4- and 1,4-Diboration of α,β-Unsaturated Carbonyl Compounds Using Bis-Pinacolatodiboron. *Chem. Commun.* **2004**, 16, 1854–1855.

(59) Kabalka, G. W.; Das, B. C.; Das, S. Rhodium-Catalyzed 1,4-Addition Reactions of Diboron Reagents to Electron Deficient Olefins. *Tetrahedron Lett.* **2002**, *43* (13), 2323–2325.

(60) Sumida, Y.; Yorimitsu, H.; Oshima, K. Nickel-Catalyzed Borylation of Aryl Cyclopropyl Ketones with Bis(Pinacolato)Diboron to Synthesize 4-Oxoalkylboronates. *J. Org. Chem.* **2009**, *74* (8), 3196–3198.

(61) Hirano, K.; Yorimitsu, H.; Oshima, K. Nickel-Catalyzed β-Boration of α,β-Unsaturated Esters and Amides with Bis(Pinacolato)Diboron. *Org. Lett.* **2007**, *9* (24), 5031–5033.

(62) Ito, H.; Yamanaka, H.; Tateiwa, J.; Hosomi, A. Boration of an α,β-Enone Using a Diboron Promoted by a Copper(I)–Phosphine Mixture Catalyst. *Tetrahedron Lett.* **2000**, *41* (35), 6821–6825.

(63) Kabalka, G. W.; Das, B. C.; Das, S. Synthesis of Novel Boron Containing Unnatural Cyclic Amino Acids as Potential Therapeutic Agents. *Tetrahedron Lett.* **2001**, *42* (41), 7145–7146.

(64) Lee, J. E.; Kwon, J.; Yun, J. Copper-Catalyzed Addition of Diboron Reagents to α,β-Acetylenic Esters: Efficient Synthesis of β-Boryl-α,β-Ethylenic Esters. *Chem. Commun.* **2008**, 6, 733–734.

(65) Lee, J.-E.; Yun, J. Catalytic Asymmetric Boration of Acyclic α,β-Unsaturated Esters and Nitriles. *Angew. Chem. Int. Ed.* **2008**, *120* (1), 151–153.

(66) Lillo, V.; Prieto, A.; Bonet, A.; Díaz Requejo, M. M.; Ramírez, J.; Pérez, P. J.; Fernández, E. Asymmetric β-Boration of α,β-Unsaturated Esters with Chiral (NHC)Cu Catalysts. *Organometallics* **2009**, *28* (2), 659–662.

(67) Sim, H. S.; Feng, X.; Yun, J. Copper-Catalyzed Enantioselective β-Boration of Acyclic Enones. *Chem. - Eur. J.* **2009**, *15* (8), 1939–1943.

(68) Mun, S.; Lee, J.-E. E.; Yun, J. Copper-Catalyzed β-Boration of α,β-Unsaturated Carbonyl Compounds: Rate Acceleration by Alcohol Additives. *Org. Lett.* **2006**, *8* (21), 4887–4889.

(69) Cragg, G. M. L. *Organoboranes in Organic Synthesis*; Dekker: New York, **1973**.

(70) Brown, H. C. *Boranes in Organic Chemistry*; Cornell University Press: Ithaca, **1972**.

(71) Brown, H. C. *Organic Synthesis via Boranes*; Wiley-Interscience: New York, **1975**.

(72) Onak, T. *Organoborane Chemistry*; Academic Press: New York, **1975**.

(73) A. Pelter, K. Smith, H. C. B. *Borane Reagents*; Academic Press: New York, **1988**.

(74) Matteson, D. S. *Stereodirected Synthesis with Organoboranes*; Springer: Berlin, **1995**.

(75) Hall, D. G. *Boronic Acids: Preparation and Applications in Organic Synthesis and Medicine*; Wiley-VCH: Weinheim, 2005.

(76) Cuenca, A. B.; Shishido, R.; Ito, H.; Fernández, E. Transition-Metal-Free B-B and B-Interelement Reactions with Organic Molecules. *Chem. Soc. Rev.* **2017**, *46* (2), 415–430.

(77) Urry, G.; Kerrigan, J.; Parsons, T. D.; Schlesinger, H. I. Diboron Tetrachloride, B_2Cl_4, as a Reagent for the Synthesis of Organoboron Compounds. I. The Reaction of Diboron Tetrachloride with Ethylene. *J. Am. Chem. Soc.* **1954**, *76* (21), 5299–5301.

(78) Kerrigan, J.; Parsons, T.; Urry, G.; Schlesinger, H. I. Cl/P Diboron Tetrachloride and Tetrafiuoride as Reagents for the Synthesis of Organo- Boron Compounds. II. The Behavior of the Diboron Tetrahalides toward Unsaturated. *J. Am. Chem. Soc.* **1958**, *3573* (5), 6368–6371.

(79) Wartik, T.; Moore, R.; Schlesinger, H. I. Derivatives of Diborine. *J. Am. Chem. Soc.* **1949**, *71* (9), 3265–3266.

(80) Finch, A.; Schlesinger, H. I. Diboron Tetrafluoride. *J. Am. Chem. Soc.* **1958**, *80* (14), 3573–3574.

(81) Bowie, R. A.; Musgrave, O. C.; Goldschmid, H. R. Organoboron Compounds. Part X. The Reaction of Lithium with Trialkyl Borates. *J. Chem. Soc. C Org.* **1970**, 16, 2228–2229.

(82) Dewhurst, R. D.; Neeve, E. C.; Braunschweig, H.; Marder, T. B. Sp^2–Sp^3 Diboranes: Astounding Structural Variability and Mild Sources of Nucleophilic Boron for Organic Synthesis. *Chem. Commun.* **2015**, *51* (47), 9594–9607.

(83) Pietsch, S.; Neeve, E. C.; Apperley, D. C.; Bertermann, R.; Mo, F.; Qiu, D.; Cheung, M. S.; Dang, L.; Wang, J.; Radius, U.; Lin, Z.; Kleeberg, C.; Marder, T. B. Synthesis, Structure, and Reactivity of Anionic Sp^2–Sp^3 Diboron Compounds: Readily Accessible Boryl Nucleophiles. *Chem. – Eur. J.* **2015**, *21* (19), 7082–7098.

(84) Lee, K.; Zhugralin, A. R.; Hoveyda, A. H. Efficient C–B Bond Formation Promoted by N-Heterocyclic Carbenes: Synthesis of Tertiary and Quaternary B-Substituted Carbons through

Metal-Free Catalytic Boron Conjugate Additions to Cyclic and Acyclic α,β-Unsaturated Carbonyls. *J. Am. Chem. Soc.* **2009**, *131* (21), 7253–7255.

(85) Kleeberg, C.; Crawford, A. G.; Batsanov, A. S.; Hodgkinson, P.; Apperley, D. C.; Cheung, M. S.; Lin, Z.; Marder, T. B. Spectroscopic and Structural Characterization of the CyNHC Adduct of B_2pin_2 in Solution and in the Solid State. *J. Org. Chem.* **2012**, *77* (1), 785–789.

(86) Ibrahem, I.; Breistein, P.; Córdova, A. One-Pot Three-Component Highly Selective Synthesis of Homoallylboronates by Using Metal-Free Catalysis. *Chem. – Eur. J.* **2012**, *18* (17), 5175–5179.

(87) Wu, H.; Radomkit, S.; O'Brien, J. M.; Hoveyda, A. H. Metal-Free Catalytic Enantioselective C–B Bond Formation: (Pinacolato)Boron Conjugate Additions to α,β-Unsaturated Ketones, Esters, Weinreb Amides, and Aldehydes Promoted by Chiral N-Heterocyclic Carbenes. *J. Am. Chem. Soc.* **2012**, *134* (19), 8277–8285.

(88) Wen, K.; Chen, J.; Gao, F.; Bhadury, P. S.; Fan, E.; Sun, Z. Metal Free Catalytic Hydroboration of Multiple Bonds in Methanol Using N-Heterocyclic Carbenes under Open Atmosphere. *Org. Biomol. Chem.* **2013**, *11* (37), 6350–6356.

(89) Bonet, A.; Gulyás, H.; Fernández, E. Metal-Free Catalytic Boration at the β-Position of α,β-Unsaturated Compounds: A Challenging Asymmetric Induction. *Angew. Chem. Int. Ed.* **2010**, *49* (30), 5130–5134.

(90) Pubill-Ulldemolins, C.; Bonet, A.; Gulyás, H.; Bo, C.; Fernández, E. Essential Role of Phosphines in Organocatalytic β-Boration Reaction. *Org. Biomol. Chem.* **2012**, *10* (48), 9677–9682.

(91) Bonet, A.; Pubill-Ulldemolins, C.; Bo, C.; Gulyás, H.; Fernández, E. Transition-Metal-Free Diboration Reaction by Activation of Diboron Compounds with Simple Lewis Bases. *Angew. Chem. Int. Ed.* **2011**, *50* (31), 7158–7161.

(92) Ishiyama, T.; Miyaura, N. Metal-Catalyzed Reactions of Diborons for Synthesis of Organoboron Compounds. *Chem. Rec.* **2004**, *3* (5), 271–280.

(93) Dembitsky, V. M.; Abu Ali, H.; Srebnik, M. Recent Developments in Bisdiborane Chemistry: B-C-B, B-C-C-B, B-C=C-B and B-C≡C-B Compounds. *Appl. Organomet. Chem.* **2003**, *17* (6–7), 327–345.

(94) Thomas, R. L.; Souza, F. E. S.; Marder, T. B. Highly Efficient Monophosphine Platinum Catalysts for Alkyne Diboration. *J. Chem. Soc. Dalton Trans.* **2001**, 10, 1650–1656.

(95) Iverson, C. N.; Smith, M. R. Efficient Olefin Diboration by a Base-Free Platinum Catalyst. *Organometallics* **1997**, *16* (13), 2757–2759.

(96) Ishiyama, T.; Yamamoto, M.; Miyaura, N. Diboration of Alkenes with Bis(Pinacolato)Diboron Catalysed by a Platinum(0) Complex. *Chem. Commun.* **1997**, 7, 689–690.

(97) Ishiyama, T.; Matsuda, N.; Murata, M.; Ozawa, F.; Suzuki, A.; Miyaura, N. Platinum(0)-Catalyzed Diboration of Alkynes with Tetrakis(Alkoxo)Diborons: An Efficient and Convenient Approach to *Cis*-Bis(Boryl)Alkenes. *Organometallics* **1996**, *15* (2), 713–720.

(98) Iverson, C. N.; Smith, M. R. Reactivity of Organoplatinum Complexes with $C_6H_4O_2B$-$BO_2C_6H_4$: Syntheses of a Platinum Diboryl Complex with, and without, Metathesis of Boron-Boron and Metal-Carbon Bonds. *J. Am. Chem. Soc.* **1995**, *117* (15), 4403–4404.

(99) Nguyen, P.; Lesley, G.; Taylor, N. J.; Marder, T. B.; Pickett, N. L.; Clegg, W.; Elsegood, M. R. J.; Norman, N. C. Oxidative Addition of B-B Bonds by Rhodium(I) Phosphine Complexes: Molecular Structures of B_2cat_2 (Cat = 1,2-$O_2C_6H_4$) and Its 4-But and 3,5-Bu^t_2 Analogs. *Inorg. Chem.* **1994**, *33* (21), 4623–4624.

(100) Ishiyama, T.; Matsuda, N.; Miyaura, N.; Suzuki, A. Platinum(0)-Catalyzed Diboration of Alkynes. *J. Am. Chem. Soc.* **1993**, *115* (23), 11018–11019.

(101) Burks, H. E.; Kliman, L. T.; Morken, J. P. Asymmetric 1,4-Dihydroxylation of 1,3-Dienes by Catalytic Enantioselective Diboration. *J. Am. Chem. Soc.* **2009**, *131* (26), 9134–9135.

(102) Kliman, L. T.; Mlynarski, S. N.; Morken, J. P. Pt-Catalyzed Enantioselective Diboration of Terminal Alkenes with $B_2(Pin)_2$. *J. Am. Chem. Soc.* **2009**, *131* (37), 13210–13211.

(103) Dai, C.; B. Marder, T.; G. Robins, E.; S. Yufit, D.; A. K. Howard, J.; B. Marder, T.; J. Scott, A.; Clegg, W. Rhodium Catalysed Diboration of Unstrained Internal Alkenes and a New and General Route to Zwitterionic [$L_2Rh(\eta^6$-CatBcat)] (Cat = 1,2-$O_2C_6H_4$) Complexes. *Chem. Commun.* **1998**, 18, 1983–1984.

(104) Morgan, J. B.; Miller, S. P.; Morken, J. P. Rhodium-Catalyzed Enantioselective Diboration of Simple Alkenes. *J. Am. Chem. Soc.* **2003**, *125* (29), 8702–8703.

(105) Trudeau, S.; Morgan, J. B.; Shrestha, M.; Morken, J. P. Rh-Catalyzed Enantioselective Diboration of Simple Alkenes: Reaction Development and Substrate Scope. *J. Org. Chem.* **2005**, *70* (23), 9538–9544.

(106) Pubill-Ulldemolins, C.; Bonet, A.; Bo, C.; Gulyás, H.; Fernández, E. Activation of Diboron Reagents with Brønsted Bases and Alcohols: An Experimental and Theoretical Perspective of the Organocatalytic Boron Conjugate Addition Reaction. *Chem. – Eur. J.* **2012**, *18* (4), 1121–1126.

(107) Zhang, J.; Wu, H.-H.; Zhang, J. Cesium Carbonate Mediated Borylation of Aryl Iodides with Diboron in Methanol. *Eur. J. Org. Chem.* **2013**, *2013* (28), 6263–6266.

(108) Nagashima, Y.; Hirano, K.; Takita, R.; Uchiyama, M. *Trans*-Diborylation of Alkynes: Pseudo-Intramolecular Strategy Utilizing a Propargylic Alcohol Unit. *J. Am. Chem. Soc.* **2014**, *136* (24), 8532–8535.

(109) Solé, C.; Gulyás, H.; Fernández, E. Asymmetric Synthesis of α-Amino Boronate Esters via Organocatalytic Pinacolboryl Addition to Tosylaldimines. *Chem. Commun.* **2012**, *48* (31), 3769–3771.

(110) Sanz, X.; Lee, G. M.; Pubill-Ulldemolins, C.; Bonet, A.; Gulyás, H.; Westcott, S. A.; Bo, C.; Fernández, E. Metal-Free Borylative Ring-Opening of Vinyl Epoxides and Aziridines. *Org. Biomol. Chem.* **2013**, *11* (40), 7004–7010.

(111) Miralles, N.; Cid, J.; Cuenca, A. B.; Carbó, J. J.; Fernández, E. Mixed Diboration of Alkenes in a Metal-Free Context. *Chem. Commun.* **2015**, *51* (9), 1693–1696.

(112) Miralles, N.; Alam, R.; Szabó, K. J.; Fernández, E. Transition-Metal-Free Borylation of Allylic and Propargylic Alcohols. *Angew. Chem. Int. Ed.* **2016**, *55* (13), 4303–4307.

(113) Davenport, E.; Fernández, E. Transition-Metal-Free Synthesis of Vicinal Triborated Compounds and Selective Functionalisation of the Internal C–B Bond. *Chem. Commun.* **2018**, *54* (72), 10104–10107.

(114) Ely, R. J.; Morken, J. P. Regio- and Stereoselective Ni-Catalyzed 1,4-Hydroboration of 1,3-Dienes: Access to Stereodefined (*Z*)-Allylboron Reagents and Derived Allylic Alcohols. *J. Am. Chem. Soc.* **2010**, *132* (8), 2534–2535.

(115) Cao, Y.; Zhang, Y.; Zhang, L.; Zhang, D.; Leng, X.; Huang, Z. Selective Synthesis of Secondary Benzylic (*Z*)-Allylboronates by Fe-Catalyzed 1,4-Hydroboration of 1-Aryl-Substituted 1,3-Dienes. *Org. Chem. Front.* **2014**, *1* (9), 1101–1106.

(116) Ely, R. J.; Yu, Z.; Morken, J. P. Diastereoselective Ni-Catalyzed 1,4-Hydroboration of Chiral Dienols. *Tetrahedron Lett.* **2015**, *56* (23), 3402–3405.

(117) Haeffner, F. Transition-Metal-Free Diboration of Non-Activated Olefins: A Reaction Mechanism Revisited. *Comput. Theor. Chem.* **2018**, *1131*, 90–98.

(118) Cid, J.; Carbó, J. J.; Fernández, E. Disclosing the Structure/Activity Correlation in Trivalent Boron-Containing Compounds: A Tendency Map. *Chem. – Eur. J.* **2012**, *18* (40), 12794–12802.

(119) García-López, D.; Cid, J.; Marqués, R.; Fernández, E.; Carbó, J. J. Quantitative Structure–Activity Relationships for the Nucleophilicity of Trivalent Boron Compounds. *Chem. – Eur. J.* **2017**, *23* (21), 5066–5075.

(120) Aguado-Ullate, S.; Saureu, S.; Guasch, L.; Carbó, J. J. Theoretical Studies of Asymmetric Hydroformylation Using the Rh-(R,S)-BINAPHOS Catalyst—Origin of Coordination Preferences and Stereoinduction. *Chem. – Eur. J.* **2012**, *18* (3), 995–1005.

(121) Aguado-Ullate, S.; Urbano-Cuadrado, M.; Villalba, I.; Pires, E.; García, J. I.; Bo, C.; Carbó, J. J. Predicting the Enantioselectivity of the Copper-Catalysed Cyclopropanation of Alkenes by Using Quantitative Quadrant-Diagram Representations of the Catalysts. *Chem. – Eur. J.* **2012**, *18* (44), 14026–14036.

(122) Maza, R. J.; Carbó, J. J.; Fernández, E. Borata-Alkene Species as Nucleophilic Reservoir. *Adv. Synth. Catal.* **2021**, *363* (9), 2274–2289.

(123) Brown, H. C.; Zweifel, G. Hydroboration. XI. The Hydroboration of Acetylenes—A Convenient Conversion of Internal Acetylenes into *Cis*-Olefins and of Terminal Acetylenes into Aldehydes. *J. Am. Chem. Soc.* **1961**, *83* (18), 3834–3840.

(124) Zweifel, G.; Arzoumanian, H. The Synthesis of Mixed Geminal Organometallic Compounds. *Tetrahedron Lett.* **1966**, *7* (23), 2535–2538.

(125) Cainelli, G.; Bello, G. D.; Zubiani, G. Gem-Dimetallic Compounds; A Novel Approach to Olefins Starting from Carbonyl Compounds and Acetylenic Derivatives. *Tetrahedron Lett.* **1966**, *7* (36), 4315–4318.

(126) Horner, L.; Hoffmann, H.; Wippel, H. G. Phosphororganische Verbindungen, XII. Phosphinoxyde Als Olefinierungsreagenzien. *Chem. Ber.* **1958**, *91* (1), 61–63.

(127) Cainelli, G.; Dal Bello, G.; Zubiani, G. Gem-Dimetallic Compounds : On the Metal-Metal Interconversion between Gem-Organoboron Compounds and n-Butyllithium. *Tetrahedron Lett.* **1965**, *6* (38), 3429–3432.

(128) Bertini, F.; Grasselli, P.; Zubiani, G.; Cainelli, G. Geminal Dimetallic Compounds: Reactivity of Methylene Magnesium Halides and Related Compounds. A General Carbonyl Olefination Reaction. *Tetrahedron* **1970**, *26* (6), 1281–1290.

(129) Kauffmann, T.; Echsler, K.-J.; Hamsen, A.; Kriegesmann, R.; Steinseifer, F.; Vahrenhorst, A. Darstellung Und Anwendungsmöglichkeiten von Diphenylarsanyl-, Diphenylstibanyl- Und Triphenylplumbyl-Methyllithium. *Tetrahedron Lett.* **1978**, *19* (45), 4391–4394.

(130) Kauffmann, T. New Possible Applications of Heavy Main-Group Elements in Organic Synthesis. *Angew. Chem. Int. Ed. English* **1982**, *21* (6), 410–429.

(131) Zweifel, G.; Arzoumanian, H. Germinal Organometallic Compounds. I. The Synthesis and Structure of 1,1-Diborohexane. *J. Am. Chem. Soc.* **1967**, *89* (2), 291–295.

(132) Matteson, D. S.; Thomas, J. R. C-Alkylation of Methanetetraboronic and Methanetriboronic Esters. *J. Organomet. Chem.* **1970**, *24* (2), 263–271.

(133) Endo, K.; Ohkubo, T.; Hirokami, M.; Shibata, T. Chemoselective and Regiospecific Suzuki Coupling on a Multisubstituted Sp^3-Carbon in 1,1-Diborylalkanes at Room Temperature. *J. Am. Chem. Soc.* **2010**, *132* (32), 11033–11035.

(134) Hong, K.; Liu, X.; Morken, J. P. Simple Access to Elusive α-Boryl Carbanions and Their Alkylation: An Umpolung Construction for Organic Synthesis. *J. Am. Chem. Soc.* **2014**, *136* (30), 10581–10584.

(135) Rathke, M. W.; Kow, R. Generation of Boron-Stabilized Carbanions. *J. Am. Chem. Soc.* **1972**, *94* (19), 6854–6856.

(136) Kow, R.; Rathke, M. W. Formation and Reactions of Boron-Stabilized Carbanions Derived from Vinylboranes. *J. Am. Chem. Soc.* **1973**, *95* (8), 2715–2716.

(137) Ashe, A. J.; Shu, P. 1-Phenylborabenzene Anion. *J. Am. Chem. Soc.* **1971**, *93* (7), 1804–1805.

(138) Kohrt, S.; Dachwitz, S.; Daniliuc, C. G.; Kehr, G.; Erker, G. Stabilized Borata-Alkene Formation: Structural Features, Reactions and the Role of the Counter Cation. *Dalton Trans.* **2015**, *44* (48), 21032–21040.

(139) Ramsey, B. G.; Isabelle, L. M. A Boron-Stabilized Carbanion from the Reaction of Trimesitylborane with Strong Bases in Tetrahydrofuran and Dimethyl Sulfoxide. *J. Org. Chem.* **1981**, *46* (1), 179–182.

(140) Matteson, D. S.; Moody, R. J. Carbanions from Deprotonation of Gem-Diboronic Esters. *J. Am. Chem. Soc.* **1977**, *99* (9), 3196–3197.

(141) Matteson, D. S.; Moody, R. J. Deprotonation of 1,1-Diboronic Esters and Reactions of the Carbanions with Alkyl Halides and Carbonyl Compounds. *Organometallics* **1982**, *1* (1), 20–28.

(142) Pelter, A.; Singaram, B.; Williams, L.; Wilson, J. W. The Dimesitylboron Group in Organic Synthesis 1. Introduction. *Tetrahedron Lett.* **1983**, *24* (6), 623–626.

(143) Pelter, A.; Williams, L.; Wilson, J. W. The Dimesitylboron Group in Organic Synthesis 2. The c-Alkylation of Alkyldimesitylboranes. *Tetrahedron Lett.* **1983**, *24* (6), 627–630.

(144) Pelter, A.; Singaram, B.; Wilson, J. W. The Dimesitylboron Group in Organic Synthesis. 3. Reactions of Allyldimesitylborane. *Tetrahedron Lett.* **1983**, *24* (6), 631–634.

(145) Pelter, A.; Singaram, B.; Warren, L.; Wilson, J. W. Hindered Organoboron Groups in Organic Chemistry. The Production of Boron Stabilised Carbanions. *Tetrahedron* **1993**, *49* (14), 2965–2978.

(146) Knochel, P. A New Approach to Boron-Stabilized Organometallics. *J. Am. Chem. Soc.* **1990**, *112* (20), 7431–7433.

(147) Cooke, M. P.; Widener, R. K. Nucleophilic Addition Reactions of Hindered Unsaturated Boranes. New Synthesis of Organoboranes. *J. Am. Chem. Soc.* **1987**, *109* (3), 931–933.

(148) Tsai, D. J. S.; Matteson, D. S. Pinanediol [α-(Trimethylsilyl)Allyl]Boronate and Related Boronic Esters. *Organometallics* **1983**, *2* (2), 236–241.

(149) Matteson, D. S.; Wilson, J. W. An α-Lithio Boronic Ester from an α-Trimethylstannyl Boronic Ester. *Organometallics* **1985**, *4* (9), 1690–1692.

(150) Pilz, M.; Allwohn, J.; Hunold, R.; Massa, W.; Berndt, A. A Monomeric Diboryldilithiomethane with a 1,3-Diborataallene Structure. *Angew. Chem. Int. Ed. English* **1988**, *27* (10), 1370–1372.

(151) Sahin, Y.; Hartmann, M.; Geiseler, G.; Schweikart, D.; Balzereit, C.; Frenking, G.; Massa, W.; Berndt, A. Nonorthogonal Dilithium-1,3-Biborataallenes Containing Planar-Tetracoordinate Carbon Atoms. *Angew. Chem. Int. Ed.* **2001**, *40* (14), 2662–2665.

(152) Hunold, R.; Allwohn, J.; Baum, G.; Massa, W.; Berndt, A. Compounds with Partial Boron-Carbon Triple Bonds. *Angew. Chem. Int. Ed. English* **1988**, *27* (7), 961–963.

(153) Braunschweig, H.; Dellermann, T.; Dewhurst, R. D.; Ewing, W. C.; Hammond, K.; Jimenez-Halla, J. O. C.; Kramer, T.; Krummenacher, I.; Mies, J.; Phukan, A. K.; Vargas, A. Metal-Free Binding and Coupling of Carbon Monoxide at a Boron–Boron Triple Bond. *Nat. Chem.* **2013**, *5* (12), 1025–1028.

(154) Takahashi, F.; Nogi, K.; Sasamori, T.; Yorimitsu, H. Diborative Reduction of Alkynes to 1,2-Diboryl-1,2-Dimetalloalkanes: Its Application for the Synthesis of Diverse 1,2-Bis(Boronate)S. *Org. Lett.* **2019**, *21* (12), 4739–4744.

(155) Chiu, C.-W.; Gabbaï, F. P. Structural Changes Accompanying the Stepwise Population of a B-C π Bond. *Angew. Chem. Int. Ed.* **2007**, *46* (36), 6878–6881.

(156) Yu, J.; Kehr, G.; Daniliuc, C. G.; Erker, G. A Unique Frustrated Lewis Pair Pathway to Remarkably Stable Borata–Alkene Systems. *Eur. J. Inorg. Chem.* **2013**, *2013* (19), 3312–3315.

(157) Möbus, J.; Kehr, G.; Daniliuc, C. G.; Fröhlich, R.; Erker, G. Borata–Alkene Derivatives Conveniently Made by Frustrated Lewis Pair Chemistry. *Dalton Trans.* **2014**, *43* (2), 632–638.

(158) Moquist, P.; Chen, G.-Q.; Mück-Lichtenfeld, C.; Bussmann, K.; Daniliuc, C. G.; Kehr, G.; Erker, G. α-CH Acidity of Alkyl–B(C_6F_5)$_2$ Compounds – the Role of Stabilized Borata-Alkene Formation in Frustrated Lewis Pair Chemistry. *Chem. Sci.* **2015**, *6* (1), 816–825.

(159) Wang, L.; Jian, Z.; Daniliuc, C. G.; Kehr, G.; Erker, G. Formation of Borata-Alkene/Iminium Zwitterions by Ynamine Hydroboration. *Dalton Trans.* **2018**, *47* (32), 10853–10856.

(160) Wang, T.; Daniliuc, C. G.; Mück-Lichtenfeld, C.; Kehr, G.; Erker, G. Formation of Reactive π-Conjugated Frustrated N/B Pairs by Borane-Induced Propargyl Amine Rearrangement. *J. Am. Chem. Soc.* **2018**, *140* (10), 3635–3643.

(161) Hoefelmeyer, J. D.; Solé, S.; Gabbaï, F. P. Reactivity of the Dimesityl-1,8-Naphthalenediylborate Anion: Isolation of the Borataalkene Isomer and Synthesis of 1,8-Diborylnaphthalenes. *Dalton Trans.* **2004**, 8, 1254–1258.

(162) Horchler von Locquenghien, K.; Baceiredo, A.; Boese, R.; Bertrand, G. New Synthesis and First X-Ray Crystal Study of a C-Borylated Phosphorus Ylide. *J. Am. Chem. Soc.* **1991**, *113* (13), 5062–5063.

(163) Lafage, M.; Pujol, A.; Saffon-Merceron, N.; Mézailles, N. BH3 Activation by Phosphorus-Stabilized Geminal Dianions: Synthesis of Ambiphilic Organoborane, DFT Studies, and Catalytic CO_2 Reduction into Methanol Derivatives. *ACS Catal.* **2016**, *6* (5), 3030–3035.

(164) Miralles, N.; Maza, R. J.; Fernández, E. Synthesis and Reactivity of 1,1-Diborylalkanes towards C–C Bond Formation and Related Mechanisms. *Adv. Synth. Catal.* **2018**, *360* (7), 1306–1327.

(165) Wu, C.; Wang, J. Geminal Bis(Boron) Compounds: Their Preparation and Synthetic Applications. *Tetrahedron Lett.* **2018**, *59* (22), 2128–2140.

(166) Cuenca, A. B.; Fernández, E. Boron-Wittig Olefination with Gem-Bis(Boryl)Alkanes. *Chem. Soc. Rev.* **2021**, *50* (1), 72–86.

(167) Castle, R. B.; Matteson, D. S. Methanetetraboroni and Methanetriboronic Esters. *J. Organomet. Chem.* **1969**, *20* (1), 19–28.

(168) Matteson, D. S.; Tripathy, P. B. Alkene-1,1-Diboronic Esters from Methanetetraboronic Ester. *J. Organomet. Chem.* **1970**, *21* (1), P6–P8.

(169) Pelter, A.; Singaram, B.; Wilson, J. W. The Dimesitylboron Group in Organic Synthesis. 4. The 'Boron Wittig' Reaction. *Tetrahedron Lett.* **1983**, *24* (6), 635–636.

(170) Pelter, A.; Buss, D.; Pitchford, A. The Dimesitylboron Group in Organic Synthesis 7. A Unique Variant of the Boron-Wittig Reaction Which Stereoselectively Yields 1,2-Diols. *Tetrahedron Lett.* **1985**, *26* (41), 5093–5096.

(171) Pelter, A.; Smith, K.; Elgendy, S.; Rowlands, M. Hindered Organoboron Groups in Organic Synthesis. 14. Stereoselective Synthesis of Alkenes by the Boron-Wittig Reaction Using Aliphatic Aldehydes. *Tetrahedron Lett.* **1989**, *30* (41), 5647–5650.

(172) Pelter, A.; Buss, E.; Colclough, E. Stereoselective Synthesis of E- and Z-Alkenes by the Boron–Wittig Reaction. *J. Chem. Soc. Chem. Commun.* **1987**, 4, 297–299.

(173) Pelter, A.; Smith, K.; Elgendy, S.; Rowlands, M. Hindered Organoboron Groups in Organic Synthesis. 13. The Direct Production of Ketones from Aliphatic Aldehydes by a Unique Variant of the Boron-Wittig Reaction. *Tetrahedron Lett.* **1989**, *30* (41), 5643–5646.

(174) Pelter, A.; Smith, K.; Jones, K. D. Allene Synthesis via Boron-Stabilised Alkenyl Carbanions. *J. Chem. Soc. Perkin Trans. 1* **1992**, 7, 747–748.

(175) Kawashima, T.; Yamashita, N.; Okazaki, R. Synthesis, Structure, and Thermolysis of a Tetracoordinate 1,2-Oxaboretanide: An Intermediate of the Boron-Wittig Reaction under Basic Conditions. *J. Am. Chem. Soc.* **1995**, *117* (22), 6142–6143.

(176) Endo, K.; Ohkubo, T.; Shibata, T. Chemoselective Suzuki Coupling of Diborylmethane for Facile Synthesis of Benzylboronates. *Org. Lett.* **2011**, *13* (13), 3368–3371.

(177) Endo, K.; Ohkubo, T.; Ishioka, T.; Shibata, T. Cross Coupling between Sp^3-Carbon and Sp^3-Carbon Using a Diborylmethane Derivative at Room Temperature. *J. Org. Chem.* **2012**, *77* (10), 4826–4831.

(178) Endo, K.; Ishioka, T.; Shibata, T. One-Pot Cross-Coupling of Diborylmethane for the Synthesis of Dithienyl-methane Derivatives. *Synlett* **2014**, *25* (15), 2184–2188.

(179) Sun, C.; Potter, B.; Morken, J. P. A Catalytic Enantiotopic-Group-Selective Suzuki Reaction for the Construction of Chiral Organoboronates. *J. Am. Chem. Soc.* **2014**, *136* (18), 6534–6537.

(180) Potter, B.; Szymaniak, A. A.; Edelstein, E. K.; Morken, J. P. Nonracemic Allylic Boronates through Enantiotopic-Group-Selective Cross-Coupling of Geminal Bis(Boronates) and Vinyl Halides. *J. Am. Chem. Soc.* **2014**, *136* (52), 17918–17921.

(181) Zhang, Z.-Q.; Yang, C.-T.; Liang, L.-J.; Xiao, B.; Lu, X.; Liu, J.-H.; Sun, Y.-Y.; Marder, T. B.; Fu, Y. Copper-Catalyzed/Promoted Cross-Coupling of Gem-Diborylalkanes with Nonactivated Primary Alkyl Halides: An Alternative Route to Alkylboronic Esters. *Org. Lett.* **2014**, *16* (24), 6342–6345.

(182) Zhang, Z.-Q.; Zhang, B.; Lu, X.-Y.; Liu, J.-H.; Lu, X.-Y.; Xiao, B.; Fu, Y. Copper-Catalyzed S_N2'-Selective Allylic Substitution Reaction of Gem-Diborylalkanes. *Org. Lett.* **2016**, *18* (5), 952–955.

(183) Li, F.; Zhang, Z.-Q.; Lu, X.; Xiao, B.; Fu, Y. Copper-Catalyzed Propargylation of Diborylmethane. *Chem. Commun.* **2017**, *53* (25), 3551–3554.

(184) Zhang, Q.; Wang, B.; Liu, J.-Q.; Fu, Y.; Wu, Y.-C. Mechanistic Insights into Solvent and Ligand Dependency in Cu(I)-Catalyzed Allylic Alkylation with Gem-Diborylalkanes. *J. Org. Chem.* **2018**, *83* (2), 561–570.

(185) Kim, J.; Park, S.; Park, J.; Cho, S. H. Synthesis of Branched Alkylboronates by Copper-Catalyzed Allylic Substitution Reactions of Allylic Chlorides with 1,1-Diborylalkanes. *Angew. Chem. Int. Ed.* **2016**, *55* (4), 1498–1501.

(186) Shi, Y.; Hoveyda, A. H. Catalytic S_N2'- and Enantioselective Allylic Substitution with a Diborylmethane Reagent and Application in Synthesis. *Angew. Chem. Int. Ed.* **2016**, *55* (10), 3455–3458.

(187) Jang, W. J.; Yun, J. Catalytic Asymmetric Conjugate Addition of a Borylalkyl Copper Complex for Chiral Organoboronate Synthesis. *Angew. Chem. Int. Ed.* **2019**, *58* (50), 18131–18135.

(188) Miralles, N.; Gómez, J. E.; Kleij, A. W.; Fernández, E. Copper-Mediated S_N2' Allyl–Alkyl and Allyl–Boryl Couplings of Vinyl Cyclic Carbonates. *Org. Lett.* **2017**, *19* (22), 6096–6099.

Chapter 2
Nucleophilic Cu-B addition to alkenes with concomitant intramolecular coupling with aldehydes

Nucleophilic Cu-B addition to alkenes with concomitant intramolecular coupling with aldehydes

2.1 Abstract and specific objectives

Catalysis with copper complexes has become one of the most powerful methods to install nucleophilic boryl units across diverse π-systems in a stereoselective manner. Additionally, this method affords difunctionalization by subsequent electrophilic trapping. In this Chapter, we study the copper(I) catalyzed borylative cyclization of γ-alkenyl aldehydes. This approach faces the challenge about the chemoselective borylation of C=C *versus* C=O by means of a copper (I) catalyst. But also, we studied the regioselective control of the intramolecular cyclization through nucleophilic attack of the organocopper intermediate to the formyl group, providing the corresponding diastereoselective cyclobutanol.

The specific goals in this chapter are:

- The study of the reaction conditions to allow the copper-boryl catalyst to be added chemoselectively on the alkene *versus* the aldehyde, with a concomitant intramolecular nucleophilic attack of the organocopper intermediate on the aldehyde.
- The study of the influence of the reaction components towards the control of the diastereoselectivity of the polysubstituted cyclobutanol formed.
- The proposal of a reaction mechanism, through theoretical calculations, identifying and evaluating the factors that determine the chemo- and diastereoselectivity

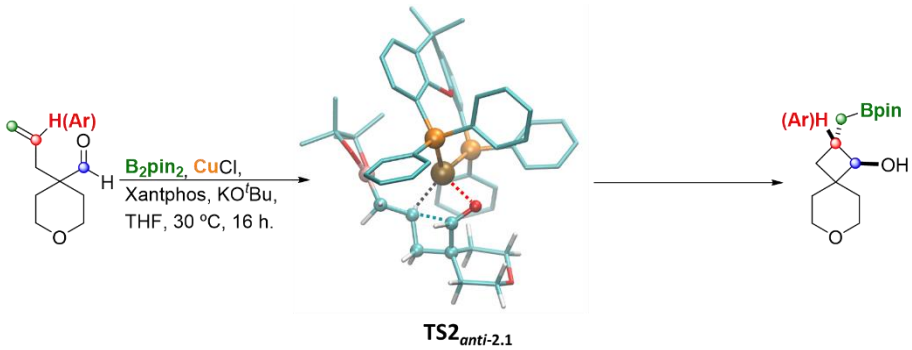

Scheme 2.1. Reaction outcome of borylative *exo*-cyclization of γ-alkenyl aldehydes.

2.2 State of the Art

Copper-catalyzed borylative ring-closing of unactivated alkenes, bearing electrophilic sites, constitutes a strategic intramolecular 1,2-carboboration process.[1] Ito and co-workers developed the concept demonstrating that CuCl/Xantphos/KO^{t}Bu catalyzed the consecutive borylcupration/C–C coupling of alkenyl halides toward the synthesis of cyclobutanes with a pending methylboryl moiety (Scheme 2.2a).[2] However, the loss of the leaving group (X= Br, I, OCO_2Me, $OP(O)(OR)_2$, OMs) reduced the atom economy of the transformation. The same authors extended the concept of copper(I)-catalyzed borylative *exo*-cyclization to γ-alkenyl aryl ketones, and they found that under similar catalytic system and reaction conditions, the regioselective borylcupration was followed by intramolecular 1,2-addition on the carbonyl group to give 2-(borylmethyl)cycloalkanols with excellent *syn*-diastereoselectivity (Scheme 2.2b).[3] An opposite *anti*-diastereselection has been found by Lautens and co-workers in the borylative cyclization of γ-alkenyl aryl ketones using $Cu(MeCN)_4PF_6$/BDPP as the catalytic system and NaO^{t}Bu as the base.[4] They found that isopropanol as an additive was critical to the reaction's success, together with MTBE as a solvent, achieving high levels of enantioselectivity when (S,S)-BDPP was the chiral ligand employed.[4] However, this new methodology is limited to using 1,1-disubstituted alkenes containing an aryl substituent (Scheme 2.2c).

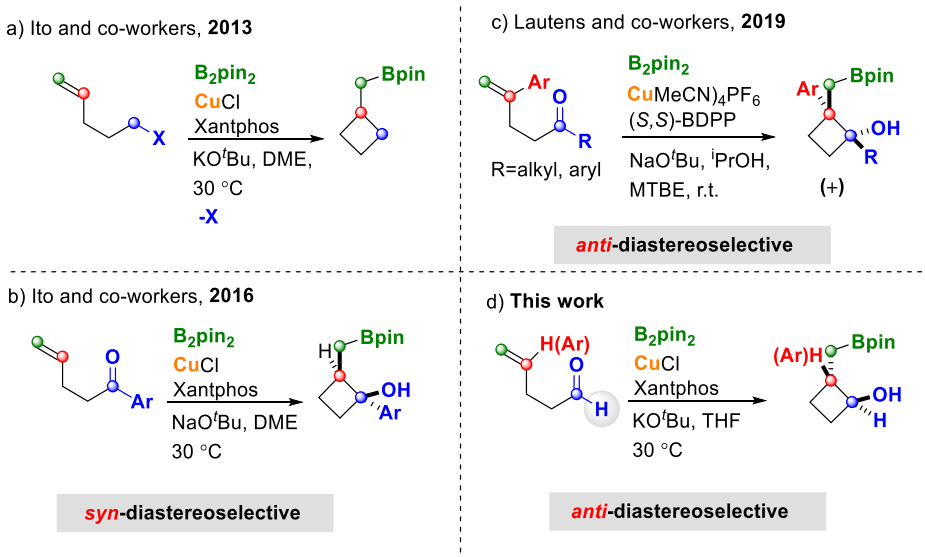

Scheme 2.2. Copper-catalyzed borylative *exo*-cyclization reactions.

Nucleophilic Cu-B addition to alkenes with concomitant intramolecular coupling with aldehydes

In the present work, we generate new knowledge about this challenging borylative ring-closing reaction demonstrating the viability of borylative cyclization of γ-alkenyl aldehydes, proving the favored chemoselective borylcupration of the double bond *versus* the carbonyl group, but also the resulting exclusive formation of 2-(borylmethyl)cycloalkanols with *anti*-diastereoselection (Scheme 2.2d). Also, based on DFT calculations, we are able to propose a new reaction mechanism identifying and evaluating the factors that control the chemo- and diastereoselectivity.

2.3 Results and Discussion

Initial experiments were conducted on the borylative cyclization of 4-allyltetrahydro-*2H*-pyran-4-carbaldehyde (**2.1**) as a model substrate in the presence of CuCl/Xantphos (Scheme 2.3). The substrate was quantitatively converted to the desired spirocyclic compound **2.2**, when bases such as NaO^{t}Bu or KO^{t}Bu were involved (Table 2.1, entry 1). To the best of our knowledge, this is the first example of a borycupration followed by intramolecular electrophilic trapping of the alkylcopper intermediate with the aldehyde, despite the fact that intermolecular versions are known.[5] Interestingly, the copper-catalyzed ring-closing reaction of **2.1** resulted in exclusive *anti*-diastereoselectivity, which was confirmed through one-dimensional Nuclear Overhauser Effect Spectroscopy (NOESY) (Figure 2.1). When proton H_a was irradiated, no positive protons were observed. However, if we irradiate H_b, a positive signal was observed for the Me groups of Bpin moiety. This favored diastereoselection is in contrast to the *syn*-diastereoselectivity observed by Ito and co-workers in the borylative cyclization of alkenyl aryl ketones where a dialkylcopper(III) species was postulated as intermediate.[3]

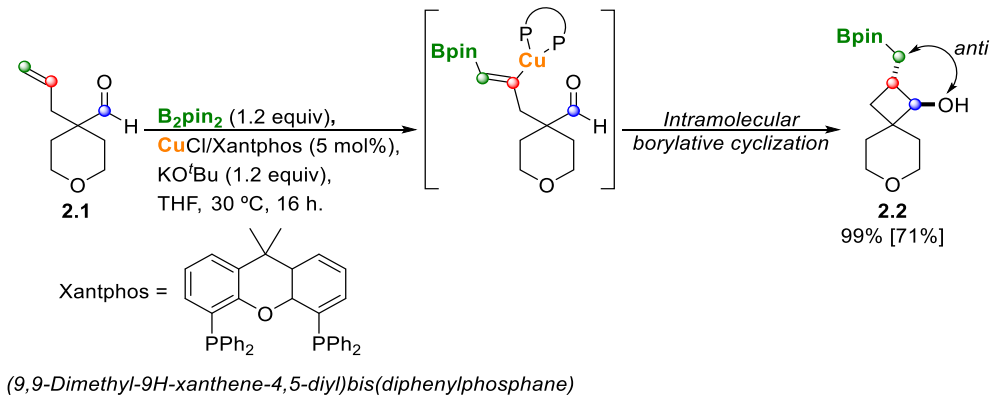

Scheme 2.3. Reaction conditions of copper-catalyzed borylative cyclization of 4-allyltetrahydro-*2H*-pyran-4-carbaldehyde (**2.1**).

Table 2.1. Cu-catalyzed diastereoselective borylative ring-closing of alkenyl aldehydes towards borylcyclobutanol compounds.[a]

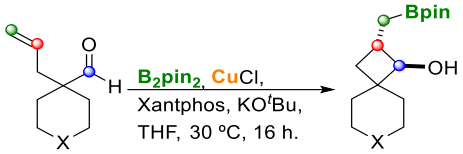

Entry	Substrate	Product	NMR Yield[b] [Isolated Yield]
1	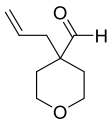 2.1	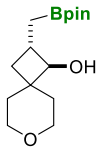 2.2	99% [71%] 99% [70%][c]
2	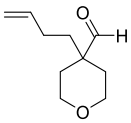 2.3	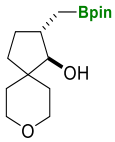 2.4	90% [45%]
3	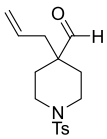 2.5	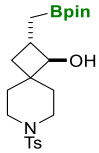 2.6	85% [67%]
4	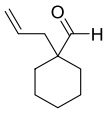 2.7	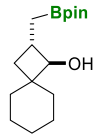 2.8	53% [50%]

[a] **Reaction conditions:** substrate (0.5 mmol), B_2pin_2 (1.2 equiv), CuCl (5 mol%), Xantphos (5 mol%), KO^{t}Bu (1.2 equiv), THF (2 mL), 30 °C, 16 h. [b] NMR yields calculated with naphthalene as internal standard, [% Isolated yields]. [c] NaO^{t}Bu used as base.

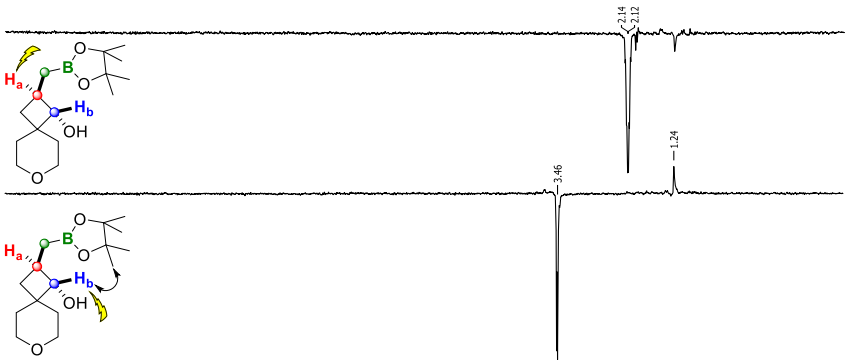

Figure 2.1. NOESY experiment to determine diastereoselectivity **2.2**.

Nucleophilic Cu-B addition to alkenes with concomitant intramolecular coupling with aldehydes

---

Next, we demonstrated the efficiency of this reaction by forming the 5-membered ring spirocyclic compound **2.4** from δ-alkenyl aldehyde **2.3**, (Table 2.1, entry 2). This result contrasts with the unsuccessful five-membered ring formation from the analogue ketone carried out by other groups.[4] The proof of concept was also applied in the transformation of 4-allyl-1-(phenylsulfonyl)piperidine-4-carbaldehyde (**2.5**) and 1-allylcyclohexane-1-carbaldehyde (**7**) towards the corresponding spirocyclic compounds **2.6** and **2.8** in 67% and 50% isolated yield, respectively (Table 2.1, entries 3 and 4). The reaction was also explored for 2,2-dimethylpent-4-enal (**2.9**) providing a direct access to 2,2-dimethyl-4-(pinacolborylmethyl)cyclobutan-1-ol (**2.10**) in moderate isolated yield (Table 2.2, entry 1). The unsymmetrical α,α-disubstituted aldehyde **2.11** followed an efficient boryl cupration with B_2pin_2 and B_2hex_2 (Table 2.2, entry 2 and 3 respectively).

Table 2.2. Cu-catalyzed diastereoselective borylative ring-closing of γ-alkyl-substituted alkenyl aldehydes. [a]

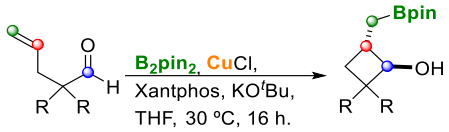

Entry	Substrate	Product	NMR Yield[b] [Isolated Yield]
1	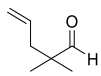 2.9	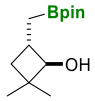 2.10	64% [59%]
2	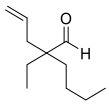 2.11	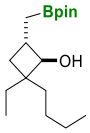 2.12	72% [34%]
3	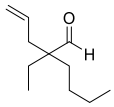 2.11	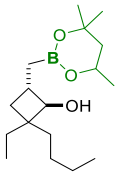 2.13	81% [51%]

[a] **Reaction conditions:** substrate (0.5 mmol), B_2pin_2 or B_2hex_2 (1.2 equiv), CuCl (5 mol%), Xantphos (5 mol%), KO^tBu (1.2 equiv), THF (2 mL), 30 °C, 16 h. [b] NMR yields calculated with naphthalene as internal standard, [% Isolated yields].

The borylative ring-closing reaction was also extended to γ-aryl-substituted alkenyl aldehydes with the aim to synthesize diastereoselective polysubstituted cyclobutanols. The

inclusion of a Ph group at the internal position of the C=C bond in substrates **2.14**, **2.16**, **2.18** and **2.20** did not change the reaction outcome, producing the desired spiro compounds in high conversion and moderate yield (Table 2.3, entries 1 to 4). The reaction proceeded with exclusive diastereoselectivity keeping the borylmethyl unit in *anti*-disposition with respect to the alcohol functional group.

Table 2.3. Cu-catalyzed diastereoselective borylative ring-closing of γ-aryl-substituted alkenyl aldehydes.[a]

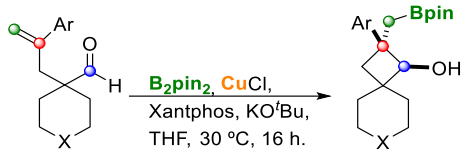

Entry	Substrate	Product	NMR Yield[b] [Isolated Yield]
1	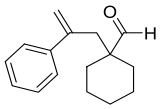 2.14	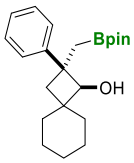 2.15	80% [76%]
2	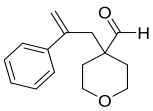 2.16	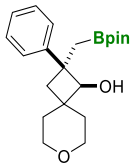 2.17	73% [24%]
3	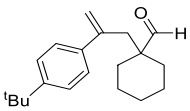 2.18	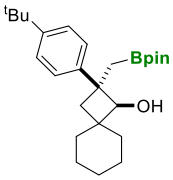 2.19	70% [25%]
4	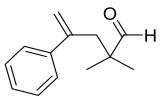 2.20	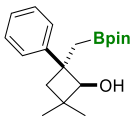 2.21	78% [27%]

[a] **Reaction conditions:** substrate (0.5 mmol), B_2pin_2 (1.2 equiv), CuCl (5 mol%), Xantphos (5 mol%), KO^{t}Bu) (1.2 equiv), THF (2 mL), 30 °C, 16 h. [b] NMR yields calculated with naphthalene as internal standard, [% Isolated yields].

When the copper (I) complex catalyzed the borylative ring-closing of 1-(2-(2-bromophenyl)allyl)cyclohexane-1-carbaldehyde (**2.22**), the expected spiro[3.5]nonan-1-ol was not observed. The unique product generated was 4'-methylene-3',4'-dihydro-*1'H*-

Nucleophilic Cu-B addition to alkenes with concomitant intramolecular coupling with aldehydes

spiro[cyclohexane-1,2'-naphthalen]-1'-ol (**2.23**) (Scheme 2.4). Since **2.23** was not formed in a blank experiment in the absence of B_2pin_2, we hypothesized that the Cu-B species might be involved in the C-Br activation with a concomitant intramolecular attack to the aldehyde, generating the spirocyclic product of six-membered ring with the exocyclic double bond in the opposite position to the alcohol functionality.

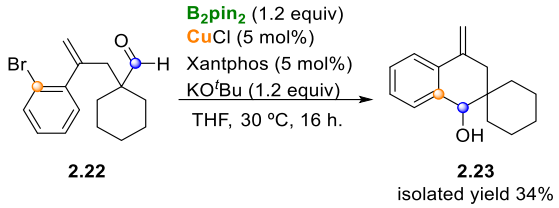

Scheme 2.4. Cu-catalyzed borylative ring-closing of 1-(2-(2-bromophenyl)allyl)cyclohexane-1-carbaldehyde (**2.22**).

Using 2-naphthyl group as the internal substituent of the alkene group in **2.24** was also tolerated in this ring-closing reaction obtaining the polysubstituted spirocyclic compound **2.25** with the expected *anti*-diastereoselectivity in 52% isolated yields (Scheme 2.5). However, the reaction also produced the boracycle with an oxaborole ring **2.26**-*syn-(B-OH)* due to the resulting cyclobutanol byproduct with *syn*-diastereoselectivity followed by the OH condensation with Bpin moiety (Scheme 2.5). The X-ray diffraction structures of products **2.25** and **2.26**-*syn-(B-OH)* are shown in Figure 2.2.

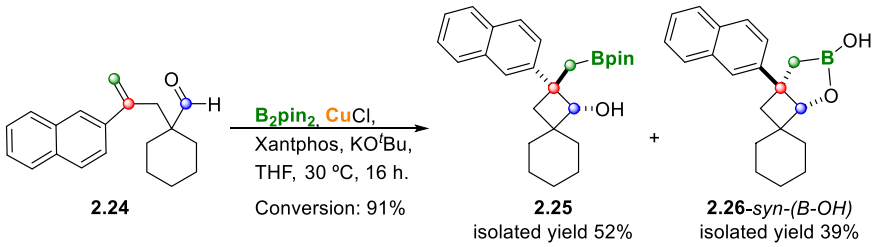

Scheme 2.5. Influence on diastereoselectivity of borylative cyclization using 2-naphthyl group as alkene substituent.

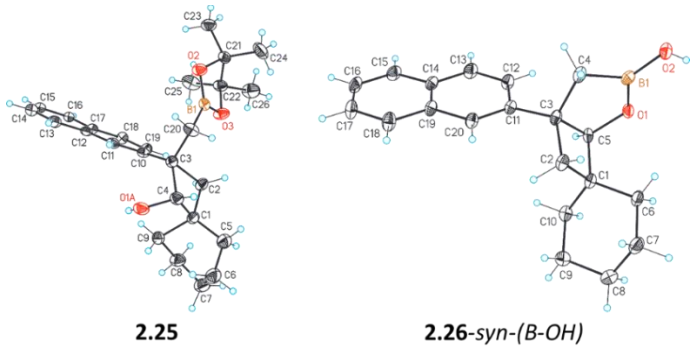

Figure 2.2. X-ray diffraction structures for **2.25** and **2.26**-*syn-(B-OH)*.

Remarkably, the copper-catalyzed ring-closing takes place chemoselectively through borylcupration on the C=C *versus* C=O. It brings added value to the borylative ring-closing method since it is known that copper-boryl complexes can efficiently catalyze the borylation of aldehydes, even at room temperature.[6,7] However γ-methyl-substituted alkenyl aldehyde substrates drive the borylcupration preferentially on the C=O bond *versus* the C=C bond. This is the case of substrate **2.27** that suffers a borylcupration on the aldehyde functional group generating the corresponding α-borylhydroxyl product **2.29** discarding the ring-closing step (Scheme 2.6).

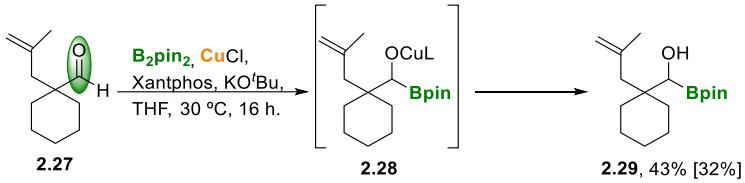

Scheme 2.6. Borylative reactivity in substrate **2.27**. Influence of alkene substituent on chemoselectivity.

The oxidation of the spirocyclic compounds with $NaBO_3{\cdot}H_2O$, allowed the isolation of the corresponding dihydroxylated cyclobutane products **2.30**-**2.35** contributing to an increase in the demand of four- and five-membered ring spirocycles (Scheme 2.7).[8] Single crystal X-ray diffraction of products **2.33** and **2.34** confirmed the *anti*-diastereoselection (Figure 2.3).

Nucleophilic Cu-B addition to alkenes with concomitant intramolecular coupling with aldehydes

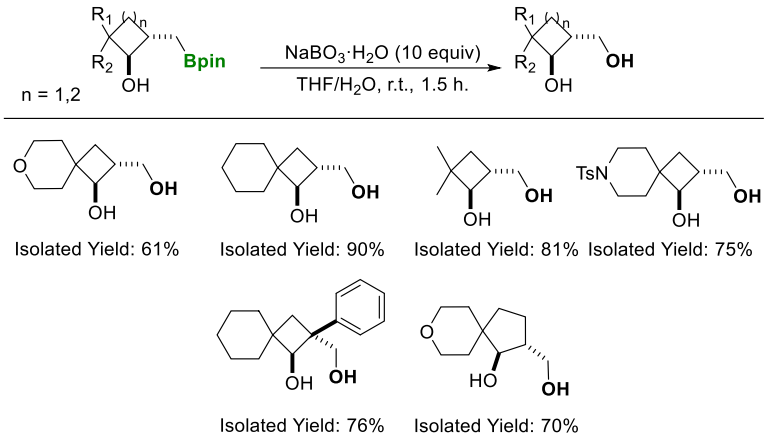

Scheme 2.7. Dihydroxylated products **2.30**-**2.35** obtained from the oxidation of the organoboron spirocyclic compounds with $NaBO_3{\cdot}H_2O$.

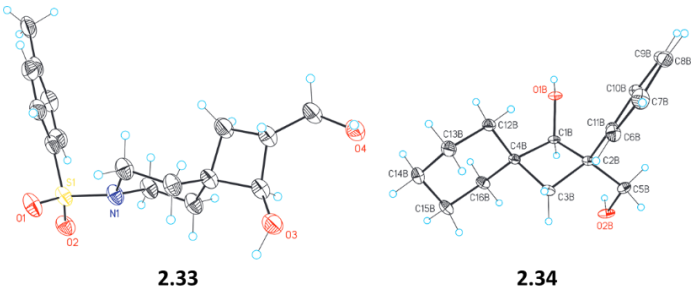

Figure 2.3. X-ray diffraction structures for **2.33** and **2.34**.

To propose a plausible mechanism and understand the factors governing the chemo- and diastereoselectivity, we performed DFT calculations (see Computational Details, section 2.5). Initially, we characterized computationally the mechanism for the Cu(I)-catalyzed borylative ring-closing reaction on substrate **2.1**, yielding the 4-membered ring spirocyclic product **2.2** with *anti* diastereoselectivity. Figure 2.4 depicts the computed potential free energy profile, as well as alternative pathways (dashed lines). Figure 2.5 shows the molecular structures of the key transition states.

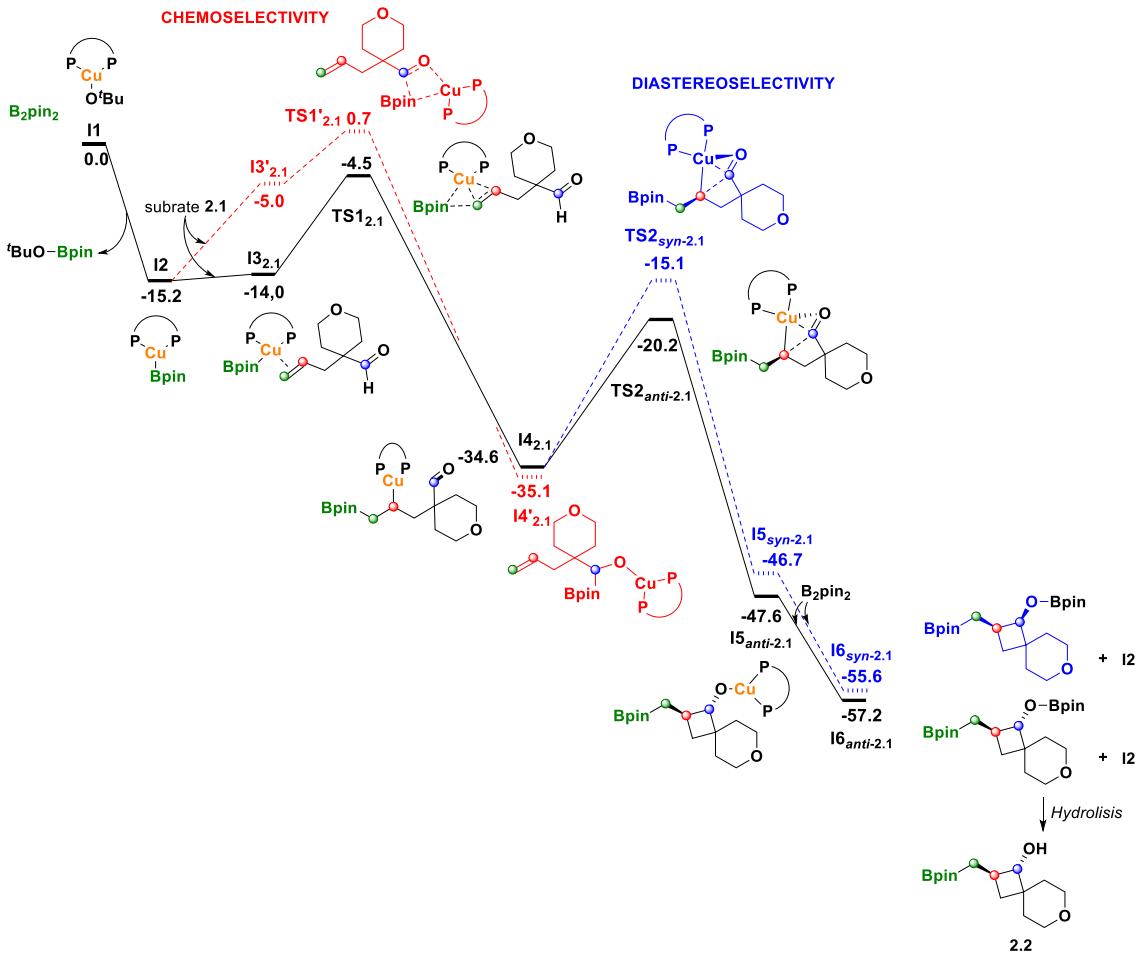

Figure 2.4. Computed free energy profile (kcal·mol^{-1}) for the formation of *syn*- and *anti*- **2.2**. Dashed lines represent alternative paths related to chemoselectivity (red lines) and diastereoselectivity (blue lines). P-P= Xantphos.

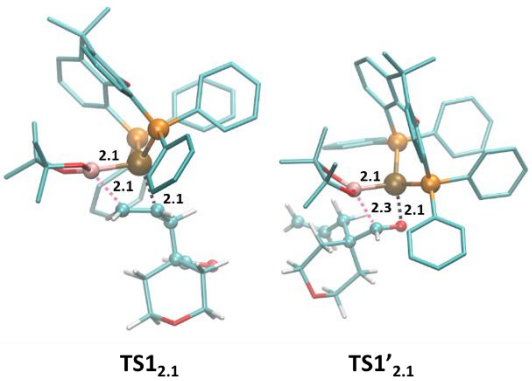

Figure 2.5. Molecular structures and main geometric parameters (Å) of the key transition states (**TS1$_{2.1}$** and **TS1'$_{2.1}$**) for the chemoselectivity of the borylative ring-closing reaction of substrate **2.1**.

Nucleophilic Cu-B addition to alkenes with concomitant intramolecular coupling with aldehydes

---

The initial steps of the mechanism were found to be similar analogous to those characterized previously for borylative ring-closing of alkenyl halides by diphosphine-Cu(I) complexes.[9] The reaction starts with the formation of Cu(O^{t}Bu) (**I1**), resulting from mixing CuCl, KO^{t}Bu and Xantphos ligand. Then, the active Cu-boryl species **I2** is generated by σ-bond metathesis between **I1** with B_2pin_2. The next step is postulated as the coordination of Cu-Bpin to the substrate **2.1** through alkene moiety (**I3$_{2.1}$**) and subsequent insertion of the C=C into the Cu-B bond to yield the alkyl-copper(I) complex **I4$_{2.1}$**. This latter process occurs via transition state **TS1$_{2.1}$** with a moderate free energy barrier of 10.7 kcal·mol^{-1} (**I2** → **TS1$_{2.1}$** in Figure 2.4).

In previous contribution,[9] it was possible to optimize the dialkylcopper(III) intermediate proposed by Ito and co-workers[2,3] resulting from the intramolecular attack of Cu(I) to the C-X with the concomitant elimination of the halide. Nevertheless, Cu(III) species corresponded to a shallow well that could not be characterised in all the studied systems. Here, the absence of the halide leaving group makes the formation of the Cu(III) complex less likely. Thus, all attempts to localize the Cu(III) intermediate were unsuccessful, including more sophisticated molecular models such as ^{t}BuO$^-$ base coordinated to Cu, the K$^+$ counter cation interacting with the alkoxy moiety, and two specific THF solvent molecules. Alternatively, an intramolecular attack of the Cu-alkyl moiety to the carbonyl carbon in complex **I4$_{2.1}$** would occur leading the ring-closing C-C coupling and the resulting alkoxy-copper(I) complex **I5$_{2.1}$**. The process needs to overcome a low energy barrier (14.4 kcal·mol^{-1}) and is exergonic by 13.0 kcal·mol^{-1}. In the corresponding transition state, **TS2$_{anti}$**, a negative charge is developed at the carbonyl oxygen, which interacts with the Cu center in order to stabilize the partial negative charge. Next, intermediate **I5$_{anti\text{-}2.1}$** can undergo another σ-bond metathesis with the diboron reagent to recover the active Cu-boryl species **I2** and yield a 4-membered ring containing the O-Bpin moiety (**I6$_{anti\text{-}2.1}$**) with *anti*-diatereoselectivity. Finally, the spirocyclic product **2.2** can be generated from species **I6$_{2.1}$** though the hydrolysis of O-B bond by the alcohol solvent or during the isolation of the product via column chromatography.

We also evaluated the chemoselective pathway for boryl addition to aldehyde, as illustrated for substrate **2.1** by red dashed lines in Figure 2.4. The Cu center in **I2** can coordinate the substrate through the carbonyl moiety (**I3'$_{2.1}$**), undergoing the 1,2-addition of Cu-Bpin to the C=O via transition state **TS1'$_{2.1}$**. The overall process has a low free energy barrier (15.9 kcal·mol^{-1}), resulting in the thermodynamically stable, intermediate **I4'$_{2.1}$**. Nevertheless, the pathway for C=C borylcupration is kinetically preferred by 5.2 kcal·mol^{-1} (**TS1$_{2.1}$** *versus* **TS1'$_{2.1}$** in Figure 2.4), agreeing with the experimental results.

Table 2.4. Calculated free energy barriers and differences in kcal·mol^{-1} for the borylcupration of C=C *versus* C=O bond, $\Delta\Delta G^{\ddagger}$(**TS1**-**TS1'**), for γ-substituted alkenyl aldehydes **2.1**, **2.7**, **2.14**, **2.24**, and **2.27**. Free energy barriers $\Delta G^{\ddagger}_{C=C}$ (**I2**→**TS1**), $\Delta G^{\ddagger}_{C=O}$ (**I2**→**TS1'**).

Substrate	C=C:C=O (exp.)	$\Delta G^{\ddagger}_{C=C}$	$\Delta G^{\ddagger}_{C=O}$	$\Delta\Delta G^{\ddagger}$
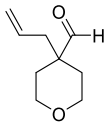 **2.1**	100:0	10.7	15.9	+5.2
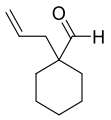 **2.7**	100:0	12.6	16.9	+4.3
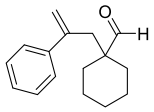 **2.14**	100:0	9.3	15.9	+6.6
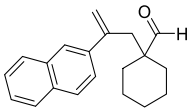 **2.24**	100:0	7.2	11.7	+9.0
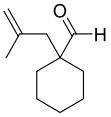 **2.27**	0:100	16.1	13.1	-2.9

Table 2.4 compares the free-energy barriers for the two competitive borylation processes in representative γ-substituted alkenyl aldehydes **2.1**, **2.7**, **2.14**, **2.24**, and **2.27**. Replacement of a tetrahydropyran group in **2.1** by cyclohexane in **2.7** has a minor effect on the barriers. Then, incorporating aromatic substituents in the alkene moiety (substrate **2.14**) decreases the energy barrier for the borylation on the C=C bond, providing the kinetic preference for ring-closing products. Since boryl-copper complexes behave as nucleophiles,[10,11] the electron-withdrawing aromatic substituents enhance the reactivity of the double bond. On the other hand, the methyl substituent in substrate **2.27** makes the alkene fragment more electron-rich, increasing the borylation energy barrier and switching the chemoselectivity towards the addition on the aldehyde moiety (intermediate **2.28** in Scheme 2.6). Figure 2.6 shows the detailed free-energy profile of the chemoselectivity determining steps for the borylation of substrate **2.27**. In this case, the coordination of substrate through the carbonyl moiety to yield intermediate $\mathbf{I3'_{2.27}}$ is slightly exergonic (-1.5 kca·mol^{-1}). Consequently, the free-energy barrier of the C=O borylation step increases slightly, $\Delta G^{\ddagger}$($\mathbf{I3'_{2.27}}$→ $\mathbf{TS1'_{2.27}}$) = 14.6 kcal·mol^{-1}, but it is still lower than that for the C=C

Nucleophilic Cu-B addition to alkenes with concomitant intramolecular coupling with aldehydes

borylation ($\Delta G^{\ddagger}$(**I2**$_{2.27}$→ **TS1**$_{2.27}$) = 16.1 kcal·mol^{-1}). Moreover, if we assume the Curtin-Hammet conditions (rapid equilibrium between species **I3'**$_{2.27}$ and **I3**$_{2.27}$ and irreversible step), the product distribution is determined by the relative free-energy of the two transition states ($\Delta\Delta G^{\ddagger}$(**TS1**$_{2.27}$→ **TS1'**$_{2.27}$)) that clearly favours the 1,2-addition of Cu-Bpin to the C=O by 2.9 kcal·mol^{-1}, in agreement with experimental observations.

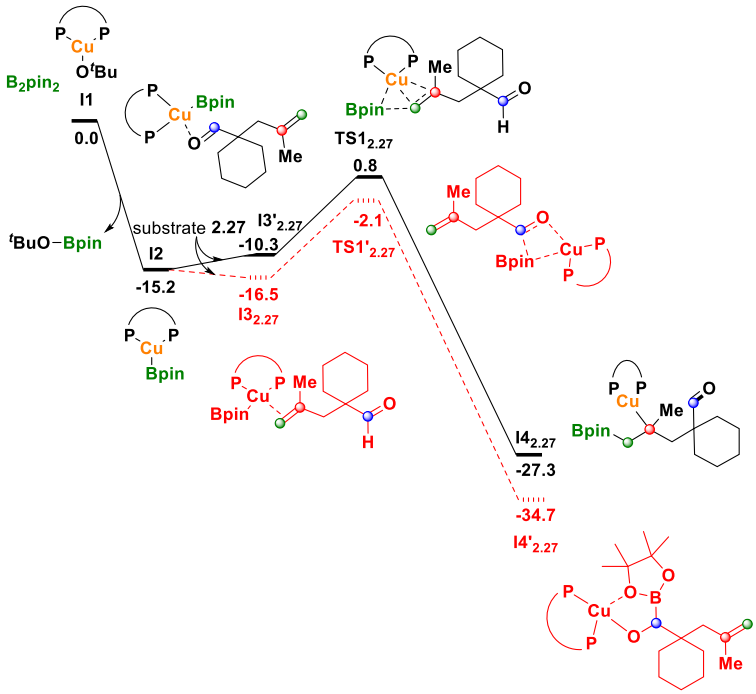

Figure 2.6. Computed free energy profile (in kcal·mol^{-1}) of chemoselectivity determining steps for substrate **2.27**. Solid, black lines represent the borylcupration of the C=C bond, and dashed, red lines represent the borylcupration of the C=O bond. P-P= Xantphos.

The diastereoselectivity is decided at the C-C coupling step where the aldehyde functional group can adopt an *anti* or a *syn* disposition respect to the borylmethyl unit (**TS2**$_{anti\text{-}2.1}$ and **TS2**$_{syn\text{-}2.1}$, Figure 2.7). In substrate **2.1**, the *anti*-configuration minimizes the 1,2 repulsion between the substituents of cyclobutane, resulting in a significantly lower free energy barrier (13.7 *versus* 17.6 kcal·mol^{-1} for **I4** → **TS2**$_{anti}$ and **I4** → **TS2**$_{syn}$, respectively). Additional calculations were performed in model systems replacing each phenyl substituent of Xantphos ligand by hydrogen and maintaining the backbone (PH_2 model) sets off ligand-substrate interactions. The results show that a free energy difference between the two diastereoselective paths is very similar to the *real-world* ligands, $\Delta\Delta G^{\ddagger}$ = +4.2 kcal·mol^{-1},

indicating that intramolecular interactions within the substrate (-CH_2Bpin···C=O) are responsible for the diastereoselectivity.

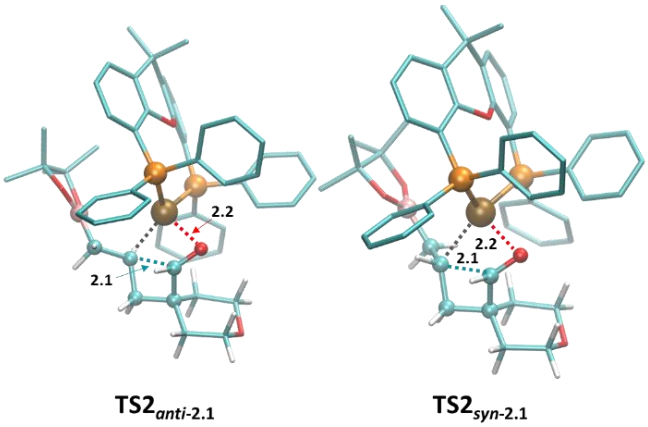

Figure 2.7. Molecular structures and main geometric parameters (Å) of the key transition states (**TS2**$_{anti\text{-}2.1}$ and **TS2**$_{syn\text{-}2.1}$).

Table 2.5. Calculated free energy barriers and differences in kcal·mol^{-1} for the borylative ring-closing of the diastereoselective *anti versus syn* paths, $\Delta\Delta G^{\ddagger}$(**TS2**$_{anti}$-**TS2**$_{syn}$) for γ-substituted alkenyl aldehydes **2.1**, **2.3** and **2.24**. Free energy barriers, $\Delta G^{\ddagger}_{anti}$ (**I4**→**TS1**$_{anti}$), and $\Delta G^{\ddagger}_{syn}$ (**I4**→**TS1**$_{syn}$).

Substrate	*anti*:*syn* (exp.)	$\Delta G^{\ddagger}_{anti}$	$\Delta G^{\ddagger}_{syn}$	$\Delta\Delta G^{\ddagger}$
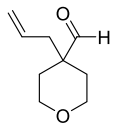 **2.1**	100:0	13.7	17.6	+5.1
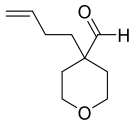 **2.3**	100:0	15.5	18.7	+3.2
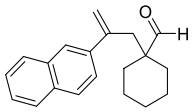 **2.24**	50:50	10.4	10.1	+0.3

Table 2.5 collects the free energy barriers of the competing paths in the diastereoselectivity determining step for several substrates, demonstrating that the mechanistic proposal is consistent with the experimental outcome. Interestingly, introducing a 2-naphthyl group on the alkene moiety (substrate **2.24**) produced a mixture of *anti* and *syn* diastereoisomers. Accordantly, the computed free energy difference between the two corresponding transition states, $\Delta\Delta G^{\ddagger}$(**TS2**$_{syn\text{-}2.24}$-**TS2**$_{anti\text{-}2.24}$), is reduced to only 0.3 kcal·mol^{-1} (Figure 2.8).

Nucleophilic Cu-B addition to alkenes with concomitant intramolecular coupling with aldehydes

---

Figure 2.8 shows the detailed free energy profiles for the two possible diastereoisomeric pathways for substrate **2.24**. In this case, the bulky naphthyl substituent leads to 1,2 repulsive interactions with the carbonyl group in the *anti*-path, similar to those between the carbonyl group and the -CH_2Bpin moiety in the *syn* isomer. Consequently, no preference for any of the two diastereoisomers is observed (see Figure 2.9 for the corresponding transition state structures).

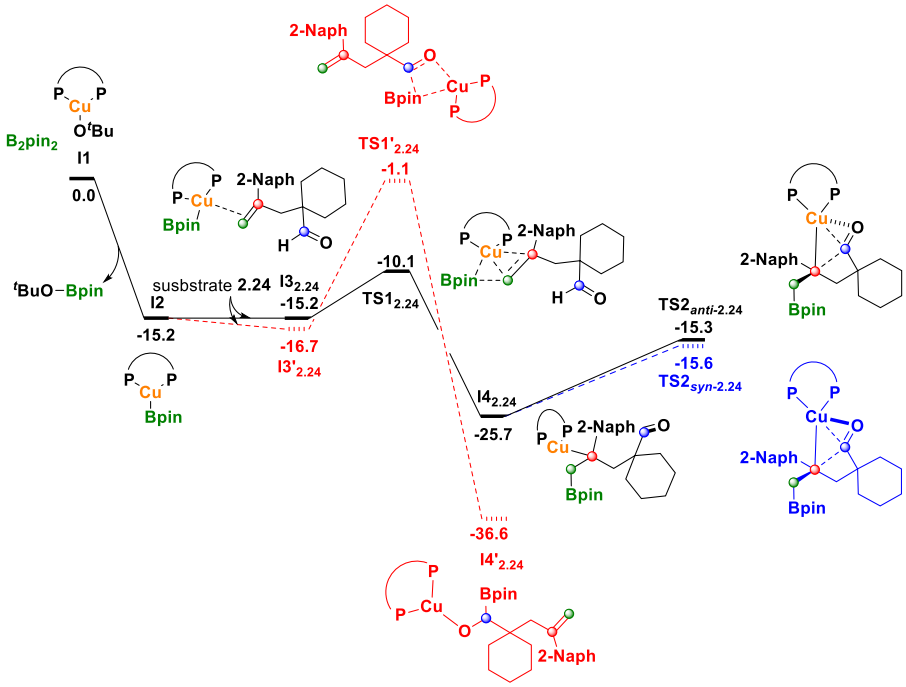

Figure 2.8. Computed free energy profile (in kcal·mol^{-1}) for the reaction of **2.24** forming two diastereoisomers, *anti* and *syn* represented with solid, black lines and dashed, blue lines, respectively. Dashed, red lines represent alternative pathway related to chemoselectivity. P-P= Xantphos.

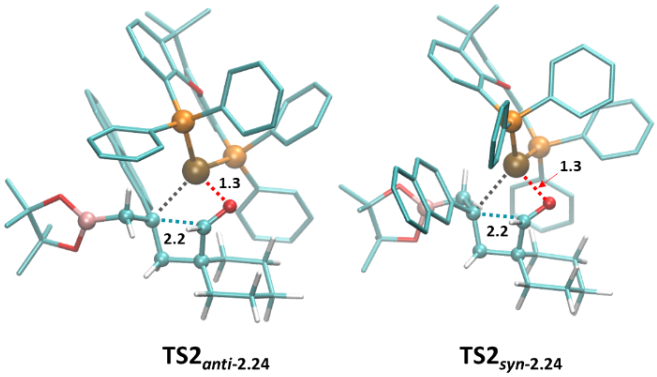

Figure 2.9. Molecular structures and main geometric parameters (Å) of transition states **TS2***anti-24* and **TS2***syn-24* for the ring-closing step in borylative cyclization of substrate **2.24**.

2.4 Conclusions

We have shown that copper(I) complex modified with Xantphos ligand is able to catalyze the borylative cyclization of γ-alkenyl aldehydes. The specific conclusions are:

- Borylcupration on C=C bond is preferred for electron-deficient alkene moieties, as described for aromatic substituted γ-alkenyl aldehydes (**2.14** and **2.24**). It could be postulated that the electron density on the nucleophile carbon could resonate with the aromatic ring.
- Despite the chemoselectivity issues arising from competitive 1,2-borylation of the aldehyde, this methodology provides access to spirocyclic cyclobutanol products with high levels of *anti*-diastereoselection in moderate to good yields.
- Substituents are required at the aldehyde α-carbon, and both four and five-membered rings can be formed.
- A variety of substituted olefins can be employed, but electron-rich olefins (**2.27**) suppress the borylation through the C=C bond favoring the borylation on the C=O bond.
- DFT studies identify and analyze the key steps of the catalytic cycle that govern the chemo- and diastereoselectivity. The addition of Cu-Bpin to C=C or C=O bond (transition states **TS1** and **TS1'**, respectively) determines the chemoselectivity. Due to the nucleophilic nature of the boryl fragment, electron-donor substituents on the alkene can switch the chemoselectivity towards the boryl addition to the aldehyde (i.e. substrate **2.27**). The diastereoselectivity-determining step corresponds to the carbon-carbon coupling process (**TS2***anti* and **TS2***syn*), where intramolecular interactions within the substrate govern the diastereoselectivity.

2.5 Computational Details

Geometry optimizations and transition state searches were performed with Gaussian 16 package.[12] The quantum mechanics calculations were performed within the framework of Density Functional Theory (DFT)[13–16] by using the ωB97X-D functional.[17] Two different basis sets were used. The first one (*basis set I*) was used for geometry optimizations, and frequency calculations, where we defined effective core potentials (ECPs) with double-ζ valence basis set (LANDL2DZ)[18–20] were employed for Cu and P, supplemented with polarized shells with the following exponents: Cu (f = 3.525) and P (d = 0.387).[21,22] For all other electrons of all other atoms, 6-31G(d) basis set was used.[23–25] All calculation was performed within solvent (THF) represented via the SMD model.[26] Potential energies were refined through single-point calculations with a larger *basis set II*, which consisted of LANL2TZ(f) for Cu,[18–22,27] LANL08(d) for P[18–22,27] and 6-311++G(d,p)[23–25] for other atoms. Free energy corrections were considered at a concentration of 1 M and a temperature of 298.15 K.

2.6 References

(1) Kubota, K.; Ito, H. Borylative Ring Closing. In *Advances in Organoboron Chemistry towards Organic Synthesis*; Science of Synthesis, Fernández, E.; ed, Georg Thieme Verlag: Stuttgart, **2019**; Vol. 2019/6, pp 227–269.

(2) Kubota, K.; Yamamoto, E.; Ito, H. Copper(I)-Catalyzed Borylative *Exo*-Cyclization of Alkenyl Halides Containing Unactivated Double Bond. *J. Am. Chem. Soc.* **2013**, *135* (7), 2635–2640.

(3) Yamamoto, E.; Kojima, R.; Kubota, K.; Ito, H. Copper(I)-Catalyzed Diastereoselective Borylative *Exo*-Cyclization of Alkenyl Aryl Ketones. *Synlett* **2016**, *27* (2), 272–276.

(4) Whyte, A.; Mirabi, B.; Torelli, A.; Prieto, L.; Bajohr, J.; Lautens, M. Asymmetric Synthesis of Boryl-Functionalized Cyclobutanols. *ACS Catal.* **2019**, *9* (10), 9253–9258.

(5) Green, J. C.; Joannou, M. V; Murray, S. A.; Zanghi, J. M.; Meek, S. J. Enantio- and Diastereoselective Synthesis of Hydroxy Bis(Boronates) via Cu-Catalyzed Tandem Borylation/1,2-Addition. *ACS Catal.* **2017**, *7* (7), 4441–4445.

(6) Laitar, D. S.; Tsui, E. Y.; Sadighi, J. P. Catalytic Diboration of Aldehydes via Insertion into the Copper−Boron Bond. *J. Am. Chem. Soc.* **2006**, *128* (34), 11036–11037.

(7) Moore, C. M.; Medina, C. R.; Cannamela, P. C.; McIntosh, M. L.; Ferber, C. J.; Roering, A. J.; Clark, T. B. Facile Formation of β-Hydroxyboronate Esters by a Cu-Catalyzed Diboration/Matteson Homologation Sequence. *Org. Lett.* **2014**, *16* (23), 6056–6059.

(8) Carreira, E. M.; Fessard, T. C. Four-Membered Ring-Containing Spirocycles: Synthetic Strategies and Opportunities. *Chem. Rev.* **2014**, *114* (16), 8257–8322.

(9) Royes, J.; Ni, S.; Farré, A.; La Cascia, E.; Carbó, J. J.; Cuenca, A. B.; Maseras, F.; Fernández, E. Copper-Catalyzed Borylative Ring Closing C–C Coupling toward Spiro- and Dispiroheterocycles. *ACS Catal.* **2018**, *8* (4), 2833–2838.

(10) Cid, J.; Carbó, J. J.; Fernández, E. Disclosing the Structure/Activity Correlation in Trivalent Boron-Containing Compounds: A Tendency Map. *Chem. – Eur. J.* **2012**, *18* (40), 12794–12802.

(11) García-López, D.; Cid, J.; Marqués, R.; Fernández, E.; Carbó, J. J. Quantitative Structure–Activity Relationships for the Nucleophilicity of Trivalent Boron Compounds. *Chem. – Eur. J.* **2017**, *23* (21), 5066–5075.

(12) Frisch, M. J.; Trucks, G. W.; Schlegel, H. B.; Scuseria, G. E.; Robb, M. A.; Cheeseman, J. R.; Scalmani, G.; Barone, V.; Petersson, G. A.; Nakatsuji, H.; Li, X.; Caricato, M.; Marenich, A. V; Bloino, J.; Janesko, B. G.; Gomperts, R.; Mennucci, B.; Hratchian, H. P.; Ortiz, J. V; Izmaylov, A. F.; Sonnenberg, J. L.; Williams-Young, D.; Ding, F.; Lipparini, F.; Egidi, F.; Goings, J.; Peng, B.; Petrone, A.; Henderson, T.; Ranasinghe, D.; Zakrzewski, V. G.; Gao, J.; Rega, N.; Zheng, G.; Liang, W.; Hada, M.; Ehara, M.; Toyota, K.; Fukuda, R.; Hasegawa, J.; Ishida, M.; Nakajima, T.; Honda, Y.; Kitao, O.; Nakai, H.; Vreven, T.; Throssell, K.; Montgomery Jr., J. A.; Peralta, J. E.; Ogliaro, F.; Bearpark, M. J.; Heyd, J. J.; Brothers, E. N.; Kudin, K. N.; Staroverov, V. N.;

Keith, T. A.; Kobayashi, R.; Normand, J.; Raghavachari, K.; Rendell, A. P.; Burant, J. C.; Iyengar, S. S.; Tomasi, J.; Cossi, M.; Millam, J. M.; Klene, M.; Adamo, C.; Cammi, R.; Ochterski, J. W.; Martin, R. L.; Morokuma, K.; Farkas, O.; Foresman, J. B.; Fox, D. J. Gaussian16 Revision A03. 2016.

(13) Hohenberg, P.; Kohn, W. Inhomogeneous Electron Gas. *Phys. Rev.* **1964**, *136* (3B), B864–B871.

(14) Kohn, W.; Sham, L. J. Self-Consistent Equations Including Exchange and Correlation Effects. *Phys. Rev.* **1965**, *140* (4A), A1133–A1138.

(15) Yang, R. G. P. and W. *Density-Functional Theory of Atoms and Molecules*; Oxford Univ. Press: Oxford, **1989**.

(16) Comstock, M. J. The Challenge of d and f Electrons, Copyright, ACS Symposium Series, Foreword. In *The Challenge of d and f Electrons*; Comstock, M. J., Ed.; ACS Symposium Series; American Chemical Society, **1989**; Vol. 394, pp i–iv.

(17) Chai, J.-D.; Head-Gordon, M. Long-Range Corrected Hybrid Density Functionals with Damped Atom–Atom Dispersion Corrections. *Phys. Chem. Chem. Phys.* **2008**, *10* (44), 6615–6620.

(18) Hay, P. J.; Wadt, W. R. Ab Initio Effective Core Potentials for Molecular Calculations. Potentials for K to Au Including the Outermost Core Orbitals. *J. Chem. Phys.* **1985**, *82* (1), 299–310.

(19) Hay, P. J.; Wadt, W. R. Ab Initio Effective Core Potentials for Molecular Calculations. Potentials for the Transition Metal Atoms Sc to Hg. *J. Chem. Phys.* **1985**, *82* (1), 270–283.

(20) Wadt, W. R.; Hay, P. J. Ab Initio Effective Core Potentials for Molecular Calculations. Potentials for Main Group Elements Na to Bi. *J. Chem. Phys.* **1985**, *82* (1), 284–298.

(21) Höllwarth, A.; Böhme, M.; Dapprich, S.; Ehlers, A. W.; Gobbi, A.; Jonas, V.; Köhler, K. F.; Stegmann, R.; Veldkamp, A.; Frenking, G. A Set of D-Polarization Functions for Pseudo-Potential Basis Sets of the Main Group Elements Al-Bi and f-Type Polarization Functions for Zn, Cd, Hg. *Chem. Phys. Lett.* **1993**, *208* (3), 237–240.

(22) Ehlers, A. W.; Böhme, M.; Dapprich, S.; Gobbi, A.; Höllwarth, A.; Jonas, V.; Köhler, K. F.; Stegmann, R.; Veldkamp, A.; Frenking, G. A Set of F-Polarization Functions for Pseudo-Potential Basis Sets of the Transition Metals Sc-Cu, Y-Ag and La-Au. *Chem. Phys. Lett.* **1993**, *208* (1), 111–114.

(23) Fukui, K. Formulation of the Reaction Coordinate. *J. Phys. Chem.* **1970**, *74* (23), 4161–4163.

(24) Gordon, M. S. The Isomers of Silacyclopropane. *Chem. Phys. Lett.* **1980**, *76* (1), 163–168.

(25) Binning Jr., R. C.; Curtiss, L. A. Compact Contracted Basis Sets for Third-Row Atoms: Ga–Kr. *J. Comput. Chem.* **1990**, *11* (10), 1206–1216.

(26) Marenich, A. V; Cramer, C. J.; Truhlar, D. G. Universal Solvation Model Based on Solute Electron Density and on a Continuum Model of the Solvent Defined by the Bulk Dielectric Constant and Atomic Surface Tensions. *J. Phys. Chem. B* **2009**, *113* (18), 6378–6396.

(27) Roy, L. E.; Hay, P. J.; Martin, R. L. Revised Basis Sets for the LANL Effective Core Potentials. *J. Chem. Theory Comput.* **2008**, *4* (7), 1029–1031.

Chapter 3
Allylic Borylation of conjugated dienes catalyzed by alkoxides

3.1 Abstract and specific objectives

This Chapter will focus on the complementary reactivity of diboron reagents with 1,3-dienes in a transition-metal-free context, in comparison with previous attempts using Pt, Ni or Cu complexes as catalysts. The sole addition of Na_2CO_3 (30 mol%) to bis(pinacolato)diboron in MeOH as solvent allows the formation of the Lewis acid-base adduct [MeO-Bpin-Bpin]$^-$ [Hbase]$^+$, responsible for the 1,4-hydroboration of cyclic and non-cyclic 1,3-dienes (Scheme 3.1). The specific goals in this Chapter are:

- The study of the optimized reaction conditions to proof our work hypothesis towards the first transition-metal-free borylation of 1,3-dienes
- The search of substrate scope to generalize the new C-B bond formation with non-cyclic and cyclic 1,3-dienes
- The study of the transformation of allylboronates esters towards valuable allylic alcohols.
- The study of the preferred stereoselectivity for *E* allylic boronate products in non-cyclic 1,3-dienes.
- The use of DFT calculations to suggest the reaction mechanism and the analysis of the factor that governs the selectivity towards 1,4-hydroboration.

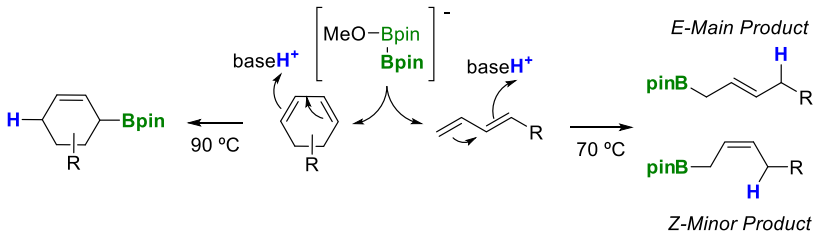

Scheme 3.1. Reaction pathway for 1,4-hydroboration with cyclic and non-cyclic conjugated dienes.

3.2 State of the Art

The borylation of 1,3-dienes represents a powerful synthetic tool to obtain diborated or monoborated allylic systems, depending on the transition-metal catalyst employed. From Miyaura and co-worker's breakthrough experiments on $Pt(PPh_3)_4$-catalyzed 1,4-diboration of 1,3-dienes to synthesize bis(allyl)boronates,[1] the field has progressed by discovering different catalytic systems based on Pt, Ni, and Cu. The most explored strategy uses Pt complexes to catalyze both 1,2- and 1,4-diboration of 1,3-dienes, even in an asymmetric fashion.[2–7] Nickel complexes are also explored as catalytic systems, and unlike Pt complexes, the Ni catalytic systems can catalyze the 1,4-selective diboration of even sterically hindered 1,3-dienes.[8–11] Contrary to Pt or Ni complexes, the Cu complexes catalyze the monoboration of 1,3-dienes with B_2pin_2 primarily forming the homoallyl boronate products (Scheme 3.2).[12,13]

Here, in this chapter, we present the results of the borylation of 1,3-dienes in a transition-metal-free context, with the sole addition of MeOH and base to generate the corresponding methoxide and form the adduct [MeO-Bpin-Bpin]$^-$[Hbase]$^+$ (Scheme 3.2, bottom right).

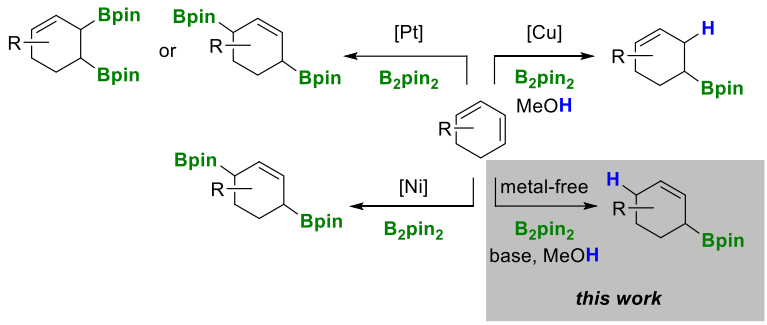

Scheme 3.2. Examples of previous transition-metal-catalyzed diboration and monoboration of 1,3-dienes for comparison with the transition-metal-free version reported in this chapter.

Transition-metal-free borylation reactions have emerged within this decade as a convenient synthetic methodology toward selective C–B bond formation.[14] Our group has previously explored the allylic borylation of tertiary allylic alcohols[15] as well as the allylic borylation of vinyl epoxides and vinyl aziridines[16] by the addition of the acid–base Lewis adduct [MeO-Bpin-Bpin]$^-$[Hbase]$^+$ through S_N2'-type mechanisms. To the best of our knowledge, the borylation of 1,3-dienes without metal catalysts was only precedented through the uncatalyzed diboration of 1,3-butadiene using the highly reactive B_2Cl_4 or B_2F_4 to produce 1,4-bis-(dihalogenoboryl)-2-butene compounds.[17,18] However, the transition-metal-free borylation of 1,3-dienes opens new questions about the preference for mono- or diborated

products, as well as whether the *E*- or the *Z*-allyl boronate products are going to be preferentially formed in non-cyclic systems.

3.3 Results and Discussion

In order to answer all of the questions raised above, we selected the model substrate *trans*-1-phenyl-1,3-butadiene (**3.1**) and we carried out the borylation with 1.1 equiv of B_2pin_2 in the presence of 15 mol% of Na_2CO_3 and MeOH as solvent (1 mL) at 90 °C. The analysis of the unpurified reaction mixture by ^{1}H NMR spectroscopy established 47% conversion toward the 1,4-hydroborated product **3.2** (*E*/*Z* = 2/1) (Scheme 3.3a) and 22% of polyborylated products (**3.3**)[19] without the consumption of all the starting material. Decreasing the temperature to 70 °C and increasing the amount of base to 30 mol% allowed the formation of **3.2** in 60% (*E*/*Z* = 3/1), minimizing the byproduct formation. Remarkably, this is the first attempt to borylate 1,3- dienes in a transition-metal-free context, and the results seem to be complementary to Huang and co-workers' work,[20] where the same substrate **3.1** underwent 1,4-hydroboration with HBpin in the presence of iminopyridine Fe complexes, but forming principally the secondary (*Z*)-allylboronate (Scheme 3.3b).

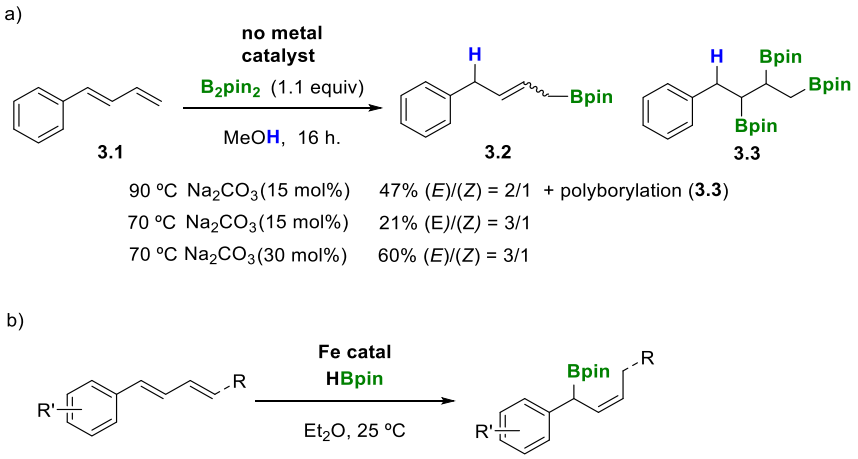

Scheme 3.3. Proof of concept in the transition-metal-free borylation of 1,3-dienes and comparison with Fe-catalyzed hydroboration towards secondary (*Z*)-allylboronate.

When *trans*-1-methyl-1,3-butadiene (**3.4**) reacted with 1.1 equivalents of B_2pin_2, 1,2-diboration of the terminal alkene took place instead to form product **3.5** in 58% NMR yield (33% isolated) (Scheme 3.4a). It seems that the competing 1,2-diboration is favored *versus* 1,4-hydroboration for alkyl substituents at the C_1 position,[21,22] in contrast to the Fe–Mg-catalyzed 1,4-hydroboration of 1-alkylsubstituted 1,3-dienes or 2-alkyl-substituted 1,3-dienes, observed by the groups of Huang and Ritter, respectively.[20,23] To confirm the

previous observation, we conducted the transition-metal free borylation of (*Z*)-penta-1,3-dien-3-ylbenzene (**3.6**), and as expected, the 1,2-diborated product **3.7** was also formed despite the presence of the phenyl group at the C_3 position (Scheme 3.4b).

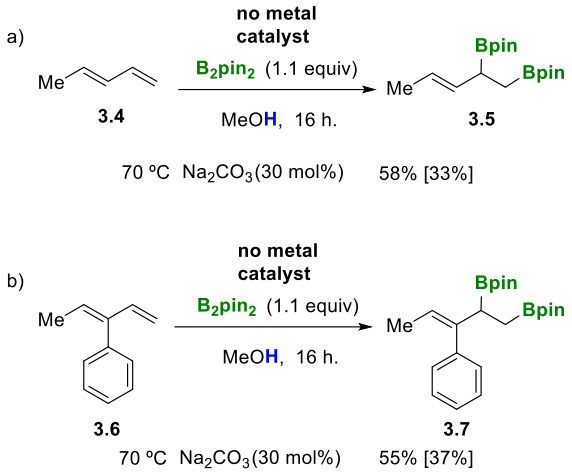

Scheme 3.4. Transition-metal-free 1,2-diboration of *trans*-1-methyl-1,3-butadiene (**3.4**) and (*Z*)-penta-1,3-dien-3- ylbenzene (**3.6**)· NMR yields calculated with naphthalene as internal standard [% isolated yields].

To extend the transition-metal-free conjugative borylation on *trans*-1-aryl-1,3-butadiene type substrates, we carried out a systematic study under the optimized reaction conditions, based on the addition of B_2pin_2 (1.1 equiv) to a solution of MeOH that contains the substrate and 30 mol% of Na_2CO_3. As can be seen in Table 3.1, *trans*-1-aryl-1,3-butadienes, that contain electron-donating and electron-withdrawing substituents on the aryl group, do not affect the reaction outcome (Table 3.1, entries 1−3). However, a slight increase in the *E*/*Z* ratio (up to 4/1) was observed for product **3.13**. It is worth mentioning that substrate buta-1,3- diene-1,1-diyldibenzene **3.14** was borylated with similar success but the enhanced *E*/*Z* ratio (up to 9/1) indicated the preference for the *E* isomer in compound **3.15** when the two aryl groups are located at the terminal position (Table 3.1, entry 4). We were also able to conduct the transition-metal-free 1,4-hydroboration of (*E*)-2-(buta-1,3-dien-1-yl)furan **3.16** toward the desired allylic boronate product **3.17**, demonstrating the compatibility with other conjugated systems (Table 3.1, entry 5).

Allylic Borylation of conjugated dienes catalyzed by alkoxides

Table 3.1. Transition-metal-free 1,4-hydroboration of *trans*-1-aryl-1,3-butadienes. [a]

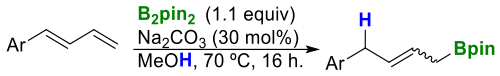

Entry	Substrate	Product	*E/Z*	NMR Yield[b] [Isolated Yield]
1	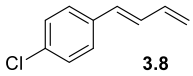 **3.8**	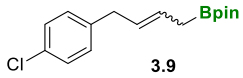 **3.9**	3/1	50% [23%]
2	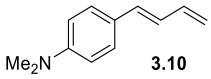 **3.10**	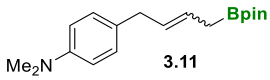 **3.11**	3/1	55% [38%]
3	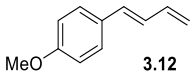 **3.12**	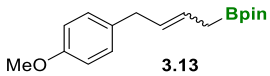 **3.13**	4/1	61% [32%]
4	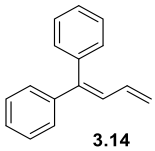 **3.14**	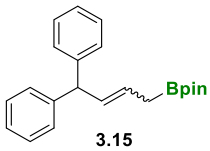 **3.15**	9/1	62% [40%]
5	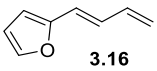 **3.16**	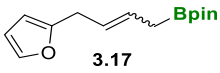 **3.17**	4/1	53% [15%]

[a] **Reaction conditions:** Substrate (0.2 mmol), B_2pin_2 (1.1 equiv) Na_2CO_3 (30 mol%), MeOH (1 mL), 70 °C, 16 h.
[b]NMR yields calculated with naphthalene as internal standard, [% Isolated yields].

The general method was also applied to internal 1,3 dienes such as ((1*E*,3*E*)-penta-1,3-dien-1-yl)benzene **3.18** and related substrates **3.20** and **3.22**. To our delight, the 1,4-hydroboration took place toward the formation of the desired allylic boronates **3.19**, **3.21**, and **3.23** without any reduction in the yield or the *E*/*Z* ratio (Table 3.2, entries 1−3). The internal substitution in substrate (*E*)-(2-methylbuta-1,3-dien-1-yl)- benzene **3.24**, also proved not to be influential to the reaction outcome as product **3.25** was formed with similar conversion and selectivity (Table 3.2, entry 4).

Table 3.2. Transition-metal-free 1,4-hydroboration of internal 1,3-dienes.[a]

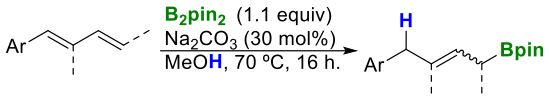

Entry	Substrate	Product	*E/Z*	NMR Yield[b] [Isolated Yield]
1	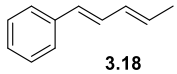 3.18	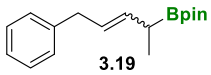 3.19	3/1	71% [16%]
2	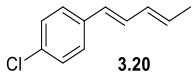 3.20	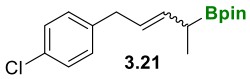 3.21	3/1	50% [23%]
3	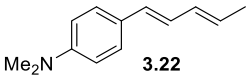 3.22	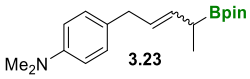 3.23	3/1	55% [38%]
4	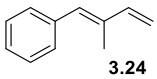 3.24	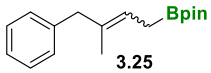 3.25	3/1	65% [60%]

[a] **Reaction conditions:** Substrate (0.2 mmol), B_2pin_2 (1.1 equiv) Na_2CO_3 (30 mol%), MeOH (1 mL), 70 °C, 16 h.
[b]NMR yields calculated with naphthalene as internal standard, [% Isolated yields].

We next considered the possibility to extend the transition-metal-free allylic borylation methodology to cyclic 1,3-dienes. We found that cyclohexadiene (**3.26**) was transformed into the corresponding allyl boronate via 1,4-hydroboration under the same reaction conditions as for non-cyclic systems except that 90 °C was required (Table 3.3, entry 1). This is interesting because in this substrate there are no aryl substituents that direct the conjugative borylation as in substrate **3.2**, and so the 1,2 diborated product could be expected to be formed as in the borylation of *trans*-1-methyl-1,3-butadiene (**3.4**) (Scheme 3.4). In extension, substrate 2-(2-ethylhexyl)cyclohexa-1,3-diene (**3.28**) could be efficiently borylated toward the allylic bororonate product **3.29**, despite the added steric hindrance provided by having a substituent at the internal position (Table 3.3, entry 2). Even the disubstituted cyclic 1,3-diene 5- isopropyl-2-methylcyclohexa-1,3-diene (**3.30**) was transformed into the allylic boronate product **3.31**, with an *anti*-configuration of the Bpin moiety with regard to the isopropyl functional group (Table 3.3, entry 3).

Table 3.3 Transition-metal-free 1,4-hydroboration of cyclic 1,3-dienes.[a]

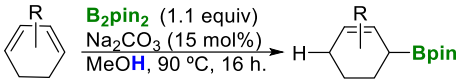

Entry	Substrate	Product	NMR Yield[b] [Isolated Yield]
10	 3.26	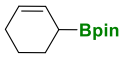 3.27	55% [35.5%]
11	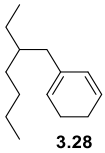 3.28	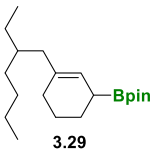 3.29	79% [59%]
12	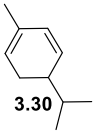 3.30	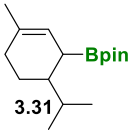 3.31	65% [59%]

[a] **Reaction conditions:** Substrate (0.2 mmol), B_2pin_2 (1.1 equiv) Na_2CO_3 (15 mol%), MeOH (1 mL), 90 °C, 16 h. [b]NMR yields calculated with naphthalene as internal standard, [% Isolated yields].

Allyl boronate products are very important building blocks,[24] and in our hands, the allyl boronate product **3.2** has been transformed into 1,2,3-triborated product **3.3** via consecutive transition-metal-free diboration of the internal double bond (Scheme 3.5). The triborated product **3.3** was quantitatively formed and isolated from the reaction as a unique product. The extension of this interesting transformation has been recently explored with a detailed study of the concomitant selective cross-coupling reaction from triborated compounds.[19]

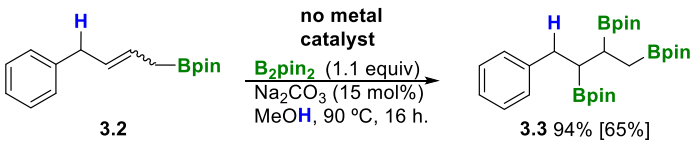

Scheme 3.5. Synthesis of 1,2,3-triborated products from the allyl boronates.

The *in situ* oxidative workup of the allylic boronate compounds, prepared in this work, provide the corresponding allylic alcohols in a transition metal-free context with a preference for the *E*-isomer (Scheme 3.6). The formation of allylic alcohols through

borylation reactions was recently reported in the Cu-catalyzed borylation of vinyl cyclic carbonates via an S_N2' mechanism, also with preference on the *E* isomer.[25]

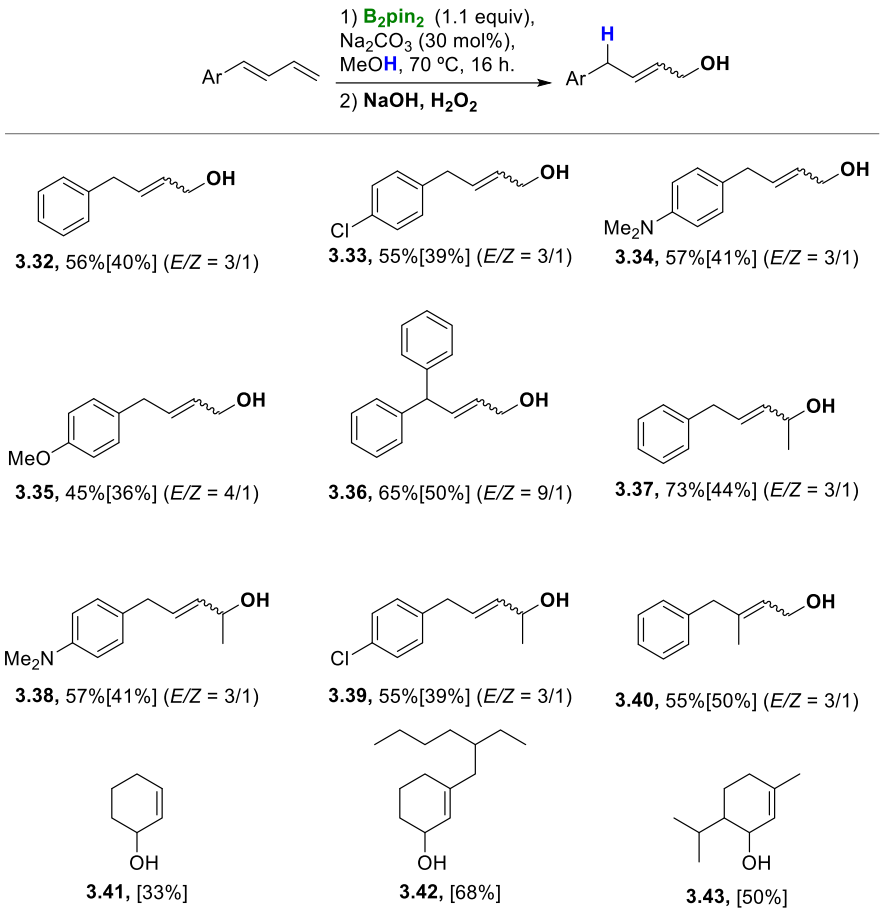

Scheme 3.6. Transition-metal-free 1,4-hydroboration/oxidation of *trans*-1-aryl-1,3-butadienes. NMR yields calculated with naphthalene as internal standard, [% isolated yields].

A proposed reaction mechanism for the transition-metal-free borylation of 1,3-dienes may involve first activation of the B_2pin_2 with MeOH/base to form adduct $[MeO\text{-}BpinBpin]^-[Hbase]^+$ followed by nucleophilic attack of the B (sp^2) moiety to the terminal double bond (Figure 3.1). The conjugative borylation may generate two isomeric allylic anion intermediates that can be protonated with MeOH, used as solvent. To evaluate this mechanistic proposal, we conducted DFT study (see Computational Details in Section 3.5).

Allylic Borylation of conjugated dienes catalyzed by alkoxides

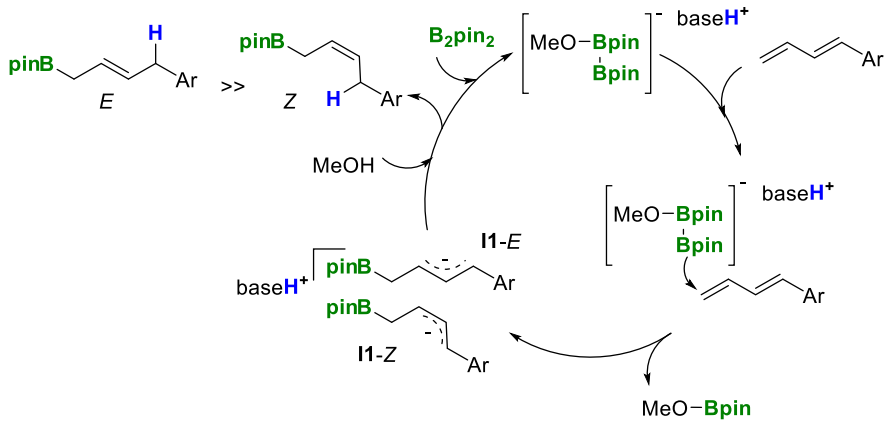

Figure 3.1. Proposed mechanism for transition-metal-free borylation of 1,3-dienes.

In order to understand the stereo- and regioselectivity of the transition-metal-free borylation of cyclic and 1-arylsubstituted 1,3-dienes. Previous computational studies have demonstrated the nucleophilic character of the B(sp^2) in the acid–base Lewis adduct [MeO-BpinBpin]$^-$[Hbase]$^+$[26–29] and that the electron-withdrawing substituents can favor the hydroboration over the diboration of C=C double bonds by stabilizing the anionic monoborylated intermediate.[30] Figure 3.2 and 3.3 displays the computed potential free-energy profile for the 1,4-hydroboration of *trans*-1-phenyl-1,3-butadiene (**3.1**) to yield both the *E* and the *Z* stereoisomeric products and the three-dimensional structures of the key transition states for the stereoselectivity control.

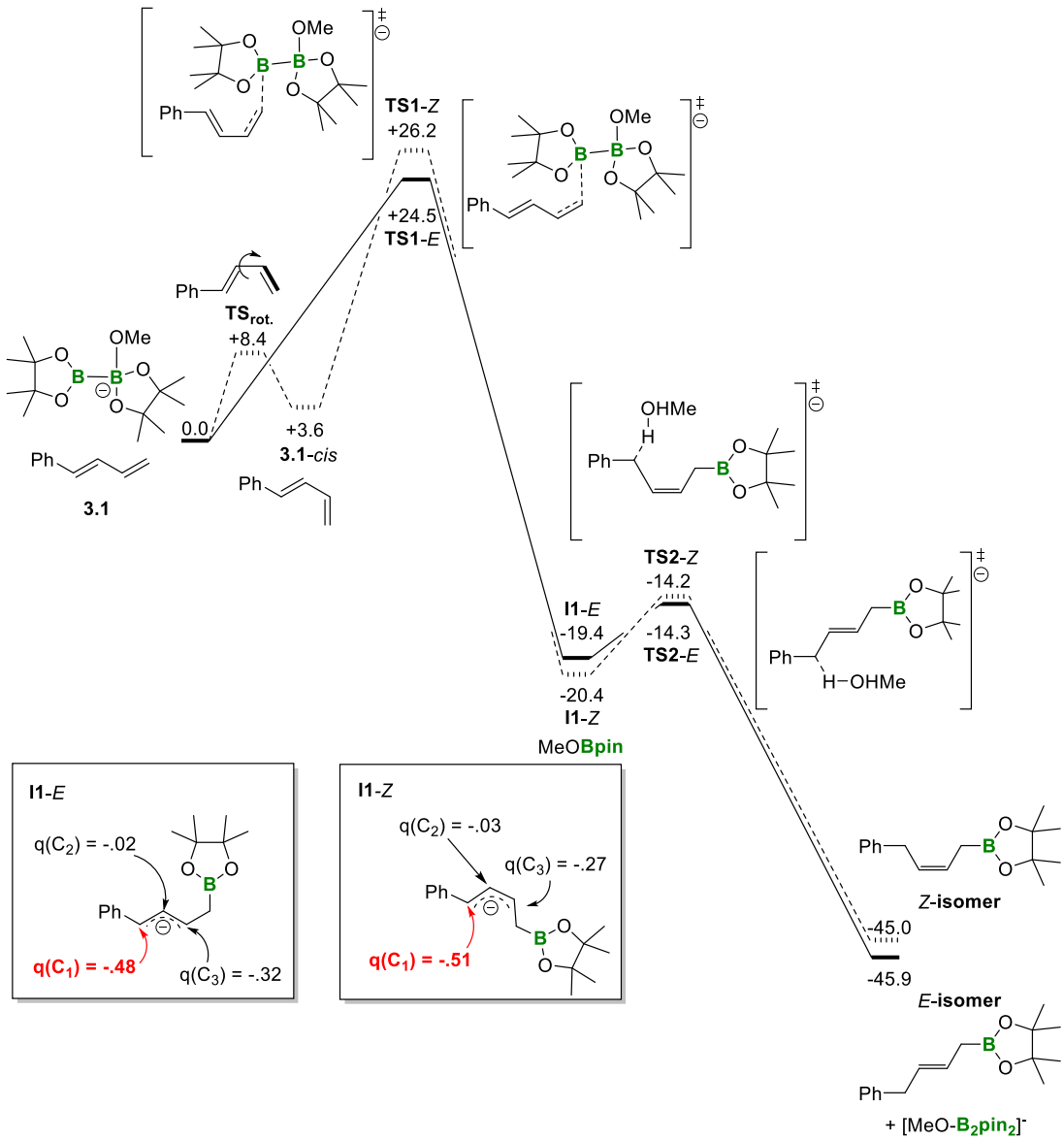

Figure 3.2. Potential free-energy profiles (kcal·mol^{-1}) for the 1,4-hydroboration of 1-*trans*-phenyl-1,3-butadiene (**3.1**) by B_2pin_2 in MeOH/base. Solid and dashed lines correspond to the paths yielding the *E* and *Z* stereoisomeric products respectively.

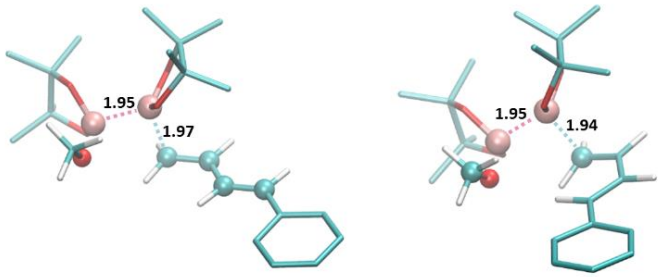

TS1-*E* **TS1-*Z***

Figure 3.3. Molecular structures of the transition states for the *E* and *Z* paths of the nucleophilic borylation of the diene **3.1** (**TS1-*E*** and **TS1-*Z***, respectively). Distances in Å.

The calculated free-energy barrier for the initial nucleophilic Bpin transfer to the terminal carbon of diene **3.1** is moderate (24.5 kcal·mol^{-1}) and leads to a stable anionic intermediate **I1**-*E* (*E*-path, solid lines). Similar to that observed for allemanides,[31] the anionic 3-membered boracycle intermediate opens to form a more stable allylic anion with an alkyl boronate group attached to the terminal carbon. Subsequent protonation of **I1**-*E* leads to the hydroborated product. The observed regioselective protonation of C_1 can be rationalized from the charge distribution in the allylic intermediate **I1**-*E* (Figure 3.2). Our calculations show that the phenyl-substituted C_1, supports a larger negative charge than the allylic C_2 and C_3. Consequently, the C_1 carbon should be more reactive toward protonation in agreement with the observed preference for 1,4- over the 3,4-hydroboration. In line with this, the estimated barrier for protonation at C_1 using a single MeOH solvent molecule is quite low (5.1 kcal·mol^{-1}).

To explain the formation of the observed *Z*-isomer, the *E* path has to undergo an isomerization process at some point in the catalytic cycle. The isomerization of the allylic intermediate **I1**-*E* to **I1**-*Z* via rotation around the C_2–C_3 bond is unlikely because the computed barrier of 19.3 kcal·mol^{-1} is significantly higher than that for the forward protonation reaction (5.1 kcal· mol^{-1}). Instead, we propose that the *trans* 1,3-diene isomerizes to the *cis* conformation. The computed barrier (8.4 kcal·mol^{-1}) and the energy difference (+3.6 kcal·mol^{-1}) might allow it. Borylation of the *cis* conformer yields intermediate **I1**-*Z* with the alkyl boronate group *cis* to C_1 (dashed lines in Figure 3.2). The lower stability of the *cis* isomer is partially compensated by a lower free-energy barrier for borylation (22.6 vs 24.5 kcal·mol^{-1}). Interestingly, the higher reactivity of *cis* conformations of α,β-unsaturated aldehydes and ketones has been explained from secondary orbital interactions which allow a better stabilization of the developing negative charge.[32,33] Overall, the transition state for the *Z* path (**TS1**-*Z*) is only 1.7 kcal·mol^{-1} higher than the

corresponding transition state for the *E* path (**TS1**-*E*). This results in a small preference for the *E* over the *Z* products, in full agreement with experimental observations.

For cyclic 1,3-dienes, we propose the same type of mechanism, in which only the *Z*-path is possible due to the *cis* configuration of the diene (Figure 3.4). The computed barrier for the nucleophilic Bpin transfer to the cyclohexadiene **3.26** is somewhat larger (27.4 kcal·mol^{-1}) than that for *E*-1-phenyl-1,3-butadiene (**3.1**) (24.5 kcal·mol^{-1}) but still reasonable for a reaction occurring at 90 °C. In this case, the absence of the phenyl substituent yields a less stable allylic anion intermediate **I1c** and makes possible the formation of the boracyclic species **I'c**. These intermediates, **I1c** and **I'c**, are close in energy and interconvert easily. In line with the observed regioselectivity toward 1,4-hydroboration, the C_1 carbon of both species supports the largest negative charge favoring its protonation, for which we found very small electronic energy barriers (<1 kcal·mol^{-1}).

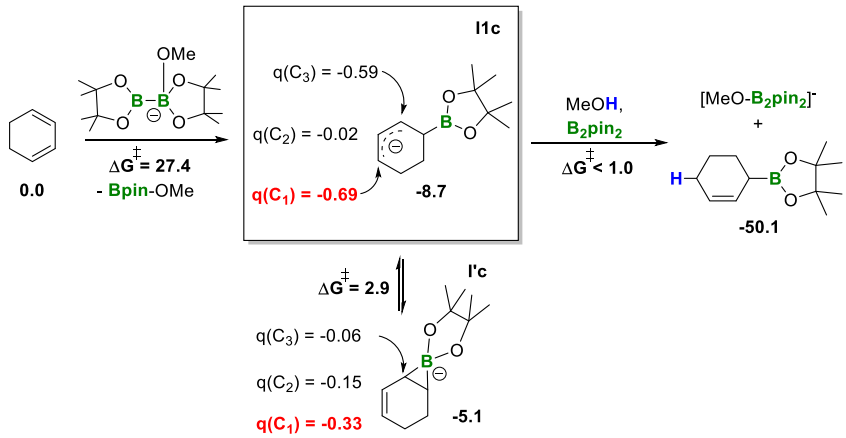

Figure 3.4. Proposed reaction mechanism for the 1,4-hydroboration of cyclohexadiene by B_2pin_2 in MeOH/base. Relative free-energies and barriers in kcal·mol^{-1}.

3.4 Conclusions

Interestingly, the sole addition of 15-30 mol% of Na_2CO_3 to B_2pin_2 in MeOH allows the 1,4-hydroboration of cyclic and non-cyclic 1,3-dienes. This unprecedented reactivity opens a new door to organoboron chemistry synthesis in a transition metal-free context. The main conclusions are depicted below:

- Transition-metal-free borylation of 1,3-dienes takes place through S_N2'-type mechanisms with a preference for the *E* stereoisomeric allylic boronate product formation. Moderate yields have been achieved for this unprecedented catalytic process and the scope of the reaction includes terminal, internal and cyclic conjugated dienes.
- Triboration of 1,3-dienes has been achieved throughout conjugated borylation followed by diboration reaction in a single operational step.
- Allylic alcohols were prepared by single *in situ* oxidation providing the *E*-major isomers.
- Computational studies identified the key steps in the transition-metal-free conjugative borylation that rationalize the preference for 1,4-hydroborated products as well as the *E* stereoisomerism in the allylic boronate products. The DFT studies show that the origin of the appearance of *Z* isomer when the starting molecule is with *E* isomer is due to the conformational rotation of the conjugated diene at the beginning of the catalytic pathway. The allylic charge distribution study shows that **I1**-*E* and **I1**-*Z* C_1 are the most reactive, being consistent with the regioselectivity found experinentally.

3.5 Computational Details

Geometry optimizations and transition state searches were performed with Gaussian 16[34] package. The quantum mechanics calculations were performed within the framework of Density Functional Theory (DFT)[35–38] by using the hybrid B3LYP functional,[39–41] a standard 6–311G(d,p) basis set[42,43] and Grimme´s dispersion approximation.[44] Full geometry optimizations were performed without constraints. The nature of the stationary points encountered was characterized either as minima or transition states by means of harmonic vibrational frequency analysis. The zero-point, thermal, and entropy corrections were evaluated to compute Gibbs free energies (T=298 K, [C]=1 M). Solvent effects were included in geometry optimizations by using the IEF-PMC model.[45] The dielectric constant (ε) used for simulation of methanol solvent was 32.613.

3.6 References

(1) Ishiyama, T.; Yamamoto, M.; Miyaura, N. Platinum(0)-Catalysed Diboration of Alka-1,3-Dienes with Bis(Pinacolato)Diboron. *Chem. Commun.* **1996**, 2073–2074.

(2) Schuster, C. H.; Li, B.; Morken, J. P. Modular Monodentate Oxaphospholane Ligands: Utility in Highly Efficient and Enantioselective 1,4-Diboration of 1,3-Dienes. *Angew. Chemie Int. Ed.* **2011**, *50* (34), 7906–7909.

(3) Clegg, W.; Johann, T. R. F.; Marder, T. B.; Norman, N. C.; Orpen, A. G.; Peakman, T. M.; Quayle, M. J.; Rice, C. R.; Scott, A. J. Platinum-Catalysed 1,4-Diboration of 1,3-Dienes. *J. Chem. Soc. Dalt. Trans.* **1998**, 1431–1438.

(4) Hong, K.; Morken, J. P. Catalytic Enantioselective Diboration of Cyclic Dienes. A Modified Ligand with General Utility. *J. Org. Chem.* **2011**, *76* (21), 9102–9108.

(5) Burks, H. E.; Kliman, L. T.; Morken, J. P. Asymmetric 1,4-Dihydroxylation of 1,3-Dienes by Catalytic Enantioselective Diboration. *J. Am. Chem. Soc.* **2009**, *131* (26), 9134–9135.

(6) Lam, H. W. TADDOL-Derived Phosphonites, Phosphites, and Phosphoramidites in Asymmetric Catalysis. *Synthesis* **2011**, 13, 2011–2043.

(7) Kliman, L. T.; Mlynarski, S. N.; Ferris, G. E.; Morken, J. P. Catalytic Enantioselective 1,2-Diboration of 1,3-Dienes: Versatile Reagents for Stereoselective Allylation. *Angew. Chemie Int. Ed.* **2012**, *51* (2), 521–524.

(8) Cho, H. Y.; Morken, J. P. Ni-Catalyzed Borylative Diene−Aldehyde Coupling: The Remarkable Effect of $P(SiMe_3)_3$. *J. Am. Chem. Soc.* **2010**, *132* (22), 7576–7577.

(9) Ely, R. J.; Morken, J. P. Ni(0)-Catalyzed 1,4-Selective Diboration of Conjugated Dienes. *Org. Lett.* **2010**, *12* (19), 4348–4351.

(10) Cho, H. Y.; Morken, J. P. Diastereoselective Construction of Functionalized Homoallylic Alcohols by Ni-Catalyzed Diboron-Promoted Coupling of Dienes and Aldehydes. *J. Am. Chem. Soc.* **2008**, *130* (48), 16140–16141.

(11) Yu, C.-M.; Youn, J.; Yoon, S.-K.; Hong, Y.-T. A Highly Stereoselective Sequential Allylic Transfer Reaction of Diene with Diboronyl Reagent and Aldehydes Promoted by Nickel Catalyst. *Org. Lett.* **2005**, *7* (20), 4507–4510.

(12) Sasaki, Y.; Zhong, C.; Sawamura, M.; Ito, H. Copper(I)-Catalyzed Asymmetric Monoborylation of 1,3-Dienes: Synthesis of Enantioenriched Cyclic Homoallyl- and Allylboronates. *J. Am. Chem. Soc.* **2010**, *132* (4), 1226–1227.

(13) Semba, K.; Shinomiya, M.; Fujihara, T.; Terao, J.; Tsuji, Y. Highly Selective Copper-Catalyzed Hydroboration of Allenes and 1,3-Dienes. *Chem. – Eur. J.* **2013**, *19* (22), 7125–7132.

(14) Cuenca, A. B.; Shishido, R.; Ito, H.; Fernández, E. Transition-Metal-Free B–B and B–Interelement Reactions with Organic Molecules. *Chem. Soc. Rev.* **2017**, *46* (2), 415–430.

(15) Miralles, N.; Alam, R.; Szabó, K. J.; Fernández, E. Transition-Metal-Free Borylation of Allylic and Propargylic Alcohols. *Angew. Chemie Int. Ed.* **2016**, *55* (13), 4303–4307.

(16) Sanz, X.; Lee, G. M.; Pubill-Ulldemolins, C.; Bonet, A.; Gulyás, H.; Westcott, S. A.; Bo, C.; Fernández, E. Metal-Free Borylative Ring-Opening of Vinyl Epoxides and Aziridines. *Org. Biomol. Chem.* **2013**, *11* (40), 7004–7010.

(17) Haubold, W.; Stanzl, K. Die Addition von Tetrahalogeno-Diboran(4)-Molekülen an Diene. *J. Organomet. Chem.* **1979**, *174* (2), 141–147.

(18) Brown, H. C.; Liotta, R.; Kramer, G. W. Hydroboration. Effect of Structure on the Selective Monohydroboration of Representative Conjugated Dienes by 9-Borabicyclo[3.3.1]Nonane. *J. Org. Chem.* **1978**, *43* (6), 1058–1063.

(19) Davenport, E.; Fernández, E. Transition-Metal-Free Synthesis of Vicinal Triborated Compounds and Selective Functionalisation of the Internal C–B Bond. *Chem. Commun.* **2018**, *54* (72), 10104–10107.

(20) Cao, Y.; Zhang, Y.; Zhang, L.; Zhang, D.; Leng, X.; Huang, Z. Selective Synthesis of Secondary Benzylic (*Z*)-Allylboronates by Fe-Catalyzed 1,4-Hydroboration of 1-Aryl-Substituted 1,3-Dienes. *Org. Chem. Front.* **2014**, *1* (9), 1101–1106.

(21) Zaidlewicz, M.; Meller, J. Syntheses with Organoboranes. VII. Monohydroboration of Conjugated Dienes with Catecholborane Catalyzed by Complexes of Nickel(II) Chloride and Cobalt(II) Chloride with Diphosphines. *Tetrahedron Lett.* **1997**, *38* (41), 7279–7282.

(22) Sardini, S. R.; Brown, M. K. Catalyst Controlled Regiodivergent Arylboration of Dienes. *J. Am. Chem. Soc.* **2017**, *139* (29), 9823–9826.

(23) Wu, J. Y.; Moreau, B.; Ritter, T. Iron-Catalyzed 1,4-Hydroboration of 1,3-Dienes. *J. Am. Chem. Soc.* **2009**, *131* (36), 12915–12917.

(24) Diner, C.; Szabó, K. J. Recent Advances in the Preparation and Application of Allylboron Species in Organic Synthesis. *J. Am. Chem. Soc.* **2017**, *139* (1), 2–14.

(25) Miralles, N.; Gómez, J. E.; Kleij, A. W.; Fernández, E. Copper-Mediated S_N2' Allyl–Alkyl and Allyl–Boryl Couplings of Vinyl Cyclic Carbonates. *Org. Lett.* **2017**, *19* (22), 6096–6099.

(26) García-López, D.; Cid, J.; Marqués, R.; Fernández, E.; Carbó, J. J. Quantitative Structure–Activity Relationships for the Nucleophilicity of Trivalent Boron Compounds. *Chem. – Eur. J.* **2017**, *23* (21), 5066–5075.

(27) Cid, J.; Carbó, J. J.; Fernández, E. Disclosing the Structure/Activity Correlation in Trivalent Boron-Containing Compounds: A Tendency Map. *Chem. – Eur. J.* **2012**, *18* (40), 12794–12802.

(28) Pubill-Ulldemolins, C.; Bonet, A.; Bo, C.; Gulyás, H.; Fernández, E. Activation of Diboron Reagents with Brønsted Bases and Alcohols: An Experimental and Theoretical Perspective of the Organocatalytic Boron Conjugate Addition Reaction. *Chem. – Eur. J.* **2012**, *18* (4), 1121–1126.

(29) Bonet, A.; Pubill-Ulldemolins, C.; Bo, C.; Gulyás, H.; Fernández, E. Transition-Metal-Free Diboration Reaction by Activation of Diboron Compounds with Simple Lewis Bases. *Angew. Chemie Int. Ed.* **2011**, *50* (31), 7158–7161.

(30) Miralles, N.; Cid, J.; Cuenca, A. B.; Carbó, J. J.; Fernández, E. Mixed Diboration of Alkenes in a Metal-Free Context. *Chem. Commun.* **2015**, *51* (9), 1693–1696.

(31) García, L.; Sendra, J.; Miralles, N.; Reyes, E.; Carbó, J. J.; Vicario, J. L.; Fernández, E. Transition-Metal-Free Stereoselective Borylation of Allenamides. *Chem. – Eur. J.* **2018**, *24* (53), 14059–14063.

(32) Barba, C.; Carmona, D.; García, J. I.; Lamata, M. P.; Mayoral, J. A.; Salvatella, L.; Viguri, F. Conformational Preferences of Methacrolein in Diels−Alder and 1,3-Dipolar Cycloaddition Reactions. *J. Org. Chem.* **2006**, *71* (26), 9831–9840.

(33) Calow, A. D. J.; Carbó, J. J.; Cid, J.; Fernández, E.; Whiting, A. Understanding α,β-Unsaturated Imine Formation from Amine Additions to α,β-Unsaturated Aldehydes and Ketones: An Analytical and Theoretical Investigation. *J. Org. Chem.* **2014**, *79* (11), 5163–5172.

(34) Frisch, M. J.; Trucks, G. W.; Schlegel, H. B.; Scuseria, G. E.; Robb, M. A.; Cheeseman, J. R.; Scalmani, G.; Barone, V.; Petersson, G. A.; Nakatsuji, H.; Li, X.; Caricato, M.; Marenich, A. V; Bloino, J.; Janesko, B. G.; Gomperts, R.; Mennucci, B.; Hratchian, H. P.; Ortiz, J. V; Izmaylov, A. F.; Sonnenberg, J. L.; Williams-Young, D.; Ding, F.; Lipparini, F.; Egidi, F.; Goings, J.; Peng, B.; Petrone, A.; Henderson, T.; Ranasinghe, D.; Zakrzewski, V. G.; Gao, J.; Rega, N.; Zheng, G.; Liang, W.; Hada, M.; Ehara, M.; Toyota, K.; Fukuda, R.; Hasegawa, J.; Ishida, M.; Nakajima, T.; Honda, Y.; Kitao, O.; Nakai, H.; Vreven, T.; Throssell, K.; Montgomery Jr., J. A.; Peralta, J. E.; Ogliaro, F.; Bearpark, M. J.; Heyd, J. J.; Brothers, E. N.; Kudin, K. N.; Staroverov, V. N.; Keith, T. A.; Kobayashi, R.; Normand, J.; Raghavachari, K.; Rendell, A. P.; Burant, J. C.; Iyengar, S. S.; Tomasi, J.; Cossi, M.; Millam, J. M.; Klene, M.; Adamo, C.; Cammi, R.; Ochterski, J. W.; Martin, R. L.; Morokuma, K.; Farkas, O.; Foresman, J. B.; Fox, D. J. Gaussian16 Revision A03. 2016.

(35) Yang, R. G. P. and W. *Density-Functional Theory of Atoms and Molecules*; Oxford Univ. Press: Oxford, 1989.

(36) Hohenberg, P.; Kohn, W. Inhomogeneous Electron Gas. *Phys. Rev.* **1964**, *136* (3B), B864–B871.

(37) Kohn, W.; Sham, L. J. Self-Consistent Equations Including Exchange and Correlation Effects. *Phys. Rev.* **1965**, *140* (4A), A1133–A1138.

(38) Comstock, M. J. The Challenge of d and f Electrons, Copyright, ACS Symposium Series, Foreword. In *The Challenge of d and f Electrons*; Comstock, M. J., Ed.; ACS Symposium Series; American Chemical Society, 1989; Vol. 394, pp i–iv.

(39) Lee, C.; Yang, W.; Parr, R. G. Development of the Colle-Salvetti Correlation-Energy Formula into a Functional of the Electron Density. *Phys. Rev. B* **1988**, *37* (2), 785–789.

(40) Becke, A. D. Density-functional Thermochemistry. III. The Role of Exact Exchange. *J. Chem. Phys.* **1993**, *98* (7), 5648–5652.

(41) Stephens, P. J.; Devlin, F. J.; Chabalowski, C. F.; Frisch, M. J. Ab Initio Calculation of Vibrational Absorption and Circular Dichroism Spectra Using Density Functional Force Fields. *J. Phys. Chem.* **1994**, *98* (45), 11623–11627.

(42) Hariharan, P. C.; Pople, J. A. The Influence of Polarization Functions on Molecular Orbital Hydrogenation Energies. *Theor. Chim. Acta* **1973**, *28* (3), 213–222.

(43) Francl, M. M.; Pietro, W. J.; Hehre, W. J.; Binkley, J. S.; Gordon, M. S.; DeFrees, D. J.; Pople, J. A. Self-consistent Molecular Orbital Methods. XXIII. A Polarization-type Basis Set for Second-row Elements. *J. Chem. Phys.* **1982**, *77* (7), 3654–3665.

(44) Grimme, S.; Antony, J.; Ehrlich, S.; Krieg, H. A Consistent and Accurate Ab Initio Parametrization of Density Functional Dispersion Correction (DFT-D) for the 94 Elements H-Pu. *J. Chem. Phys.* **2010**, *132* (15), 154104.

(45) Mennucci, B.; Cancès, E.; Tomasi, J. Evaluation of Solvent Effects in Isotropic and Anisotropic Dielectrics and in Ionic Solutions with a Unified Integral Equation Method: Theoretical Bases, Computational Implementation, and Numerical Applications. *J. Phys. Chem. B* **1997**, *101* (49), 10506–10517.

Chapter 4

α-Boryl Carbanions: Mapping the structure and the reactivity trends

4.1 Abstract and specific objectives

The chemistry of stabilized α-boryl carbanions show a remarkable diversity, and can enable many different synthetic routes towards efficient C-C bond formation. The electron-deficient, trivalent boron-atom stabilizes the carbanion facilitating its generation and tuning its reactivity. Chapter 4 describes the electronic structure and the reactivity trends of a large dataset of α-boryl carbanions, using DFT-derived parameters capturing their electronic and steric properties, computational reactivity towards model substrates, and crystallographic analysis within the Cambridge Structural Database (CSD). This study maps the reactivity space by varying the nature of the boryl moiety (Scheme 4.1a), the number of α-boryl motifs (Scheme 4.1b), the substituents of the carbanionic carbon (Scheme 4.1c), and the metal cation interacting with the carbanion (Scheme 4.1d).

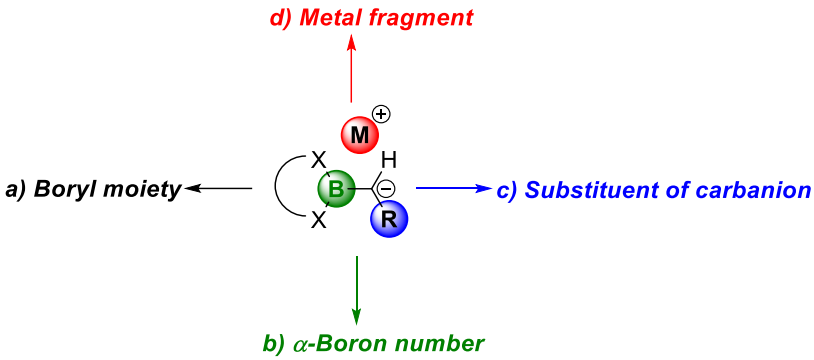

Scheme 4.1. Summary of the different features of α-boryl carbanions studied in Chapter 4.

In general, the free carbanionic intermediates are described as borata-alkene species with C-B π-interaction polarized towards the carbon, showing an inverse stability-reactivity relationship. Furthermore, we have classified the α-boryl alkylidene metal precursors into three classes directly related to their reactivity: 1) Nucleophilic borata-alkene salts with alkali and alkali-earth metals, 2) nucleophilic η^2-(C-B) borata-alkene complexes with early transition metals, Cu and Ag, and 3) α-boryl alkyl complexes with late transition metals. This trend map aids the selection of the appropriate reactive synthon depending on the reactivity sought.

Here, we aim to identify reliable descriptors derived from ground-state structures that correlate with the stability and reactivity of α-boryl carbanions and allow to build a map of trends for these species.

4.2 State of the art

The access to primary, secondary, and tertiary alkylboronic esters, through the generation of α-boryl carbanions and subsequent electrophilic trapping, is a new and powerful synthetic tool towards efficient C-C bond formation. The generation of α-boryl carbanions can be conducted through four complementary pathways (Scheme 4.2), including a) deborylation of 1,1-diboryl alkanes,[1–9] b) deprotonation of the α-hydrogen from an organoborane compound,[10–16] c) metallation of α-halo boronic esters,[17] and d) transmetallation of α-borylmethide metal salts with organometallic reagents.[18,19] α-Boryl carbanions show a remarkable stability due to the valence deficiency of the adjacent three coordinate boron centre, and they can be also described by their borata-alkene resonance forms (see Scheme 4.3).[20–24]

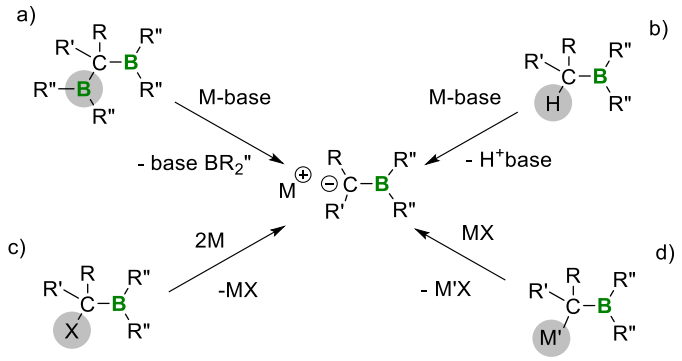

Scheme 4.2. Strategic methods to access α-boryl carbanions.

The experimental outcomes are consistent with the delocalization of the electron density of the anion throughout the empty *p* orbital of the adjacent boron. This is demonstrated by the chemical shifts displacement on ^{11}B (highfield) and ^{13}C (downfield) NMR data for R_2B-CH_2^- in comparison with the corresponding α-boryl alkane.[12,25] IR spectra of boron-stabilized anions in the gas phase, in combination with DFT calculations, also suggest the double bond character of C=B bond in $Me_2BCH_2^-$ α-monoborlyl anions.[26]

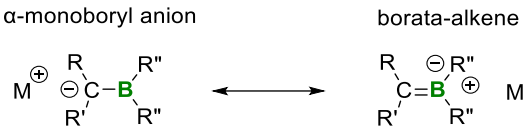

Scheme 4.3. Resonance structures for α-boryl carbanion and borata-alkene.

In the solid state, the shortened B-C bond lengths[27–29] of the borata-alkene species provide an additional evidence of the their "boron ylide" character, which can be related to the

analogs containing boron-carbon double bonds.[30] Computational studies have also supported the borata-alkene character of α-boryl carbanions by means of detailed analysis of their electronic structures.[29,31,32] The natural bond orbital (NBO) analysis on $[Mes_2B{=}CR_2]^-$ anion by Gabbaï and co-workers showed one σ- and one π-interaction between the carbon and the boron atoms, where the π bond was polarized towards the carbon.[31] Erker and co-workers described a similar B-C interaction for related species, in which the HOMO formally corresponds to a C-B π-orbital strongly polarized towards the carbanionic atom.[29]

The study by Erker and co-workers,[29] compared three different α-boryl moieties, $B(C_6F_5)_2$, $BMes_2$ and 9-boryilbicyclo[3.3.1]nonane (Figure 4.1). The authors concluded that the high degree of carbanion stabilization when the boryl moiety $B(C_6F_5)_2$ is involved might be due to the presence of fluorine substituents on the aryl group. The mesityl substituents at boron led to a decrease of stabilization by about 16 kcal·mol^{-1}, followed by the borata-alkenes containing the 9-boryilbicyclo[3.3.1]nonane which showed a lower degree of carbanion stabilization (Figure 4.1). The steric protection of the boron center seems to be necessary to ensure an appropriate proton abstraction of the α-hydrogen from the organoborane (Scheme 4.2b), since there is a strong tendency to form a four-coordinate boron"ate" salt upon addition of a base. For that reason, most of the borata-alkenes reported so far bear bulky substituents on boron, generating boryl moieties such as $B(C_6F_5)_2$, $BMes_2$ or 9-boryilbicyclo[3.3.1]nonane. Eventually, the pronounced α-boryl carbanion stabilization represents an extra advantage to explore the significant reactivity of the borata-alkenes.[29,33]

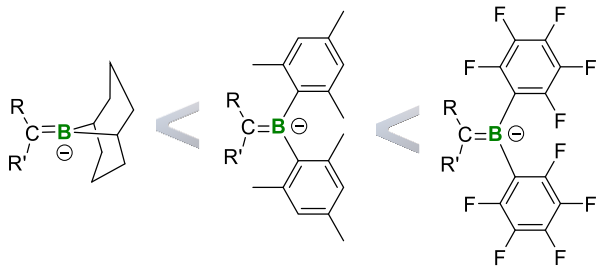

Figure 4.1. Stabilizing order for selected borata-alkene species.

To gain more insight into the electronic structure and the reactivity trends of α-boryl carbanions, we conduct here a detailed computational study based on density functional calculations (See Computational Details, section 4.5) and wave function analysis. The study is performed on a varied dataset of compounds bearing commonly used boryl moieties, such as Bpin (pinacolboryl) and Bdan (naphthodiazaboryl). As illustrated in Figure 4.2, we have gauged the influence of several structural features of the α-boryl carbanions: 1) the

nature of the boryl moiety, 2) the substituents on the carbanionic carbon, 3) the comparison between α-mono-, α-di- and α-triboryl carbanions, and 4) the nature of the metal involved.

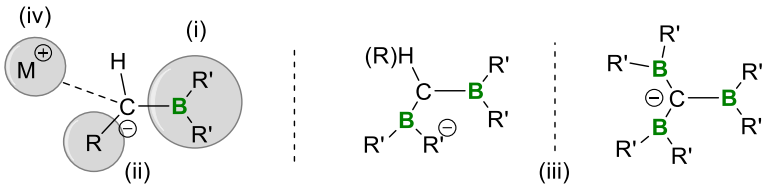

Figure 4.2. Analyzed structural features influencing the nature of the α-boryl carbanions.

4.3 Results and Discussion

4.3.1 Influence of the nature of the boryl moiety

Using as starting point, the early work by Erker and co-workers,[29] we have initially gauged the electronic structure and reactivity of α-monoboryl carbanions as a function of boryl fragment nature. We started with the comparison of the previously analyzed α-monoboryl carbanions, containing the boryl moieties $BMes_2$ and $B(C_6F_5)_2$ (**1a**^{mes} and **1a**^{PhF}), with those that include the commonly used Bpin and Bdan moieties in the structure, (**1a**^{pin} and **1a**^{dan,} respectively). Here, we have explored different geometric, electronic and energy descriptors aiming to rationalize the stability and reactivity trends along the carbanion series. Table 4.1 collects the values of the most meaningful descriptors for **1a**^{PhF}, **1a**^{mes}, **1a**^{dan} and **1a**^{pin} species. Tables 6.1 and 6.2 of the Experimental Section (Chapter 6) lists all the computed descriptors and their values.

Table 4.1. Calculated protonation Gibbs energies ($\Delta G_{prot.}$) and free-energy barriers for nucleophilic substitution with bromoethane ($\Delta G^{\ddagger}_{SN2}$) in kcal·mol^{-1}, energy of the HOMO orbital (E_{HOMO}) in eV, and Wiberg bond orders ($\sum$C-B$_{bo}$) upon variation of boryl moiety nature, species **1a^{PhF}**, **1a^{mes}**, **1a^{dan}** and **1a^{pin}**.

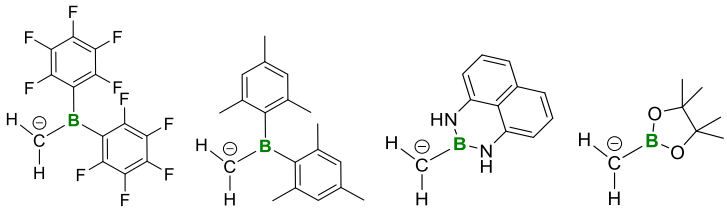

Species	1a^{PhF}	1a^{mes}	1a^{dan}	1a^{pin}
$\Delta G_{prot.}$	+19.7	-0.2	-23.2	-33.6
$\Delta G^{\ddagger}_{SN2}$	19.3	18.8	6.9	4.2
$\sum$C-B$_{bo}$	1.73	1.69	1.57	1.56
E_{HOMO}	-2.87	-2.20	-1.19	-0.58

In line with the analysis reported by Erker,[29] the stabilization of α-boryl carbanions can be assessed by calculating the protonation energies of the carbanions respect to the cyclopentadienyl anion (ΔG_{prot}) as illustrated in Scheme 4.4. Note that this procure is equivalent to compute absolute proton affinities of carbanions but using cyclopenatadienyl as reference to set the zero, *i.e.*, subtracting the proton affinity of cyclopentadienyl (368.4 kcal·mol^{-1}) to each species. Moreover, we have determined the free-energy barriers ($\Delta G^{\ddagger}_{SN2}$) for the S_N2 nucleophilic substitution reaction between the carbanions and bromoethane (Scheme 4.5) in order to quantify the nucleophilic reactivity of α-boryl carbanions towards organic electrophiles. The values of energy barriers in Table 4.1 indicate the following trend on the reactivity **1a^{pin}** > **1a^{dan}** > **1a^{mes}** > **1a^{PhF}**.

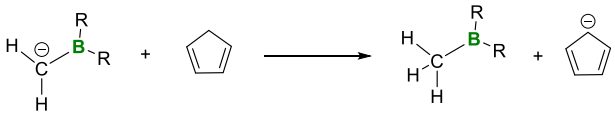

Scheme 4.4. Protonation reaction of α-boryl carbanion with cyclopentadiene.

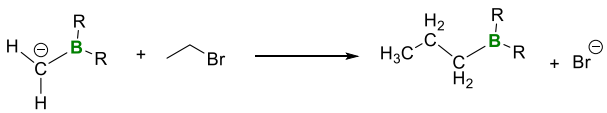

Scheme 4.5. Alkylation reaction of α-boryl carbanion with bromoethane.

The reactivity trend is inversely correlated to the stability of the α-monoboryl carbanions. The least reactive species **1a**^{mes} and **1a**^{PhF} show a marked stabilization as reflected in isoenergetic or endergonic, relative protonation free-energies (ΔG_{prot} = -0.2 and +19.7 kcal·mol^{-1}, respectively). Whereas the boron atom in **1a**^{PhF} and **1a**^{mes} is protected by the steric bulkiness of Mes and C_6F_5 groups, the Bpin and Bdan boryl fragments depict the π-donor ability from the O and N heteroatoms to the empty *p* orbital of the B atom. Consequently, in **1a**^{mes} and **1a**^{PhF} the electron deficient boron center is fully available for delocalizing the carbanion negative charge. This also correlates with the Wiberg C-B bond order whose values increase from **1a**^{pin} < **1a**^{dan} < **1a**^{mes} < **1a**^{PhF} (Table 4.1). Moreover, the values are significantly larger than 1 (from 1.56 to 1.73), supporting the borata-alkene character of these species.

The nucleophilic reactivity of organic reagents has been traditionally correlated with the energy level of HOMO orbital, or with the NBO atomic charges as it was reported for related nucleophilic boryl species.[34,35] Here, the energy of the HOMO, formally corresponding to a C-B π-orbital strongly polarized towards the carbanionic atom (Figure 4.3), clearly correlates with the nucleophilic reactivity. The higher the energy is, the lower thefree energy barrier (compare 2nd and 4th files in Table 4.1).

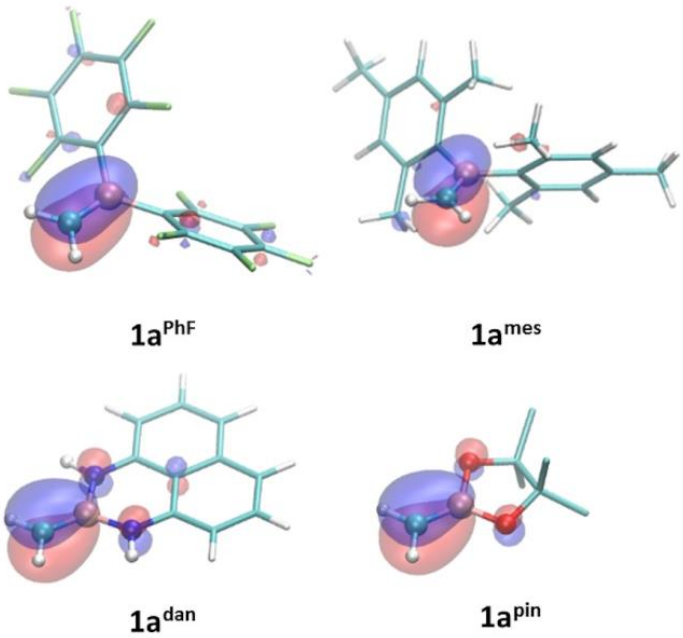

Figure 4.3. Representation of HOMO orbitals, formally corresponding to a C-B π-orbital polarized towards the carbon, for **1a**^{PhF}, **1a**^{mes}, **1a**^{dan} and **1a**^{pin}.

Interestingly, the **1a**^{pin} species is computed to be more reactive than **1a**^{dan} ($\Delta G^{\ddagger}_{SN2}$= 4.2 and 6.9 kcal·mol^{-1}, respectively). As illustrated in the HOMO representations of Figure 4.3, the aromatic fragment of Bdan **1a**^{dan} moiety contributes to the delocalization of the carbanionic charge through the π-channel, resulting in lower energy-laying HOMO compared to **1a**^{pin}. In fact, this effect had been observed in a previous study on boron-stabilized carbanions generated from deborylation of 1,1-diborylalkanes with alkoxides.[36] Since the N atoms bound to B in Bdan are better π-donors than O atoms in Bpin, one can envisage that in the absence of the aromatic fragment, the diazoboryl moieties should enhance carbanion nucleophilicity. To evaluate this effect, we computed the unprecedented compound **1a**^{Npin} (Figure 4.4), in which the O substituents on **1a**^{pin} were replaced by NH fragments. In line with previous reasoning, the **1a**^{Npin} is the most reactive species with a computed free energy barrier $\Delta G^{\ddagger}_{SN2}$ of only 3.2 kcal·mol^{-1}.

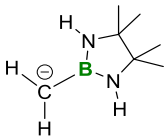

1a^{Npin}

Figure 4.4. Schematic representation of the newly 4,4,5,5-tetramethyl-1,3,2-diazaboryl methide anion **1a**^{Npin}.

Finally, it is worth to mention that in this subset, the computed atomic charges at the carbanionic carbon (-0.88, -0.98, -1.14 and -1.20 a.u. for **1a**^{PhF}, **1a**^{mes}, **1a**^{dan} and **1a**^{pin}, respectively) are consistent with the nucleophilicity of the α-boryl methyl fragment, but this correlation is not observed for the other subsets in this work. A similar trend was suggested by Erker and co-workers,[29] who attributed the observation to their borata-alkane behavior. Therefore, HOMO energies will be used hereafter as a suitable descriptor of the reactivity of α-boryl carbanions.

4.3.2 Influence of the substituents on the carbanionic carbon

Next, we explored how the reactivity/stability and electronic structural properties can be affected by the influence of Me and Ph substituents on α-monoboryl carbanions. The calculated ΔG_{prot} energies for **1c**^{pin} (Table 4.2) demonstrates that the Ph group stabilizes the carbanion lone pair. This is also reflected in a larger sum of Wiberg bond orders for the three bonds of carbanion (3.68 for **1c**^{pin} vs. 3.55 and 3.62 for **1a**^{pin} and **1b**^{pin} respectively), and in the lower energy-laying HOMO (-1.27 for **1c**^{pin} vs. -0.58 and -0.56 eV for **1a**^{pin} and **1b**^{pin}

respectively). Both descriptors capture the electron withdrawing effect of the Ph group. Alike stability trend, **1c^{pin}** shows lower reactivity for the S_N2 nucleophilic substitution of bromoethane than for **1a^{pin}** ($\Delta G^{\ddagger}_{SN2}$ = 9.8 and 4.2 kcal·mol^{-1} for **1c^{pin}** and **1a^{pin}**, respectively).

Table 4.2. Calculated protonation Gibbs free energies ($\Delta G_{prot.}$), free-energy barriers for nucleophilic substitution in bromoethane ($\Delta G^{\ddagger}_{SN2}$) in kcal·mol^{-1}, energy of the HOMO (E_{HOMO}) in eV, and Wiberg bond orders upon variation of carbanion substituents, species **1c^{pin}**, **1a^{pin}** and **1b^{pin}**.

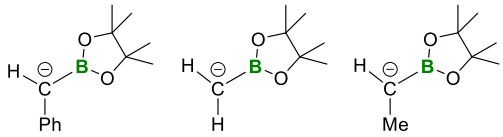

Species	1c^{pin}	1a^{pin}	1b^{pin}
$\Delta G_{prot.}$	-7.2	-33.6	-30.6
$\Delta G^{\ddagger}_{SN2}$	9.8 (13.0)	4.2 (9.3)	4.2 (8.5)
$\sum$C-R$_3$	3.68	3.55	3.62
E_{HOMO}	-1.27	-0.58	-0.56

The presence of the Me group (**1b^{pin}**) does not alter significantly the nucleophilic character of the carbanion with respect to hydrogen-substituted **1a^{pin}**. Although it is usually considered that alkyl groups destabilize carbanions due to their electron-donating inductive effect, here calculations show that other subtle effects need to be considered since they do not provide a clear picture of stability/reactivity order between **1a^{pin}** and 1**b^{pin}** (Table 4.2). Besides the inductive effect, one should considerer an electrostatic size effect, in which the negative charge in **1b^{pin}** is more stabilized by the larger molecular volume that reduces its charge density. Thus, calculations in vacuum pointed out that methyl-substituted **1b^{pin}** is more stable (less negative ΔG_{prot}) than **1a^{pin}**, whereas its HOMO is higher in energy (-0.58 and -0.56 eV for **1a^{pin}** and **1b^{pin}**, respectively). However, the inclusion of the effect of polar solvent (DMSO) reduces the influence of electrostatic–size effect, and the corresponding calculations predict that methyl-substitued **1b^{pin}** is more reactive than **1a^{pin}** (see values in parenthesis in Table 4.2).

4.3.3 Influence of the number of boryl substituents

We next explored the influence of the number of boryl fragments in the stability/reactivity of the corresponding carbanions. Table 4.3 compares the main computed parameters for α-mono-, di-, and triboryl carbanions **1a^{pin}**, **2a^{2pin}** and **3^{3pin}**, respectively. Increasing the

number of boryl moieties the stability of the carbanion is enhanced (**1a**^{pin} < **2a**^{2pin} < **3**^{3pin}) whereas the nucleophilicity is reduced (**1a**^{pin} > **2a**^{2pin} > **3**^{3pin}).

Table 4.3. Calculated protonation free Gibbs energies ($\Delta G_{prot.}$) and free-energy barriers for nucleophilic substitution in bromoethane ($\Delta G^{\ddagger}_{SN2}$) in kcal·mol^{-1}, energy of the HOMO orbital (E_{HOMO}) in eV, Wiberg bond orders ($\sum$C-R$_3$), and average C-B distances in Å upon variation of the number of boryl substituents, species **1a**^{pin}, **2a**^{2pin} and **3**^{3pin}.

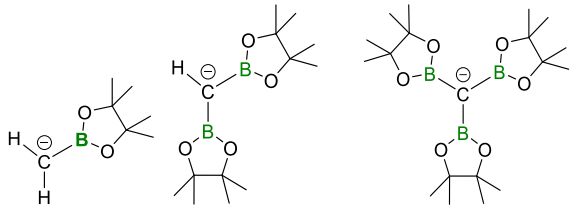

Species	1a^{pin}	2a^{2pin}	3^{3pin}
$\Delta G_{prot.}$	-33.6	-10.0	-1.8
$\Delta G^{\ddagger}_{SN2}$	4.2	10.3	14.0
$\sum$C-R$_3$	3.55	3.51	3.39
C-B$_{bo\text{-}av.}$	1.56	1.23	1.07
$d_{C\text{-}B\text{-}av.}$	1.44	1.47	1.50
E_{HOMO}	-0.58	-1.85	-2.61

Figure 4.5 shows the HOMO orbitals for **2a**^{2pin} and **3**^{3pin}, where it can be clearly observed that each boryl moiety contributes to the stabilization of the carbanion through a strong delocalization of the carbanion *p*-type electron density into the π-channel. Consequently, the α-triboryl carbanion **3**^{3pin} has lower-energy laying HOMO (-2.61 eV) than those for **2a**^{2pin} and **1a**^{pin} (-1.85 and -0.58 eV, respectively), being the former the least prone to react with electrophiles and the most stable.

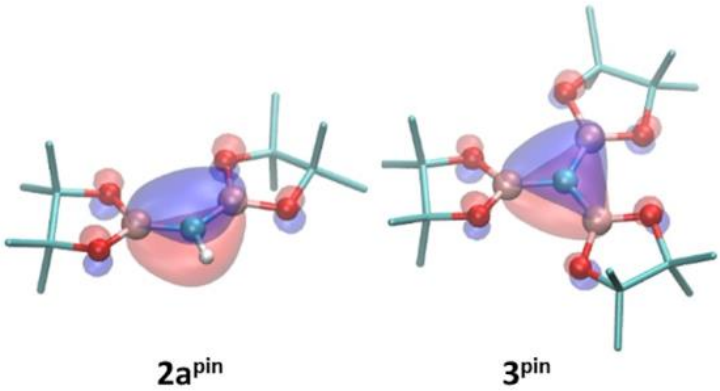

Figure 4.5. Representation of HOMO orbitals, formally corresponding to a C-B π-orbital polarized towards the carbon, for **2a**^{2pin} and **3**^{3pin}.

Remarkably, the sums of Wiberg bond order of the carbanion for species **1a**^{pin}, **2a**^{2pin} and **3**^{3pin} (3.55, 3.51 and 3.39, respectively) do not seem to be consistent with their stability. In this case, the most stable **3**^{3pin} species has the lowest overall bond order. This might be due to the loss of borata-alkane character when the negative charge of carbanion has to be shared between several boryl moieties. In fact, the averaged individual C-B bond order in **3**^{3pin} is low (1.07) and the averaged C-B bond distance (1.50 Å) is significantly longer than that for monoborylated species **1a**^{pin} (1.44 Å). Thus, multi-boryl carbanions can be viewed as carbanionic species with polar C-B bonds, in which the excess of negative charge is electrostatically stabilized by the boron substituents, as well as by some amount of charge transfer to the empty perpendicular boron *p* orbitals. Figure 4.6 depicts the evolution of computed atomic charges from mono- to di-, and to tri-boryl carbanions, showing an increasing charge separation (polarization) at the C-B bonds. The estimated amount of charge transferred from the carbanion to the perpendicular boron *p* orbitals is still significant for **3**^{3pin} (0.21 a.u.), contributing to the overall stabilization of this species.

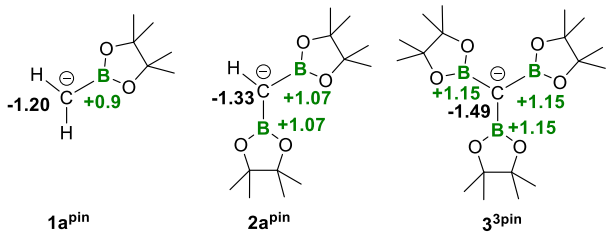

Figure 4.6. NBO atomic charges for mono-, di-, and triboryl carbanions **1a**^{pin} ($\Delta q_{B\text{-}C}$= 2.1), **2a**^{2pin} ($\Delta q_{B\text{-}C}$= 2.4) and **3**^{3pin} ($\Delta q_{B\text{-}C}$= 2.64).

4.3.4 Mapping the nucleophilicity of α-boryl carbanions

Once it has been discussed in detail the influence of electronic and structural features on the stability/reactivity of several model α-boryl carbanions, our next objective is the construction of a map from a full set of structures, in order to classify and identify certain trends in the chemical space. To this end, we additionally analyzed 14 α-boryl carbanions depicted in Figure 4.7. Overall, the full dataset (**set 1**) comprises 22 anionic species, which were selected by varying systematically the number and the type of boryl moieties, as well as, the type of substituents on carbon (R = H, Me and Ph). The dataset also includes the α-boryl vinyl system (**1e^{pin}**), in order to compare the borata-alkene character between $[R_2B{=}CH_2]^-$ and $[R_2B{=}CH{=}CH_2]^-$. Interestingly, we found an inverse, linear correlation (correlation coefficient r^2 = 0.91) between the protonation energies of the carbanions and the HOMO energies, which can be consequently used as reliable descriptor to gauge the stability/reactivity trends in α-boryl carbanions (see Figure 4.8).

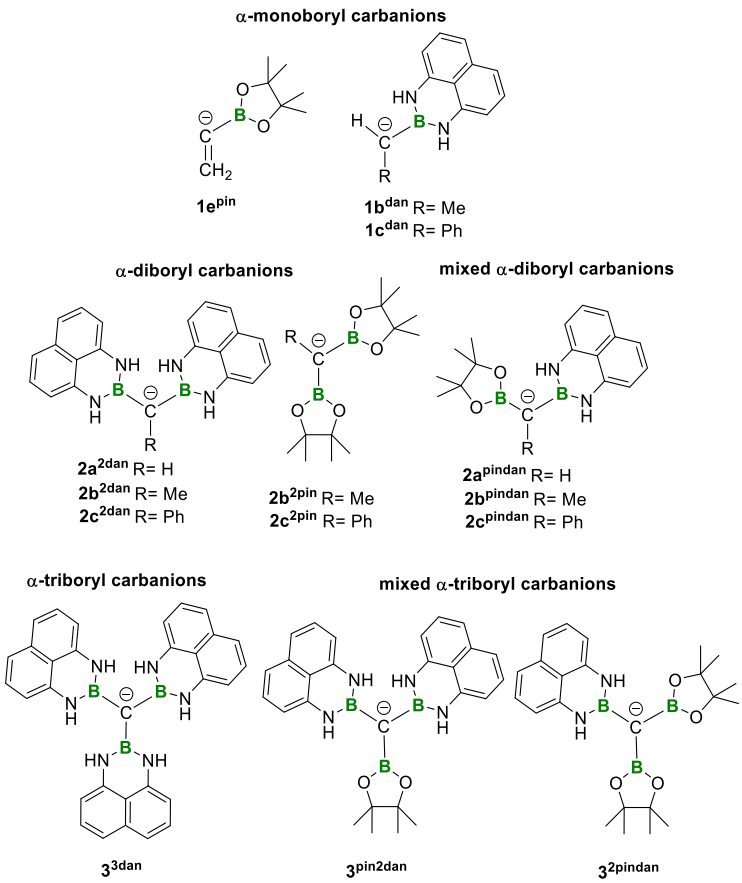

Figure 4.7. Additional α-boryl carbanion species forming dataset set1.

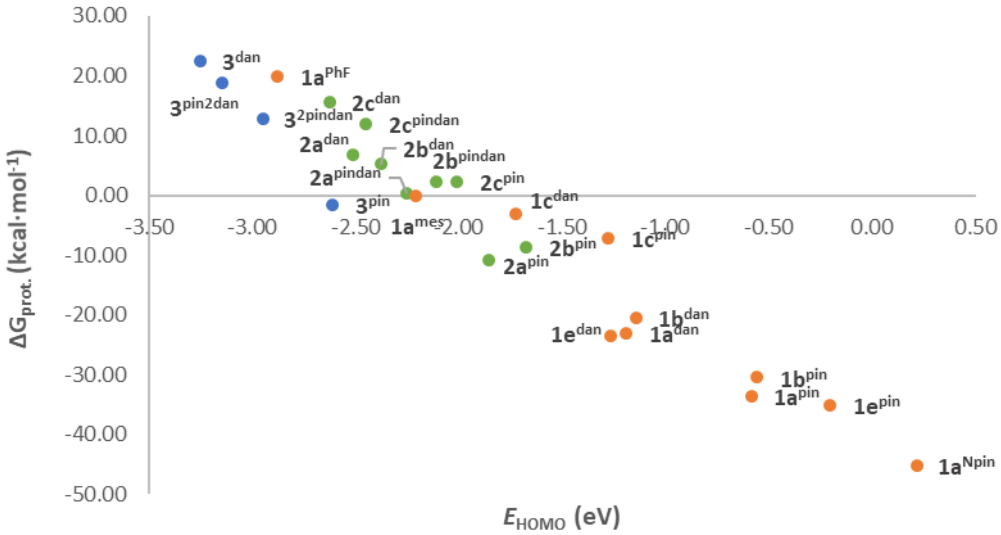

Figure 4.8. Representation of the linear correlation between the energy of the HOMO (eV) and the protonation free-energies (kcal·mol^{-1}) for the α-boryl carbanions. α-Monoboryl are represented in orange circles, α-diboryl carbanions in green circles, and α-triboryl carbanions in blue circles.

Figure 4.9 maps the full dataset using two descriptors, the energy of the HOMO (E_{HOMO}) and the sum of Wiberg C-B bond order (∑C-B_{bo}). The E_{HOMO} descriptor can be directly related to the stability/reactivity trends, while the ∑C-B_{bo} is a useful descriptor allowing to separate the mono-, di- and triborylated species, and to differentiate between Me and Ph substituents on carbon. First, we identified a clear correlation between the number of boryl substituents and the carbanion nucleophilicity as reflected in the HOMO energy. α-Triboryl carbanions are the least nucleophilic, with HOMO energies ranging from -3.3 to -2.6 eV, presumably due to the accumulation of the three stabilizing boryl substituents. The reactivity on these species follows the trend **3**^{3pin} > **3**^{2pindan} > **3**^{pin2dan} > **3**^{3dan} in agreement with the observation that Bdan moieties have an extra stabilization effect on the carbanion.[36] Within the α-diboryl cabanions, the calculated HOMO energies are found between -2.6 to -1.7 eV, conforming a specific group where once again the species containing Bdan units become less reactive and more stabilized than the ones with Bpin moieties. In fact, the values for HOMO energy for **2a**^{2dan} and **2c**^{2dan} carbanions reach values close to the next group to the left, the α-triboryl carbanions (Figure 4.9). The mixed α-diboryl cabanions (**2a**^{pindan}, **2b**^{pindan}, and **2c**^{pindan}) have intermediate energy HOMO values, and the **2b**^{2pin} might be the most reactive among the α-diboryl carbanions.

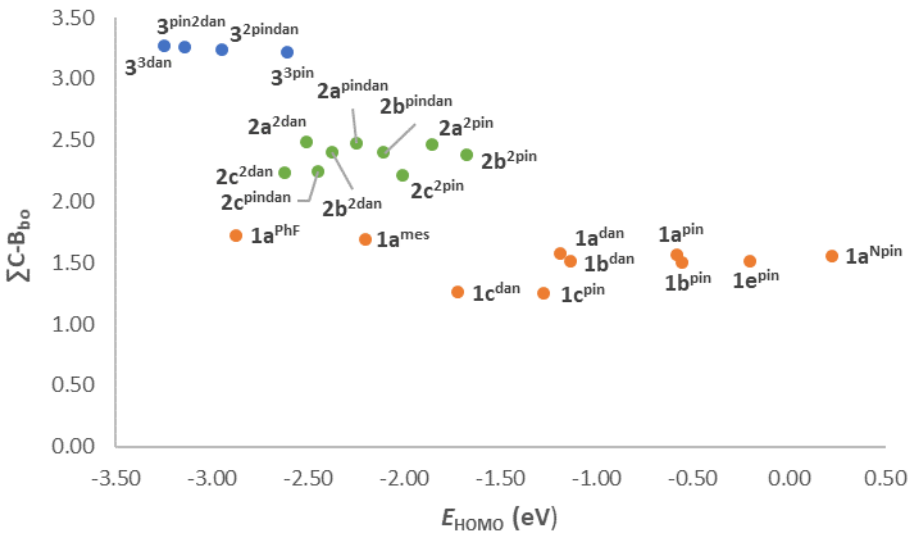

Figure 4.9. Representation of the sum of C-B Wiberg bond orders *versus* the energy of the HOMO (eV) for the carbanions. α-Monoboryl carbanions are represented in orange circles, α-diboryl carbanions in green circles, and α-triboryl carbanions in blue circles.

The subset formed by the α-monoborylated species with Bpin or Bdan boryl fragments shows higher HOMO energies (-1.3 to -0.2 eV). Among them, we predicted the vinyl carbanionic species **1e^{pin}**, that contains a sp^2 carbanion, as highly nucleophlic. Even more to the right, we found the newly design species **1a^{Npin}** (Figure 4.7). Whereas the sum of Wiberg C-B bond order for **1a^{Npin}** is similar to **1a^{pin}**, the higher energy of the HOMO orbital of **1a^{Npin}** indicates that combining N-substituted boron and non-aromatic scaffold causes the largest nucleophilicity. On the other side, the species containing highly-acidic BMes or BC_6H_5 moieties (**1a^{mes}** and **1a^{PhF}**) have E_{HOMO} values that lay in the range of di- and triborylated species (-2.2 and -2.9 eV, respectively). This clearly indicates that boryl substituents in **1a^{mes}** and **1a^{PhF}** cause a strong stabilization on the carbanion because in the absence of heteroatom substituents on boron, its perpendicular *p* orbital is fully available for the overlap with the lone pair of the carbanion.

The structures with the phenyl substituents (**1c^{pin}**, **1c^{dan}**, **2c^{2pin}**, **2c^{pindan}** and **2c^{2dan}**) show the lowest C-B bond orders due to the electron-releasing effect of the phenyl groups, which compete with electron delocalization through the borata-akene structure. On the other hand, the structures containing methyl substituents (**1b^{pin}**, **1b^{dan}**, **2b^{2pin}**, **2b^{pindan}** and **2b^{2dan}**) have slightly lower C-B bond orders than those

species with hydrogen substituents. This latter trend can be correlated with a subtle effect of alkyl substituents, which induce some electrostatic delocalization.

4.3.5 Influence of the nature of the metal

The practical applications of borata-alkenes as reactive synthons are achieved by different strategies which involve the preparation of boryl alkylidene metal salts and α-boryl alkyl transition metal complexes. Here, we study the influence of those metals and transition metals in their stability/reactivity. Figure 4.10 depicts the selected structures including Li^+, Cu^+, Ag^+ and Pd^{2+} α-boryl methide metal salts, and Table 4.4 collects the most representative computed parameters. In this case, to evaluate the nucleophilic reactivity, we have determined the free-energy barriers ($\Delta G^{\ddagger}_{Ald}$) required to transfer the carbanions to the electrophilic carbon atom of the model substrate formaldehyde (Scheme 4.6). This substrate is a simple species that have been used to quantify the reactivity of related metal-boryl compounds,[35,37,38] and constitute a model of observed reactions such as the nucleophilic borylmethylation of aldehydes with α-boryl alkyl copper[39,40] and silver[41] complexes, and with lithium dimesithylboron substituted carbanions [$(Mes)_2BC(H)RLi$].[42]

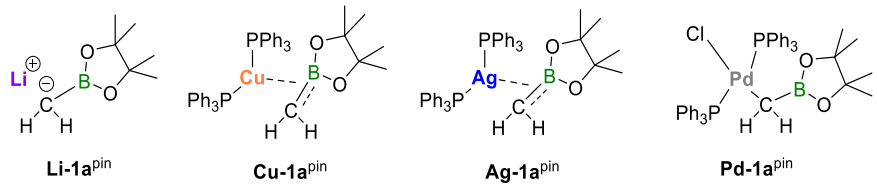

Figure 4.10. Selected structures for the analysis of metal cation (Li^+, Cu^+, Ag^+, and Pd^{2+}) effect on the stability/reactivity of α-boryl carbanionic species.

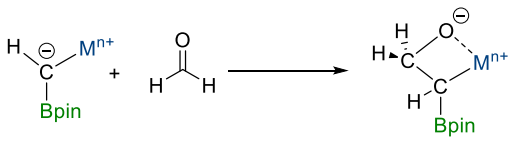

Scheme 4.6. Nucleophilic addition of α-boryl methide metals to formaldehyde.

It is important to note that for Li, Cu and Ag species the nucleophilic additions to several organic electrophiles have been reported,[39–45] while for transition metals such as Pd the observed reactivity involves mainly transmetallation processes.[46,47] Thus, we should expect low to moderate free-energy barriers for Li, Cu and Ag salts, and larger barrier for Pd indicating a less favorable nucleophilic reactivity.

Table 4.4. Calculated free-energy barriers for carbanion addition to formaldehyde ($\Delta G^{\ddagger}_{Ald}$) in kcal·mol^{-1}, overall charge of carbanion fragment (*q*[C]), Wiberg bond orders, C-B lengths (d_{C-B}) and steric distance-weight volume (V_W) upon variation the cationic fragment in **1a^{pin}-Li**, **1a^{pin}-Cu**, **1a^{pin}-Ag** and **1a^{pin}-Pd**

Structures	1a^{pin}-Li	1a^{pin}-Cu	1a^{pin}-Ag	1a^{pin}-Pd
$\Delta G^{\ddagger}_{Ald}$[a]	2.2[a]	15.0	18.4	52.7
q[C]	-0.88	-0.66	-0.64	-0.21
C-B bond order	1.36	1.17	1.17	0.97
d_{C-B}	1.48	1.51	1.51	1.55
V_w	0.0	40.6	38.1	46.3

[a] The free-energy barrier is computed from a precursor complex in which the carbonyl oxygen of aldehyde is coordinated side-on to lithium.

The computed $\Delta G^{\ddagger}_{Ald}$ values (Table 4.4) predict an order of nucleophilic reactivity that is consistent with experimental background (Li > Cu > Ag > Pd, with $\Delta G^{\ddagger}_{Ald}$ = 2.2, 15.0, 18.4 and 52.7 kcal·mol^{-1}, respectively). Here, we identify the overall charge of carbanionic fragment (*q*[C]) as descriptor correlating with nucleophilicity; thus, the more negatively charged the carbanionic fragment, the lower is the energy barrier (Table 4.4, second row). The formation of coordination complexes changes the nature of the HOMO orbital which cannot be univocally assigned to the C-B π-interaction, and consequently, we discarded it as descriptor in this case. Additionally, we evaluated the steric effects of the different metal fragments on the reactivity using the distance-weighted volume (V_W) parameter.[48–50] The V_W parameter measures the steric bulkiness of the metal fragment and its impact on carbanion center (see Computational Details, section 4.5). Comparison of the closely related [$(PPh_3)_2Cu(H_2CBpin)$] and [$(PPh_3)_2Ag(H_2CBpin)$] complexes shows that the silver fragment induces less steric hindrance on the reactive carbanion due to the larger size of Ag^+ ion, which move away the ligand substituents. However, the larger polarization of the metal-carbon bond in Cu complex determines its higher nucleophilicity, indicating that steric effects are less influential than electronic ones when comparing different metals. Along the series we observe substantial structural changes in the boron-carbon moiety and in its interaction with the metal (Table 4.4, third and fourth rows). This indicates a continuous switch on the compound nature from borata-alkene lithium salt to an α-boryl alkyl palladium complex. In lithium species **1a^{pin}-Li**, both the Wiberg C-B bond order (1.36) and

the C-B distance (1.48 Å) are indicative of borata-alkene character. The Li cation interacts electrostatically with the 3 atoms of O-C-B moiety (See Figure 4.11). Although Li^+ does not change the nature of the species, it induces some C-B lengthening (+0.04 Å) and pyramidalization of the carbanionic carbon (-30º), with respect to the free carbanion **1a^{pin}**. Note that introducing specific solvation molecules solvating Li^+ cation[51] would diminish its effect on the electronic structure borata-alkene.

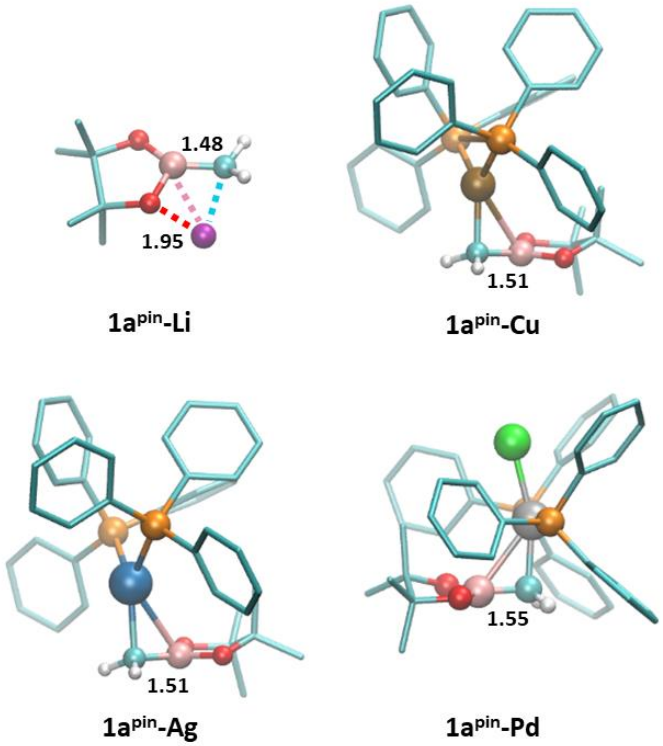

Figure 4.11. Three-dimensional representation of computed structures for metal complexes **1a^{pin}-Li**, **1a^{pin}-Cu**, **1a^{pin}-Ag** and **1a^{pin}-Pd**. Selected distances in Å.

On the other extreme, the computed C-B bond order of palladium complex **1a^{pin}-Pd** is close to 1 and the corresponding distance (1.55 Å) is significantly larger than for **1a^{pin}-Li**. Thus, this Pd compound can be better defined as an α-boryl alkyl palladium complex. At an intermediate situation, the Bpin=CH_2^- fragment in Cu and Ag compounds acts as an anionic η^2-(C,B) ligand whose interaction with the transition metal is shifted toward the C atom (See Figure 4.11). In line with bonding description, the HOMO orbital in **1a^{pin}-Cu** and **1a^{pin}-Ag** shows an overlap between transition metal *d* orbitals and the C=B π orbital (Figure 4.12). Note that borata-alkenes acting as anionic ligands with η^2 coordination to transition metals are known.[52]

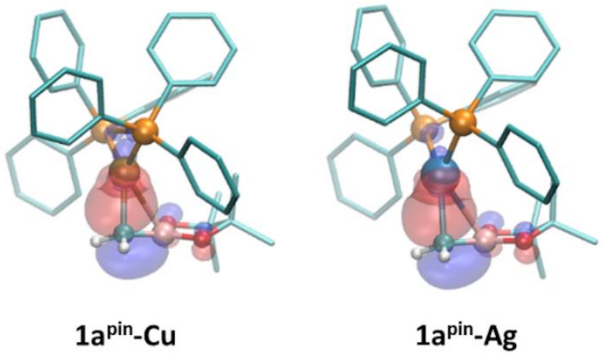

Figure 4.12. Representation of HOMO orbitals, formally corresponding to the overlap of *d* metal complex orbital and C-B π-orbital, for **1a^{pin}-Cu** and **1a^{pin}-Ag**.

4.3.6 Trend map for the metal salts and complexes

To further assess the variation in the nature of α-boryl carbanions with regard to the metal involved, we performed a systematic structural search within the Cambridge Structural Database (CSD; see Computational Details, section 4.5), and constructed a histogram of the C=B distances (Figure 4.13). The graph separates the crystallographic data for boryl methide salts into three main groups: red bars represent boryl methide Li salts, green bars cover boryl methyde Cu salts, and other metals from group 4 and 5, and blue bars inlvolve boryl methide salts of late transition metals including Pd^{2+}. For each group, the $d_{C\text{-}B}$ values lie within a relatively wide range (0.1 Å), but their distributions are centered at different distances. To the far left we found the boryl alkylidene lithium salts, most of whose C-B distances range from 1.44 to 1.49 Å. Moving to the right, from 1.47 to 1.54 Å, there are several early transition metal complexes (Ti^{4+}, Zr^{4+}, Hf^{4+}, and Ta^{5+}), and within this distance range we also found the Cu^{+} complexes at 1.51 and 1.52 Å. At longer C-B distances (> 1.52 Å), we find most of the late transition metal complexes such as Pd, Pt, Ru, Rh or Zn (for a complete list, see Table 6.4 in Chapter 6, section 6.4). Overall, our computed values fit quite well with the structural data available in CSD, allowing to classify the nature of α-boryl carbanionic species into three main groups and to establish structure-reactivity relationships.

The borata-alkene lithium salts, and the η^2-(C,B) borata-alkene copper and silver complexes show highly polarized metal-carbon interactions with a significant nucleophilic character. They are prone to generate carbanionic fragments stabilized by boryl moiety that are able to react with organic electrophiles as observed experimentally.[39–45] Other promising species for nucleophilic additions are those based on early transition metals, although to the best of our knowledge their reactivity has not been tested yet.[43–45] Only few examples are

currently reported on the use of silver salts for nucleophilic additions.[41] The α-boryl alkyl palladium complexes have less polarized and stronger metal-carbon bond. As consequence, the reported reactivity for Pd differs from Li, Cu and Ag. Although these palladium complexes do not serve as nucleophilic agents, they have been applied in C-C bond forming reactions, for example, via transmetalllation.[46,47] Figure 4.13 shows that other late transition metals have similar structural features to Pd, suggesting that this reactivity can be extended to other complexes.

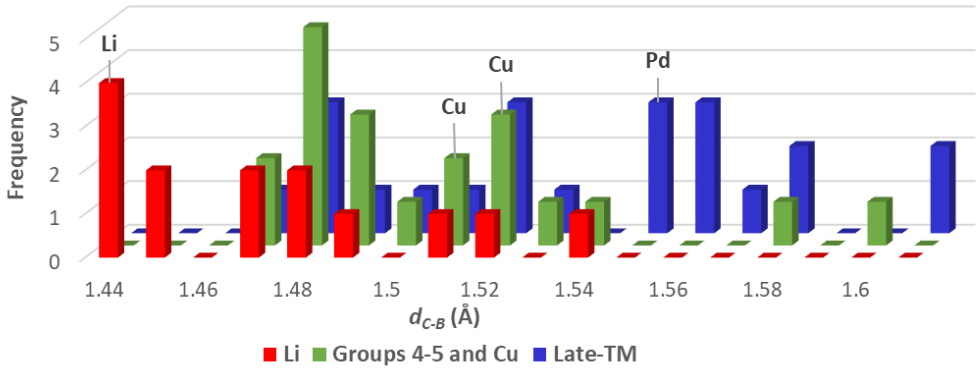

Figure 4.13. Histograms for B-C bond lengths of α-boryl carbanionic species separates into 3 groups as a function of carbanion nature 1) Li salts (red bars), 2) Cu and groups 4 and 5 including Ti, Zr, Hf, and Ta complexes (green bars), and 3) late transition metals including Fe, Ru, Rh, Ni, Pd, Pt, Au, Zn and Hg (blue bars). All bonds lengths are rounded to the nearest 0.01 Å. Data obtained from crystallographic data in the CSD.

Finally, Figure 4.14 provides an extension of the electronic structure analysis for Li, Cu, Ag and Pd compounds with different type and number of boryl moieties and substituents on the carbanionic atom. The overall charge of the carbanionic fragment (q[C]) and the average C-B bond order (C-$B_{bo\text{-}av.}$) can be used as descriptors to evaluate the nucleophilicity and the nature of the α-boryl carbanionic species, respectively. Clearly, the extent of the nucleophilicity (increasing to the left of the graph) is mainly ruled by the type of metal, but it can be tuned by α-borly carbanionic fragment. We also observe that the decrease of C-B bond order, that is, the reduction of borata-alkene character, has the following trend: Li > Cu ≅ Ag > Pd. The C-$B_{bo\text{-}av.}$ descriptor is more sensitive to the nature of the carbanionic fragment. Interestingly, among Cu species, calculations suggest that the vinyl carbanionic **1e^{pin}-Cu** complex is located at a different area of the chemical space (see Figure 4.14), and therefore, it could lead to new reactivity.

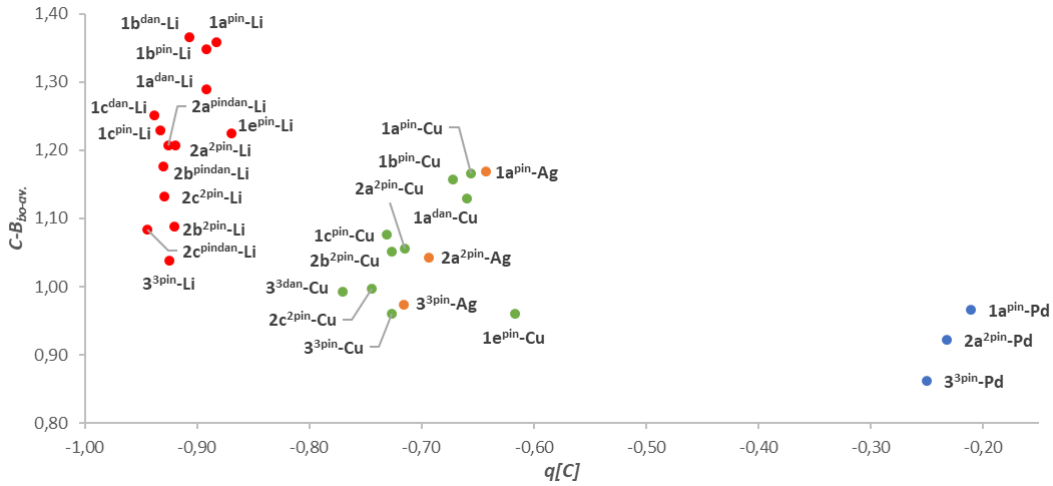

Figure 4.14. Representation of the average of C-B Wiberg bond orders (C-$B_{bo\text{-}av.}$) *versus* the overall charge of the carbanionic fragment (*q*[C]) for the α-boryl carbanionic Li (red circles), Cu (green circles), Ag (orange circles) and Pd (blue circles) species.

4.4 Conclusions

We have systematically studied several types of α-boryl carbanions analyzing their electronic structures and reactivity trends as a function of the nature of boryl moieties, the type of carbanionic substituents, the number of boryl motifs, and the metal interaction with the carbanion. In general, the free carbanionic intermediates are better described as borata-alkene species with a C-B π-interaction strongly polarized towards the carbanionic atom. By taking into consideration the energy of the HOMO and Wiberg bond order, we were able to establish a gradient of stability and nucleophilic reactivity for these intermediates that can be summarized as follows:

- π-Acidic boron atoms (i.e. $BMes_2$ or $B(C_5F_5)_2$), aromatic substituents on boron (i.e. Bdan), or electron withdrawing substituents on carbon (i.e. Ph) induce a larger delocalization of the carbanionic charge through the π-channel resulting in more stable and less reactive intermediates.
- The multi-boryl carbanionic species loss part of their borata-akene character but enhance their stability electrostatically through the additive effect of several polar C-B bonds.

This map of the reactivity landscape has predicted a novel α-boryl carbanion, the newly design 4,4,5,5-tetramethyl-1,3,2-diazaboryl methide anion **1a**^{Npin} $[H_2CB(NH)_2R_2]^-$, that could show enhanced nucleophilicity.

From the analysis of a large dataset for α-boryl alkylidene metal precursors, both computational and crystallographic analysis, we remark:

- There are three different types of carbanionic species that can be directly related to the observed reactivity: 1) borata-alkene salts with alkali and alkali earth metals such as Li, 2) η^2-(C-B) borata-alkene complexes with early transition metals, Cu and Ag, and 3) α-boryl alkyl complexes with late transition metals such as Pd.
- The two first groups show highly polarized metal-carbon interactions with a significant nucleophilic character that make them suitable synthons for reacting with organic electrophiles.
- The third group has a less polarized and stronger metal-carbon bond and they are prone to undergo other type of C-C bond forming reactions such as cross coupling through transmetallation strategies.

4.5 Computational details

Geometry optimizations and transition state searches were performed with Gaussian16 package.[53] The quantum mechanics calculations were performed within the framework of Density Functional Theory (DFT)[54–57] by using the ωB97X-D functional.[58] The basis set employed effective core potentials (ECPs) with double-ζ valence basis set (LANDL2DZ)[59–61] for Cu, Ag, Pd, Cl, Br and P, and were supplemented with polarized shells with the following exponents: Cu (f = 3.525), Ag (f = 1.611), Pd (f = 1.472), Cl (d = 0.650), Br (d = 0.428) and P (d = 0.387).[62,63] For all other electrons of all other atoms 6-31G(d) basis set was used.[64–66] The solvent effects of DMSO were included by means of SMD model[67] as implemented in Gaussian16. [53] The bonding of the molecules as well as the fragment charges were analyzed by using the NBO method,[68] from which we derived the Wiberg bond order and carbanion fragment charge (*q*[C]) descriptors. The NBO method analyses the resultant wave function in terms of optimally chosen localized orbitals, corresponding to a Lewis structure representation of chemical bonding. For computing orbital populations consistently, we had defined the carbanion carbon bonded to 3 substituents with single bonds.

To quantify the steric hindrance of metal fragments, we used the distance-weighed volume parameter (V_W).[48–50] which measures the steric bulkiness of the molecular environment and its impact on the carbanion center. The descriptor quantifies the bulk produced the metal fragment by considering three parameters: 1) The number of atoms, excluding the metal,

2) the size of the atom (*r* = van der Waals radii in Å), and 3) the distance (*d*) from the atom to the boron center (in Å). The factor r^3 is divided by *d* for each atom and the sum is extended to all of the atoms in the given fragment. Finally, the crystallographic structure search was carried out by Cambridge Structural Database (CSD) software, using the February 2020 version. A data set collection of computational results is available in the ioChem-BD repository[69] and can be accessed via https://doi.org/10.19061/iochem-bd-2-52.

4.6 References

(1) Horner, L.; Hoffmann, H.; Wippel, H. G. Phosphororganische Verbindungen, XII. Phosphinoxyde Als Olefinierungsreagenzien. *Chem. Ber.* **1958**, *91* (1), 61–63.

(2) Cainelli, G.; Dal Bello, G.; Zubiani, G. Gem-Dimetallic Compounds : On the Metal-Metal Interconversion between Gem-Organoboron Compounds and n-Butyllithium. *Tetrahedron Lett.* **1965**, *6* (38), 3429–3432.

(3) Zweifel, G.; Steele, R. B. Transmetalation Reactions with 1,1-Dialuminohexane. A Novel Synthesis of Cn+1 1-Alkenes from Cn 1-Alkynes. *Tetrahedron Lett.* **1966**, *7* (48), 6021–6025.

(4) Schmidbauer, H.; Tronich, W. Ein NMR-Beitrag Zum Problem Der Struktur Metallierter Methylenphosphorane. *Chem. Ber.* **1968**, *101* (10), 3556–3561.

(5) Kauffmann, T.; Echsler, K.-J.; Hamsen, A.; Kriegesmann, R.; Steinseifer, F.; Vahrenhorst, A. Darstellung Und Anwendungsmöglichkeiten von Diphenylarsanyl-, Diphenylstibanyl- Und Triphenylplumbyl-Methyllithium. *Tetrahedron Lett.* **1978**, *19* (45), 4391–4394.

(6) Kauffmann, T. New Possible Applications of Heavy Main-Group Elements in Organic Synthesis. *Angew. Chemie Int. Ed. English* **1982**, *21* (6), 410–429.

(7) Bertini, F.; Grasselli, P.; Zubiani, G.; Cainelli, G. Geminal Dimetallic Compounds: Reactivity of Methylene Magnesium Halides and Related Compounds. A General Carbonyl Olefination Reaction. *Tetrahedron* **1970**, *26* (6), 1281–1290.

(8) Zweifel, G.; Arzoumanian, H. Germinal Organometallic Compounds. I. The Synthesis and Structure of 1,1-Diborohexane. *J. Am. Chem. Soc.* **1967**, *89* (2), 291–295.

(9) Zweifel, G.; Fisher, R. P. The Insertion of Alkylidene Groups into Diene Systems. A Convenient Synthesis of Alkylidenecycloalkanes via Monohydroboration of 1-Bromo-1-Alkynes with Bisboracyclanes. *Synthesis* **1972**, 10, 557–558.

(10) Rathke, M. W.; Kow, R. Generation of Boron-Stabilized Carbanions. *J. Am. Chem. Soc.* **1972**, *94* (19), 6854–6856.

(11) Kow, R.; Rathke, M. W. Formation and Reactions of Boron-Stabilized Carbanions Derived from Vinylboranes. *J. Am. Chem. Soc.* **1973**, *95* (8), 2715–2716.

(12) Ashe, A. J.; Shu, P. 1-Phenylborabenzene Anion. *J. Am. Chem. Soc.* **1971**, *93* (7), 1804–1805.

(13) Pelter, A.; Singaram, B.; Williams, L.; Wilson, J. W. The Dimesitylboron Group in Organic Synthesis 1. Introduction. *Tetrahedron Lett.* **1983**, *24* (6), 623–626.

(14) Pelter, A.; Williams, L.; Wilson, J. W. The Dimesitylboron Group in Organic Synthesis 2. The c-Alkylation of Alkyldimesitylboranes. *Tetrahedron Lett.* **1983**, *24* (6), 627–630.

(15) Pelter, A.; Singaram, B.; Wilson, J. W. The Dimesitylboron Group in Organic Synthesis. 3. Reactions of Allyldimesitylborane. *Tetrahedron Lett.* **1983**, *24* (6), 631–634.

(16) Pelter, A.; Singaram, B.; Warren, L.; Wilson, J. W. Hindered Organoboron Groups in Organic Chemistry. The Production of Boron Stabilized Carbanions. *Tetrahedron* **1993**, *49* (14), 2965–2978.

(17) Knochel, P. A New Approach to Boron-Stabilized Organometallics. *J. Am. Chem. Soc.* **1990**, *112* (20), 7431–7433.

(18) Matteson, D. S.; Wilson, J. W. An α-Lithio Boronic Ester from an α-Trimethylstannyl Boronic Ester. *Organometallics* **1985**, *4* (9), 1690–1692.

(19) Tsai, D. J. S.; Matteson, D. S. Pinanediol [α-(Trimethylsilyl)Allyl]Boronate and Related Boronic Esters. *Organometallics* **1983**, *2* (2), 236–241.

(20) Brown, H. C.; Zweifel, G. Hydroboration. XI. The Hydroboration of Acetylenes—A Convenient Conversion of Internal Acetylenes into *cis*-Olefins and of Terminal Acetylenes into Aldehydes. *J. Am. Chem. Soc.* **1961**, *83* (18), 3834–3840.

(21) Zweifel, G.; Arzoumanian, H. The Synthesis of Mixed Geminal Organometallic Compounds. *Tetrahedron Lett.* **1966**, *7* (23), 2535–2538.

(22) Matteson, D. S. Methanetetraboronic and Methanetriboronic Esters as Synthetic Intermediates. *Synthesis* **1975**, 3, 147–158.

(23) Paetzold, P.; Boeke, B. Darstellung Und Deprotonierung von 9-Borylfluorenen. *Chem. Ber.* **1976**, *109* (3), 1011–1016.

(24) Maza, R. J.; Carbó, J. J.; Fernández, E. Borata-Alkene Species as Nucleophilic Reservoir. *Adv. Synth. Catal.* **2021**, *363* (9), 2274–2289.

(25) Hong, K.; Liu, X.; Morken, J. P. Simple Access to Elusive α-Boryl Carbanions and Their Alkylation: An Umpolung Construction for Organic Synthesis. *J. Am. Chem. Soc.* **2014**, *136* (30), 10581–10584.

(26) Oomens, J.; Steill, J. D.; Morton, T. H. IR Spectra of Boron-Stabilized Anions in the Gas Phase. *Inorg. Chem.* **2010**, *49* (15), 6781–6783.

(27) Bartlett, R. A.; Power, P. P. X-Ray Crystal Structure of the Boron-Stabilized Carbanion [Li(12-Crown-4)$_2$][$CH_2C_6H_2$(3,5-Me_2)(4-B{2,4,6-$Me_3C_6H_2$}$_2$)]·Et_2O: Evidence for "Boron Ylide" Character. *Organometallics* **1986**, *5* (9), 1916–1917.

(28) Olmstead, M. M.; Power, P. P.; Weese, K. J.; Doedens, R. J. Isolation and X-Ray Crystal Structure of the Boron Methylidenide Ion [Me_2BCH_2]$^-$ (Mes = 2,4,6-$Me_3C_6H_2$): A Boron-Carbon Double Bonded Alkene Analog. *J. Am. Chem. Soc.* **1987**, *109* (8), 2541–2542.

(29) Moquist, P.; Chen, G.-Q.; Mück-Lichtenfeld, C.; Bussmann, K.; Daniliuc, C. G.; Kehr, G.; Erker, G. α-CH Acidity of Alkyl–B(C_6F_5)$_2$ Compounds – the Role of Stabilized Borata-Alkene Formation in Frustrated Lewis Pair Chemistry. *Chem. Sci.* **2015**, *6* (1), 816–825.

(30) Power, P. P. π-Bonding and the Lone Pair Effect in Multiple Bonds between Heavier Main Group Elements. *Chem. Rev.* **1999**, *99* (12), 3463–3504.

(31) Chiu, C.-W.; Gabbaï, F. P. Structural Changes Accompanying the Stepwise Population of a B-C π Bond. *Angew. Chemie Int. Ed.* **2007**, *46* (36), 6878–6881.

(32) Lafage, M.; Pujol, A.; Saffon-Merceron, N.; Mézailles, N. BH3 Activation by Phosphorus-Stabilized Geminal Dianions: Synthesis of Ambiphilic Organoborane, DFT Studies, and Catalytic CO_2 Reduction into Methanol Derivatives. *ACS Catal.* **2016**, *6* (5), 3030–3035.

(33) Klis, Tomasz and Lulinski, Sergiusz and Serwatowski, J. Formation and Synthetic Applications of Metalated Organoboranes. *Curr. Org. Chem.* **2010**, *14* (20), 2549–2566.

(34) Cid, J.; Carbó, J. J.; Fernández, E. Disclosing the Structure/Activity Correlation in Trivalent Boron-Containing Compounds: A Tendency Map. *Chem. – Eur. J.* **2012**, *18* (40), 12794–12802.

(35) García-López, D.; Cid, J.; Marqués, R.; Fernández, E.; Carbó, J. J. Quantitative Structure–Activity Relationships for the Nucleophilicity of Trivalent Boron Compounds. *Chem. – Eur. J.* **2017**, *23* (21), 5066–5075.

(36) Cuenca, A. B.; Cid, J.; García-López, D.; Carbó, J. J.; Fernández, E. Unsymmetrical 1,1-Diborated Multisubstituted sp^3-Carbons Formed via a Metal-Free Concerted-Asynchronous Mechanism. *Org. Biomol. Chem.* **2015**, *13* (37), 9659–9664.

(37) Wagner, M.; van Eikema Hommes, N. J. R.; Noeth, H.; Schleyer, P. v. R. Lithioboranes. A Theoretical Study. *Inorg. Chem.* **1995**, *34* (3), 607–614.

(38) Zhao, H.; Dang, L.; Marder, T. B.; Lin, Z. DFT Studies on the Mechanism of the Diboration of Aldehydes Catalyzed by Copper(I) Boryl Complexes. *J. Am. Chem. Soc.* **2008**, *130* (16), 5586–5594.

(39) Joannou, M. V; Moyer, B. S.; Meek, S. J. Enantio- and Diastereoselective Synthesis of 1,2-Hydroxyboronates through Cu-Catalyzed Additions of Alkylboronates to Aldehydes. *J. Am. Chem. Soc.* **2015**, *137* (19), 6176–6179.

(40) Murray, S. A.; Green, J. C.; Tailor, S. B.; Meek, S. J. Enantio- and Diastereoselective 1,2-Additions to α-Ketoesters with Diborylmethane and Substituted 1,1-Diborylalkanes. *Angew. Chemie Int. Ed.* **2016**, *55* (31), 9065–9069.

(41) Joannou, M. V; Moyer, B. S.; Goldfogel, M. J.; Meek, S. J. Silver(I)-Catalyzed Diastereoselective Synthesis of Anti-1,2-Hydroxyboronates. *Angew. Chemie Int. Ed.* **2015**, *54* (47), 14141–14145.

(42) Pelter, A.; Buss, D.; Colclough, E.; Singaram, B. Hindered Organoboron Groups in Organic Chemistry. 23. The Interactions of Dimesitylboron Stabilized Carbanions with Aromatic Ketones and Aldehydes to Give Alkenes. *Tetrahedron* **1993**, *49* (32), 7077–7103.

(43) Wu, C.; Wang, J. Geminal Bis(Boron) Compounds: Their Preparation and Synthetic Applications. *Tetrahedron Lett.* **2018**, *59* (22), 2128–2140.

(44) Miralles, N.; Maza, R. J.; Fernández, E. Synthesis and Reactivity of 1,1-Diborylalkanes towards C–C Bond Formation and Related Mechanisms. *Adv. Synth. Catal.* **2018**, *360* (7), 1306–1327.

(45) Nallagonda, R.; Padala, K.; Masarwa, A. Gem-Diborylalkanes: Recent Advances in Their Preparation, Transformation and Application. *Org. Biomol. Chem.* **2018**, *16* (7), 1050–1064.

(46) Zhang, C.; Wu, X.; Wang, C.; Zhang, C.; Qu, J.; Chen, Y. Pd/Cu-Catalyzed Domino Cyclization/Deborylation of Alkene-Tethered Carbamoyl Chloride and 1,1-Diborylmethane. *Org. Lett.* **2020**, *22* (16), 6376–6381.

(47) Li, C.; Li, M.; Li, J.; Wu, W.; Jiang, H. Palladium-Catalyzed Oxidative Allylation of Bis[(Pinacolato)Boryl]Methane: Synthesis of Homoallylic Boronic Esters. *Chem. Commun.* **2018**, *54* (1), 66–69.

(48) Aguado-Ullate, S.; Urbano-Cuadrado, M.; Villalba, I.; Pires, E.; García, J. I.; Bo, C.; Carbó, J. J. Predicting the Enantioselectivity of the Copper-Catalyzed Cyclopropanation of Alkenes by Using Quantitative Quadrant-Diagram Representations of the Catalysts. *Chem. – Eur. J.* **2012**, *18* (44), 14026–14036.

(49) Aguado-Ullate, S.; Saureu, S.; Guasch, L.; Carbó, J. J. Theoretical Studies of Asymmetric Hydroformylation Using the Rh-(R,S)-BINAPHOS Catalyst—Origin of Coordination Preferences and Stereoinduction. *Chem. – Eur. J.* **2012**, *18* (3), 995–1005.

(50) MolQuO Application (Accessed Sep 2021): Http://Rodi.Urv.Es/~carbo/Quadrants/Index.Html.

(51) Royes, J.; Ni, S.; Farré, A.; La Cascia, E.; Carbó, J. J.; Cuenca, A. B.; Maseras, F.; Fernández, E. Copper-Catalyzed Borylative Ring Closing C–C Coupling toward Spiro- and Dispiroheterocycles. *ACS Catal.* **2018**, *8* (4), 2833–2838.

(52) Emslie, D. J. H.; Cowie, B. E.; Kolpin, K. B. Acyclic Boron-Containing π-Ligand Complexes: H2- and H3-Coordination Modes. *Dalton* **2012**, *41* (4), 1101–1117.

(53) Frisch, M. J.; Trucks, G. W.; Schlegel, H. B.; Scuseria, G. E.; Robb, M. A.; Cheeseman, J. R.; Scalmani, G.; Barone, V.; Petersson, G. A.; Nakatsuji, H.; Li, X.; Caricato, M.; Marenich, A. V; Bloino, J.; Janesko, B. G.; Gomperts, R.; Mennucci, B.; Hratchian, H. P.; Ortiz, J. V; Izmaylov, A. F.; Sonnenberg, J. L.; Williams-Young, D.; Ding, F.; Lipparini, F.; Egidi, F.; Goings, J.; Peng, B.; Petrone, A.; Henderson, T.; Ranasinghe, D.; Zakrzewski, V. G.; Gao, J.; Rega, N.; Zheng, G.; Liang, W.; Hada, M.; Ehara, M.; Toyota, K.; Fukuda, R.; Hasegawa, J.; Ishida, M.; Nakajima, T.; Honda, Y.; Kitao, O.; Nakai, H.; Vreven, T.; Throssell, K.; Montgomery Jr., J. A.; Peralta, J. E.; Ogliaro, F.; Bearpark, M. J.; Heyd, J. J.; Brothers, E. N.; Kudin, K. N.; Staroverov, V. N.; Keith, T. A.; Kobayashi, R.; Normand, J.; Raghavachari, K.; Rendell, A. P.; Burant, J. C.; Iyengar, S. S.; Tomasi, J.; Cossi, M.; Millam, J. M.; Klene, M.; Adamo, C.; Cammi, R.; Ochterski, J. W.; Martin, R. L.; Morokuma, K.; Farkas, O.; Foresman, J. B.; Fox, D. J. Gaussian16 Revision A03. 2016.

(54) Hohenberg, P.; Kohn, W. Inhomogeneous Electron Gas. *Phys. Rev.* **1964**, *136* (3B), B864–B871.

(55) Kohn, W.; Sham, L. J. Self-Consistent Equations Including Exchange and Correlation Effects. *Phys. Rev.* **1965**, *140* (4A), A1133–A1138.

(56) Yang, R. G. P. and W. *Density-Functional Theory of Atoms and Molecules*; Oxford Univ. Press: Oxford, 1989.

(57) Comstock, M. J. The Challenge of d and f Electrons, Copyright, ACS Symposium Series, Foreword. In *The Challenge of d and f Electrons*; Comstock, M. J., Ed.; ACS Symposium Series; American Chemical Society, 1989; Vol. 394, pp i–iv.

(58) Chai, J.-D.; Head-Gordon, M. Long-Range Corrected Hybrid Density Functionals with Damped Atom–Atom Dispersion Corrections. *Phys. Chem. Chem. Phys.* **2008**, *10* (44), 6615–6620.

(59) Hay, P. J.; Wadt, W. R. Ab Initio Effective Core Potentials for Molecular Calculations. Potentials for the Transition Metal Atoms Sc to Hg. *J. Chem. Phys.* **1985**, *82* (1), 270–283.

(60) Wadt, W. R.; Hay, P. J. Ab Initio Effective Core Potentials for Molecular Calculations. Potentials for Main Group Elements Na to Bi. *J. Chem. Phys.* **1985**, *82* (1), 284–298.

(61) Hay, P. J.; Wadt, W. R. Ab Initio Effective Core Potentials for Molecular Calculations. Potentials for K to Au Including the Outermost Core Orbitals. *J. Chem. Phys.* **1985**, *82* (1), 299–310.

(62) Ehlers, A. W.; Böhme, M.; Dapprich, S.; Gobbi, A.; Höllwarth, A.; Jonas, V.; Köhler, K. F.; Stegmann, R.; Veldkamp, A.; Frenking, G. A Set of F-Polarization Functions for Pseudo-Potential Basis Sets of the Transition Metals Sc-Cu, Y-Ag and La-Au. *Chem. Phys. Lett.* **1993**, *208* (1), 111–114.

(63) Höllwarth, A.; Böhme, M.; Dapprich, S.; Ehlers, A. W.; Gobbi, A.; Jonas, V.; Köhler, K. F.; Stegmann, R.; Veldkamp, A.; Frenking, G. A Set of D-Polarization Functions for Pseudo-Potential Basis Sets of the Main Group Elements Al-Bi and f-Type Polarization Functions for Zn, Cd, Hg. *Chem. Phys. Lett.* **1993**, *208* (3), 237–240.

(64) Fukui, K. Formulation of the Reaction Coordinate. *J. Phys. Chem.* **1970**, *74* (23), 4161–4163.

(65) Gordon, M. S. The Isomers of Silacyclopropane. *Chem. Phys. Lett.* **1980**, *76* (1), 163–168.

(66) Binning Jr., R. C.; Curtiss, L. A. Compact Contracted Basis Sets for Third-Row Atoms: Ga–Kr. *J. Comput. Chem.* **1990**, *11* (10), 1206–1216.

(67) Marenich, A. V; Cramer, C. J.; Truhlar, D. G. Universal Solvation Model Based on Solute Electron Density and on a Continuum Model of the Solvent Defined by the Bulk Dielectric Constant and Atomic Surface Tensions. *J. Phys. Chem. B* **2009**, *113* (18), 6378–6396.

(68) Reed, A. E.; Curtiss, L. A.; Weinhold, F. Intermolecular Interactions from a Natural Bond Orbital, Donor-Acceptor Viewpoint. *Chem. Rev.* **1988**, *88* (6), 899–926.

(69) Álvarez-Moreno, M.; de Graaf, C.; López, N.; Maseras, F.; Poblet, J. M.; Bo, C. Managing the Computational Chemistry Big Data Problem: The IoChem-BD Platform. *J. Chem. Inf. Model.* **2015**, *55* (1), 95–103.

Chapter 5
Conclusions

Conclusions

In this Thesis, we have developed new synthetic methodologies that give access to unprecedented organoboron compounds via addition of nucleophilic boryl synthons to carbon π-systems. We have also generated new knowledge on the stability/reactivity trends of α-boryl carbanions, attending structural and electronic issues. The close combination of experimental and computational tools have provided a deep understanding of the reaction mechanism and trends, which have allowed to rationalize observations and to propose newly designed reagents.

The specific conclusions of the work conducted in this Thesis are listed below:

- In Chapter 2, we have shown that copper(I), modified with Xantphos ligand, can catalyze the borylative cyclization of γ-alkenyl aldehydes. We could observe that borylcupration on C=C bond is preferred for electron-deficient alkene moieties, as described for aromatic substituted γ-alkenyl aldehydes. It could be postulated that the electron density on the nucleophile carbon could resonate with the aromatic ring. A variety of substituted olefins can be employed, but electron-rich olefins suppress the borylation through the C=C bond favoring the borylation on the C=O bond. In addition, substituents are required at the aldehyde α-carbon, and both four and five-membered rings can be formed.

  Despite the chemoselectivity issues arising from competitive 1,2-borylation of the aldehyde, this methodology provides access to various spirocyclic cyclobutanol products with high levels of *anti*-diastereoselection in moderate to good yields. DFT studies identify and analyze the key steps of the catalytic cycle that govern the chemo- and diastereoselectivity. The preference in the addition of Cu-Bpin to C=C or C=O bond (transition states **TS1** and **TS1'**, respectively) determines the chemoselectivity. Due to the nucleophilic nature of the boryl fragment, electron-donor substituents on the alkene can switch the chemoselectivity towards the boryl addition to the aldehyde (i.e. substrate **2.27**). The diastereoselectivity-determining step corresponds to the carbon-carbon coupling process (**TS2**$_{anti}$ and **TS2**$_{syn}$), where intramolecular interactions within the substrate govern the diastereoselectivity.

- In Chapter 3, we have demonstrated that the sole addition of 15-30 mol% of Na_2CO_3 to B_2pin_2 in MeOH, allows the 1,4-hydroboration of cyclic and non-cyclic 1,3-dienes. We have observed that transition-metal-free borylation of 1,3-dienes occurs through S_N2'-type mechanisms with a preference for the *E* stereoisomeric allylic boronate product formation. Moderate yields have been achieved for this unprecedented catalytic process and the scope of the reaction includes terminal, internal and cyclic conjugated dienes. On the other hand, we have postulated that triboration of 1,3-dienes has been

achieved throughout conjugated borylation followed by diboration reaction in a single operational step.

Computational studies have identified the key steps in the transition-metal-free conjugative borylation that rationalize the preference for 1,4-hydroborated products as well as the *E* stereoisomerism in the allylic boronate products. The origin of the Z isomer involves an initial isomerization of the *trans* diene to the *cis* conformer, which has lower stability but it is compensated by the higher reactivity towards borylation. The analysis of the charge distribution in the allylic intermediate shows that protonation is favoured at the C_1 position, explaioning the regioselectivity in the 1,4-hydroboration.

- In Chapter 4, we have systematically studied several types of α-boryl carbanions analyzing their electronic structures and reactivity trends as a function of the nature of boryl moieties, the type of carbanionic substituents, the number of boryl motifs, and the metal interaction with the carbanion. In general, the free carbanionic intermediates are better described as borata-alkene species with a C-B π-interaction strongly polarized towards the carbanionic atom. By taking into consideration the energy of the HOMO and Wiberg bond order, we were able to establish a gradient of stability and nucleophilic reactivity for these intermediates that can be summarized as follow: 1) π-acidic boron atoms (i.e. $BMes_2$ or $B(C_5F_5)_2$), aromatic substituents on boron (i.e. Bdan), or electron-withdrawing substituents on carbon (i.e. Ph), induce a larger delocalization of the carbanionic charge through the π-channel that is resulting in more stable and less reactive intermediates, 2) the multi-boryl carbanionic species, lose part of their borata-akene character but enhance their stability electrostatically through the additive effect of several polar C-B bonds. This map of the reactivity landscape has predicted a novel α-boryl carbanion, the newly designed 4,4,5,5-tetramethyl-1,3,2-diazaboryl methide anion (**1a**$^{\mathbf{Npin}}$), that could show enhanced nucleophilicity.

  From a computational and crystallographic analysis conducted for a large dataset for α-boryl alkylidene metal precursors, we can conclude that there are three different types of carbanionic species that can be directly related to the observed reactivity: 1) borata-alkene salts with alkali and alkali earth metals such as Li, 2) η^2-(C-B) borata-alkene complexes with early transition metals, Cu and Ag, and 3) α-boryl alkyl complexes with late transition metals such as Pd. The two first groups show highly polarized metal-carbon interactions with a significant nucleophilic character, making them suitable synthons for reacting with organic electrophiles, and the third group has a less polarized and stronger metal-carbon bond, and they are prone to undergo another type of C-C bond forming reactions such as cross-coupling through transmetallation strategies.

Chapter 6
Experimental Section

6.1 General Considerations

Solvents and reagents were obtained from commercial suppliers and dried and/or purified (if needed) by standard procedures[1]. Solvents and reagents were obtained from commercial suppliers as Sigma-Aldrich Inc. Appollo Scientific, Fluka, Stream or Fluorochem. Bis(pinacolato)diboron (B_2pin_2) was purchased from Ally Chem and used without further purification. All reactions were conducted in oven and flame-dried glassware under an inert atmosphere of argon, using Schlenk-type techniques. Flash chromatography was performed on standard silica gel (Merck Kieselgel 60 Å 230-400 mesh particle size). Thin layer chromatography was performed on Merck Kieselgel 60 F_{254} which was developed using standard visualizing agents: UV fluorescence (254 and 366 nm) or potassium permanganate/Δ. NMR spectra were recorded at a Varian 400 spectrometer. ^{1}H NMR and ^{13}C NMR chemical shifts (δ) are reported in ppm with the solvent resonance as the internal standard ($CHCl_3$: 7.26 ppm (^{1}H)) and ($CDCl_3$: 77.16 ppm (^{13}C). ^{11}B NMR chemical shifts (δ) are reported in ppm relative to $(CH_3)_2O\cdots BF_3$. Data are reported as follows: chemical shift, multiplicity (s = singlet, d = doublet, t = triplet, q = quartet, hept = heptuplet, br = broad, m = multiplet), coupling constants (Hz) and integration. High resolution mass spectra (HRMS) were recorded using a 6210 Time of Flight (TOF) mass spectrometer from Agilent Technologies (Waldbronn, Germany) with an ESI interface and it was performed at the Servei de Recursos Científics i Tècnics (Universidad Rovira i Virgili, Tarragona) or using a BIOTOF II Time of Flight (TOF) mass spectrometer from Bruker with an APCI interface or EI interface and it was performed at the Unida de de Espectrometría de Masas e Proteómica (Universidad de Santiago de Compostela, Santiago de Compostela). GC-MS analyses were performed on a HP6890 gas chromatograph and an Agilent Technologies 5973 Mass selective detector (Waldbronn, Germany) equipped with an achiral capillary column HP-5 (30 m, 0.25 mm i.d., 0.25 µm thickness) using He as the carrier gas.

6.2 Experimental section for Chapter 2

6.2.1 General procedure for the protection of amines with sulfonyl chloride derivative

N,N-diisopropyletilamina (DIPEA, 2 equiv, 20 mmol) and the tosyl chloride derivative (1 equiv, 10 mmol) were added to a solution of methyl piperidine-4-carboxylate (1 equiv, 10 mmol) in dry dichlorometane (DCM, 0.14 M) at room temperature. The mixture was stirred for 4-16 hours until complete consumption of the corresponding arenesulfonyl chloride. The organic phase was washed with 10% of $NaHCO_3$. The aqueous phase was extracted with ethyl acetate. The organic extracts were combined, washed with H_2O and NaCl sat. solution, dried ($MgSO_4$), filtered and the volatiles removed in *vacuo*. The crude product was purified by flash column chromatography.[2]

6.2.2 Characterization of sulfonyl chloride derivative

Methyl 1-tosylpiperidine-4-carboxylate (S2.1)

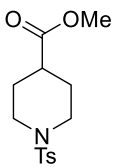

S2.1

The product **S2.1** was purified by flash column chromatography using pentane:ethyl acetate (100:0 to 60:40) as eluent. It was obtained as white solid (4458.3 mg, 60% yield). **^{1}H NMR ($CDCl_3$, 400 MHz) δ =** 7.62 (d, *J* = 7.9 Hz, 2H), 7.31 (d, *J* = 7.9 Hz, 2H), 3.64 (s, 3H), 3.61 (m, 2H), 2.43 (td, J = 11.4, 2.9 Hz, 2H), 2.42 (s, 3H), 2.24 (dt, *J* = 10.7, 4.0 Hz, 1H), 1.95 (m, 2H), 1.79 (m, 2H). **^{13}C NMR ($CDCl_3$, 100 MHz) δ =** 174.2, 143.5, 132.9, 129.6, 127.6, 51.8, 45.3, 39.8, 27.4, 21.5. **HRMS (ESI) for $C_{28}H_{38}N_2NaO_8S_2$ $[2M+Na]^+$:** calculated: 617.1968, found: 617.1985.

6.2.3 General procedure for the preparation of alkyl bromides

This protocol covers two consecutive synthetic procedures:

A) Wittig reaction on aryl methyl ketones:[3] a mixture of methyltriphenylphosphonium bromide (1.2 equiv) in dry THF (0.5 M) under argon atmosphere was cooled to 0 °C. Then, nBuLi (2.5 M solution in hexane, 1.2 equiv) was added slowly under stirring. After, the resulting orange mixture was maintained at 0 °C for 1 hour, a solution of the corresponding ketone (15 mmol, 1.0 equiv) in dry THF was added dropwise, at 0 °C. The reaction was allowed to warm up to r.t., stirred overnight, and finally quenched with a saturated aqueous solution of NaCl. The resulting mixture was extracted with diethyl ether. The combined organic phases were washed with brine, dried over Mg_2SO_4, and concentrated under reduced pressure. The resulting crude

product was purified by flash column chromatography to give the corresponding alkene.

B) Bromination of 1,1-disubstituted alkenes; **Method B1**:[4–6] The previously prepared alkene (1 equiv) was dissolved in a round bottom flask containing DCM (10 mL x 3 mmol alkene). N-bromosuccinimide (NBS, 2 equiv) was added to the solution which was then allowed to stir at 45 °C for 18 hours. Then the reaction mixture was concentrated and petroleum ether was added. The precipitate formed was filtered off and then the organic layer was dried over Mg_2SO_4 and concentrated under vacuum. The crude product was purified by flash column chromatography to give the corresponding brominated product. **Method B2**:[7] To a mixture of the α-methylstyrene derivative (1.0 equiv) and TMS-Cl (10 mol%) in dry CH_2Cl_2/THF (4:1, 3 mL x 1 mmol) under an argon atmosphere were added NBS (1.2 equiv) and $Yb(OTf)_3$ (10 mol%) in one portion. After stirring for 1 hour, the mixture was concentrated under reduced pressure. The resulting residue was filtered three times with pentane or diethyl ether, and the combined filtrates were concentrated under reduced pressure. The crude product mixture was then purified by silica gel chromatography.

6.2.4 Characterization of 1,1-disubstituted products prepared via Wittig Reaction (Method A)

Prop-1-en-2-ylbenzene (S2.2)

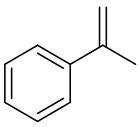

S2.2

The product **S2.2** was purchased from Sigma-Aldrich.

1-(tert-butyl)-4-(prop-1-en-2-yl)benzene (S2.4)

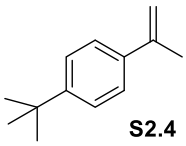

S2.4

The product **S2.4** was purified by flash column chromatography using pentane:diethyl ether (10:1) as eluent. It was obtained as colorless oil (2385.5 mg, 91% yield). **^{1}H NMR ($CDCl_3$, 400 MHz) δ =** 7.49 (d, *J* = 8.3 Hz, 2H) – 7.35 (d, *J* = 8.2 Hz, 2H), 5.41 – 5.37 (m, 1H), 5.09 – 5.05 (m, 1H), 2.18 (s, 3H), 1.36 (s, 9H). **^{13}C NMR ($CDCl_3$, 100 MHz) δ** = 150.4, 142.9, 138.3, 125.1, 125.1, 111.6, 34.5, 31.3, 21.7.

2-(prop-1-en-2-yl)naphthalene (S2.6)

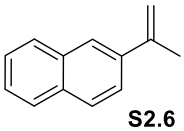

S2.6

The product **S2.6** was purified by flash column chromatography using pentane:diethyl ether (10:1) as eluent. The product was obtained as white solid (2132.2 mg, 85% yield). **^{1}H NMR ($CDCl_3$, 400 MHz) δ** = 7.82 – 7.68 (m, 4H), 7.60 (dd, *J* = 8.6, 1.9 Hz, 1H), 7.46 – 7.30 (m, 2H), 5.46 (d, *J* = 1.5Hz, 1H), 5.12 (d, *J* = 1.5 Hz, 1H), 2.20 (s, 3H). **^{13}C NMR ($CDCl_3$, 100 MHz) δ** = 143.0, 138.3, 133.3, 132.8, 128.2, 127.6, 127.5, 126.1, 125.8, 124.2, 123.9, 113.0, 21.8.

1-bromo-2-(prop-1-en-2-yl)benzene (S2.8)

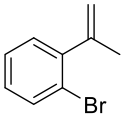

S2.8

The product **S2.8** was purified by flash column chromatography using pentane:diethyl ether (10:1) as eluent. It was obtained as colorless oil (2388.8 mg, 79% yield). **^{1}H NMR ($CDCl_3$, 400 MHz) δ** = 7.23 (d, *J* = 8.0 Hz, 1H), 7.12 (dd, *J* = 7.6, 1.9 Hz, 1H), 7,08 (d, *J* = 7.9 Hz, 1H), 7.04 (dd, *J* = 8.0, 1.9 Hz, 1H), 5.15 (d, *J* = 1.7 Hz, 1H), 4.86 (d, *J* = 2.0 Hz, 1H), 2.02 (s, 2H). **^{13}C NMR ($CDCl_3$, 100 MHz) δ** = 145.8, 144.8, 132.7, 129.7, 128.3, 127.2, 121.5, 116.0, 23.5.

6.2.5 Characterization of products from bromination Reaction (Method B1)

(3-bromoprop-1-en-2-yl)benzene (S2.3)

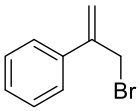

S2.3

The product **S2.3** was purified by flash column chromatography using pentane:diethyl ether (10:1) as eluent. It was obtained as colorless oil (1434.8 mg, 52% yield). **^{1}H NMR ($CDCl_3$, 400 MHz) δ** = 7.42 (dd, *J* = 8.3, 1.5 Hz, 2H), 7.39 – 7.20 (m, 4H), 5.49 (d, *J* = 0.7 Hz, 1H), 5.42 (d, *J* = 0.8 Hz, 1H), 4.32 (s, 2H). **^{13}C NMR ($CDCl_3$, 100 MHz) δ** = 144.2, 137.6, 128.5, 128.3, 127.8, 126.1, 126.0, 117.2, 34.2.

1-(3-bromoprop-1-en-2-yl)-4-(tert-butyl)benzene (S2.5)

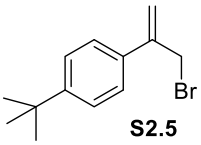

S2.5

The product **S2.5** was purified by flash column chromatography using pentane:diethyl ether (10:1) as eluent. It was obtained as a yellow oil (1556.9 mg, 45% yield). **^{1}H NMR ($CDCl_3$, 400 MHz) δ** = 7.42 (dd, *J* = 8.1, 1.7 Hz, 2H) 7.28 (dd, *J* = 8.4, 1.5 Hz, 2H)), 5.48 (d, *J* = 0.8 Hz, 1H), 5.38 (d, *J* = 0.8 Hz, 1H), 4.31 (s, 2H), 1.26 (s, 9H). **^{13}C NMR ($CDCl_3$, 100 MHz) δ** = 151.3, 143.8, 134.5, 125.7, 125.4, 116.5, 34.6, 34.2, 31.2.

2-(3-bromoprop-1-en-2-yl)naphthalene (S2.7)

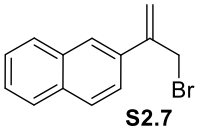

S2.7

The product **S2.7** was purified by flash column chromatography using pentane:ethyl acetate (10:1) as eluent. It was obtained as a yellow oil (2536.5 mg, 81% yield). **^{1}H NMR ($CDCl_3$, 400 MHz) δ =** 7.97 (d, *J* = 1.9 Hz, 1H), 7.94 – 7.81 (m, 3H), 7.65 (dd, *J* = 8.6, 1.9 Hz, 1H), 7.57 – 7.46 (m, 2H), 5.73 (t, *J* = 0.8 Hz, 1H), 5.62 (t, *J* = 0.8 Hz, 1H), 4.53 (s, 2H). **^{13}C NMR ($CDCl_3$, 100 MHz) δ** = 144.1, 134.7, 133.2, 133.1, 128.3, 128.20, 127.6, 126.3, 126.3, 125.2, 124.0, 117.6, 34.1.

6.2.6 Characterization of products from Bromination Reaction (Method B2)

1-bromo-2-(3-bromoprop-1-en-2-yl)benzene (S2.9)

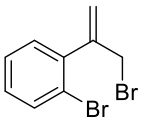

S2.9

The product **S2.9** was purified by flash column chromatography using pentane:ethyl acetate (10:1) as eluent. It was obtained as colorless oil (795.1 mg, 20% yield). **^{1}H NMR ($CDCl_3$, 400 MHz) δ =** 7.60 (d, *J* = 8.0 Hz, 1H), 7.39 – 7.29 (m, 2H), 7.25 – 7.20 (m, 1H), 5.67 (d, *J* = 1.0 Hz, 1H), 5.24 (d, *J* = 1.0 Hz, 1H), 4.38 (d, *J* = 0.9 Hz, 2H). **^{13}C NMR ($CDCl_3$, 100 MHz) δ =** 145.6, 140.2, 136.2, 132.7, 131.6, 129.4, 127.2, 120.8, 35.4.

6.2.7 General procedure for the alkylation of ester substrates with alkyl bromides followed by reduction to alcohols and oxidation to aldehydes

The initial step proceeded towards **the alkylation of ester substrates with alkyl bromides**:[8] To a 0 °C solution of ^{i}Pr$_2$NH (1.5 equiv, 15 mmol) in THF (15 mL), was added dropwise a solution of nBuLi 2.0 M (1.1 equiv, 11 mmol) in hexane. The reaction mixture was stirred for 20 minutes and then cooled to -78 °C. The substrate with the ester functionality (1 equiv, 10 mmol) was added dropwise and the reaction mixture was stirred for 1 hour at -78 °C. The corresponding alkyl halide (1.5 equiv, 15 mmol) was then added dropwise into the reaction mixture. The reaction mixture was then warmed naturally to room temperature and stirred until consumption of the starting ester. The reaction mixture was quenched by addition of saturated NH_4Cl aq. and extracted with diethyl ether three times. The combined organic layers were then dried ($MgSO_4$) filtered and concentrated under reduced pressure. The crude product of the alkylated ester was purified by flash column chromatography.

Next step proceeded towards **the reduction of the ester group to the corresponding alcohol**:[9] to a slurry of $LiAlH_4$ (1.5 equiv, 6 mmol) in anhydrous diethyl ether (0.9 M) was added a solution of the alkenyl ester (1 equiv, 4 mmol) in diethyl ether (1 M) dropwise at 0 °C. The mixture was stirred for 2 hours (or until consumption of the substrate). The reaction was then quenched by addition of diethyl ether dropwise after no observation of bubbles.

Then, water was added and the mixture was stirred until a white solid was formed. The mixture was then filtered and extracted with ethyl acetate. The organic layers were separated, dried ($MgSO_4$), filtered and concentrated under reduced pressure to obtain the alcohol without need of further purification for the next reaction step.

The last step involves a **general procedure for the oxidation of primary alcohols to aldehydes**:[10] to a solution of the alkenyl alcohol (2 mmol, 1 equiv) in dichloromethane (2 mL) was added Dess-Martin periodinane (DMP, 5 mmol, 2 equiv) and stirred at room temperature for 16 hours. Then $NaHCO_3$ saturated solution was added and extracted few times with dichloromethane. The organic layer was separated, dried ($MgSO_4$), filtered and the solvent removed in vacuum. The crude was purified by flash column chromatography.

6.2.8 Characterization of alkylated esters and aldehydes

Methyl 4-allyltetrahydro-2*H*-pyran-4-carboxylate (S2.10)

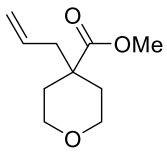

S2.10

The product **S2.10** was purified by flash column chromatography using hexane:ethyl acetate (20:1) as eluent. It was obtained as a colorless oil (2485.5 mg, 90% yield). **^{1}H NMR ($CDCl_3$, 400 MHz) δ** = 5.63 (ddt, *J* = 16.8, 10.2, 6.5 Hz, 1H), 5.08 – 4.94 (m, 2H), 3.74 (m, 2H), 3.67 (s, 3H), 3.40 (t, *J* = 10.4 Hz, 2H), 2.20 (dd, *J* = 7.4, 1.0 Hz, 2H), 2.02 - 1.94 (m, 2H), 1.52 (m, 2H). **^{13}C NMR ($CDCl_3$, 100 MHz) δ** = 175.5, 132.5, 118.2, 65.2, 51.6, 45.1, 44.7, 33.7. **HRMS (ESI) for $C_{10}H_{16}O_3$ [M]$^+$**: calculated: 184.1102, found: 184.1099.

Methyl 4-allyl-1-tosylpiperidine-4-carboxylate (S2.11)

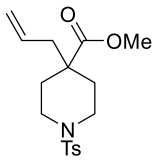

S2.11

The product **S2.11** was purified by flash column chromatography using pentane:ethyl acetate (100:0 to 60:40) as eluent. It was obtained as white solid (3135.4 mg, 62% yield). **^{1}H NMR ($CDCl_3$, 400 MHz) δ** = 7.59 (d, *J* = 8.2 Hz, 2H), 7.28 (d, *J* = 8.2 Hz, 2H), 5.58 (ddt, *J* = 14.9, 10.1, 7.5 Hz, 1H), 5.06 – 4.90 (m, 2H), 3.60 – 3.50 (m, 2H), 3.55 (s, 3H), 2.40 (s, 3H), 2.37 (dd, *J* = 12.0, 2.1 Hz, 2H), 2.19 (d, *J* = 7.5 Hz, 2H), 2.15 (m, 2H), 1.54 (t, *J* = 7.5 Hz, 2H). **^{13}C NMR ($CDCl_3$, 100 MHz) δ** = 174.8, 143.3, 133.3, 132.1, 129.5, 127.5, 118.6, 51.7, 45.2, 44.2, 43.6, 32.4, 21.4. **HRMS (ESI) for $C_{17}H_{24}NO_4S$ [M+H]$^+$:** calculated: 338.1421, found: 338.1425.

Methyl 4-(but-3-en-1-yl)tetrahydro-2*H*-pyran-4-carboxylate (S2.12)

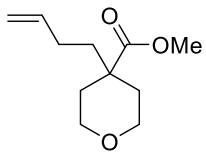

S2.12

The product **S2.12** was purified by flash column chromatography using hexane:ethyl acetate (20:1) as eluent. It was obtained as a colorless oil (2229.0 mg, 75% yield). **^{1}H NMR ($CDCl_3$, 400 MHz) δ** = 5.74 (ddt, *J* = 16.8, 10.2, 6.5 Hz, 1H), 4.97 – 4.80 (m, 2H), 3.82 (m, 2H), 3.71 (s, 3H), 3.42 (t, *J* = 7.5 Hz, 2H), 2.15 (d, *J* = 6.5 Hz, , 2H), 1.98 – 1.90 (m, 2H), 1.67 – 1.57

(m, 2H), 1.50 (m, 2H). **^{13}C NMR ($CDCl_3$, 100 MHz) δ** = 176.0, 137.8, 114.8, 65.4, 51.8, 44.8, 39.9, 34.2, 28.0. **HRMS (ESI) for $C_{11}H_{18}O_3$ [M]$^+$:** calculated: 198.1255, found: 198.1256.

4-Allyltetrahydro-2*H*-pyran-4-carbaldehyde (2.1)

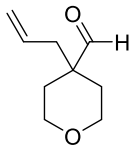

2.1

The product **2.1** was purified by flash column chromatography using pentane:diethyl ether (100:0 to 60:40) as eluent. It was obtained as a colorless oil (1081.8 mg, 52% yield). **^{1}H NMR ($CDCl_3$, 400 MHz) δ** = 9.50 (s, 1H), 5.66 (m, 1H), 5.10 (m, 2H), 3.81 (d, *J* = 12.0 Hz, 2H), 3.43 (dt, *J* = 12.0, 4.3 Hz, 2H), 2.25 (d, *J* = 7.5 Hz, 2H), 1.93 (d, *J* = 13.7 Hz, 2H), 1.60 (m, 2H). **^{13}C NMR ($CDCl_3$, 100 MHz) δ** = 204.6, 131.2, 118.5, 64.0, 46.9, 40.4, 30.2. **HRMS (ESI) for $C_9H_{15}O_2$ [M+H]$^+$:** calculated: 155.1067, found: 155.1053.

4-(But-3-en-1-yl)tetrahydro-2*H*-pyran-4-carbaldehyde (2.3)

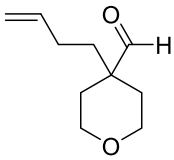

2.3

The product **2.3** was purified by flash column chromatography using pentane:diethyl ether (100:0 to 60:40) as eluent. It was obtained as a colorless oil (1437.3 mg, 76% yield). **^{1}H NMR ($CDCl_3$, 400 MHz) δ** = 9.42 (s, 1H), 5.67 (ddt, *J* = 16.8, 10.1, 6.5 Hz, 1H), 4.92 (m, 2H), 3.76 (dt, *J* = 11.8, 4.0 Hz, 2H), 3.36 (td, *J* = 11.5, 2.6 Hz, 2H), 1.94 – 1.81 (m, 4H), 1.59 – 1.45 (m, 4H). **^{13}C NMR ($CDCl_3$, 100 MHz) δ** = 205.3, 137.4, 115.1, 64.5, 47.3, 35.9, 30.9, 27.3. **HRMS (ESI) for $C_{10}H_{17}O_2$ [M+H]$^+$**: calculated: 169.1223, found: 169.1221.

4-Allyl-1-tosylpiperidine-4-carbaldehyde (2.5)

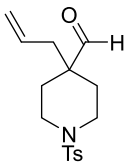

2.5

The product **2.5** was purified by flash column chromatography using pentane:ethyl acetate (100:0 to 60:40) as eluent. It was obtained as a colorless oil (2199.3 mg,77% yield). **^{1}H NMR ($CDCl_3$, 400 MHz) δ** = 9.32 (s, 1H), 7.57 (d, *J* = 7.9 Hz, 2H), 7.28 (d, *J* = 7.9 Hz, 2H), 5.56 (m, 1H), 5.05 (m, 2H), 3.54 (dt, *J* = 11.8, 3.2 Hz, 2H), 2.40 (s, 3H), 2.33 (td, *J* = 12.1, 2.8 Hz, 2H), 2.16 (d, *J* = 7.5 Hz, 2H), 2.05 (m, 2H), 1.64 (td, *J* = 12.0, 2.7 Hz, 2H). **^{13}C NMR ($CDCl_3$, 100 MHz) δ** = 204.7, 143.6, 132.8, 130.9, 129.6, 127.4, 119.5, 47.6, 43.2, 40.6, 29.6, 21.4. **HRMS (ESI) for $C_{16}H_{22}NO_3S$ [M+H]$^+$:** calculated: 308.1315, found: 308.1315.

4-(2-phenylallyl)tetrahydro-2*H*-pyran-4-carbaldehyde (2.16)

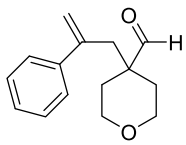

2.16

The product **2.16** was purified by flash column chromatography using pentane:ethyl acetate:methanol (10:4:1) as eluent. It was obtained as a colorless oil (280.5 mg, 88% yield). **^{1}H NMR ($CDCl_3$, 400 MHz) δ** = 9.23 (s, 1H), 7.31 – 7.16 (m, 5H), 5.21 (d, *J* = 1.5 Hz, 1H), 5.01 (m, 1H), 3.67 (ddd, *J* = 12.0, 4.4, 3.2 Hz, 2H), 3.31 – 3.20 (m, 2H), 2.68 (d, *J* = 0.9 Hz, 2H), 1.81 –

1.71 (m, 2H), 1.55 – 1.43 (m, 2H). **^{13}C NMR ($CDCl_3$, 100 MHz) δ** = 204.9, 143.9, 141.6, 128.5, 127.8, 126.5, 117.8, 64.6, 48.0, 43.6, 31.5. **HRMS (ESI) for $C_{15}H_{18}O_2$ [M]$^+$:** calculated: 230.1308, found: 230.1307.

6.2.9 General procedure for the alkylation of aldehyde substrates with alkyl bromides

To a 0 °C solution of ^{i}Pr$_2$NH (1.5 equiv, 15 mmol) in THF (15 mL), was added dropwise a solution of nBuLi 2.0 M (1.1 equiv, 11 mmol) in hexane. The reaction mixture was stirred for 20 minutes and then cooled to -78 °C. The substrate with the aldehyde functionality (1 equiv, 10 mmol) was added dropwise and the reaction mixture was stirred for 1 hour at -78 °C. The corresponding alkyl halide (1.5 equiv, 15 mmol) was then added dropwise into the reaction mixture. The reaction mixture was then warmed naturally to room temperature and stirred until consumption of the starting aldehyde. The reaction mixture was quenched by addition of saturated NH_4Cl aq. and extracted with diethyl ether three times. The combined organic layers were then dried ($MgSO_4$) filtered and concentrated under reduced pressure. The crude product of the alkylated aldehyde was purified by flash column chromatography.[8]

6.2.10 Characterization of alkylaldehydes from alkylbromides

1-(2-phenylallyl)cyclohexane-1-carbaldehyde (2.14)

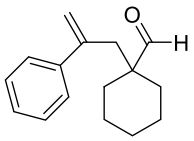

2.14

The product **2.14** was purified by flash column chromatography using pentane:ethyl acetate (10:1) as eluent. It was obtained as a colorless oil (233.8 mg, 56% yield). **^{1}H NMR ($CDCl_3$, 400 MHz) δ** = 9.18 (s, 1H), 7.28 – 7.18 (m, 5H), 5.17 (d, *J* = 1.5 Hz, 1H), 4.97 (dd, *J* = 1.6, 0.9 Hz, 1H), 2.61 (d, *J* = 0.9 Hz, 2H), 1.80 – 1.67 (m, 2H), 1.51 – 1.32 (m, 3H), 1.22 – 1.01 (m, 5H). **^{13}C NMR ($CDCl_3$, 100 MHz) δ** = 206.5, 144.7, 142.1, 128.3, 127.6, 126.6, 117.3, 50.2, 43.5, 31.5, 25.5, 22.6.

1-(2-(4-(tert-butyl)phenyl)allyl)cyclohexane-1-carbaldehyde (2.18)

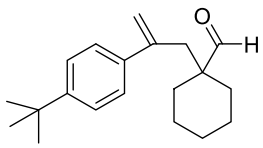

2.18

The product **2.18** was purified by flash column chromatography using pentane:ethyl acetate (10:1) as eluent. It was obtained as a colorless oil (1449.5 mg, 91% yield). **^{1}H NMR ($CDCl_3$, 400 MHz) δ** = 9.18 (s, 1H), 7.23 (d, *J* = 8.5 Hz, 2H), 7.15 (d, *J* = 8.5 Hz, 2H), 5.16 (d, *J* = 1.6 Hz, 1H), 4.94 – 4.89 (m, 1H), 2.58 (d, *J* = 0.9 Hz, 2H), 1.81 – 1.69 (m, 2H), 1.50 – 1.37 (m, 3H), 1.23 (s, 9H), 1.20 – 1.04 (m, 5H). **^{13}C NMR ($CDCl_3$, 100 MHz) δ** = 206.6, 150.6, 144.3, 139.0, 126.1, 125.2, 116.6, 50.1, 43.4, 34.5, 31.6, 31.3, 31.3, 25.6, 22.7. **HRMS (ESI) for $C_{20}H_{29}O$ [M+H]$^+$:** calculated: 285.2199, found: 285.2218.

2,2-dimethyl-4-phenylpent-4-enal (2.20)

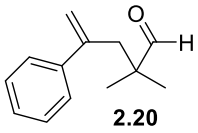

2.20

The product **2.20** was purified by flash column chromatography using pentane:diethyl ether (10:1) as eluent. It was obtained as a colorless oil (520.4 mg, 64% yield). **^{1}H NMR ($CDCl_3$, 400 MHz) δ** = 9.26 (s, 1H), 7.29 – 7.14 (m, 5H), 5.20 (d, *J* = 1.6 Hz, 1H), 5.03 – 4.97 (m, 1H), 2.67 (d, *J* = 0.9 Hz, 2H), 0.91 (s, 6H). **^{13}C NMR ($CDCl_3$, 100 MHz) δ** = 205.3, 145.3, 142.1, 128.3, 127.6, 126.5, 117.2, 46.4, 43.2, 21.8. **HRMS (ESI) for $C_{13}H_{16}O$ [M]$^{+}$:** calculated: 188.1201, found: 188.1200.

1-(2-(2-bromophenyl)allyl)cyclohexane-1-carbaldehyde (2.22)

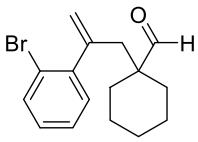

2.22

The product **2.22** was purified by flash column chromatography using pentane:ethyl acetate (10:1) as eluent. It was obtained as a colorless oil (198.2 mg, 25% yield). **^{1}H NMR ($CDCl_3$, 400 MHz) δ** = 9.20 (s, 1H), 7.46 (dd, *J* = 7.9, 1.2 Hz, 1H), 7.18 (td, *J* = 7.5, 1.3 Hz, 1H), 7.11 – 7.00 (m, 2H), 5.17 (d, *J* = 1.3 Hz, 1H), 5.04 (d, *J* = 1.5 Hz, 1H), 2.70 (d, *J* = 1.0 Hz, 2H), 1.81 – 1.73 (m, 2H), 1.47 – 1.38 (m, 3H), 1.26 – 1.13 (m, 5H). **^{13}C NMR ($CDCl_3$, 100 MHz) δ** = 206.2, 145.1, 143.2, 133.0, 130.9, 128.8, 127.3, 121.7, 120.6, 50.4, 31.3, 25.5, 22.4. **HRMS (ESI) for $C_{16}H_{19}BrO$ [M]$^{+}$:** calculated: 306.0622, found: 306.0619.

1-(2-(naphthalen-2-yl)allyl)cyclohexane-1-carbaldehyde (2.24)

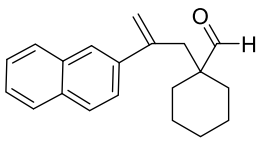

2.24

The product **2.24** was purified by flash column chromatography using pentane:ethyl (10:1) as eluent. It was obtained as a yellow oil (750 mg, 30% yield). **^{1}H NMR ($CDCl_3$, 400 MHz) δ** = 9.22 (s, 1H), 7.82 – 7.66 (m, 4H), 7.45 – 7.33 (m, 3H), 5.32 (d, *J* = 1.5 Hz, 1H), 5.07 (d, *J* = 1.4 Hz, 1H), 2.72 (d, *J* = 0.9 Hz, 2H), 1.84 – 1.75 (m, 2H), 1.50 – 1.34 (m, 3H), 1.16 (tdd, *J* = 19.4, 10.5, 5.0 Hz, 6H). **^{13}C NMR ($CDCl_3$, 100 MHz) δ** = 128.0, 127.6, 126.2, 125.9, 125.2, 125.0, 118.0, 50.3, 43.4, 31.6, 25.5, 22.6. **HRMS (ESI) for $C_{20}H_{22}O$ [M]$^{+}$:** calculated: 278.1677, found: 278.1671.

6.2.11 General procedure for the alkylation of aldehyde substrates with allyl alcohols

To a dry reaction vessel equipped with a magnetic stirrer bar was introduced 1,1'-bis(diphenylphosphino)ferrocene (0.4 mmol, 0.1 equiv) and bis(1,5-cyclooctadiene)nickel (0.16 mmol, 0.04 equiv) in methanol (MeOH, 2 mL) into a glove box. The mixture was stirred and the corresponding allyl alcohol (4 mmol, 1 equiv) and aldehyde (4 mmol, 1 equiv) were added dropwise. Finally, the Schlenk tube was sealed then warmed up to 80 °C and stirred

for 16 hours. Once the reaction was finished, the solvent was removed, and the crude was purified by silica-gel column chromatography to give the desired alkylated aldehyde.[11]

6.2.12 Characterization of alkylated aldehydes from allyl alcohols

1-Allylcyclohexane-1-carbaldehyde (2.7)

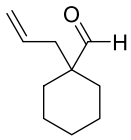

2.7

The product **2.7** was purified by flash column chromatography using pentane:dichloromethane (80:20) as eluent. It was obtained as a colorless oil (223.9 mg, 82% yield). **^{1}H NMR ($CDCl_3$, 400 MHz) δ =** 9.38 (s, 1H), 5.69 – 5.48 (m, 1H), 4.97 (dd, *J* = 10.8, 2.7 Hz, 2H), 2.11 (d, *J* = 7.5 Hz, 2H), 1.86 – 1.76 (m, 2H), 1.56 – 1.43 (m, 3H), 1.31 – 1.16 (m, 5H). **^{13}C NMR ($CDCl_3$, 100 MHz) δ =** 206.8, 132.6, 118.2, 49.6, 40.7, 30.7, 29.6, 25.6, 22.4.

2,2-dimethylpent-4-enal (2.9)

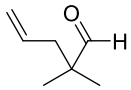

2.9

The product **2.9** was purified by flash column chromatography using pentane:dichloromethane (4:1) as eluent. It was obtained as a colorless oil (400.3 mg, 89% yield). **^{1}H NMR ($CDCl_3$, 400 MHz) δ =** 9.42 (s, 1H), 5.73 – 5.53 (m, 1H), 5.06 – 4.92 (m, 2H), 2.15 (d, *J* = 7.3 Hz, 2H), 0.99 (s, 6H). **^{13}C NMR ($CDCl_3$, 100 MHz) δ =** 205.5, 133.1, 118.4, 53.4, 53.1, 41.4, 21.1.

2-allyl-2-ethylhexanal (2.11)

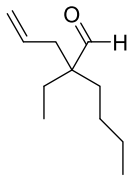

2.11

The product **2.11** was purified by flash column chromatography using pentane:dichloromethane (4:1) as eluent. It was obtained as a colorless oil (359.8 mg, 54% yield). **^{1}H NMR ($CDCl_3$, 400 MHz) δ =** 9.39 (s, 1H), 5.59 (ddt, *J* = 17.6, 10.2, 7.4 Hz, 1H), 5.06 – 4.95 (m, 2H), 2.19 (dd, *J* = 7.4, 1.0 Hz, 2H), 1.52 – 1.38 (m, 4H), 1.28 – 1.15 (m, 2H), 1.15 – 1.00 (m, 2H), 0.82 (t, *J* = 7.3 Hz, 3H), 0.73 (t, *J* = 7.6 Hz, 3H). **^{13}C NMR ($CDCl_3$, 100 MHz) δ =** 206.8, 133.1, 118.2, 52.2, 35.4, 31.7, 25.6, 24.7, 23.2, 13.8, 7.8.

1-(2-methylallyl)cyclohexane-1-carbaldehyde (2.27)

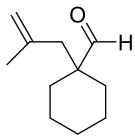

2.27

The product **2.27** was purified by flash column chromatography using pentane:dichloromethane (4:1) as eluent. It was obtained as a colorless oil (359.8 mg, 54% yield). **^{1}H NMR ($CDCl_3$, 400 MHz) δ =** 9.45 (s, 1H), 4.76 (d, *J* = 1.2 Hz, 1H), 4.60 (d, *J* = 0.8 Hz, 1H), 2.14 (s, 2H), 1.87 – 1.72 (m, 2H), 1.57 (s, 3H), 1.56 – 1.41 (m, 3H), 1.33 – 1.13 (m, 5H). **^{13}C NMR ($CDCl_3$, 100 MHz) δ =** 207.1, 141.0, 115.0, 49.6, 45.2, 31.3, 25.6, 24.3, 22.5.

6.2.13 General procedure for the copper catalyzed borylative cyclization

Copper chloride (0.98 mg, 5 mol%, 0.01 mmol) and bis(pinacolato)diboron (60.9 mg, 1.2 equiv, 0.24 mmol), 4,5-Bis(diphenylphosphino)-9,9-dimethylxanthene (Xantphos, 138.8 mg, 5 mol%, 0.01 mmol) were placed in an oven-dried reaction vial. The vial was sealed with a screw cap containing a Teflon-coated rubber septum and connected to a vacuum/nitrogen manifold through a needle, evacuated and backfilled with nitrogen and THF (0.24 ml, 1 M). KO^{t}Bu (26.9 mg, 1.2 equiv, 0.24 mmol) in THF (0.24 ml, 1 M) were added in the vial through the rubber septum. Then, substrate alkenyl aldehyde (1 equiv, 0.2 mmol) in THF (0.2 ml, 1 M) was added dropwise at 30 °C. After the reaction was complete, the reaction mixture was filtered over Celite. The organic extract was then concentrated in *vacuo*. The crude product was purified by flash chromatography.

6.2.14 Characterization of spirocyclic borylcyclobutanol products

***anti*-2-((4,4,5,5-tetramethyl-1,3,2-dioxaborolan-2-yl)methyl)-7-oxaspiro[3.5]nonan-1-ol (2.2)**

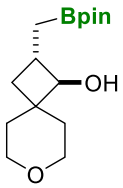

2.2

The product **2.2** was purified by flash column chromatography using pentane:ethyl acetate (3:2) as eluent. It was obtained as a colorless oil (100.2 mg, 71% yield). **^{1}H NMR ($CDCl_3$, 400 MHz) δ =** 3.87 (dt, *J* = 10.8, 4.4 Hz, 1H), 3.72 (dt, *J* = 10.9, 4.4 Hz, 1H), 3.59 (m, 1H), 3.46 (d, *J* = 8 Hz, 1H), 3.43 (dd, *J* = 11.5, 2.3 Hz, 1H), 2.14 (m, 1H), 1.93 (m, 2H), 1.76 (ddd, *J* = 13.3, 9.6, 3.9 Hz, 1H), 1.49 (m, 1H), 1.39 (m, 1H), 1.25 (s, 12H), 1.09 (dd, *J* = 16.4, 5.1 Hz, 1H), 0.95 (t, *J* = 10.2 Hz, 1H), 0.86 (dd, *J* = 16.4, 10.6 Hz, 1H). **^{13}C NMR ($CDCl_3$, 100 MHz) δ =** 83.3, 80.9, 64.9, 64.7, 39.4, 38.8, 36.3, 33.6, 30.5, 24.7, 24.7. **^{11}B NMR ($CDCl_3$, 128.3 MHz) δ =** 33.8. **HRMS (ESI) for $C_{15}H_{26}BO_3$ $[M-OH]^+$:** calculated: 265.1975, found: 265.1964.

2-((4,4,5,5-tetramethyl-1,3,2-dioxaborolan-2-yl)methyl)-7-oxaspiro[3.5]nonan-1-ol (2.4)

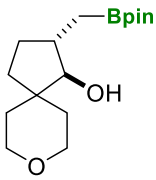

2.4

The product **2.4** was purified by flash column chromatography using pentane:ethyl acetate (1:1) as eluent. It was obtained as a colorless oil (66.6 mg, 45% yield). **^{1}H NMR ($CDCl_3$, 400 MHz) δ =** 3.82 (m, 2H), 3.49 (m, 2H), 3.12 (d, *J* = 8.3 Hz, 1H), 1.84 (m, 4H), 1.72 (m, 1H), 1.40 (m, 2H), 1.24 (s, 12H), 1.13 (m, 2H), 1.06 – 0.93 (m, 2H). **^{13}C NMR ($CDCl_3$, 100 MHz) δ =** 87.0, 83.3, 65.3, 64.5, 42.2, 40.6, 36.9, 31.9, 30.2, 29.3, 24.7. **^{11}B NMR ($CDCl_3$, 128.3 MHz) δ** = 33.8. **HRMS (ESI) for $C_{16}H_{30}BO_4$ $[M+H]^+$:** calculated: 297.2237, found: 297.2238.

anti-2-((4,4,5,5-tetramethyl-1,3,2-dioxaborolan-2-yl)methyl)-7-tosyl-7-azaspiro [3.5] nonan-1-ol (2.6)

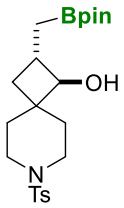

2.6

The product **2.6** was purified by flash column chromatography using pentane:ethyl acetate (3:2) as eluent. It was obtained as a colorless oil (145.8 mg, 67% yield). **^{1}H NMR ($CDCl_3$, 400 MHz) δ =** 7.63 (d, *J* = 8.0 Hz, 2H), 7.30 (d, *J* = 8.0 Hz, 2H), 3.43 (d, *J* = 7.8 Hz, 1H), 3.38 (m, 1H), 3.21 (m, 1H), 2.84 (s, 1H), 2.79 (m, 1H), 2.42 (s, 3H), 2.07 (m, 1H), 1.95 (m, 1H), 1.77 (m, 1H), 1.73 (t, *J* = 10.2 Hz, 1H), 1.63 (m, 1H), 1.52 (m, 1H), 1.22 (s, 12H), 1.04 (dd, *J* = 16.7, 4.9 Hz, 1H), 0.81 (t, *J* = 10.2 Hz, 1H), 0.76 (m, 1H). **^{13}C NMR ($CDCl_3$, 100 MHz) δ =** 143.1, 133.5, 129.4, 127.5, 83.4, 80.4, 43.4, 43.2, 39.4, 37.5, 36.2, 29.4, 24.7, 21.4. **^{11}B NMR ($CDCl_3$, 128.3 MHz) δ =** 33.0. **HRMS (ESI) for $C_{22}H_{35}BNO_5S$ $[M+H^+]^+$:** calculated: 436.2329, found: 436.2330.

anti-2-(4,4,5,5-tetramethyl-1,3,2-dioxaborolan-2-yl)spiro[3.5]nonan-1-ol (2.8)

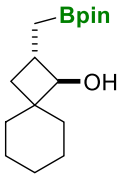

2.8

The product **2.8** was purified by flash column chromatography using pentane:ethyl acetate (3:2) as eluent. It was obtained as a colorless oil (70.1 mg, 50% yield). **^{1}H NMR ($CDCl_3$, 400 MHz) δ =** 3.33 (d, *J* = 7.6 Hz, 1H), 2.09 – 1.95 (m, 1H), 1.84 – 1.76 (m, 1H), 1.64 – 1.24 (m, 10H), 1.18 (s, 12H), 0.99 (dd, *J* = 16.4, 5.6 Hz, 1H), 0.83 – 0.79 (m, 1H), 0.77 (d, *J* = 10.5 Hz, 1H). **^{13}C NMR ($CDCl_3$, 100 MHz) δ =** 83.3, 81.8, 42.1, 39.4, 36.6, 34.0, 29.9, 26.4, 24.8, 23.3, 23.0, 22.5. **^{11}B NMR ($CDCl_3$, 128.3 MHz) δ =** 34.0. **HRMS (ESI) for $C_{16}H_{33}BNO_3$ $[M+NH_4^+]^+$:** calculated: 298.2557, found: 298.2553.

2,2-dimethyl-4-((4,4,5,5-tetramethyl-1,3,2-dioxaborolan-2-yl)methyl)cyclobutan-1-ol (2.10)

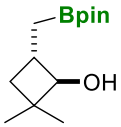

2.10

The product **2.10** was purified by flash column chromatography using pentane:ethyl acetate (3:2) as eluent. It was obtained as a colorless oil (78 mg, 59% yield). **^{1}H NMR ($CDCl_3$, 400 MHz) δ =** 3.34 (dd, *J* = 7.7, 3.1 Hz, 1H), 2.76 (d, *J* = 3.4 Hz, 1H), 2.10 – 1.93 (m, 1H), 1.65 (t, *J* = 9.9 Hz, 1H), 1.18 (s, 12H), 1.13 (dd, *J* = 4.7, 1.5 Hz, 1H), 1.00 (d, *J* = 2.5 Hz, 6H), 0.89 (t, *J* = 10.2 Hz, 1H), 0.78 (dd, *J* = 16.3, 10.5 Hz, 1H). **^{13}C NMR ($CDCl_3$, 100 MHz) δ =** 83.3, 81.0, 37.5, 36.7, 36.6, 28.8, 24.8, 21.0. **^{11}B NMR ($CDCl_3$, 128.3 MHz) δ** = 33.8. **HRMS (ESI) for $C_{13}H_{29}NBO_2$ $[M-NH_4^+]^+$:** calculated: 258.2240, found: 258.2242.

2-butyl-2-ethyl-4-((4,4,5,5-tetramethyl-1,3,2-dioxaborolan-2-yl)methyl)cyclobutan-1-ol (2.12) ***(as a mixture of two diastereoisomers)***

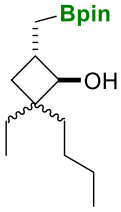

2.12

The product **2.12** was purified by flash column chromatography using pentane:diethyl ether (3:2) as eluent. It was obtained as a colorless oil as a mixture of two diastereoisomers (1:1) (50.9 mg, 34% yield). **^{1}H NMR ($CDCl_3$, 400 MHz) δ =** 3.43 (t, J = 7.6 Hz, 1H), 2.02 (dddd, J = 9.4, 7.7, 4.0, 2.4 Hz, 1H), 1.73 (td, J = 10.5, 9.8, 2.4 Hz, 1H), 1.62 – 1.49 (m, 2H), 1.42 – 1.25 (m, 4H), 1.18 (s, 12H), 0.98 (dd, J = 16.3, 5.3 Hz, 1H), 0.89 – 0.65 (m, 10H). **^{13}C NMR ($CDCl_3$, 100 MHz) δ =** 83.3, 81.2, 81.0, 44.3, 44.2, 38.6, 36.6, 36.5, 33.6, 33.5, 31.7, 29.3, 26.2, 25.8, 24.8, 24.8, 23.7, 23.4, 22.5, 14.2, 14.1, 8.3, 7.9. **^{11}B NMR ($CDCl_3$, 128.3 MHz) δ** = 34.7. **HRMS (ESI) for $C_{17}H_{34}BO_3$ $[M+H^+]^+$:** calculated: 297.2611, found: 297.2601.

2-butyl-2-ethyl-4-((4,4,6-trimethyl-1,3,2-dioxaborinan-2-yl)methyl)cyclobutan-1-ol (2.13) ***(as a mixture of two diastereoisomers)***

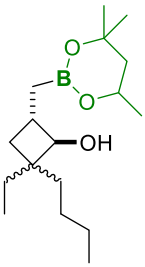

2.13

The product **2.13** was purified by flash column chromatography using pentane:diethyl ether (3:2) as eluent. It was obtained as a colorless oil as a mixture of two diastereoisomers (1:1) (75.9 mg, 51% yield). **^{1}H NMR ($CDCl_3$, 400 MHz) δ =** 4.11 (dqd, J = 12.3, 6.1, 2.9 Hz, 1H), 3.42 (td, J = 7.5, 0.9 Hz, 1H), 2.07 – 1.89 (m, 1H), 1.70 (dd, J = 14.0, 2.9 Hz, 2H), 1.62 – 1.49 (m, 1H), 1.47 – 1.25 (m, 5H), 1.22 (s, 6H), 1.18 (d, J = 6.1 Hz, 5H), 0.97 – 0.63 (m, 10H). **^{13}C NMR ($CDCl_3$, 100 MHz) δ =** 81.4, 81.4, 81.1, 71.0, 65.8, 64.8, 64.8, 45.7, 44.0, 43.9, 38.6, 36.6, 36.5, 33.6, 33.4, 31.8, 31.2, 31.1, 29.4, 29.3, 28.1, 28.0, 26.2, 25.8, 25.8, 23.7, 23.4, 23.1, 23.0, 22.6, 22.6, 15.2, 14.2, 14.1, 8.3, 8.0, 7.9. **^{11}B NMR ($CDCl_3$, 128.3 MHz) δ** = 30.2. **HRMS (ESI) for $C_{17}H_{32}BO_2$ $[M-H_2O]^+$:** calculated: 279.2498, found: 279.2495.

2-phenyl-2-((4,4,5,5-tetramethyl-1,3,2-dioxaborolan-2-yl)methyl)spiro[3.5]nonan-1-ol (2.15)

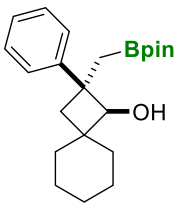

2.15

The product **2.15** was purified by flash column chromatography using pentane:diethyl ether (3:2) as eluent. It was obtained as a colorless oil (131.6 mg, 76% yield). **^{1}H NMR ($CDCl_3$, 400 MHz) δ =** 7.33 (dd, *J* = 8.3, 1.4 Hz, 2H), 7.24 (dd, *J* = 8.5, 7.1 Hz, 2H), 7.17 – 7.07 (m, 1H), 3.83 (s, 1H), 2.57 (d, *J* = 12.6 Hz, 1H), 1.54 (d, *J* = 12.7 Hz, 1H), 1.46 (d, *J* = 6.0 Hz, 6H), 1.25 (d, *J* = 15.0 Hz, 3H), 1.12 (s, 4H), 0.97 (s, 6H), 0.96 (s, 6H). **^{13}C NMR ($CDCl_3$, 100 MHz) δ =** 143.1, 128.5, 128.0, 125.8, 84.2, 82.7, 46.6, 41.4, 39.7, 37.6, 30.0, 26.1, 24.7, 24.6, 23.2, 21.9. **^{11}B NMR ($CDCl_3$, 128.3 MHz) δ** = 33.2. **HRMS (ESI) for $C_{22}H_{34}O_3$ $[M+H]^+$:** calculated: 357.2601, found: 357.260.

2-phenyl-2-((4,4,5,5-tetramethyl-1,3,2-dioxaborolan-2-yl)methyl)-7-oxaspiro[3.5] nonan-1-ol (2.17)

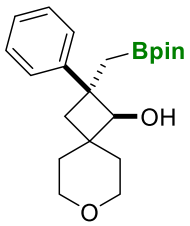

2.17

The product **2.17** was purified by flash column chromatography using pentane:diethyl ether (3:2) as eluent. It was obtained as a colorless oil (131.6 mg, 24% yield). **^{1}H NMR ($CDCl_3$, 400 MHz) δ =** 7.36 – 7.29 (m, 2H), 7.29 (s, 2H), 7.19 – 7.07 (m, 1H), 3.93 (s, 1H), 3.67 (ddt, *J* = 13.5, 11.3, 4.4 Hz, 2H), 3.50 – 3.36 (m, 2H), 2.65 (d, *J* = 12.7 Hz, 1H), 1.78 (ddd, *J* = 13.4, 9.6, 4.0 Hz, 2H), 1.66 (d, *J* = 12.8 Hz, 1H), 1.47 (dd, *J* = 14.3, 5.0 Hz, 2H), 1.27 (d, *J* = 15.2 Hz, 2H), 0.97 (s, 6H), 0.96 (s, 6H). **^{13}C NMR ($CDCl_3$, 100 MHz) δ =** 142.9, 128.2, 128.2, 126.1, 83.4, 82.9, 65.0, 64.3, 46.6, 39.3, 38.9, 37.8, 30.9, 24.8, 24.7. **^{11}B NMR ($CDCl_3$, 128.3 MHz) δ =** 33.6. **HRMS (ESI) for $C_{21}H_{32}BO_4$ $[M+H]^+$:** calculated: 359.2397, found: 359.2394**.**

2-(4-(tert-butyl)phenyl)-2-((4,4,5,5-tetramethyl-1,3,2-dioxaborolan-2-yl)methyl) spiro[3.5]nonan-1-ol (2.19)

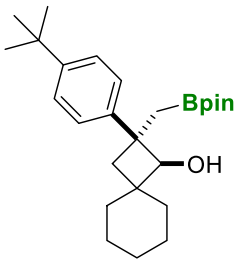

2.19

The product **2.19** was purified by flash column chromatography using pentane:diethyl ether (10:1) as eluent. It was obtained as a colorless oil (50.5 mg, 25% yield). **^{1}H NMR ($CDCl_3$, 400 MHz) δ** = 7.28 – 7.21 (m, 4H), 3.80 (s, 1H), 2.57 (dd, *J* = 12.7, 1.0 Hz, 2H), 1.57 – 1.37 (m, 6H), 1.24 (d, *J* = 4.1 Hz, 3H), 1.22 (s, 9H), 1.15 – 1.07 (m, 3H), 0.94 (s, 6H), 0.89 (s, 6H). **^{13}C NMR ($CDCl_3$, 100 MHz) δ =** 148.6, 139.5, 128.1, 124.9, 84.0, 82.6, 46.1, 41.3, 39.8, 37.5, 34.2, 31.4, 31.3, 30.1, 26.1, 24.6, 24.6, 23.2, 22.0. **^{11}B NMR ($CDCl_3$, 128.3 MHz) δ** = 33.7. **HRMS (ESI) for $C_{26}H_{42}BO_3$ $[M+H]^+$:** calculated: 413.3235, found: 413.3227.

2,2-dimethyl-4-phenyl-4-((4,4,5,5-tetramethyl-1,3,2-dioxaborolan-2-yl)methyl) cyclobutan-1-ol (2.21)

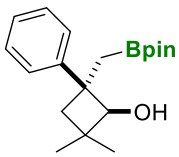

2.21

The product **2.21** was purified by flash column chromatography using pentane:diethyl ether (3:2) as eluent. It was obtained as a colorless oil (36.5 mg, 27% yield). **^{1}H NMR ($CDCl_3$, 400 MHz) δ =** 7.35 (dd, *J* = 8.4, 1.3 Hz, 2H), 7.24 (dd, *J* = 8.6, 7.0 Hz, 2H), 7.15 – 7.04 (m, 1H), 3.90 (m, 1H), 2.46 (dd, *J* = 12.5, 1.0 Hz, 1H), 1.62 (d, *J* = 12.5 Hz, 1H), 1.44 (d, *J* = 15.1 Hz, 1H), 1.26 (7, *J* = 15.1 Hz, 1H), 1.11 (s, 3H), 0.99 (s, 6H), 0.97 (s, 6H), 0.68 (s, 3H). **^{13}C NMR ($CDCl_3$, 100 MHz) δ =** 143.2, 128.5, 128.0, 125.8, 83.8, 82.8, 47.0, 40.1, 37.3, 29.8, 24.7, 24.6, 21.3. **^{11}B NMR ($CDCl_3$, 128.3 MHz) δ** = 33.4. **HRMS (ESI) for $C_{19}H_{33}NBO_3$ $[M+NH_4^+]^+$:** calculated: 334.2554, found 334.2553.

2-(naphthalen-2-yl)-2-((4,4,5,5-tetramethyl-1,3,2-dioxaborolan-2-yl)methyl) spiro[3.5]nonan-1-ol (2.25)

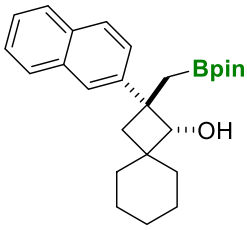

2.25

The product **2.25** was purified by flash column chromatography using pentane:diethyl ether (3:2) as eluent. It was obtained as a colorless oil (208.3 mg, 52% yield). **^{1}H NMR ($CDCl_3$, 400 MHz) δ =** 7.79 (d, *J* = 1.9 Hz, 1H), 7.77 – 7.69 (m, 3H), 7.49 (dd, *J* = 8.6, 1.9 Hz, 1H), 7.44 – 7.31 (m, 2H), 3.93 (s, 1H), 2.69 (d, *J* = 12.6 Hz, 1H), 1.64 (d, *J* = 12.7 Hz, 1H), 1.53 (dd, *J* = 5.7, 1.7 Hz, 3H), 1.45 – 1.29 (m, 6H), 1.16 – 1.06 (m, 3H), 0.92 (s, 6H), 0.89 (s, 6H). **^{13}C NMR ($CDCl_3$, 100 MHz) δ =** 141.2, 133.2, 131.9, 127.9, 127.4, 127.3, 126.7, 125.6, 125.3, 84.5, 82.8, 46.8, 41.5, 39.7, 38.0, 30.0, 26.1, 24.7, 24.6, 23.2, 21.9. **^{11}B NMR ($CDCl_3$, 128.3 MHz) δ** 33.7. **HRMS (ESI) for $C_{26}H_{39}NBO_3$ $[M+NH_4^+]^+$:** calculated: 424.3026, found: 424.3023.

1-(naphthalen-2-yl)-4-oxa-3-boraspiro[bicyclo[3.2.0]heptane-6,1'-cyclohexan]-3-ol (2.26-*syn-(B-OH)*)

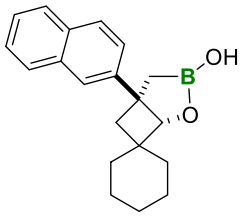

2.26-*syn-(B-OH)*

The product **2.26**-*syn-(B-OH)* was purified by flash column chromatography using pentane:diethyl ether (3:2) as eluent. It was obtained as a colorless oil (78.5 mg, 39% yield). **^{1}H NMR ($CDCl_3$, 400 MHz) δ =** 7.72 (dt, *J* = 6.4, 3.4 Hz, 3H), 7.58 (d, *J* = 2.2 Hz, 1H), 7.43 – 7.31 (m, 2H), 7.28 (dd, *J* = 8.5, 2.0 Hz, 1H), 4.64 (d, *J* = 2.4 Hz, 1H), 2.36 – 2.26 (m, 1H), 1.90 (dd, *J* = 12.0, 2.0 Hz, 1H), 1.56 – 1.46 (m, 2H), 1.35 – 1.18 (m, 10H). **^{13}C NMR ($CDCl_3$, 100 MHz) δ =** 147.3, 133.3, 131.6, 128.5, 127.6, 127.5, 126.1, 125.3, 124.6, 122.6, 90.2, 65.8, 46.8, 44.4, 40.7, 36.7, 32.4, 25.8, 22.6, 22.3, 15.2. **^{11}B NMR ($CDCl_3$, 128.3 MHz) δ** = 36.5. **HRMS (ESI) for $C_{20}H_{23}BO_2$ $[M+H]^+$:** calculated: 307.1870, found: 307.1869.

(1-(2-methylallyl)cyclohexyl)(4,4,5,5-tetramethyl-1,3,2-dioxaborolan-2-yl)methanol (2.29)

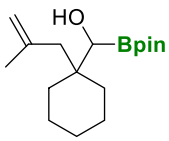

2.29

The product **2.29** was purified by flash column chromatography using pentane:diethyl ether (3:2) as eluent. It was obtained as a colorless oil (95.4 mg, 32% yield). **^{1}H NMR ($CDCl_3$, 400 MHz) δ =** 4.86 – 4.77 (m, 1H), 4.73 (s, 1H), 3.51 (d, *J* = 5.9 Hz, 1H), 2.19 (d, *J* = 13.2 Hz, 1H), 2.10 – 2.01 (m, 1H), 1.75 (s, 3H), 1.60 (d, *J* = 6.0 Hz, 1H), 1.54 – 1.26 (m, 10H), 1.21 (s, 12H). **^{13}C NMR ($CDCl_3$, 100 MHz) δ =** 144.4, 114.7, 84.0, 41.1, 33.1, 31.5, 26.4, 25.5, 25.0, 24.7, 21.8, 21.6. **^{11}B NMR ($CDCl_3$, 128.3 MHz) δ** = 33.0. **HRMS (ESI) for $C_{17}H_{32}BO_3$ $[M+H^+]^+$:** calculated: 295.2441, found: 295.2445.

6.2.15 General procedure for the oxidation of spiroboronate compounds

The oxidation was performed in a reaction vial, $NaBO_3 \cdot H_2O$ (2 mmol) was dissolved in THF/H_2O (3:2, 0.2 M) and the boronate (1 equiv, 0.2 mmol) was then added at room temperature. After stirred for 1.5 hours, the reaction mixture was extracted three times with ethyl acetate, dried ($MgSO_4$), filtered and concentrated in *vacuo*. The crude mixture was further purified by flash column chromatography.[12]

2-(hydroxymethyl)-7-oxaspiro[3.5]nonan-1-ol (2.30)

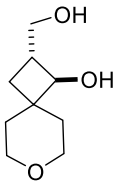

2.30

The product **2.30** was purified by flash column chromatography using pentane:ethyl acetate (100:0 to 0:100) as eluent. It was obtained as a colorless oil (52.5 mg, 61% yield). **^{1}H NMR ($CDCl_3$, 400 MHz) δ =** 3.89 (dt, *J* = 11.3, 4.1 Hz, 1H), 3.73 (m, 3H), 3.59 (m, 2H), 3.43 (td, *J* = 11.1, 2.6 Hz, 1H), 2.33 (m, 1H), 1.88 (m, 2H), 1.77 (m, 1H), 1.50 (m, 1H), 1.40 (m, 1H), 1.09 (t, *J* = 10.1 Hz, 1H). **^{13}C NMR ($CDCl_3$, 100 MHz) δ =** 77.2, 76.6, 64.9, 64.5, 42.6, 40.1, 38.1, 30.4, 29.6, 27.2. **HRMS (ESI) for $C_9H_{17}O_3$ $[M+H]^+$:** calculated: 173.1172, found: 173.1185.

2-(hydroxymethyl)spiro[3.5]nonan-1-ol2-(hydroxymethyl)spiro[3.5]nonan-1-ol (2.31)

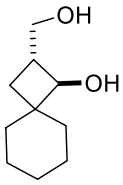

2.31

The product **2.31** was purified by flash column chromatography using pentane:ethyl acetate (100:0 to 0:100) as eluent. It was obtained as a colorless oil (27.3 mg, 90% yield). **^{1}H NMR ($CDCl_3$, 400 MHz) δ =** 3.63 (dd, *J* = 10.9, 5.1 Hz, 1H), 3.53 – 3.44 (m, 2H), 3.37 (m, 2H), 2.28 – 2.14 (m, 1H), 1.65 (t, *J* = 10.3 Hz, 1H), 1.62 – 1.24 (m, 8H), 1.24 – 1.09 (m, 2H), 0.85 (t, *J* = 10.2 Hz, 1H). **^{13}C NMR ($CDCl_3$, 100 MHz) δ =** 78.0, 65.7, 42.7, 42.6, 38.7, 29.8, 27.4, 26.3, 23.1, 22.3. **HRMS (ESI) for $C_{10}H_{18}O_2$ $[M]^+$:** calculated: 170.1307, found: 170.1309.

(1R,4R)-4-(hydroxymethyl)-2,2-dimethylcyclobutan-1-ol (2.32)

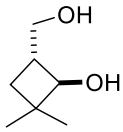

2.32

The product **2.32** was purified by flash column chromatography using pentane:diethyl ether:methanol (3:2:1) as eluent. It was obtained as a colorless oil (73.8 mg, 81% yield). **^{1}H NMR ($CDCl_3$, 400 MHz) δ =** 3.70 – 3.58 (m, 1H), 3.58 – 3.44 (m, 2H), 3.25 (s, 1H), 2.65 (s, 1H), 2.29 – 2.14 (m, 1H), 1.57 – 1.46 (m, 1H), 1.01 (d, *J* = 8.1 Hz, 6H). **^{13}C NMR ($CDCl_3$, 100 MHz) δ =** 65.5, 42.9, 38.3, 30.0, 28.3, 21.0. **HRMS (ESI) for $C_7H_{14}O_2$ $[M]^+$:** calculated: 130.0992, found: 130.0994.

2-(hydroxymethyl)-7-tosyl-7-azaspiro[3.5]nonan-1-ol (2.33)

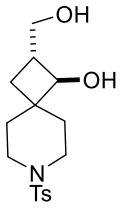

2.33

The product **2.33** was purified by flash column chromatography using pentane:ethyl acetate (100:0 to 0:100) as eluent. It was obtained as a colorless oil (121.9 mg, 75% yield). **^{1}H NMR ($CDCl_3$, 400 MHz) δ =** 7.63 (d, *J* = 8.0 Hz, 2H), 7.31 (d, *J* = 8.0 Hz, 2H), 3.72 (d, *J* = 7.5 Hz, 1H), 3.67 (dd, *J* = 10.9, 5.3 Hz, 1H), 3.59 (dd, *J* = 10.9, 5.3 Hz, 1H), 3.49 (m, 1H), 3.32 (m, 1H), 2.67 (t, *J* = 11.4 Hz, 1H), 2.53 (t, *J* = 11.4 Hz, 1H), 2.43 (s, 3H), 2.27 (m, 1H), 1.90 (m, 1H), 1.78 (m, 1H), 1.64 (m, 1H), 1.59 (t, *J* = 10.8 Hz, 1H), 1.51 (m, 1H), 0.97 (t, *J* = 10.8 Hz, 1H). **^{13}C NMR ($CDCl_3$, 100 MHz) δ =** 143.3, 133.3, 129.6, 127.6, 75.6, 64.4, 43.3, 42.9, 42.4, 40.1, 36.7, 29.2, 26.5, 21.5. **HRMS (ESI) for $C_{16}H_{24}NO_4S$ $[M+H]^+$:** calculated: 326.1421, found: 326.1427.

2-(hydroxymethyl)-2-phenylspiro[3.5]nonan-1-ol (2.34)

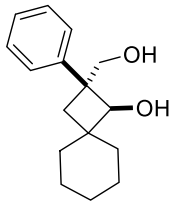

2.34

The product **2.34** was purified by flash column chromatography using pentane:diethyl ether (3:2) as eluent. It was obtained as a colorless oil (148.7 mg, 76% yield). **^{1}H NMR ($CDCl_3$, 400 MHz) δ =** 7.41 – 7.25 (m, 4H), 7.25 – 7.20 (m, 1H), 3.89 (s, 1H), 3.67 (dt, *J* = 10.9, 0.8 Hz, 1H), 3.58 (dd, *J* = 10.9, 0.8 Hz, 1H), 2.33 (d, *J* = 12.5 Hz, 1H), 1.67 (d, *J* = 12.5 Hz, 1H), 1.50 – 1.43 (m, 5H), 1.35 – 1.26 (m, 2H), 1.13 (d, *J* = 3.4 Hz, 2H), 1.11 – 1.04 (m, 1H). **^{13}C NMR ($CDCl_3$, 100 MHz) δ =** 139.0, 128.8, 128.6, 126.8, 77.8, 72.7, 51.1, 41.5, 38.6, 33.2, 30.7, 26.0, 23.0, 21.9. **HRMS (ESI) for $C_{16}H_{22}O_2$ $[M]^+$:** calculated: 246.1620, found: 246.1617.

2-(hydroxymethyl)-8-oxaspiro[4.5]decan-1-ol (2.35)

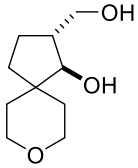

2.35

The product **2.35** was purified by flash column chromatography using pentane:ethyl acetate (3:2) as eluent. It was obtained as a colorless oil (50 mg, 70% yield). **^{1}H NMR ($CDCl_3$, 400 MHz) δ =** 3.81 (m, 3H), 3.62 – 3.46 (m, 2H), 3.46 – 3.35 (m, 2H), 1.87 – 1.77 (m, 3H), 1.71 (dtd, *J* = 13.2, 9.1, 5.7 Hz, 1H), 1.36 – 1.29 (m, 1H), 1.25 – 1.05 (m, 4H). **^{13}C NMR ($CDCl_3$, 100 MHz) δ =** 84.8, 66.8, 65.4, 64.4, 45.3, 42.6, 36.3, 31.3, 29.3, 21.9. **HRMS (ESI) for $C_{10}H_{18}O_2$ $[M]^+$:** calculated: 186.1256, found: 186.1252.

6.2.16 Characterization of spirocyclic 2.23

4'-methylene-3',4'-dihydro-1'H-spiro[cyclohexane-1,2'-naphthalen]-1'-ol (2.23)

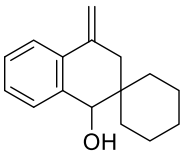

2.23

The product **2.23** was purified by flash column chromatography using pentane:diethyl ether (3:2) as eluent. It was obtained as a colorless oil (38.8 mg, 34% yield). **^{1}H NMR ($CDCl_3$, 400 MHz) δ =** 7.65 – 7.55 (m, 1H), 7.41 – 7.29 (m, 1H), 7.25 – 7.16 (m, 2H), 5.51 (s, 1H), 5.01 (s, 1H), 4.29 (s, 1H), 2.71 – 2.61 (m, 1H), 2.29 – 2.20 (m, 1H), 1.51 – 1.33 (m, 6H), 1.37 – 1.08 (m, 4H). **^{13}C NMR ($CDCl_3$, 100 MHz) δ =** 140.5, 137.4, 133.7, 129.8, 128.4, 127.9, 123.7, 110.0, 37.2, 37.0, 32.6, 31.4, 31.4, 26.2, 24.5. **HRMS (ESI) for $C_{16}H_{18}$ $[M-H_2O]^+$:** calculated: 210.1416, found: 210.1409.

6.3 Experimental section for Chapter 3

6.3.1 General procedure for the preparation of 1,3-dienes via Wittig olefination

To a dry reaction vessel equipped with a magnetic stirrer bar, alkyl phosphonium bromide (3.75 mmol, 1.25 equiv) and potassium tert-butoxide (3.9 mmol, 1.3 equiv) were added. The flask was flushed with argon 3 times and dry THF (8 mL) was added slowly with stirring at room temperature. The mixture was left for 30 minutes before the corresponding aldehyde, dissolved in dry THF (4 mL), was added dropwise over 10 minutes at room temperature. The mixture was then left to stir for 16 hours. The reaction was quenched with aqueous saturated ammonium chloride solution (25 mL). The aqueous layer was then extracted three times with diethyl ether before the combined organic extracts were washed with brine and dried over sodium sulphate. After filtration, the volatile components were removed under reduced pressure. The crude residue was purified by silica gel flash chromatography to afford the diene product.[3]

6.3.2 Characterization of 1,3-dienes via Wittig Olefination

(*E*)-penta-1,3-dien-3-ylbenzene (3.6)

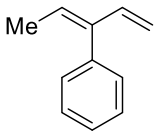

3.6

The product **3.6** was purified by flash column chromatography using pentane as eluent. It was obtained as a colorless liquid (290.7 mg, 67% yield). **^{1}H NMR (400 MHz, $CDCl_3$) δ** = 7.34 – 7.27 (m, 2H), 7.26 – 7.18 (m, 1H), 7.11 – 7.00 (m, 2H), 6.49 (dd, *J* = 17.3, 10.5 Hz, 1H), 5.75 (q, *J* = 7.0 Hz, 1H), 4.89 (d, *J* = 10.7 Hz, 1H), 4.60 (d, *J* = 17.3 Hz, 1H), 1.52 (d, *J* = 7.1 Hz, 3H). **^{13}C NMR (100 MHz, $CDCl_3$) δ** = 142.4, 140.7, 137.6, 129.7, 128.1, 126.8, 113.9, 14.9.

(*E*)-1-(buta-1,3-dien-1-yl)-4-chlorobenzene (3.8)

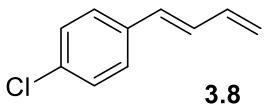

3.8

The product **3.8** was purified by flash column chromatography using pentane:ethyl acetate (40:1) as eluent. It was obtained as an orange oil (401.6 mg, 81% yield). **^{1}H NMR (400 MHz, $CDCl_3$) δ** = 7.28 – 7.15 (m, 4H), 6.74 – 6.60 (m, 1H), 6.49 – 6.34 (m, 2H), 5.31 – 5.22 (d, J = 16.2 Hz, 1H), 5.12 (d, J = 9.2 Hz, 1H). **^{13}C NMR (100 MHz, $CDCl_3$) δ** = 136.9, 135.7, 133.2, 131.5, 130.2, 128.8, 127.6, 118.2.

(*E*)-4-(buta-1,3-dien-1-yl)-*N*,*N*-dimethylaniline (3.10)

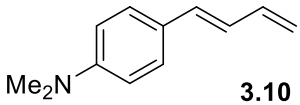

3.10

The product **3.10** was purified by flash column chromatography using pentane:ethyl acetate (10:1) as eluent. It was obtained as a yellow solid (484.0 mg, 95% yield). **^{1}H NMR (400 MHz, $CDCl_3$)**

δ = 7.35 – 7.28 (m, 2H), 6.73 – 6.58 (m, 1H), 6.56 – 6.43 (m, 2H), 5.24 (d, *J* = 17.4 Hz, 1H), 5.05 (d, *J* = 10.0 Hz, 1H), 2.97 (s, 6H). **^{13}C NMR (100 MHz, $CDCl_3$) δ** = 150.1, 137.8, 133.1, 127.5, 125.6, 125.6, 115.0, 112.4, 40.5.

(*E*)-1-(buta-1,3-dien-1-yl)-4-methoxybenzene (3.12)

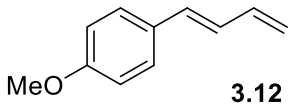

3.12

The product **3.12** was purified by flash column chromatography using pentane:ethyl acetate (4:1) as eluent. It was obtained as a colorless oil (449.6 mg, 94% yield). **^{1}H NMR (400 MHz, $CDCl_3$) δ =** 7.28 (d, *J* = 8.7 Hz, 2H), 6.79 (d, *J* = 8.8 Hz, 2H), 6.60 (dd, *J* = 15.4, 10.6 Hz, 1H), 6.49 – 6.34 (m, 2H), 5.21 (d, *J* = 15.4 Hz, 1H), 5.05 (d, *J* = 9.2 Hz, 1H), 3.74 (s, 3H). **^{13}C NMR (100 MHz, $CDCl_3$) δ =** 159.3, 137.4, 132.4, 129.9, 127.7, 116.5, 114.1, 55.3.

Buta-1,3-diene-1,1-diyldibenzene (3.14)

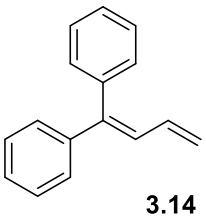

3.14

The product **3.14** was purified by flash column chromatography using pentane:ethyl acetate (30:1) as eluent. It was obtained as a yellow liquid (587.7 mg, 95% yield). **^{1}H NMR (400 MHz, $CDCl_3$) δ** = 7.27 (m, 3H), 7.20 – 7.09 (m, 7H), 6.63 (d, *J* = 11.0 Hz, 1H), 6.35 (ddd, *J* = 16.8, 11.0, 10.1 Hz, 1H), 5.34 – 5.25 (dd, *J* = 16.9, 1.5 Hz, 1H), 5.03 (dd, *J* = 10.1, 1.9 Hz, 1H). **^{13}C NMR (100 MHz, $CDCl_3$) δ** = 143.2, 142.1, 139.7, 135.0, 130.4, 128.5, 128.2, 127.6, 127.5, 127.4, 118.6.

(*E*)-2-(buta-1,3-dien-1-yl)furan (3.16)

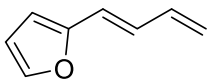

3.16

The product **3.16** was purified by flash column chromatography using pentane as eluent. It was obtained as a yellow oil (191.0 mg, 53% yield). **^{1}H NMR (400 MHz, $CDCl_3$) δ =** 7.29 (d, *J* = 1.8 Hz, 1H), 6.63 (dd, *J* = 15.6, 10.8 Hz, 1H), 6.44 – 6.24 (m, 3H), 6.20 (d, *J* = 3.3 Hz, 1H), 5.25 (d, *J* = 17.7 Hz, 1H), 5.08 (d, *J* = 10.0 Hz, 1H). **^{13}C NMR (100 MHz, $CDCl_3$) δ =** 153.0, 142.2, 136.7, 128.2, 120.4, 117.8, 111.6, 108.6.

((1*E*)-penta-1,3-dien-1-yl)benzene (3.18)

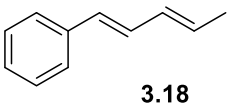

3.18

The product **3.18** was purified by flash column chromatography using pentane as eluent. It was obtained as a yellow oil (317.2 mg, 72% yield) (*E:Z* = 78:22). **^{1}H NMR (400 MHz, $CDCl_3$) δ** = (*E*): 7.38 – 7.29 (m, 2H), 7.25 – 7.16 (m, 2H), 7.15 – 7.05 (m, 1H), 6.99 (dd, *J* = 15.6, 11.1 Hz, 1H), 6.43 (d, *J* = 15.6 Hz, 1H), 6.19 – 6.02 (m, 1H), 5.58 – 5.45 (m, 1H), 1.77 (dd, *J* = 7.2, 1.8 Hz, 3H). (*Z*):7.29 – 7.25 (m, 2H), 7.25 – 7.16 (m, 2H), 7.15 – 7.05 (m, 1H), 6.65 (dd, *J* = 15.7, 10.4 Hz, 1H), 6.33 (d, *J* = 15.7 Hz, 1H), 6.19 – 6.02 (m, 1H), 5.74 (dq, *J* = 14.0, 6.8 Hz,

1H), 1.73 (dd, *J* = 6.8, 1.6 Hz, 3H). **^{13}C NMR (100 MHz, $CDCl_3$) δ** = (*E:Z* = 78:22) 137.7, 131.9, 130.3, 129.8, 129.7, 129.4, 128.6, 128.5, 127.3, 127.1, 127.1, 126.3, 126.1, 124.2, 18.3, 13.6.

1-chloro-4-((1*E*)-penta-1,3-dien-1-yl)benzene (3.20)

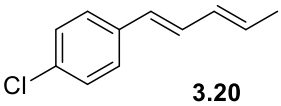

3.20

The product **3.20** was purified by flash column chromatography using pentane as eluent. It was obtained as a yellow solid (464.4 mg, 87% yield) (*E:Z* = 56:44). **^{1}H NMR (400 MHz, $CDCl_3$) δ** = (*E)*: 7.29 – 7.15 (m, 4H), 6.63 (dd, *J* = 15.7, 10.4 Hz, 1H), 6.28 (d, *J* = 15.7 Hz, 1H), 6.19 – 6.03 (m, 1H), 5.83 – 5.70 (m, 1H), 1.74 (dd, *J* = 6.8, 1.6 Hz, 3H). (*Z)*: 7.29 – 7.15 (m, 4H), 6.98 (ddd, *J* = 15.6, 11.1, 1.2 Hz, 1H), 6.38 (d, *J* = 15.6 Hz, 1H), 6.19 – 6.03 (m, 1H), 5.61 – 5.48 (m, 1H), 1.78 (dd, *J* = 7.2, 1.8 Hz, 3H). **^{13}C NMR (100 MHz, $CDCl_3$) δ** = (*E:Z* = 56:44) 136.2, 132.8, 132.5, 131.6, 131.1, 130.5, 130.0, 129.4, 128.8, 128.7, 128.4, 127.9, 127.5, 127.3, 124.7, 18.5, 13.7.

***N*,*N*-dimethyl-4-((1*E*)-penta-1,3-dien-1-yl)aniline (3.22)**

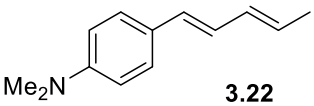

3.22

The product **3.22** was purified by flash column chromatography using pentane as eluent. It was obtained as a yellow solid (476,6 mg, 85% yield) (*E:Z* = 56:44). **^{1}H NMR (400 MHz, $CDCl_3$) δ** = (*E)*: 7.29 – 7.15 (m, 4H), 6.63 (dd, *J* = 15.7, 10.4 Hz, 1H), 6.28 (d, *J* = 15.7 Hz, 1H), 6.19 – 6.03 (m, 1H), 5.83 – 5.70 (m, 1H), 1.74 (dd, *J* = 6.8, 1.6 Hz, 3H). (*Z)*: 7.29 – 7.15 (m, 4H), 6.98 (ddd, *J* = 15.6, 11.1, 1.2 Hz, 1H), 6.38 (d, *J* = 15.6 Hz, 1H), 6.19 – 6.03 (m, 1H), 5.61 – 5.48 (m, 1H), 1.78 (dd, *J* = 7.2, 1.8 Hz, 3H). **^{13}C NMR (100 MHz, $CDCl_3$) δ** = (*E:Z* = 56:44) 150.0, 133.3, 131.1, 129.8, 129.7, 127.3, 126.9, 125.1, 121.2, 111.3, 40.2, 19.1, 13.7.

(*E*)-(2-methylbuta-1,3-dien-1-yl)benzene (3.24)

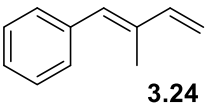

3.24

The product **3.24** was purified by flash column chromatography using pentane as eluent. It was obtained as a colorless oil (380.7 mg, 88% yield). **^{1}H NMR (400 MHz, $CDCl_3$) δ** = 7.31 – 7.17 (m, 4H), 7.17 – 7.10 (m, 1H), 6.47 (dd, *J* = 17.2, 10.6, 1H), 6.43 (s, 1H), 5.21 (d, *J* = 17.5 Hz, 1H), 5.04 (d, *J* = 10.8 Hz, 1H), 1.91 (s, 3H). **^{13}C NMR (100 MHz, $CDCl_3$) δ** = 141.9, 137.7, 136.0, 131.7, 129.2, 128.2, 126.6, 113.0, 13.2.

Cyclohexadiene (3.26)

3.26

The product **3.26** was purchased from Sigma-Aldrich.

2-Methyl-5-(1-methylethyl)-1,3-cyclohexadiene (3.30)

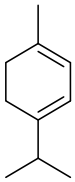

3.30

The product **3.30** was purchased from Sigma-Aldrich.

6.3.3 General Procedure for the preparation of cyclic 1,3-dienes via Kumada Coupling

To a dry reaction vessel equipped with a magnetic stirrer bar at 0 °C was added diidopropylamine (0.77 mL, 5.5 mmol) in dry THF (10 mL) and nBuLi (5.5 mmol). After 30 minutes at 0 °C the solution was cooled to -78 °C and cyclohexenone (0.48 mL, 5 mmol) in dry THF (10 mL) was added dropwise. The mixture was left to stir for an additional 30 minutes before a solution of N-phenyl-bis(trifluoromethanesulfonimide) (1.78g, 5 mmol) in THF (7 mL) was added slowly and the reaction was allowed to warm to 0 °C. It was then left to stir at 0 °C. After 3 hours, the mixture was washed with water and extracted with diethyl ether before being dried over magnesium sulphate to yield the crude triflate. To a new dry reaction vessel equipped with a magnetic stirrer bar was added the crude triflate (ca. 5 mmol) and copper(I) Iodide (10 mol%, 95 mg) in dry THF (14 mL). The solution was cooled to 0 °C before the relevant Grignard reagent (1.1 equiv, 5.5 mmol) was added dropwise. The reaction was running until judged complete by TLC (ca. 1 hour) and quenched with saturated aqueous ammonium chloride (10 mL). The aqueous phase was extracted with Et_2O and the combined organic extracts were dried over magnesium sulfate. After filtration, the volatile components were removed under reduced pressure. The crude residue was purified by silica gel flash chromatography to afford the diene product.[13]

6.3.4 Characterization of cyclic 1,3-dienes via Kumada Coupling

2-(2-ethylhexyl)cyclohexa-1,3-diene (3.28)

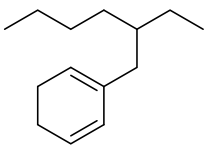

3.28

The product **3.28** was purified by flash column chromatography using synthesized using petroleum ether as eluent. It was obtained as a colorless liquid (480 mg, 69% yield). **^{1}H NMR (400 MHz, $CDCl_3$) δ** = 5.81 (m, 2H), 5.45 (m, 1H), 2.09 (m, 4H), 1.92 (dd, J = 7.0, 1.0 Hz, 2H), 1.25 (m, 9H), 0.88 (m, 3H), 0.83 (m, 3H). **^{13}C NMR (100 MHz, $CDCl_3$) δ** = 135.1, 127.7, 126.5, 121.5, 40.2, 37.8, 32.5, 28.9, 25.7, 23.2, 22.6, 14.3, 10.9.

6.3.5 General Procedure for the transition metal-free 1,4-hydroboration reaction for non-cyclic 1,3-dienes

To an oven-dried Schlenk-flask equipped with a magnetic stir bar, B_2pin_2 (0.55 mmol, 1.1 equiv), sodium carbonate (30 mol%), dry methanol as solvent (1 mL), and 1,3-diene (0.5 mmol, 1 equiv) were added. The vial was sealed with a plastic cap and heated to 70 °C in an oil bath for 8 hours. After that period an extra amount of sodium carbonate (0.075 mmol, 0.15 equiv) was added and the reaction stirred for 8 hours. Upon completion, the reaction mixture was concentrated under reduced pressure and a known amount of naphthalene (ca. 10 mg) as internal standard was added. An aliquot was taken to determine the conversion and selectivity by ^{1}HNMR and GC-MS analysis. The crude residue was purified by silica gel flash chromatography to afford the hydroborated product.

6.3.6 Characterization of 1,4-hydroborated non-cyclic 1,3-dienes

4,4,5,5-tetramethyl-2-(4-phenylbut-2-en-1-yl)-1,3,2-dioxaborolane (3.2)

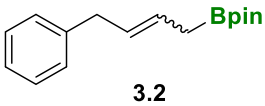

3.2

The product **3.2** was purified by flash column chromatography using pentane:ethyl acetate (20:1) as eluent. It was obtained as a colorless liquid (27 mg, 21% yield) (*E:Z* = 4:1). **^{1}H NMR (400 MHz, $CDCl_3$) δ =** (*E*) 7.35 – 7.13 (m, 5H), 5.70 – 5.51 (m, 2H), 3.44 – 3.36 (d, *J* = 6.5 Hz, 2H), 1.80 (d, *J* = 7.6 Hz, 2H). (*Z*) 7.35 – 7.13 (m, 5H), 5.70 – 5.51 (m, 2H), 3.33 (d, *J* = 5.5 Hz, 2H), 1.69 (d, *J* = 5.8 Hz, 2H), 1.25 (s, 12H). **^{13}C NMR (100 MHz, $CDCl_3$) δ =** 141.3, 132.8, 128.5, 128.3, 128.3, 128.1, 126.7, 125.9, 125.8, 125.3, 83.3, 83.1, 39.2, 33.3, 27.4, 24.9, 24.8, 24.6. **^{11}B NMR (128 MHz, $CDCl_3$) δ =** 33.01. **HRMS-(ESI+) for $C_{16}H_{23}BO_2$ $[M]^+$**: calculated: 258.1791, found: 258.1786.

2-(4-(4-chlorophenyl)but-2-en-1-yl)-4,4,5,5-tetramethyl-1,3,2-dioxaborolane (3.9)

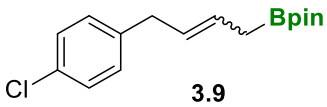

3.9

The product **3.9** was purified by flash column chromatography using as eluent a mixture of pentane:ethyl acetate (10:1). It was obtained as colorless oil (31.5 mg, 23% yield) (*E:Z* = 3:1). **^{1}H NMR (400 MHz, $CDCl_3$) δ =** 7.24 (t, *J* = 5.1 Hz, 2H), 7.12 (dd, *J* = 11.0, 8.6 Hz, 2H), 5.71 – 5.59 (m, 1H), 5.58 – 5.44 (m, 1H), 3.35 (d, *J* = 7.2 Hz, 2H), 3.28 (d, *J* = 6.3 Hz, 0,5H), 1.77 (d, *J* = 7.9 Hz, 2H), 1.69 (d, *J* = 6.8 Hz, 0,5H), 1.24 (s, 15H). **^{1}H NMR (400 MHz, $CDCl_3$) δ =** 129.8, 128.5, 128.3, 127.4, 127.1, 125.8, 83.39, 24.8, 24.7, 24.5. **^{11}B NMR (128 MHz, $CDCl_3$) δ =** 33.1. **HRMS-(ESI+) for $C_{16}H_{23}BClO_2$ $[M+H]^+$:** calculated: 293.1480, found: 293.1474.

_N,N_-dimethyl-4-(4-(4,4,5,5-tetramethyl-1,3,2-dioxaborolan-2-yl)but-2-en-1-yl)aniline (3.11)

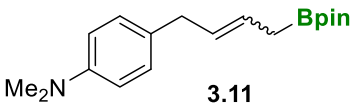

3.11

The product **3.11** was purified by flash column chromatography using as eluent a mixture of pentane:ethyl acetate (25:1). It was obtained as colorless oil (57.8 mg, 38% yield) (*E*:*Z* = 3:1). **^{1}H NMR(400 MHz, $CDCl_3$) δ** = 7.02 (t, *J* = 8.8 Hz, 2,5H), 6.68 (s, 2,5H), 5.63 – 5.39 (m, 2,5H), 3.24 (d, *J* = 6.4 Hz, 2H), 3.17 (d, *J* = 5.2 Hz, 0,5H), 2.84 (s, 7H), 1.72 (d, *J* = 7.1 Hz, 2H), 1.61 (d, *J* = 5.5 Hz, 0,5H), 1.19 (s, 15H). **^{13}C NMR (100 MHz, $CDCl_3$) δ** = 129.1, 124.6, 83.3, 41.3, 38.2, 32.3, 29.7, 24.8. **^{11}B NMR (128 MHz, $CDCl_3$) δ** = 33.1. **HRMS-(ESI+) for $C_{18}H_{29}BNO_2$ $[M+H]^+$**: calculated: 302.2291, found: 302.2258.

2-(4-(4-methoxyphenyl)but-2-en-1-yl)-4,4,5,5-tetramethyl-1,3,2-dioxaborolane (3.13)

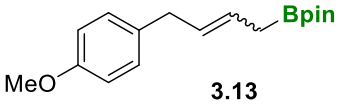

3.13

The product **3.13** was purified by flash column chromatography using as eluent a mixture of pentane:ethyl acetate (10:1). It was obtained as colorless oil (46 mg, 32% yield) (*E*:*Z* = 4:1). **^{1}H NMR(400 MHz, $CDCl_3$) δ** = 7.04 (t, J = 9.3 Hz, 2,5H), 6.79 – 6.71 (m, 3H), 5.61 – 5.38 (m, 2,5H), 3.71 (s, 5H), 3.26 (d, J = 6.9 Hz, 2H), 3.20 (d, J = 5.4 Hz, 0,5H), 1.72 (d, J = 7.6 Hz, 2H), 1.61 (d, J = 5.7 Hz, 0,5H), 1.18 (s, 15H). **^{13}C NMR (100 MHz, $CDCl_3$) δ** = 133.3, 129.3, 129.3, 128.5, 126.9, 124.9, 113.8, 113.7, 113.6, 83.3, 55.2, 32.3, 24.8, 24.8. **^{11}B NMR (128 MHz, $CDCl_3$) δ** = 32.8. **HRMS-(ESI+) for $C_{17}H_{25}NaBO_3$ $[M+Na]^+$**: calculated: 311.1794, found: 311.1794.

2-(4,4-diphenylbut-2-en-1-yl)-4,4,5,5-tetramethyl-1,3,2-dioxaborolane (3.15)

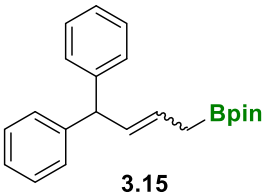

3.15

The product **3.15** was purified by flash column chromatography using as eluent a mixture of pentane:ethyl acetate (10:1). It was obtained as colorless oil (68 mg, 40% yield) (*E*:*Z* = 9:1). **^{1}H NMR(400 MHz, $CDCl_3$) δ** = 7.26 – 7.15 (m, 5H), 7.14 – 7.05 (m, 5H), 5.86 – 5.72 (m, 1H), 5.45 (ddd, J = 15.0, 8.0, 6.8 Hz, 1H), 4.61 (d, J = 7.9 Hz, 1H), 1.65 (d, J = 7.3 Hz, 2H), 1.17 (d, J = 1.1 Hz, 12 H). **^{13}C NMR (100 MHz, $CDCl_3$) δ** = 144.5, 132.8, 128.5, 128.2, 127.2, 126.0, 83.2, 54.0, 24.7. **^{11}B NMR (128 MHz, $CDCl_3$) δ** = 32.9. **HRMS-(ESI+) for $C_{22}H_{28}BO_2$ $[M+H]^+$:** calculated: 335.2182, found: 335.2177.

2-(4-(furan-2-yl)but-2-en-1-yl)-4,4,5,5-tetramethyl-1,3,2-dioxaborolane (3.17)

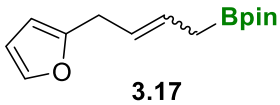

3.17

The product **3.17** was purified by flash column chromatography using as eluent a mixture of pentane:ethyl acetate (10:1). It was obtained as colorless oil (7 mg, 15% yield) (*E*:*Z* = 4:1). **^{1}H NMR(400 MHz, $CDCl_3$) δ** = 7.33 – 7.28 (s, 1H), 6.32 (dt, *J* = 7.9, 3.9 Hz, 0,25H), 6.30 – 6.24 (m, 1H), 6.12 – 6.09 (m, 0,25H), 6.02 – 5.94 (m, 1H), 5.74 – 5.44 (m, 2H), 3.39 (d, *J* = 6.7 Hz, 1), 3.33 (d, *J* = 6.5 Hz, 0,25H), 1.75 (d, *J* = 7.8 Hz, 2H), 1.70 (d, *J* = 6.7 Hz, 0,25H), 1.25 (s, 3H), 1.25 (s, 12H). **^{13}C NMR (100 MHz, $CDCl_3$) δ =** 140.9, 126.7, 110.1, 104.8, 83.3, 26.1, 24.7. **^{11}B NMR (128 MHz, $CDCl_3$) δ** = 33.0. **HRMS-(ESI+) $C_{14}H_{22}BO_3$ [M+H]$^+$**: calculated: 249.1662, found: 249.1654.

4,4,5,5-tetramethyl-2-(5-phenylpent-3-en-2-yl)-1,3,2-dioxaborolane (3.19)

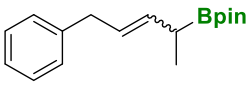

3.19

The product **3.19** was purified by flash column chromatography using as eluent a mixture of pentane:ethyl acetate (10:1). It was obtained as colorless oil (21 mg, 16% yield) (*E*:*Z* = 3:1). **^{1}H NMR(400 MHz, $CDCl_3$) δ** = 7.35 – 7.24 (m, 3H), 7.23 – 7.14 (m, 2H), 5.71 – 5.58 (m, 1H), 5.57 – 5.40 (m, 1H), 3.43 – 3.38 (m, 0,3H), 3.35 (d, J = 6.6 Hz, 3H) 1.94 – 1.84 (m, 1H), 1.24 (s, 12H), 1.23 (s, 3H), 1.09 (d, J = 7.3 Hz, 3H), 1.02 (d, J = 7.4 Hz, 1H). **^{13}C NMR (100 MHz, $CDCl_3$) δ** = 134.0, 128.4, 128.2, 126.6, 125.7, 83.1, 39.1, 24.7, 24.6, 14.9. **^{11}B NMR (128 MHz, $CDCl_3$) δ** = 33.8. **HRMS-(ESI+) for $C_{17}H_{26}BO_2$ [M+H]$^+$**: calculated 273.2026, found: 273.2025.

2-(5-(4-chlorophenyl)pent-3-en-2-yl)-4,4,5,5-tetramethyl-1,3,2-dioxaborolane (3.21)

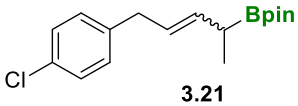

3.21

The product **3.21** was purified by flash column chromatography using as eluent a mixture of pentane:ethyl acetate (25:1). It was obtained as colorless oil (36 mg, 23% yield) (*E*:*Z* = 3:1). **^{1}H NMR(400 MHz, $CDCl_3$) δ** = 7.18 – 7.12 (m, 2.5H), 7.05 (t, *J* = 10.8 Hz, 2.5H), 5.55 (dd, *J* = 15.3, 7.4 Hz, 1.25H), 5.40 (m, 1.25H), 3.29 (d, *J* = 6.1 Hz, 0.5H), 3.23 (d, *J* = 6.7 Hz, 2H), 1.86 – 1.76 (m, 1H), 1.16 (s, 15H), 1.01 (d, *J* = 7.3 Hz, 4H). **^{13}C NMR (100 MHz, $CDCl_3$) δ** = 134.6, 129.8, 128.3, 126.0, 83.1, 38.4, 24.7, 24.6, 14.9. **^{11}B NMR (128 MHz, $CDCl_3$) δ** = 33.6. **HRMS-(ESI+) for $C_{17}H_{25}BClO$ [M+H]$^+$:** calculated: 307.1636, found: 307.1617.

***N*,*N*-dimethyl-4-(4-(4,4,5,5-tetramethyl-1,3,2-dioxaborolan-2-yl)pent-2-en-1-yl)aniline (3.23)**

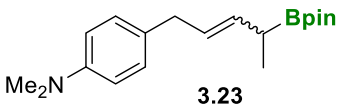

3.23

The product **3.23** was purified by flash column chromatography using as eluent a mixture of pentane:ethyl acetate (25:1). It was obtained as colorless oil (59.9 mg, 38%

yield)(*E:Z* = 3:1). **^{1}H NMR(400 MHz, $CDCl_3$) δ** = 7.08 (d, *J* = 8.3 Hz, 2H), 6.73 (s, 2H), 5.68 – 5.38 (m, 2H), 3.26 (d, *J* = 6.5 Hz, 2H), 2.92 (s, 6H), 1.92 – 1.82 (m, 1H), 1.24 (s, 12H), 1.08 (d, *J* = 7.3 Hz, 3H). **^{13}C NMR (100 MHz, $CDCl_3$) δ** = 133.3, 129.0, 129.0, 127.9, 127.3, 83.0, 65.8, 38.1, 24.7, 24.6, 24.6, 15.0. **^{11}B NMR (128 MHz, $CDCl_3$) δ** = 34.0. **HRMS (ESI) for $C_{19}H_{31}BNO_2$ [M+H]$^+$**: calculated: 316.2449, found: 316.2448.

4,4,5,5-tetramethyl-2-(3-methyl-4-phenylbut-2-en-1-yl)-1,3,2-dioxaborolane (3.25)

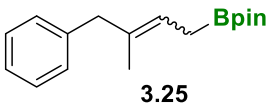

3.25

The product **3.25** was purified by flash column chromatography using as eluent a mixture of pentane:ethyl acetate (25:1). It was obtained as colorless oil (81.6 mg, 60% yield) (*E:Z* = 3:1). **^{1}H NMR(400 MHz, $CDCl_3$) δ** = 7.27 – 7.03 (m, 8H), 5.36 (m, 2H), 3.28 (s, 2H), 3.23 (s, 1H), 1.70 (d, J = 7.7 Hz, 2H), 1.59 (d, J = 7.7 Hz, 1H), 1.54 (d, J = 1.1 Hz, 3H), 1.43 (s, 1.5H), 1.18 (s, 18H). **^{13}C NMR (100 MHz, $CDCl_3$) δ** = 140.8, 140.3, 134.1, 133.8, 128.8, 128.7, 128.6, 128.2, 128.1, 127.9, 125.8, 125.7, 120.6, 83.2, 46.2, 37.6, 24.8, 24.8, 24.8, 23.4. **^{11}B NMR (128 MHz, $CDCl_3$) δ** = 33.3. **HRMS (ESI) for $C_{17}H_{25}BNaO_2$ [M+Na]$^+$**: calculated: 295.1845, found: 295.1867.

6.3.7 General Procedure for the transition metal-free 1,4-hydroboration reaction for cyclic 1,3-dienes

To an oven-dried Schlenk-flask equipped with a magnetic stir bar, B_2pin_2 (0.55 mmol, 1.1 equiv) sodium carbonate (0.075 mmol, 0.15 equiv), dry methanol as solvent (1 mL), and 1,3-diene (0.5 mmol, 1 equiv) were added. The vial was sealed with a plastic cap and heated to 90 °C in an oil bath 16 hours. Upon completion, the reaction mixture was concentrated under reduced pressure and a known amount of naphthalene (ca. 10 mg) as internal standard was added. An aliquot was taken to determine the conversion and selectivity by ^{1}HNMR and GC-MS analysis. The crude residue was purified by silica gel flash chromatography to afford the hydroborated product.

6.3.8 Characterization of 1,4-hydroborated cyclic 1,3-dienes

2-(cyclohex-2-en-1-yl)-4,4,5,5-tetramethyl-1,3,2-dioxaborolane (3.27)

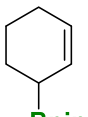

3.27

The product **3.27** was purified by flash column chromatography using as eluent a mixture of pentane:dichloromethane (4:1). It was obtained as colorless oil (37 mg, 35.5% yield). **^{1}H NMR (400 MHz, $CDCl_3$) δ** = 5.75 – 5.50 (m, 2H), 1.98 – 1.86 (m, 2H), 1.69 (ddd, *J* = 9.2, 8.1 Hz, 2H), 1.65 - 1.45 (m, 4H), 1.17 (s,12H). **^{13}C NMR (100 MHz, $CDCl_3$) δ** = 127.5, 126.0, 83.1, 24.9, 24.7, 24.6, 24.1, 22.5. **^{11}B NMR (128 MHz, $CDCl_3$) δ** = 33.5 (br s). **HRMS-(ESI+) for $C_{12}H_{21}BO_2$ [M]$^+$:** calculated: 209.1713, found: 209,1707.

2-((1S)-3-(2-ethylhexyl)cyclohex-2-en-1-yl)-4,4,5,5-tetramethyl-1,3,2-dioxaborolane (3.29)

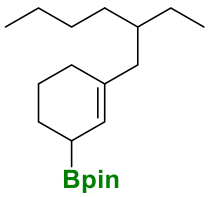

3.29

The product **3.29** was purified by flash column chromatography using as eluent a mixture of pentane:ethyl acetate (40:1). It was obtained as colorless oil (37.8 mg, 59% yield). **^{1}H NMR(400 MHz, $CDCl_3$) δ** = 5.39 (m, 1H), 1.85 (m, 4H), 1.67 (m, 2H), 1.56 (m, 1H), 1.37 (m, 1H), 1.35 (m, 5H), 1.23 (s, 12H), 1.19 (m, 5H), 0.87 (m, 3H), 0.81 (td, J = 7.4, 3.7 Hz, 3H). **^{13}C NMR (100 MHz, $CDCl_3$) δ** = 43.2, 36.7, 32.6, 28.9, 28.2, 25.8, 24.8, 24.1, 23.2, 23.1, 14.3, 10.8. **^{11}B NMR (128 MHz, $CDCl_3$) δ** = 33.9 (br s).

2-(6-isopropyl-3-methylcyclohex-2-en-1-yl)-4,4,5,5-tetramethyl-1,3,2-dioxaborolane (3.31)

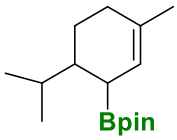

3.31

The product **3.31** was purified by flash column chromatography using as eluent a mixture of pentane:ethyl acetate (20:1). It was obtained as colorless oil (78 mg, 59% yield). **^{1}H NMR(400 MHz, $CDCl_3$) δ** = 5.23 (br s, 1H), 1.94 (m, 2H), 1.67 (m, 2H), 1.63 (s, 3H), 1.56 (m, 1H), 1.49 (m, 1H), 1.26 (m, 1H), 1.23 (d, J = 1.6 Hz, 12H), 0.91 (d, J = 6.7 Hz, 3H), 0.83 (d, J = 6.8 Hz, 3H). **^{13}C NMR (100 MHz, $CDCl_3$) δ** = 133.3, 120.5, 83.1, 40.4, 31.3, 29.9, 24.9, 24.7, 24.2, 24.1, 21.4, 18.5. **^{11}B NMR (128 MHz, $CDCl_3$) δ** = 33.8 (br s). **HRMS (ESI) for $C_{16}H_{29}BO_2$ [M]$^{+}$**: calculated: 265.2339, found: 265.2331.

6.3.9 General procedure for the transition metal free 1,2-diboration reaction

To an oven-dried Schlenk-flask equipped with a magnetic stir bar, B_2pin_2 (0.55 mmol, 1.1 equiv), sodium carbonate (30 mol%), dry methanol as solvent (1 mL), and substrate **3.1**, **3.4** or **3.6** (0.5 mmol, 1 equiv) were added. The vial was sealed with a plastic cap and heated to 70 °C in an oil bath for 16 hours. Upon completion, the reaction mixture was concentrated under reduced pressure and a known amount of naphthalene as internal standard was added. An aliquot was taken to determine the conversion and selectivity by ^{1}HNMR and GC-MS analysis. The crude residue was purified by silica gel flash chromatography to afford the diborated product.

6.3.10 Characterization of 1,2-diborated and 1,2,3-triborated products

(*E*)-2,2'-(pent-3-ene-1,2-diyl)bis(4,4,5,5-tetramethyl-1,3,2-dioxaborolane) (3.5)

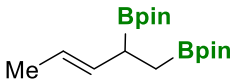

3.5

The product **3.5** was purified by flash column chromatography using pentane:ethyl acetate (20:1) as eluent. It was obtained as a colorless oil (41.2 mg, 33% yield). **^{1}H NMR(400 MHz, $CDCl_3$) δ** = 5.49 (ddd, J = 15.3, 7.6, 1.5 Hz, 1H), 5.41 – 5.30 (m, 1H), 1.90 (m, 1H), 1.61 (d, J = 6.2 Hz, 3H), 1.20 (s, 24H), 0.98 (dd, J = 15.9, 9.2 Hz, 1H), 0.87 (dd, J = 15.9, 6.3 Hz, 1H). **^{13}C NMR (100 MHz, $CDCl_3$) δ** = 133.6, 122.7, 83.0, 82.9, 82.8, 28.6, 25.7, 24.9, 24.8, 24.7, 18.2. **^{11}B NMR (128 MHz, $CDCl_3$) δ** = 33.41 (br s). **HRMS-(ESI+) for $C_{17}H_{33}B_2O_4$ $[M+H^+]^+$:** calculated: 323.2565, found: 323.2562.

(Z)-2,2'-(3-phenylpent-3-ene-1,2-diyl)bis(4,4,5,5-tetramethyl-1,3,2-dioxaborolane) (3.7)

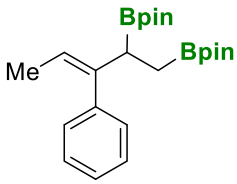

3.7

The product **3.7** was purified by flash column chromatography using as eluent a mixture of pentane:ethyl acetate (25:1). It was obtained as colorless oil (74 mg, 37% yield). **^{1}H NMR(400 MHz, $CDCl_3$) δ** = 7.30 – 7.16 (m, 2H), 7.15 – 7.03 (m, 3H), 5.53 – 5.39 (m, 1H), 2.20 (t, *J* = 8.2 Hz, 1H), 1.42 (dd, *J* = 6.8, 0.8 Hz, 3H), 1.14 (d, *J* = 2.8 Hz, 12H), 1.07 (d, *J* = 7.0 Hz, 12H), 1.00 – 0.93 (m, 2H). **^{13}C NMR (100 MHz, $CDCl_3$) δ** = 144.5, 142.2, 129.0, 127.6, 126.0, 119.3, 83.0, 82.9, 24.9, 24.7, 24.7, 24.6, 14.8. **^{11}B NMR (128 MHz, $CDCl_3$) δ** = 34.5. **HRMS-(ESI+) for $C_{23}H_{36}B_2O_4Na$ $[M+Na^+]^+$**: calculated: 421.2697, found: 421.2701.

2,3',2''-(4-phenylbutane-1,2,3-triyl)tris(4,4,5,5-tetramethyl-1,3,2-dioxaborolane) (3.3)

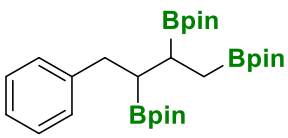

3.3

The product **3.3** was purified by flash column chromatography using pentane:ethyl acetate (10:1) as eluent. It was obtained as a colorless liquid (167 mg, 65% yield). **^{1}H NMR(400 MHz, $CDCl_3$) δ** = 7.20 (m, 4H), 7.08 (m, 1H), 2.72 (m, 2H), 1.50 (m, 1H), 1.31. (m, 1H), 1.21-1.19 (m, 24H), 1.10 (s, 6H), 1.08 (s, 6H), 0.91-0.78 (m, 2H). **^{13}C NMR (100 MHz, $CDCl_3$) δ** = 143.0, 129.1, 129.1, 127.8, 127.8, 125.2, 82.8, 82.8, 82.7, 36.3, 24.9. **^{11}B NMR (128 MHz, $CDCl_3$) δ** = 33.15 (br s). **HRMS-(ESI+) for $NaC_{28}H_{47}B_3O_6$ $[M+Na]^+$**: calculated: 535.3549, found: 535.3549.

6.3.11 General procedure for oxidative reaction of borylated 1,4-hydroborated compounds

The allylic alcohols were synthetized according to an adapted version of the general procedure using an oxidative work-up with hydrogen peroxide and sodium hydroxide. Once

1,4-hydroboration reaction of substrate is completed, the solvent was removed in *vacuo* and resolved within 2 mL of diethyl ether in a flask equipped with a magnetic stirrer. A solution of NaOH 3 M (2 mL) was added followed by of hydrogen peroxide 30 % of volume (1 mL). The reaction was allowed to stir 3 hours and then it was quenched with sodium thiosulfate. The mixture was washed with diethyl ether, dried over magnesium sulfate and filtered. Finally, the solution was concentrated under *vacuo* and purified by silica gel flash chromatography.

6.3.12 Characterization of allylic alcohols

4-phenylbut-2-en-1-ol (3.32)

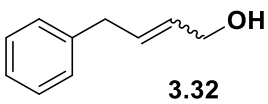

3.32

The product **3.32** was purified by flash column chromatography using pentane:ethyl acetate (1:1) as eluent. It was obtained as a colorless oil (28.9 mg, 40% yield) (*E:Z* = 3:1). **^{1}H NMR(400 MHz, $CDCl_3$) δ** = 7.27 – 7.20 (m, 3H), 7.15 – 7.06 (m, 4H), 5.84 – 5.57 (m, 3H), 4.25 (d, *J* = 5.1 Hz, 2H), 4.06 (ddd, *J* = 5.7, 2.2, 1.1 Hz, 1H), 3.38 (d, *J* = 5.4 Hz, 2H), 3.32 (d, *J* = 6.6 Hz, 1H). **^{13}C NMR (100 MHz, $CDCl_3$) δ** = 131.1, 129.3, 128.5, 128.4, 128.3, 126.1, 58.6, 38.6, 33.6. **HRMS-(ESI+) for $C_{10}H_{13}O$ $[M+H^+]^+$**: calculated: 147.0810 found: 147.0804.

4-(4-chlorophenyl)but-2-en-1-ol (3.33)

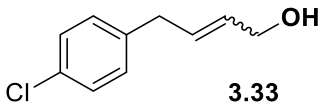

3.33

The product **3.33** was purified by flash column chromatography using as eluent a mixture of pentane:ethyl acetate (4:1). It was obtained as colorless oil (35.1 mg, 17% yield) (*E:Z* = 3:1). **^{1}H NMR(400 MHz, $CDCl_3$) δ** = 7.26 (d, *J* = 3.1 Hz, 3H), 7.11 (d, *J* = 8.2 Hz, 3H), 5.88 – 5.63 (m, 3H), 4.30 (s, 2H), 4.13 (s, 1H), 3.41 (d, *J* = 7.1 Hz, 2H), 3.35 (d, *J* = 6.6 Hz, 1H). **^{13}C NMR (100 MHz, $CDCl_3$) δ** = 138.6, 130.7, 130.6, 129.9, 129.6, 128.6, 128.5, 58.55, 33.0. **HRMS-(ESI+) for $C_{10}H_{12}ClO[M+H^+]^+$**: calculated: 181.0420 found: 181.0415.

4-(4-(dimethylamino)phenyl)but-2-en-1-ol (3.34)

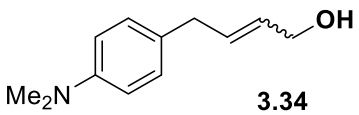

3.34

The product **3.34** was purified by flash column chromatography using as eluent a mixture of pentane:ethyl acetate (4:1). It was obtained as colorless oil (39.2 mg, 41% yield) (*E:Z* = 3:1). **^{1}H NMR(400 MHz, $CDCl_3$) δ** = 7.09 (d, *J* = 8.5 Hz, 3H), 6.81 (br s, 2H), 6.73 (br s, 1H), 6.02 – 5.61 (m, 3H), 4.31 (t, *J* = 4.7 Hz, l,2H), 4.12 (t, *J* = 5.1 Hz, 1H), 3.37 (d, *J* = 5.7 Hz, 2H), 3.31 (d, *J* = 6.6 Hz, 1H), 2.96 (s, 1,5H), 2.94 (s, 3H). **^{13}C NMR (100 MHz, $CDCl_3$) δ** = 129.3, 129.0, 128.8, 127.0, 63.6, 58.5, 37.7, 36.5, 32.6, 29.7. **HRMS-(ESI+) for $C_{12}H_{17}NO$ $[M]^+$**: calculated: 191.1310, found: 191.1308.

4-(4-methoxyphenyl)but-2-en-1-ol (3.35)

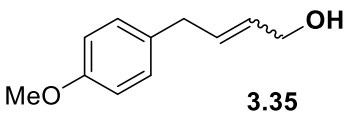

3.35

The product **3.35** was purified by flash column chromatography using as eluent a mixture of pentane:ethyl acetate (4:1). It was obtained as colorless oil (34.4 mg, 36% yield) (*E:Z* = 4:1). **^{1}H NMR(400 MHz, $CDCl_3$) δ** = 7.12 – 7.07 (m, 3.5H), 6.84 (d, *J* = 8.6 Hz, 3.5H), 5.89 – 5.79 (m, 0.7H), 5.78 – 5.64 (m, 2.7H), 4.33 – 4.30 (m, 2H), 4.13 (dd, *J* = 5.8, 1.0 Hz, 1.4H), 3.79 (s, 5.2H), 3.39 (d, *J* = 5.8 Hz, 2H), 3.33 (d, *J* = 6.8 Hz, 1.5H), 1.25 (s, 1.7H). **^{13}C NMR (100 MHz, $CDCl_3$) δ** = 157.99, 132.24, 131.62, 129.96, 129.52, 129.24, 128.97, 127.22, 113.97, 113.89, 63.60, 62.11, 58.56, 55.31, 37.76, 36.42, 32.75. **HRMS-(ESI+) for $C_{11}H_{14}O_2$ [M]$^+$**: calculated: 178.0994, found: 178.0988.

4,4-diphenylbut-2-en-1-ol (3.36)

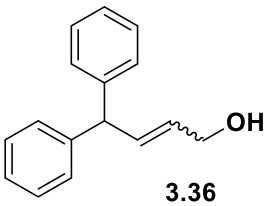

3.36

The product 3.**36** was purified by flash column chromatography using as eluent a mixture of pentane:ethyl acetate (4:1). It was obtained as colorless oil (0.27 mmol, 60.1 mg, 50% yield) (*E:Z* = 9:1). **^{1}H NMR(400 MHz, $CDCl_3$) δ** = 7.36 – 7.26 (m, 5H), 7.24 – 7.15 (m, 5H), 6.28 – 6.12 (ddt, *J* = 15.3, 7.5, 1.5 Hz, 1H), 5.63 (dtd, *J* = 15.4, 5.7, 1.3 Hz, 1H), 4.75 (d, *J* = 7.5 Hz, 1H), 4.19 (d, *J* = 5.7, 2H). **^{13}C NMR (100 MHz, $CDCl_3$) δ** = 143.3, 134.4, 130.9, 128.5, 128.5, 126.4, 63.4, 53.6. **HRMS-(ESI+) for $C_{16}H_{16}O$ [M]$^+$**: calculated: 224.1201 found: 224.1196.

5-phenylpent-3-en-2-ol (3.37)

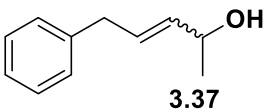

3.37

The product **3.37** was purified by flash column chromatography using as eluent a mixture of pentane:ethyl acetate (4:1). It was obtained as colorless oil (35.6 mg, 44% yield) (*E:Z* = 3:1). **^{1}H NMR(400 MHz, $CDCl_3$) δ** = 7.30 (m, 2H), 7.20 (m, 3H), 5.89 – 5.70 (m, 1H), 5.70 – 5.49 (m, 1H), 4.41 – 4.24 (m, 1H), 3.47 (m, 0.5H), 3.37 (d, *J* = 6.7 Hz, 2H), 1.54 (s, 1H), 1.28 (d, *J* = 6.4 Hz, 3H). **^{13}C NMR (100 MHz, $CDCl_3$) δ** = 140.1, 135.5, 129.5, 128.5, 128.8, 126.1, 68.7, 65.9, 38.5, 23.3, 15.3. **HRMS-(ESI+) for $C_{11}H_{15}O$ [M+H]$^+$**: calculated: 163.1123 found: 163.1117.

4-(4-(dimethylamino)phenyl)but-2-en-1-ol (3.38)

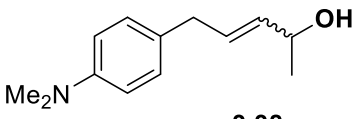

3.38

The product **3.38** was purified by flash column chromatography using as eluent a mixture of pentane:ethyl acetate (4:1). It was obtained as colorless oil (42.0 mg, 41% yield) (*E:Z* = 3:1). **^{1}H NMR(400 MHz, $CDCl_3$) δ** = 7.00 (d, *J* = 8.5 Hz, 2.5H), 6.77 – 6.54 (m, 2.5H), 5.80 – 5.60 (m, 1.25H), 5.61 – 5.35 (m, 1.25H), 4.30 – 4.12 (m, 1H), 3.30 (d, *J* = 6.9 Hz, 0.5H), 3.20 (d, *J* = 6.7 Hz, 2H), 2.88 (s, 1H),

2.86 (s, 6H), 1.23 (d, *J* = 6.3 Hz, 0.75H), 1.20 (d, *J* = 6.4 Hz, 3H). **^{13}C NMR (100 MHz, $CDCl_3$) δ** = 134.8, 130.3, 129.2, 128.9, 127.0, 113.2, 112.6, 68.8, 67.4, 41.0, 40.6, 37.6, 23.7, 23.3. **HRMS-(ESI+) for $C_{12}H_{19}NO$ [M]$^+$**: calculated 205.1467 found: 205.1467.

5-(4-chlorophenyl)pent-3-en-2-ol (3.39)

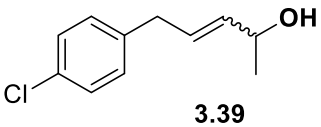

3.39

The product **3.39** was purified by flash column chromatography using as eluent a mixture of pentane:ethyl acetate (4:1). It was obtained as colorless oil (38.0 mg, 39% yield)(*E:Z* = 3:1). **^{1}H NMR(400 MHz, $CDCl_3$) δ** = 7.26 (m, 2H), 7.11 (d, *J* = 8.2 Hz, 2H), 5.76 (m, 1H), 5.64 – 5.53 (m, 1H), 4.31 (m, 1H), 3.33 (d, *J* = 6.7 Hz, 2H), 1.27 (dd, *J* = 6.4, 0.6 Hz, 3H). **^{13}C NMR (100 MHz, $CDCl_3$) δ** = 143.3, 134.4, 130.9, 129.9, 128.6, 128.5, 128.4, 128.1, 126.4, 63.5, 53.6. **HRMS-(ESI+) for $C_{11}H_{14}ClO$ [M+H]$^+$**: calculated: 197.0733, found: 197.0728.

3-methyl-4-phenylbut-2-en-1-ol (3.40)

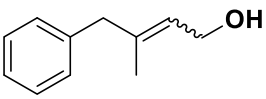

3.40

The product **3.40** was purified by flash column chromatography using as eluent a mixture of pentane:ethyl acetate (4:1). It was obtained as colorless oil (41.0 mg, 50% yield)(*E:Z* = 3:1). **^{1}H NMR(400 MHz, $CDCl_3$) δ** = 7.27 – 7.17 (m, 2H), 7.17 – 7.04 (m, 3H), 5.52 (t, *J* = 6.7 Hz, 1H), 4.21 (d, *J* = 7.1 Hz, 2H), 3.35 (s, 2H), 1.61 (d, *J* = 0.9 Hz, 3H). **^{13}C NMR (100 MHz, $CDCl_3$) δ** = 128.6, 128.5, 128.4, 128.2, 126.1, 125.2, 59.3, 37.9, 23.5. **HRMS-(ESI+) for $C_{11}H_{15}O$ [M+H]$^+$**: calculated: 163.1123, found: 163.1117.

Cyclohex-2-en-1-ol (3.41)

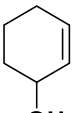

3.41

The product **3.41** was purified by flash column chromatography using as eluent a mixture of pentane:ethyl acetate (4:1). It was obtained as colorless oil (16.0 mg, 33% yield). **^{1}H NMR(400 MHz, $CDCl_3$) δ** = 5.84 (dtd, *J* = 10.0, 3.6, 1.2 Hz, 1H), 5.80 – 5.71 (m, 1H), 4.20 (s, 1H), 2.10 – 1.94 (m, 4H), 1.94 – 1.80 (m, 3H), 1.79 – 1.67 (m, 3H), 1.66 – 1.52 (m, 7H). **^{13}C NMR (100 MHz, $CDCl_3$) δ** = 130.6, 129.8, 65.5, 32.0, 29.7, 25.0, 18.9. **HRMS-(ESI+) for $C_6H_{11}O$ [M+H]$^+$**: calculated: 99.0810, found: 99.0804.

3-(2-ethylhexyl)cyclohex-2-en-1-ol (3.42)

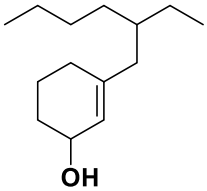

3.42

The product **3.42** was purified by flash column chromatography using as eluent a mixture of pentane:ethyl acetate (4:1). It was obtained as colorless oil (37.1 mg, 68% yield). **^{1}H NMR(400 MHz, $CDCl_3$) δ** = 5.52 – 5.44 (m, 2H), 4.19 (s, 2H), 1.89 (d, *J* = 7.2 Hz, 6H), 1.84 – 1.65 (m, 5H), 1.64 – 1.51 (m, 5H), 1.45 – 1.32 (m, 4H), 1.32 – 1.12 (m, 17H), 0.93 – 0.76 (m, 12H). **^{13}C NMR (100 MHz, $CDCl_3$) δ** =141.6, 125.1, 125.0, 65.9, 65.9, 42.4, 36.5, 36.4, 32.6, 32.4, 31.9, 31.9, 28.8, 28.7, 28.4, 28.4, 25.7, 25.5, 23.0, 19.1, 19.1, 14.1, 10.7, 10.6. **HRMS-(ESI+) for $C_{14}H_{26}O$ [M]$^{+}$**: calculated: 210.1984, found: 210.1934.

6-isopropyl-3-methylcyclohex-2-en-1-ol (3.43)

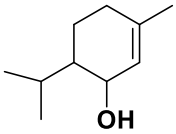

3.43

The product **3.43** was purified by flash column chromatography using as eluent a mixture of pentane:ethyl acetate (20:1). It was obtained as colorless oil (38.0 mg, 50% yield). **^{1}H NMR(400 MHz, $CDCl_3$) δ** = 5.37 (s, 1H),4.01 (d, *J* = 6.7 Hz, 1H), 2.00 (hept, *J* = 3.6 Hz, 1H), 1.91 (m, 2H), 1.67 (s, 3H), 1.65 (m, 1H), 1.25 (m, 2H), 0.96 (d, *J* = 6.9 Hz, 3H), 0.83 (d, *J* = 6.9 Hz, 3H). **^{13}C NMR (100 MHz, $CDCl_3$) δ** = 137.8, 125.4, 69.3, 48.0, 30.2, 26.6, 23.3, 21.4, 21.0, 17.5. **HRMS-(ESI+) for $C_{10}H_{18}O$ [M]$^{+}$**: calculated: 154.1358, found: 154.1355.

6.4 Experimental section for Chapter 4

6.4.1 Descriptors

The descriptors computed in this work are collected in Table 6.1 and 6.2 for anionic intermediates and Table 6.3 for boryl alkylidene lithium salts and α-boryl alkyl transition metal complexes. The computed descriptors include: 1) the calculated protonation Gibbs free-energies ($\Delta G_{prot.}$) for the acid-base reaction of cyclopentadiene with α-borylcarbanion, resulting in the corresponding cyclopentadienyl anion and neutral α-boryl species; 2) the energy of the Highest Occupied Molecular Orbital (E_{HOMO}), formally corresponding to the C-B π-orbital in eV; 3) the bond distance averaged for all the C-B bonds ($d_{C\text{-}B\ av.}$) in Å; 4) the NBO atomic charge supported on carbanion atom (q(C)); 5) the average atomic charge for the boron atoms ($q(B)_{av.}$); 6) the charge of borata-alkene fragment including the atomic charge of the carbanion and the averaged atomic charge of boron atoms ($B_{av.}$=C); 7) the charge of borata-alkene fragment including also the substituents of the carbanion ($B_{av.}=C_{(R1R2)}$); 8) the total Wiberg bond order of the carbanion (∑C-R_3 bond order); 9) the sum of Wiberg bond orders for the C-B bonds (∑C-B_{bo}); 10) the average of Wiberg bond orders for the C-B bonds (C-$B_{bo\text{-}av.}$); forcing a Lewis structure with the carbanion forming 3 bonds, 11) the NBO population of the perpendicular boron *p* orbital ($p^{\perp}$(B)) in the anionic species, 12) the increase of the NBO population in the perpendicular *p* orbital from the corresponding neutral, protonated species ($\Delta[p^{\perp}(B)\text{-}p^{\perp}(B)_{prot}] = p^{\perp}(B)_{prot} - p^{\perp}(B)$); 13) the NBO population of the lone pair electron for the carbanionic atom (p(C)); 14) the p/s ratio in carbanion-metal bonds, defined as the ratio between the *p* and *s* atomic orbitals of carbon in the C-M σ bond; 15) the free-energy for the dissociation of the carbanion ligand from the metal (ΔG_{bond}), shown in Figure 6.1; and 16) the *distance-weighed volume* parameter (V_W) used to evaluate the impact of steric hindrance, using equation 6.1 (see also Computational Details in Chapter 4):

$$V_W = \sum_{i=1}^{N} \frac{r^3}{d_i}$$

Equation 6.1. Equation for the distance-weighted volume (V_W) parameter.

Table 6.1. Values of the computed descriptors described above for α-boryl carbanion species. Gibbs free energies ($\Delta G_{prot.}$) in kcal·mol^{-1}, HOMO energy (E_{HOMO}) in eV, distances ($d_{C\text{-}B\ av.}$) in Å, charges in a.u., and Wiberg bond orders.

Entry	$\Delta G_{prot.}$	E_{HOMO}	$d_{C\text{-}B\ av.}$	q(C)	$q(B)_{av.}$	$B_{av.}$=C	$B_{av.}$=C$_{(R1R2)}$	∑C-R$_3$ bond order	∑C-B$_{bo}$	C-B$_{bo\text{-}av.}$
1a^{PhF}	19.7	-2.87	1.44	-0.88	0.33	-0.54	-0.13	3.79	1.73	1.73
1a^{mes}	-0.2	-2.20	1.45	-0.98	0.39	-0.59	-0.20	3.73	1.69	1.69
1a^{dan}	-23.2	-1.19	1.45	-1.14	0.74	-0.40	-0.03	3.60	1.57	1.57
1b^{dan}	-20.5	-1.14	1.45	-0.89	0.75	-0.13	-0.22	3.66	1.52	1.52
1e^{pin}	-35.1	-0.20	1.43	-0.52	0.84	0.32	0.10	3.68	1.51	1.51
1c^{dan}	-3.1	-1.72	1.48	-0.84	0.86	0.02	-0.11	3.71	1.26	1.26
1a^{pin}	-33.6	-0.58	1.44	-1.20	0.91	-0.30	0.08	3.55	1.56	1.56
1b^{pin}	-30.6	-0.56	1.45	-0.95	0.92	-0.03	-0.12	3.62	1.50	1.50
1c^{pin}	-7.2	-1.27	1.47	-0.89	1.04	0.14	-0.20	3.68	1.25	1.25
1a^{Npin}	-45.3	0.22	1.58	-1.06	0.75	-0.31	0.03	3.55	1.56	1.56
2a^{2dan}	6.7	-2.51	1.48	-1.24	0.90	-0.34	-0.12	3.56	2.48	1.24
2b^{2dan}	5.1	-2.38	1.48	-1.01	0.91	-0.10	-0.15	3.61	2.40	1.20
2c^{2dan}	15.5	-2.62	1.48	-1.00	0.94	-0.06	-0.25	3.61	2.23	1.12
2a^{pindan}	0.3	-2.25	1.48	-1.20	0.98	-0.22	0.01	3.54	2.48	1.24
2b^{pindan}	2.2	-2.11	1.48	-1.05	1.00	-0.05	-0.10	3.59	2.39	1.20
2c^{pindan}	11.8	-2.45	1.50	-1.04	1.03	-0.01	-0.18	3.59	2.24	1.12
2a^{2pin}	-10.9	-1.85	1.47	-1.33	1.07	-0.26	-0.02	3.51	2.46	1.23
2b^{2pin}	-8.7	-1.67	1.48	-1.10	1.09	-0.01	-0.05	3.56	2.38	1.19
2c^{2pin}	2.2	-2.01	1.50	-1.08	1.12	0.05	-0.15	3.57	2.20	1.10
3^{3dan}	22.4	-3.25	1.51	-1.37	0.97	-0.40	-0.40	3.46	3.27	1.09
3^{2pindan}	18.7	-2.95	1.52	-1.40	1.03	-0.37	-0.37	3.44	3.26	1.09
3^{pin2dan}	12.6	-3.14	1.50	-1.44	1.09	-0.35	-0.35	3.42	3.24	1.08
3^{3pin}	-1.8	-2.61	1.50	-1.49	1.15	-0.33	-0.33	3.39	3.21	1.07

Table 6.2. Values of the computed descriptors described above for α-boryl carbanion species. NBO population analysis of the wave function corresponding to a Lewis structure defining a carbanion bonded to 3 substituents with single bonds.

Entry	$p^{\perp}(B)$	$p^{\perp}(B)_{prot}$	$\Delta[p^{\perp}(B)-p^{\perp}(B)_{prot}]$	p(C)
1a^{PhF}	0.72	0.18	0.54	1.19
1a^{mes}	0.65	0.15	0.50	1.29
1a^{dan}	0.63	0.39	0.24	1.49
1b^{dan}	0.64	0.39	0.24	1.45
1e^{pin}	0.67	0.38	0.28	1.40
1c^{dan}	0.52	0.40	0.12	1.38
1a^{pin}	0.67	0.36	0.32	1.31
1b^{pin}	0.63	0.36	0.27	1.47
1c^{pin}	0.52	0.36	0.16	1.38
1a^{Npin}	0.69	0.41	0.28	1.36
2a^{2dan}	0.99	0.80	0.20	1.41
2b^{2dan}	0.99	0.80	0.20	1.39
2c^{2dan}	0.94	0.81	0.13	1.38
2a^{pindan}	0.99	0.76	0.23	1.41
2b^{pindan}	0.99	0.76	0.23	1.39
2c^{pindan}	0.94	0.75	0.19	1.38
2a^{2pin}	0.98	0.72	0.26	1.42
2b^{2pin}	0.98	0.72	0.25	1.40
2c^{2pin}	0.91	0.73	0.18	1.38
3^{3dan}	1.35	1.21	0.14	1.38
3^{2pindan}	1.33	1.17	0.16	1.37
3^{pin2dan}	1.32	1.13	0.18	1.38
3^{3pin}	1.29	1.08	0.21	1.40

Table 6.3. Values of the computed descriptors described above and charge of the carbanion fragment (*q*[C]) for borly alkylidene lithium salts and α-boryl alkyl Cu^+, Ag^+ and Pd^{2+} complexes. Gibbs free energies ($\Delta G_{bond.}$) in kcal·mol^{-1}, HOMO energy (E_{HOMO}) in eV, distances in Å, charges in a.u., and the steric descriptor *distance-weight volume* (V_W).

Entry	E_{HOMO}	C-B$_{bo\text{-}av.}$	$d_{C\text{-}B\ av.}$	*q*[C]	*p/s*	V_W	ΔG_{bond}
1a^{pin}-Li	-6.46	1.36	1.48	-0.88	-	0.0	29.9
1b^{pin}-Li	-6.14	1.35	1.48	-0.89	-	0.0	22.4
1c^{pin}-Li	-5.95	1.23	1.49	-0.93	-	0.0	29.2
1a^{dan}-Li	-6.27	1.29	1.50	-0.89	-	0.0	20.1
1b^{dan}-Li	-6.18	1.37	1.49	-0.91	-	0.0	23.0
1c^{dan}-Li	-6.09	1.25	1.50	-0.94	-	0.0	16.2
1e^{pin}-Li	-6.27	1.23	1.50	-0.87	-	0.0	28.7
2a^{2pin}-Li	-6.52	1.21	1.49	-0.92	-	0.0	30.0
2b^{2pin}-Li	-6.18	1.09	1.49	-0.92	-	0.0	16.7
2c^{2pin}-Li	-6.08	1.13	1.50	-0.93	-	0.0	29.2
2a^{pindan}-Li	-6.36	1.21	1.50	-0.93	-	0.0	15.8
2b^{pindan}-Li	-6.33	1.18	1.50	-0.93	-	0.0	23.8
2c^{pindan}-Li	-5.81	1.08	1.52	-0.94	-	0.0	12.0
3^{3pin}-Li	-6.73	1.04	1.51	-0.92	-	0.0	15.8
1a^{pin}-Cu	-6.32	1.17	1.51	-0.66	6.45	4.5	37.5
1b^{pin}-Cu	-5.98	1.16	1.51	-0.67	7.75	4.4	36.2
1c^{pin}-Cu	-5.76	1.08	1.52	-0.73	-	40.8	25.3
1a^{dan}-Cu	-5.89	1.13	1.53	-0.66	5.75	40.6	34.7
1e^{pin}-Cu	-6.34	0.96	1.55	-0.62	2.60	41.1	36.6
2a^{2pin}-Cu	-6.49	1.06	1.52	-0.71	-	39.7	28.4
2b^{2pin}-Cu	-6.15	1.05	1.52	-0.73	-	40.2	27.1
2c^{2pin}-Cu	-6.06	1.00	1.53	-0.74	-	39.9	19.7
3^{3pin}-Cu	-6.52	0.96	1.52	-0.73	25.73	40.3	25.8
3^{3dan}-Cu	-6.16	0.99	1.54	-0.77	-	39.5	23.6
1a^{pin}-Ag	-6.26	1.17	1.51	-0.64	8.84	38.1	37.1
2a^{2pin}-Ag	-6.44	1.04	1.52	-0.69	16.84	39.1	14.4
3^{3pin}-Ag	-10.35	0.97	1.52	-0.72	-	38.5	25.6
1a^{pin}-Pd	-7.80	0.97	1.55	-0.21	0.97	46.3	67.1
2a^{2pin}-Pd	-7.66	0.92	1.54	-0.23	0.92	46.4	55.4
3^{3pin}-Pd	-7.50	0.86	1.57	-0.25	0.86	44.6	43.4

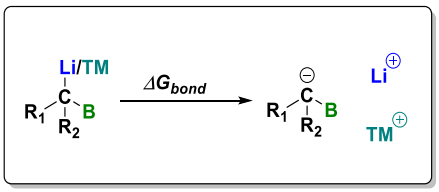

Figure 6.1. Schematic representation of the process for carbanion dissociation from the metals, used in the calculation of the bond dissociation free-energies (ΔG_{bond}).

6.4.2 Cambridge Structure Database (CSD) search

We defined different search queries (Figure 6.2 and 6.3) to produce the histogram of C-B distances depicted in Chapter 4. For boryl alkylidene lithium salts, we combined two queries (Figure 6.2). Both the carbon and the boron atoms in borata-alkene motif are defined as trivalent atoms, bonded to each other with *any-type* bond, and to other non-metal groups (NM). Then, the negative charge can be supported on the carbon atom (Figure 6.2a), or on the boron atom (Figure 6.2b). This search resulted in 14 hits.

For transition-metal α-boryl carbanions (Figure 6.3), the C-B bond is defined as *any-type*, both the carbon and the boron are linked to non-metal groups (NM). Then, we combined three possible queries in which the boron is defined as a trivalent atom, and the carbanion is bonded to the transition metal group (Figure 6.3a); the boron is defined as a negative tetravalent atom bonded to a transition metal (Figure 6.3b); or both, the carbon and the boron are defined as tetravalent atoms, linked to a transition metal (Figure 6.3c). This structural search resulted in 46 hits (Table 6.4).

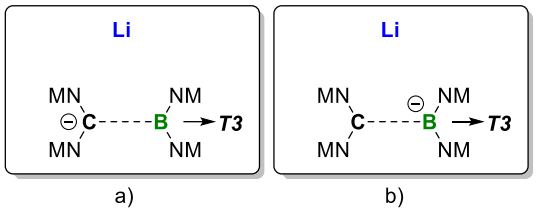

Figure 6.2. Structural motifs combined for the search query of X-ray structures in CSD for boryl alkylidene lithium salts.

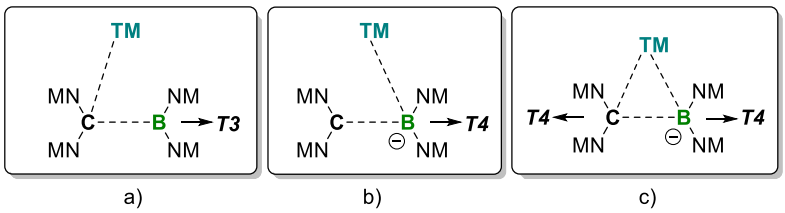

Figure 6.3. Structural motifs combined for the search query of X-ray structures in CSD for α-boryl alkyl transition metal complexes.

Table 6.4. Structures found in the CSD searches are defined in the structural motifs of Figures 6.2 and 6.3. The results are divided into three sets: lithium salts in red, carbanions interacting with early transition-metals and Cu in green, and carbanion interacting with other late transition-metals in blue.

CSD Entry	Metal	$d_{C\text{-}B\ av.}$ (Å)	CSD Entry	Metal	$d_{C\text{-}B\ av.}$ (Å)	CSD Entry	Metal	$d_{C\text{-}B\ av.}$ (Å)
EXINOO	Li	1.48	HOVWAQ	Ti	1.48	CAFCAP	Hg	1.55
FALGAA	Li	1.52	HOKSEI	Cu	1.51	OVUBEO	Ru	1.53
FEBLUW	Li	1.45	KEYGOK	Zr	1.48	NADXEY	Pd	1.55
FEBMAD	Li	1.44	NAJXIF	Ti	1.50	KOLFAU	Ru	1.56
FEBNIM	Li	1.44	QIZTUO	Ti	1.48	JARXIJ	Au	1.56
FEWWUZ	Li	1.44	SAKWEG	Ti	1.60	JOHXAH	Pt	1.52
GODKAO	Li	1.48	TIYGIS	Hf	1.49	XUVKIL	Rh	1.48
GIZQUEO	Li	1.54	TIYGOY	Hf	1.47	YOHNUE	Pt	1.55
HULCUP	Li	1.47	XOWFAR	Zr	1.48	TUCRIV	Zn	1.52
JIXXAS	Li	1.44	XOWFEV	Zr	1.48	TUCRUH	Zn	1.61
OPAXAG	Li	1.47	WUVFUR	Cr	1.52	IHAFAA	Fe	1.56
PILKIH	Li	1.45	YORGIY	Mn	1.48	JOHKUO	Pt	1.52
YUNJEY	Li	1.51	TABWAU	Ta	1.58	PATLEE	Ni	1.61
ZEKTEQ	Li	1.49	BOMYAF	Ta	1.51	SAPCAN	Pt	1.51
DEGVUH	Cu	1.52	MAPJES	Ta	1.52	VUFMER	Rh	1.49
DOGGEN	Zr	1.47	OVUBIS	Ru	1.66	VUFMIV	Rh	1.47
GIVCEV	Zr	1.53	QEXFAD	Ru	1.58	WUVFOL	Au	1.50
HAYGUJ	Zr	1.54	QEXFIL	Ru	1.58	XUVKIL	Rh	1.48
HOBCOQ	Ti	1.49	AQUYAM	Ru	1.57	XUVRAK	Rh	1.48
HOBCOQ01	Ti	1.49	AQUYIU	Ru	1.56	ROKBID	Fe	1.56

6.5 References

(1) Perrin, D. D.; Amarego, W. L. F. *Purification of Laboratory Chemicals*, 3rd ed.; Pergamin Press, Ed.; 1988.

(2) Mendiola, J.; García-Cerrada, S.; de Frutos, Ó.; de la Puente, M. L.; Gu, R. L.; Khau, V. V. Enzymatic Resolution of N-Substituted-β-Prolines. *Org. Process Res. Dev.* **2009**, *13* (2), 292–296.

(3) Sardini, S. R.; Brown, M. K. Catalyst Controlled Regiodivergent Arylboration of Dienes. *J. Am. Chem. Soc.* **2017**, *139* (29), 9823–9826.

(4) Pizey, J. S. Synthetic Reagents Vol. 2; John Wiley & Sons, Ed.; New York, 1974; pp 1–63.

(5) Hans-Günther, S. *Encyclopedia of Reagents for Organic Synthesis*; John Wiley & Sons, Ed.; New York, 1995.

(6) Djerassi, C. Brominations with N-Bromosuccinimide and Related Compounds. The Wohl-Ziegler Reaction. *Chem. Rev.* **1948**, *43* (2), 271–317.

(7) Pratsch, G.; Overman, L. E. Synthesis of 2,5-Diaryl-1,5-Dienes from Allylic Bromides Using Visible-Light Photoredox Catalysis. *J. Org. Chem.* **2015**, *80* (22), 11388–11397.

(8) Stevens, C. V; Rammeloo, T.; De Kimpe, N. Directing the Regioselectivity of the Alkylation of Pyroglutamate Carbamates by Formation of a Stable Counter-Ion Complex. *Synlett* **2001**, *2001* (10), 1519–1522.

(9) Tavares, F. X.; Deaton, D. N.; Miller, A. B.; Miller, L. R.; Wright, L. L.; Zhou, H.-Q. Potent and Selective Ketoamide-Based Inhibitors of Cysteine Protease, Cathepsin K. *J. Med. Chem.* **2004**, *47* (21), 5049–5056.

(10) Yamano, Y.; Chary, M. V.; Wada, A. Carotenoids and Related Polyenes, Part 12. *Chem. Pharm. Bull.* **2010**, *58* (10), 1362–1365.

(11) Bernhard, Y.; Thomson, B.; Ferey, V.; Sauthier, M. Nickel-Catalyzed α-Allylation of Aldehydes and Tandem Aldol Condensation/Allylation Reaction with Allylic Alcohols. *Angew. Chemie Int. Ed.* **2017**, *56* (26), 7460–7464.

(12) Yamamoto, E.; Takenouchi, Y.; Ozaki, T.; Miya, T.; Ito, H. Copper(I)-Catalyzed Enantioselective Synthesis of α-Chiral Linear or Carbocyclic (*E*)-(γ-Alkoxyallyl)Boronates. *J. Am. Chem. Soc.* **2014**, *136* (47), 16515–16521.

(13) Karlström, A. S. E.; Rönn, M.; Thorarensen, A.; Bäckvall, J.-E. A Versatile Route to 2-Substituted Cyclic 1,3-Dienes via a Copper(I)-Catalyzed Cross-Coupling Reaction of Dienyl Triflates with Grignard Reagents. *J. Org. Chem.* **1998**, *63* (8), 2517–2522.

Chapter 7
Summary

Summary

Organoboron chemistry has become a fundamental pillar in synthesis, as it has been demonstrated over the last decades. Figure 7.1 shows a graphic that represents the number of publications that mention the use of bis(pinacolato)diboron, as a reference boron source, over the years. The picture clearly shows the exponential trend up to almost 2500 publications in 2020 that involves the use of bis(pinacolato)diboron. This pronounced upward trend demonstrates the usefulness of organoboron chemistry as an efficient tool in organic synthesis since the organoboron compounds can be easily transformed into desired functional groups. Here we contribute to expand the field through new methodologies that give access to unprecedented organoboron compounds with the emphasis on the efficiency of the protocols and the versatility of the products. The deep understanding of the experimental observations and the predictions on the efficient C-B bond formation have attracted our attention and efforts by conducting computational studies on the mechanisms and the reactivity trends. They have been performed in combination with experiments.

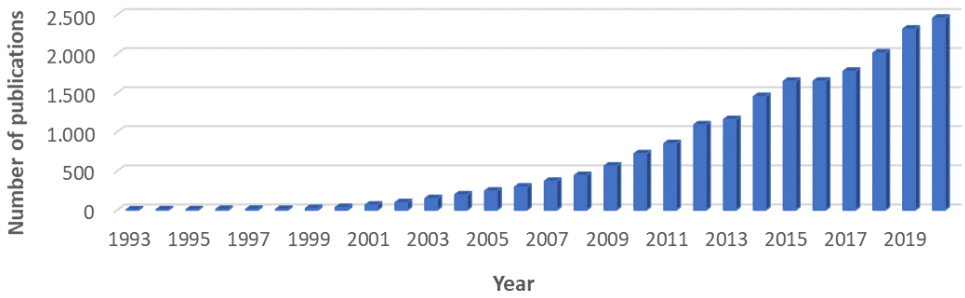

Figure 7.1. Representation of the publications about the use of bis(pinacolato)diboron boron source over the decades until October 2021. Source: SciFinder.

As discussed in Chapters 2 and 3, we aimed to develop an efficient and selective manner to borylate π-systems, due to the importance of selective organoboron compounds in synthesis, medicinal and material science.

Chapter 2 disclosed the copper-catalyzed borylation of π-systems to generate chemo- and diastereoselective 2-(borylmethyl)cycloalkanols up to five member-ring from alkenyl aldehydes. We demonstrated that the Cu-Bpin intermediate regioselectively reacts with electron-deficient C=C bonds followed by concomitant intramolecular Cu-C addition to the carbonyl moiety, giving the corresponding 2-(borylmethyl)cycloalcohol. However, the electron-rich C=C bonds seem to be less reactive with Cu-Bpin species, and consequently, the borylcuppration of C=O is favoured towards the formation of α-hydroxyboronate esters (Figure 7.2). The diastereoselectivity observed in the formation of 2-(borylmethyl)cycloalcohols was the *anti* configuration proved by NOE experiments and X-

Ray diffraction data (Figure 7.2). An exception was observed when a bulky group was bonded to the double bond, such as the 2-naphthyl group, giving as a result, a mixture of *anti* and *syn* diastereoisomers, this last one, as oxaborole bicyclic ring species, which was confirmed by X-Ray diffraction analysis (Figure 7.2). In addition, DFT calculations disclosed the mechanism, suggesting the intermediacy of Cu^{I} complex instead of Cu^{III}, as it was postulated by Ito and co-workers using ketones instead of aldehydes. The key steps that explain the origin of the chemo- and diastereoselectivity were calculated. The first transition state (**TS1** vs **TS1'**, Figure 7.2) decides the chemoselectivity through the boryl-copper complex, that attacks to the C=C *versus* C=O bonds. The second transition state explains the diastereoselectivity (**TS2**$_{anti}$ vs **TS2**$_{syn}$, Figure 7.2), since the intramolecular attack of organocopper to the formyl group can adopt two stereoconfiguration.

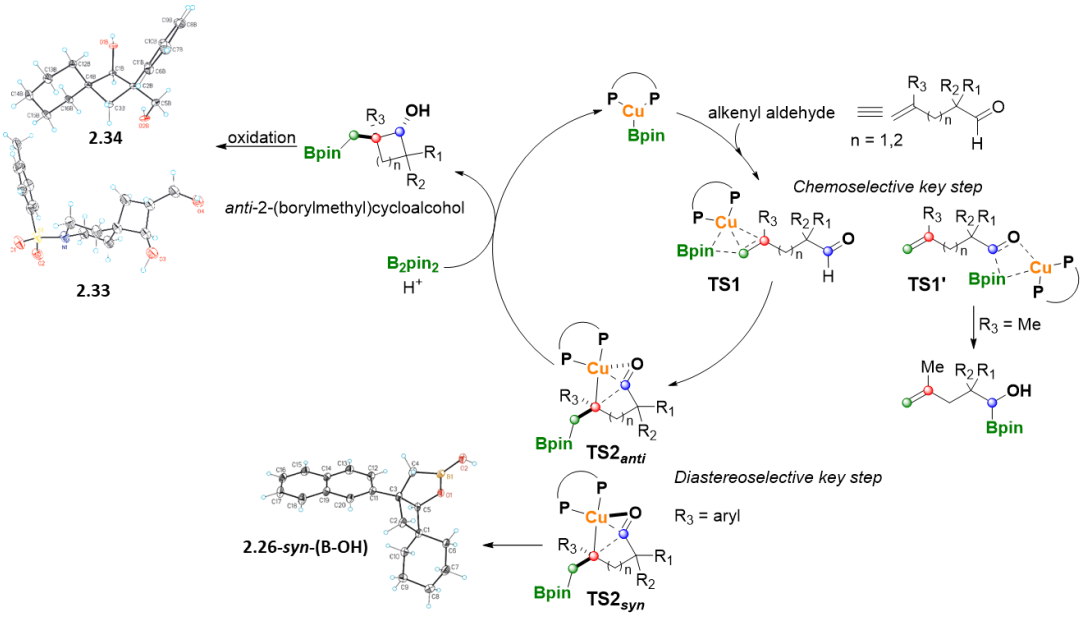

Figure 7.2. The general outlook discussed in Chapter 2 of copper-catalyzed borylative intramolecular cyclization using γ-alkenyl aldehydes.

Chapter 3 focused on the transition-metal-free borylation of the conjugated π-system 1,3-dienes. We developed a novel method optimizing the 1,4-hydroboration with the sole addition of base (Na_2CO_3) and methanol as solvent. We found that arylbutadiene substrates were essential in developing the 1,4-hydroboration (Scheme 7.1a), contrary to non-activated dienes, which gives the 1,2-diboration (Scheme 7.1b). Interestingly, the transition-metal-free 1,4-hydroboration provides a stereoselective preference for the *E*-isomer as the main product (Scheme 7.1a). On the other hand, we extended this reactivity to cyclic 1,3-

dienes, enhancing the usefulness of this transition-metal-free catalysis (Scheme 7.1c). DFT calculations in cyclic and non-cyclic systems provide us insight into this reactivity, allowing to understand the regioselectivity towards 1,4-hydroboration and the stereoselectivity towards the *E*-isomer. We postulated that the preference for the *E*-isomers comes from a previous isomerization of the *trans* 1,3-diene to the *cis* conformer. Thus the **TS1**-*Z* is 1.7 kcal·mol^{-1} higher than the *E*-isomer **TS1**-*E* (Scheme 7.1a). Interestingly, cyclic dienes react to give the 1,4-hydroborated product, going through a less stabilized allylic intermediate, which is in equilibrium with a boracyclic one. This reaction was less efficient, so we had to warm up until 90 °C. The DFT calculation agrees with the experimental results, showing a higher energy demand for the boryl attack to the diene. The observed regioselectivity was explained from the charge distribution of the allylic intermediate formed upon borylation that shows a large negative charge on the C_1 (Scheme 7.1c).

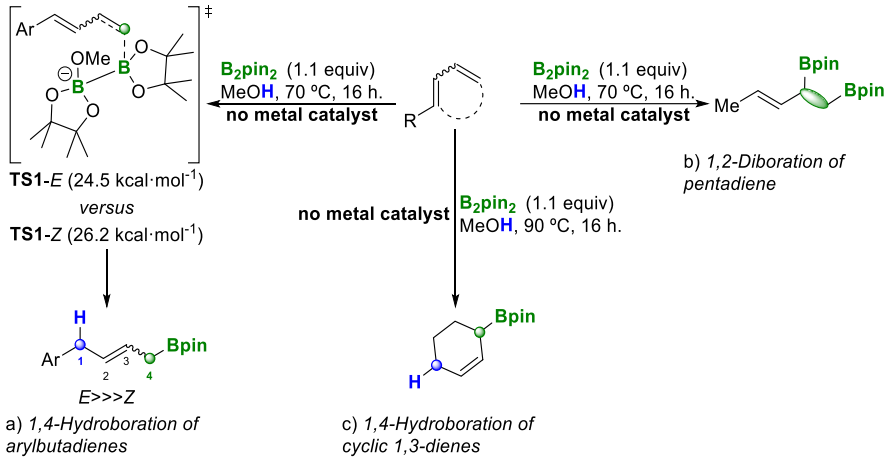

Scheme 7.1. The general outlook discussed in Chapter 3 for intermolecular transition-metal-free borylation of 1,3-dienes.

Finally, Chapter 4 was focused on building tendency maps of α-boryl carbanions employing computational descriptors to gauge their structural and electronic features and correlate them with the stability and reactivity of the carbanionic species. We started with the analysis of bare anionic species in order to evaluate the influence of the boryl moiety, the substituents on the carbanionic carbon and the number of boryl substituents. We found that HOMO energy (E_{HOMO}) describes the reactivity/stability of these carbanions efficiently, having an inverse linear correlation with the free energy of protonation ($\Delta G_{prot.}$). The sum of the Widberg bond-order ($\Sigma C\text{-}B_{bo}$) is useful to classify the mono-, di- or triborylated species and to differentiate between carbon substituents. These two descriptors and a set of 22 structures allowed us to build a tendency map, in which the nucleophilic reactivity increases

right (higher HOMO energies) and down (lower ΣC-B_{bo} values). Here, we identify a newly designed α-boryl carbanion with potential enhanced nucleophilicity, the 4,4,5,5-tetramethyl-1,3,2-diazaboryl methide anion (**1a**^{Npin}). Then, we expanded our study to more realistic systems consisting of α-boryl carbanions stabilized with metals such as lithium, copper, silver and palladium. Computational and crystallographic analysis classify these species into three different families that can be directly related to their reactivity: 1) borata-alkene salts with alkali and alkaline earth metals such as Li, 2) η^2-(C,B) borata-alkene complexes with early transition metals, Cu and Ag and 3) α-boryl alkyl complexes with late transition metals salt such palladium. Figure 7.3 maps this dataset using two descriptors, the negative charge of the non-metal fragment (*q*[C]) and the C-B bond order (*C-B*$_{bo\text{-}av.}$), which can be used to predict the nucleophilicity and the nature of the α-boryl carbanionic species, respectively. The map shows an order of nucleophilic reactivity that is consistent with experimental background, Li > Cu ≅ Ag > Pd; Moreover, vinyl carbanionic **1e**$^{pin\text{-}Cu}$ complex is placed in a different area of the chemical space, suggesting a new reactivity for this copper α-boryl carbanion compound. We hope that this map and the underlying dataset will facilitate the optimization of novel α-boryl carbanion reagents and assist their selection along with the desired reactivity.

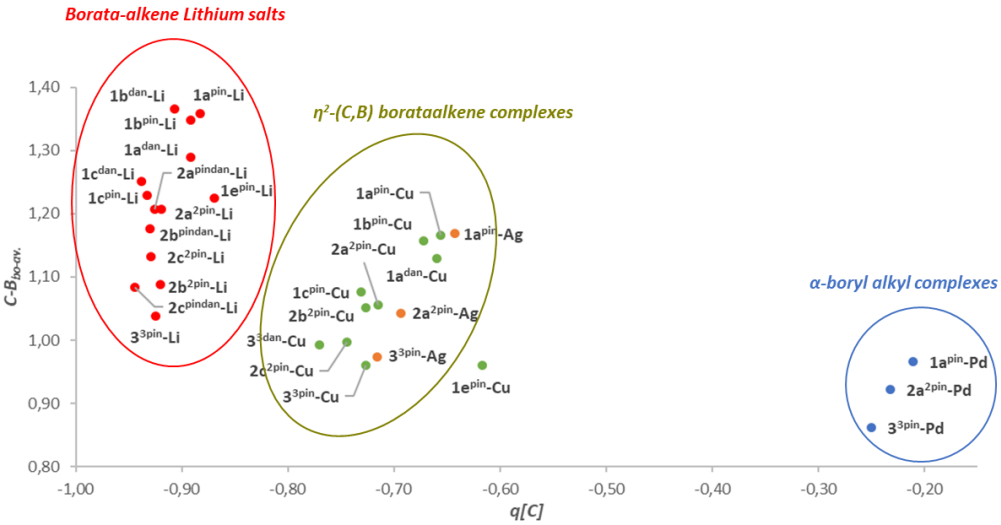

Figure 7.3. Representation of the average of C-B Wiberg bond orders (C-$B_{bo\text{-}av.}$) *versus* the overall charge of the carbanionic fragment (*q*[C]) divided into three different types of species: 1) borata-alkene lithium salts highlighted in red circle, 2) η^2-(C,B) borataalkene complexes highlighted in ochre circle, and 3) α-boryl alkyl complexes highlighted in blue circle.

Chapter 8
List of publications

8.1 List of publications

Related with this Thesis

Miralles, N.; Maza, R. J.; Fernández, E. Synthesis and Reactivity of 1,1-Diborylalkanes towards C–C Bond Formation and Related Mechanisms. *Adv. Synth. Catal.* **2018**, *360* (7), 1306–1327.

Maza, R. J.; Davenport, E.; Miralles, N.; Carbó, J. J.; Fernández, E. Transition-Metal-Free Allylic Borylation of 1,3-Dienes. *Org. Lett.* **2019**, *21* (7), 2251–2255.

Maza, R. J.; Royes, J.; Carbó, J. J.; Fernández, E. Consecutive Borylcupration/C–C Coupling of γ-Alkenyl Aldehydes towards Diastereoselective 2-(Borylmethyl)Cycloalkanols. *Chem. Commun.* **2020**, *56* (44), 5973–5976.

Maza, R. J.; Fernández, E.; Carbó, J. J. Mapping the Electronic Structure and the Reactivity Trends for Stabilized α-Boryl Carbanions. *Chem. – A Eur. J.* **2021**, *27* (48), 12352–12361.

Maza, R. J.; Carbó, J. J.; Fernández, E. Borata-Alkene Species as Nucleophilic Reservoir. *Adv. Synth. Catal.* **2021**, *363* (9), 2274–2289.

Other publication

Dominguez-Molano, P.; Bru, G.; Salvado, O.; Maza, R. J.; Carbó, J. J.; Fernández, E. Transborylation of alkenylboranes with diboranes. *Under revision* **2021**.

UNIVERSITAT
ROVIRA i VIRGILI